

**DNA-Binding and Photocleavage by Metallo-  
Polypyridyl, Porphyrin and Diazoarene Chromophores**

A Thesis  
Submitted for the Degree of  
**DOCTOR OF PHILOSOPHY**

By  
*S. Arounagiri*



School of Chemistry  
**University of Hyderabad**  
Hyderabad - 500 046  
India

March 1998

## CONTENTS

Statement	i
Certificate	ii
Acknowledgements	iii
Synopsis	v
<b>CHAPTER 1: Introduction</b>	<b>1</b>
<b>CHAPTER 2: Materials and Methods</b>	<b>53</b>
<b>CHAPTER 3: A New Metallointercalator Containing an Electroactive Dipyridophenazine Ligand: DNA Binding, Photonuclease Activity and Luminescence Properties</b>	<b>77</b>
<b>CHAPTER 4: DNA Binding, Photonuclease Activity and Luminescence Properties of a Series of Ruthenium(II) Complexes Containing 6,7-Dicyanodipyridoquinoxaline</b>	<b>118</b>
<b>CHAPTER 5: Dipyridophenazine Complexes of Cobalt(III) and Nickel(II): DNA-Binding and Photocleavage Studies</b>	<b>152</b>
<b>CHAPTER 6: Photonuclease Activity of Porphyrin-Anthraquinone Diads and Diazoarene Chromophores</b>	<b>177</b>
<b>CHAPTER 7: Conclusions</b>	<b>206</b>
<b>APPENDIX I: List of Publications</b>	<b>224</b>

## STATEMENT

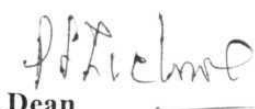
I hereby declare that the matter embodied in this Thesis is the result of investigations carried out by me in the School of Chemistry, University of Hyderabad, India under the supervision of Dr. Bhaskar G. Maiya.

In keeping with general practice of reporting scientific observations due acknowledgements have been made wherever the work described is based on the findings of other investigations.

  
**S. Arounagiri**

## CERTIFICATE

Certified that the work contained in this thesis entitled “**DNA-Binding and Photocleavage by Metallo-Polypyridyl, Porphyrin and Diazoarene Chromophores**” has been carried out by **S. Arounagiri** under my supervision and that the same has not been submitted elsewhere for a degree.



Dean

School of Chemistry



Bhaskar G. Maiya

Thesis Supervisor

## ACKNOWLEDGEMENTS

I am grateful to Dr. Bhaskar G. Maiya, my supervisor for his indispensable guidance, kind cooperation, unfaltering encouragement and help throughout this work.

I thank Professor P. S. Zacharias, Dean and all the faculty members of the school of chemistry for training me in various aspects of chemistry.

I owe special thanks to Professor G. Mehta and Professor M. Nagarajan for providing me samples for some of the studies. I am especially grateful to Dr. Aparna Dattagupta for her guidance and co-operation while carrying out the biochemical experiments involved in this study. I also thank Dr. T. P. Radhakrishnan for his help in computational work.

I am grateful to Professor C. K. Mitra for the timely help with laser printing

I thank my labmates Dr. M. Sirish, T. Anita Rao, L. Giribabu, D. Raghunath, Ashok kumar and C. V. Sastri for all their help and suggestions. I specially thank Dr. C. V. Ramana for his valuable help.

It is great pleasure to thank my friends and colleagues U. Radhakrishnan, K. Narkunan, M. C. Raja, P. Nachimuthu, Amanullah, G. Ambedkar, S. Prasanna, Prasad, M. Ravi, Prabavathi, A. Manjula, A. Sudha, C. Rameshkumar, C. R. Ramanathan, L. Venkatraman, P. Bharathi, K. Muthukumaran, S. Gopal, B. Doss, K. Gurubaran, C. Muthaiah, Ramakrishnan, Selvam, Srinivasan, V. Senthilkumar, Sivakumar, Sivaprakasam, Arul, Senthivel, Manohar, T. Venkat, T. Rajesh, B. Ramachandram, Sathyan, M. Bhaskar, RK, Kiran, Ramkumar, Vinay,

Mustafa, Samba, Giri, Jena, Chita, Jayakar, Tharakan, Murali. They have made my stay in the campus an unforgettable one.

I thank Satyanarayana, Bhaskar Rao, Mrs. Vijayalakshmi, V. Bhaskar, Manjunath, Mishra and Venkatramana for their technical help. I acknowledge Ananta Rao, Santosh, Shetty and all other non-teaching staff.

Financial assistance from the University Grants Commission and Jawaharlal Nehru Centre for Advanced Scientific Research are gratefully acknowledged.

RSIC, Central Drug Research Institute, Lucknow is acknowledged for the mass spectral data.

Lastly, I thank my parents and brothers for their love and constant encouragement throughout my education.

## Synopsis

This thesis entitled “**DNA-Binding and Photocleavage by Metallo-Polypyridyl, Porphyrin and Diazoarene Chromophores**” deals mainly with studies on the design, synthesis, characterization as well as DNA-binding and photonuclease activity of mixed-ligand or tris- complexes of cobalt(III), nickel(II) and ruthenium(II) derived from phenanthroline and modified phenanthroline ligands. It also deals with similar studies carried out with covalently linked porphyrin-anthraquinone diads and diazoarene chromophores. While the major interest in DNA-binding and photocleavage chemistry of metallo-intercalators stems from their use as structural/spectroscopic probes and site-specific cleavage agents for DNA, that of porphyrins is related to their ability to act as effective photosensitizers in the photodynamic therapy (PDT) of cancer and allied diseases. The strategy adopted in the design of all of the new chromophores investigated in this study largely relies on means of maximizing their DNA intercalation. Attempts to understand their mode of DNA-binding and mechanism of DNA-photocleavage has been done by the application of various physicochemical and biochemical techniques.

Metal complexes of the type  $[M(\text{phen}^*)_3]^{n+}$ , where phen\* is either 1, 10-phenanthroline (phen) or a modified phen ligand, are particularly attractive species for developing new diagnostic and therapeutic agents that can recognise and cleave DNA. Currently, a great deal of attention is being paid to DNA interactions of mixed-ligand complexes that contain both phen (or bpy = 2, 2'-bipyridyl) and modified phen (or modified bpy) ligands, the

latter of which so designed to augment the intercalative interaction by the complexes. Unique among the host of such modified ligands reported so far is dipyrdo[3,2-*a*:2',3'-*c*]-phenazine (dppz) - a near-planar, hetero-aromatic entity obtained by fusing a phenazine subunit to bpy. During the course of the present work, it was realized that further derivatization of this ligand with suitable electron donating/withdrawing group(s) or change of metal ion complexing this ligand might not only accentuate DNA-binding and photocleavage efficiencies of the ensuing complexes but also serve to explore other interesting functional aspects associated therein. We chose to derivatize dppz with electron-deficient functional groups such as for example, a quinone or a cyano group. Chapter 3 of this thesis describes the design, synthesis, characterization as well as DNA-binding and photonuclease activity of two new ruthenium(II) complexes containing dppz-based ligands endowed with electrochemically interconvertible quinone or hydroquinone functionality. Similar studies carried out with mixed-ligand and tris- ruthenium(II) complexes containing a "dicyano derivative" of dppz are described in Chapter 4. In Chapter 5 are described the results of studies carried out with an aim of evaluating the effect/s due to change of the metal ion on the DNA-binding and photocleavage abilities of the mixed-ligand complexes containing dppz.

Photodynamic therapy (PDT), in which light activates a photosensitizing drug and elicits a cytotoxic action, has recently emerged as a promising modality against cancer and allied diseases. Currently, hematoporphyrin derivative (or its commercial variant Photofrin II<sup>®</sup>) is the most widely used photosensitizer in PDT. However, application of this drug is known to cause undesirable, post-treatment phototoxic response, probably

due to the non-specific subcellular level activity during its photodynamic action. One possible way to circumvent this problem involves the use of targeted drug-delivery approach. In this regard, photoactive porphyrins which bind selectively to DNA owing to their linkage to either an intercalator (e.g. acridone, phenothiazine), a minor groove binder (e.g. ellipticine) or a cross-linking agent (e.g. chlorambucil) have been reported recently. During the above-mentioned studies on metallointercalators, it occurred to us that utilization of a photoactive, *intercalatable* moiety, such as an anthraquinone subunit, in conjunction with the porphyrin chromophore might accentuate the photochemical activity of the so-derived 'hybrid' molecules leading to an efficient DNA cleavage. DNA-binding and photocleavage studies on a series of tailor-made, covalently linked, porphyrin-anthraquinone diads are described in Chapter 6. Also described, in brief, in this chapter are similar studies carried out with *intercalatable* diazoarene chromophores which are shown to photocleave DNA *via* a carbene-mediated pathway.

The work embodied in this thesis has been divided into seven chapters and, a brief, chapter-wise account of the results is presented below.

## **Chapter 1. Introduction**

In this chapter, recent literature related to DNA-binding and photocleavage by metallointercalators has been discussed in light of their applicability as foot-printing and site-specific agents, spectroscopic and structural probes, molecular "light switches" and redox switches of luminescence has been reviewed. Also given is a brief survey on the

development of new, porphyrin-based photosensitizers for PDT with emphasis laid on the aspects related to photocleavage of DNA.

## **Chapter 2. Materials and Methods**

A general description of the synthetic methods as well as the spectroscopic, electrochemical, magnetic resonance and biochemical techniques employed during the research work is presented in this chapter.

## **Chapter 3. A New Metallointercalator Containing an Electroactive Dipyridophenazine Ligand: DNA Binding, Photonuclease Activity and Luminescence Properties**

A new mixed-ligand ruthenium(II) complex  $[\text{Ru}(\text{phen})_2(\text{qdppz})]^{2+}$  incorporating a quinone-fused dipyridophenazine ligand (where phen = 1,10-phenanthroline and qdppz = naphtho[2,3-a]dipyrido[3,2-h:2',3'-f] phenazine-5,18-dione) has been synthesized and fully characterized by spectroscopic (UV-visible, infra-red,  $^1\text{H}$  and  $^{13}\text{C}$  NMR and FAB-MS) and electrochemical methods. Chemical or electrochemical reduction of  $[\text{Ru}(\text{phen})_2(\text{qdppz})]^{2+}$  lead to the generation of  $[\text{Ru}(\text{phen})_2(\text{hqdpz})]^{2+}$  - a complex containing the hydroquinone form (hqddz = 5,18-dihydroxynaphtho[2,3-a]dipyrido[3,2-h:2',3'-f] phenazine) of qdppz. Three important aspects of these two redox-related complexes have been addressed in this chapter: (i) DNA binding (ii) DNA photocleavage and (iii) luminescence characteristics. Absorption and viscometric titration, thermal denaturation, topoisomerase assay and differential-pulse voltammetric studies reveal that  $[\text{Ru}(\text{phen})_2(\text{qdppz})]^{2+}$  is avid binder ( $K_b$ , apparent binding constant  $> 10^6 \text{ M}^{-1}$ ) of calf-thymus

(CT) DNA due to a strong intercalation by the ruthenium-bound qdppz while,  $[\text{Ru}(\text{phen})_2(\text{hqdpzz})]^{2+}$  binds to DNA less strongly than the parent ‘quinone’ containing complex ( $K_b = (1 \pm 0.2) \times 10^5 \text{ M}^{-1}$ ). The DNA photocleavage efficiencies of these complexes also follow a similar trend in that the MLCT excited state of  $[\text{Ru}(\text{phen})_2(\text{qdppz})]^{2+}$  is more effective than that of  $[\text{Ru}(\text{phen})_2(\text{hqdpzz})]^{2+}$  in cleaving the supercoiled plasmid pBR 322 DNA ( $\lambda_{\text{exc}} = 440 \pm 5 \text{ nm}$ ) as revealed by the results of agarose gel electrophoresis experiments. While  $[\text{Ru}(\text{phen})_2(\text{qdppz})]^{2+}$  has been found to be weakly luminescent or totally non-luminescent in non-aqueous solvents and also in aqueous buffered, aqueous  $\text{CH}_3\text{CN}$  (10%  $\text{H}_2\text{O}$ ), micellar (SDS) and DNA solutions, the reduced complex, on the other hand, shows its MLCT luminescence in both aqueous  $\text{CH}_3\text{CN}$  and micellar media but not in aqueous buffered and DNA solutions. These results have been rationalized by invoking (i) a photoinduced electron transfer from the MLCT state to the quinone acceptor in  $[\text{Ru}(\text{phen})_2(\text{qdppz})]^{2+}$  and (ii) quenching of the excited state due to a proton transfer from water to the dipyrrophenazine ligand in both the complexes. Finally, by the combined application of exhaustive bulk-electrolysis and steady state fluorescence spectroscopic methods, it is demonstrated that the “ $2e^-/2H^+$ ” redox related couple  $[\text{Ru}(\text{phen})_2(\text{qdppz})]^{2+}/[\text{Ru}(\text{phen})_2(\text{hqdpzz})]^{2+}$  represents a molecular “light switching” device displaying interconversion between the non-fluorescent ‘quinone’ and luminescent ‘hydroquinone’ states in aqueous  $\text{CH}_3\text{CN}$  solutions, Fig. 1 (*Proc. Indian Acad. Sci. (Chem. Sci)*, **1997**, 109, 155-158).

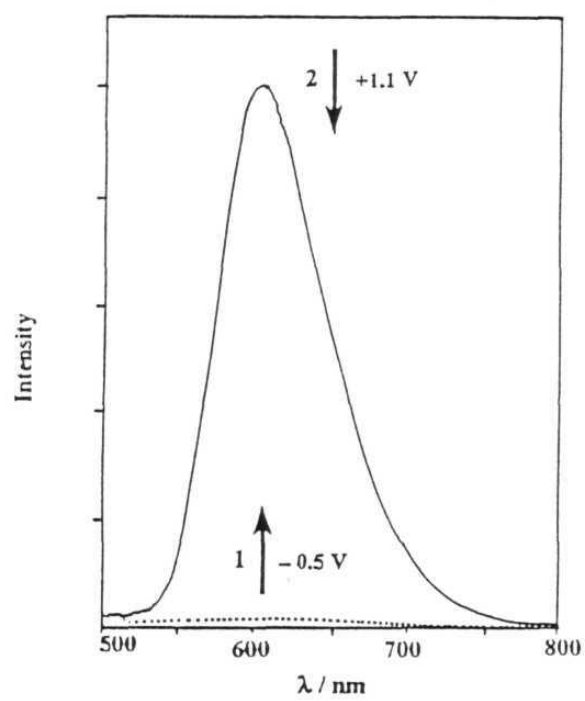
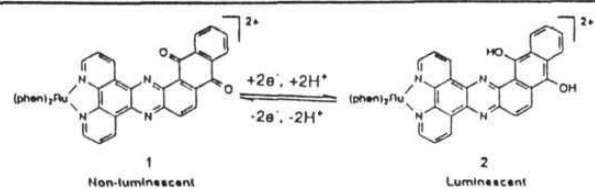
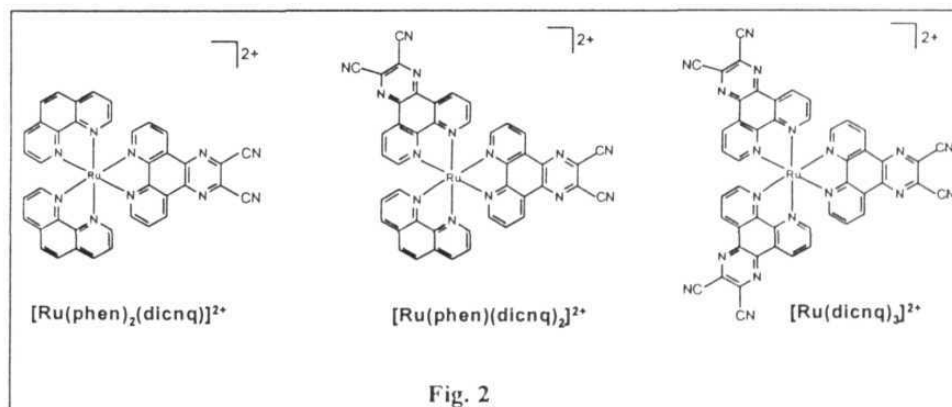


Fig. 1

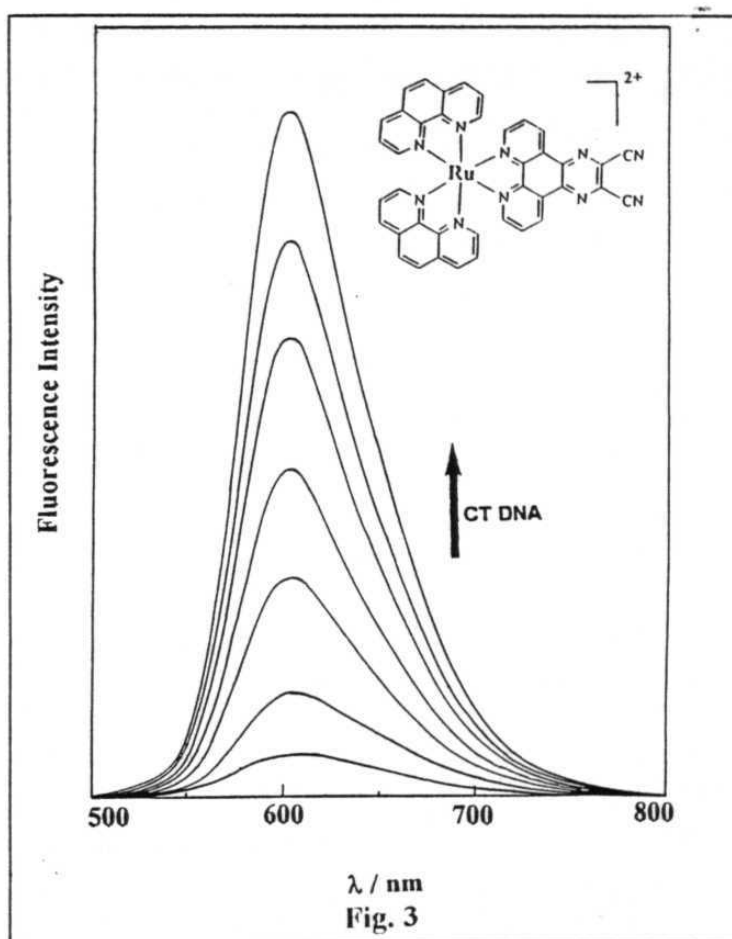
#### Chapter 4. DNA Binding, Photonuclease Activity and Luminescence Properties of a Series of Ruthenium(II) Complexes Containing 6,7-Dicyanodipyrido Quinoxaline

A new, phenanthroline-derived ligand (dicnq, 6,7-dicyanodipyrido quinoxaline) endowed with electron-withdrawing cyano groups on the dppz frame-work has been synthesized by the condensation of 1,10-phenanthroline-5,6-dione with diaminomaleonitrile. Mono- ( $[\text{Ru}(\text{phen})_2(\text{dicnq})]^{2+}$ ), bis- ( $[\text{Ru}(\text{phen})(\text{dicnq})_2]^{2+}$ ) and tris- ( $[\text{Ru}(\text{dicnq})_3]^{2+}$ ) ruthenium(II) complexes of dicnq (Fig. 2) have been synthesized in good to-moderate yields and these complexes have been fully characterized by elemental analysis, FAB-MS,  $^1\text{H}$  NMR and cyclic voltammetric methods. All the new complexes



show MLCT band around 445 nm in the UV-visible spectra - typical of any ruthenium(II) polypyridyl complex.. Results of absorption titration and thermal denaturation studies reveal that  $[\text{Ru}(\text{phen})_2(\text{dicnq})]^{2+}$ ,

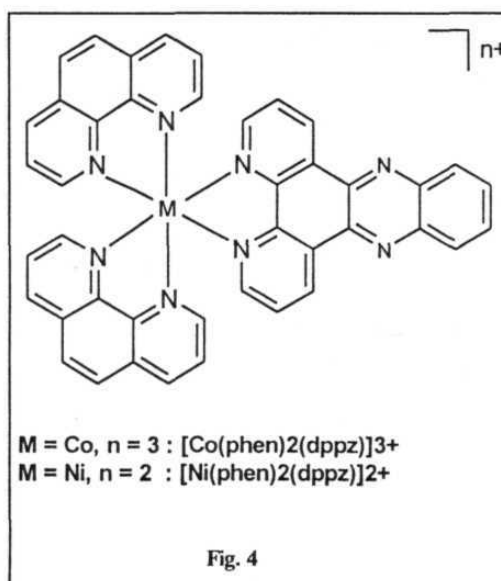
$[\text{Ru}(\text{phen})(\text{dicnq})_2]^{2+}$  and  $[\text{Ru}(\text{dicnq})_3]^{2+}$  bind with CT DNA predominantly *via* an intercalative mode with  $K_b$  values of  $4.30 \times 10^4$ ,  $4.01 \times 10^4$  and  $9.10 \times 10^3 \text{ M}^{-1}$ , respectively. While no lesion was observed in the dark for samples containing pBR 322 DNA and the individual complex, each complex was observed to be active against the plasmid in the presence of light ( $440 \pm 5 \text{ nm}$ ). Under identical set of experimental conditions of concentration and light dose, photonuclease activity was seen to follow the order  $[\text{Ru}(\text{phen})_2(\text{dicnq})]^{2+} > [\text{Ru}(\text{phen})(\text{dicnq})_2]^{2+} > [\text{Ru}(\text{dicnq})_3]^{2+}$ . Interestingly, the emission quantum yield values ( $\Phi_f$ ) of these complexes also follow the same order. Steady state luminescence studies reveal that both  $[\text{Ru}(\text{phen})_2(\text{dicnq})]^{2+}$  and  $[\text{Ru}(\text{phen})(\text{dicnq})_2]^{2+}$  are moderately luminescent in both water and  $\text{CH}_3\text{CN}$  ( $\Phi_f = 0.012$  and  $0.003$ , respectively) whereas,  $[\text{Ru}(\text{dicnq})_3]^{2+}$  is totally non-emissive in nature. An intramolecular electron transfer involving the electron deficient dicnq ligand/s can probably rationalize the observed variation in the  $\Phi_f$  values of these complexes. An interesting aspect related to the emission from  $[\text{Ru}(\text{phen})_2(\text{dicnq})]^{2+}$  and  $[\text{Ru}(\text{phen})(\text{dicnq})_2]^{2+}$  is concerned with the molecular “light switch” effect exhibited by these complexes in the presence of DNA. Successive addition of CT DNA to buffered solutions containing these complexes ( $10 \mu\text{M}$ ) results in an enhancement of the emission in each case, with the enhancement factors at saturation being approximately 16 and 8 for  $[\text{Ru}(\text{phen})_2(\text{dicnq})]^{2+}$  (see Fig. 3) and  $[\text{Ru}(\text{phen})(\text{dicnq})_2]^{2+}$ , respectively. No such emission enhancement was noticed for  $[\text{Ru}(\text{dicnq})_3]^{2+}$  in the presence of DNA.



## Chapter 5. Dipyridophenazine Complexes of Cobalt(III) and Nickel(II): DNA-Binding and Photocleavage Studies

Results of studies carried out with an aim of evaluating the effects due to change of the metal ion on the DNA-binding and photocleavage abilities of the mixed-ligand complexes containing dppz are described in this chapter.

$[\text{Co}(\text{phen})_2(\text{dppz})]^{3+}$  and  $[\text{Ni}(\text{phen})_2(\text{dppz})]^{2+}$  (Fig. 4) have been synthesized and characterized by elemental analysis, FAB-MS,  $^1\text{H}$  NMR, electrochemical and magnetic susceptibility measurements. UV-visible spectra of aqueous buffered solutions containing  $[\text{Co}(\text{phen})_2(\text{dppz})]^{3+}$  and  $[\text{Ni}(\text{phen})_2(\text{dppz})]^{2+}$  show strong hypochromism with red shift in the



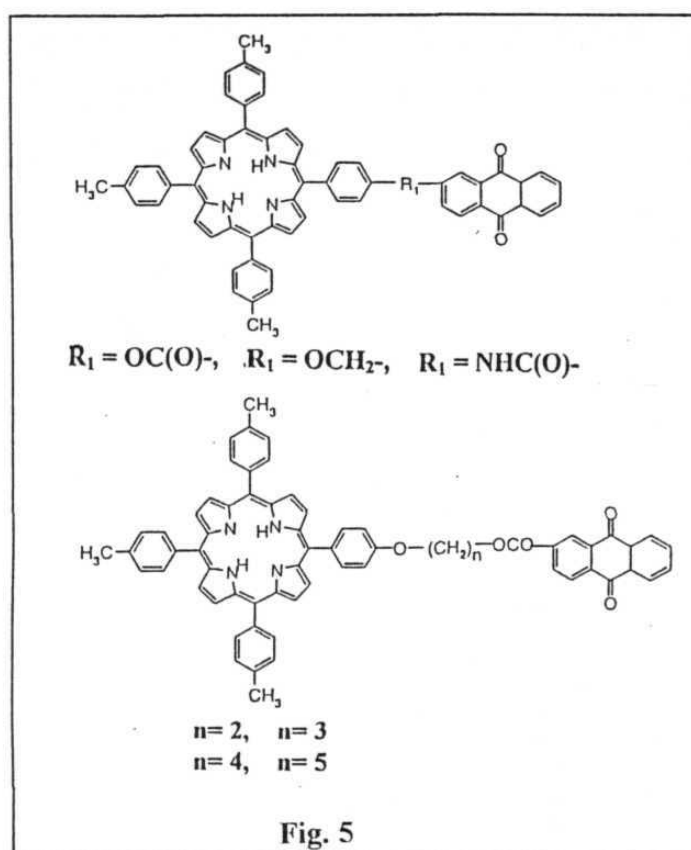
respective peak maximum upon addition of CT DNA. A 6-7° shift in the melting temperature of DNA in the presence of each complex was also noticed. In addition, differential-pulse voltammetric experiments carried out for  $[\text{Co}(\text{phen})_2(\text{dppz})]^{3+}$  (0.1 mM) both in the presence and absence of CT DNA have revealed a decrease in the peak-current due to  $\text{Co}^{\text{III}}/\text{Co}^{\text{II}}$  redox couple in the presence of 10 - 30 fold molar excess of DNA. All these results are reminiscent of those reported for DNA interactions of several tris-chelated, mixed-ligand complexes containing phen and/or dppz including  $[\text{Ru}(\text{phen})_2(\text{dppz})]^{2+}$  and suggest an intercalative mode of binding by both

$[\text{Co}(\text{phen})_2(\text{dppz})]^{3+}$  and  $[\text{Ni}(\text{phen})_2(\text{dppz})]^{2+}$  with the duplex. The intrinsic binding constant,  $K_b$ , as obtained by the absorption titration method is  $(9 \pm 2) \times 10^5 \text{ M}^{-1}$  for both the complexes. On the other hand, only  $[\text{Co}(\text{phen})_2(\text{dppz})]^{3+}$  was found to be effective in sensitizing the single strand cleavage of pBR 322 DNA with the nickel(II) analogue being ineffective under the similar set of experimental conditions. While control experiments in the absence of light show no discernible nicking of the plasmid, excitation of the cobalt(III) complex at  $350 \pm 5 \text{ nm}$  was seen to affect an efficient DNA photocleavage. An attempt to identify the species responsible for the DNA cleavage using various 'inhibitors' in the irradiation/gel electrophoresis experiments and also ESR experiments carried out in conjunction with spin trapping agents has indicated that  $\cdot\text{OH}$  may be involved in the DNA photodamage. (*Inorg. Chem.* **1996**, 35, 4267-4270)

## Chapter 6. Photonuclease Activity of Porphyrin-Anthraquinone Diads and Diazoarene Chromophores

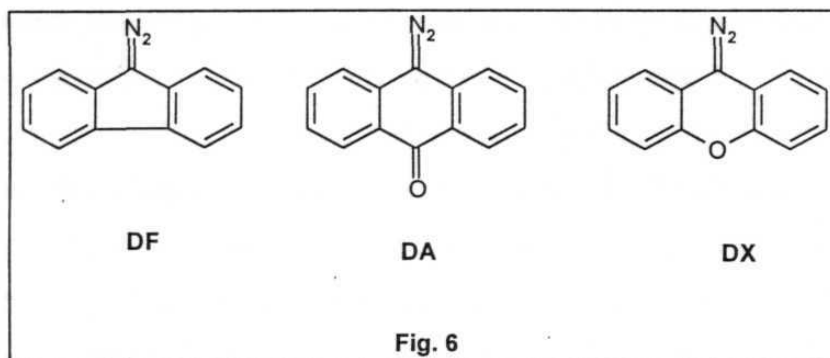
This chapter deals with (i) photocleavage of DNA by porphyrin-anthraquinone hybrids and (ii) carbene mediated DNA photodamage by diazoarene compounds.

Spectral, photophysical and DNA photocleavage studies of a series of photosensitizers in which a tetraaryl porphyrin has been linked to an anthraquinone subunit *via* various spacers (see Fig. 5) are described first. The UV-visible and the redox potential data of these new porphyrin-anthraquinone diads were found to be in the same range as those of the corresponding reference compounds (i. e. meso-5,10,15,20-



tetratolylporphyrin or anthraquinone/substituted anthraquinone). This indicates that there exists minimal ground state interaction between the porphyrin and anthraquinone subunits. However, their fluorescence ( $\Phi_f$ ) and singlet oxygen ( $\Phi(^1O_2)$ ) quantum yields were seen to be drastically reduced in comparison with the corresponding values for the control porphyrin. These photophysical data have been interpreted in terms of a intramolecular photoinduced electron transfer reaction from the porphyrin singlet state to the appended quinone, as is true for the covalently-linked, porphyrin-anthraquinone systems reported earlier. The photonuclease activity of these hybrid sensitizers has been studied by irradiating the supercoiled plasmid pBR 322 DNA samples at 350 (anthraquinone absorption) and 550 nm (porphyrin absorption) light and monitoring the photodamage by the gel electrophoresis method. The photonuclease activity was found to be more effective when the samples were irradiated at 350 nm than at 550 nm indicating the superior photonicking ability of the anthraquinone chromophore. These results have been rationalized in terms of an overall scheme involving several reactive species including anthraquinone triplet and anion radical, porphyrin triplet, singlet oxygen etc. (*Tetrahedron Lett.* **1997**, 38, 7125-7128).

Results of DNA-binding and photocleavage studies carried out with three diazoarene compounds (9-diazofluorene (**DF**), 9-diazoanthrone (**DA**) and 9-dizoxanthene (**DX**), Fig. 6)) are described next. Absorption titration experiments have revealed that all the three diazoarene species bind to CT DNA with comparable binding constants ( $1-3 \times 10^4 \text{ M}^{-1}$ ). Irradiation of samples containing each of these diazoarenes and pBR 322 DNA resulted in



DNA photodamage as monitored by agarose gel electrophoresis. Under similar experimental conditions, the DNA-nicking efficiency follows the order: **DX** > **DA** > **DF**. 'Inhibitor' studies have suggested that the DNA photodamage has been brought about by a carbene-mediated pathway (*Bioorg. & Med. Chem. Lett.* 1997, **7**, 2141-2144).

## Chapter 7. Conclusions

A summary of the investigations is presented in this chapter.

## CHAPTER 1

### *Introduction*

Considerable attention is currently being focused on the design of small molecules that can bind and cleave DNA. These molecules, commonly referred to as artificial nucleases, have numerous biochemical and biomedical applications. While most of the hitherto reported DNA-cleaving agents have been activated thermally, in recent years, there is an increasing emphasis on photoactivated cleavage agents, because this methodology possesses significant practical advantages. In particular, photonucleases can be triggered by exposure to light; light is an attractive 'co-factor' since it is easy to manipulate. This study deals with the design, DNA-binding and DNA-cleavage of new, rationally-designed photonucleases based, mainly, on metallo-polypyridyl complexes. It also deals with the DNA photocleavage by porphyrin and diazo-arene chromophores. Interest in the DNA-binding and photocleavage chemistry of these chromophores is related to the use of metallo-intercalators as structural/spectroscopic probes for DNA and that of porphyrins as photosensitizers in the photodynamic therapy (PDT) of malignant tumors.

DNA is a polyelectrolyte composed of monomers of deoxyribonucleotide (mononucleotides) that are covalently attached to each other (Fig. 1.1). It consists of a  $\beta$ -D-2'-deoxyribose sugar bound to a negatively charged phosphate *via* the C<sub>5</sub>' and C<sub>3</sub>' hydroxyl and to one of the four possible bases *via* the C<sub>1</sub>' hydroxyl (glycosidic bonds). The four bases are:

adenine (A), guanine (G) (both purine bases), cytosine (C) and thymine (T) (both pyrimidine bases). The purines are linked to the sugar via their  $N_9$  and

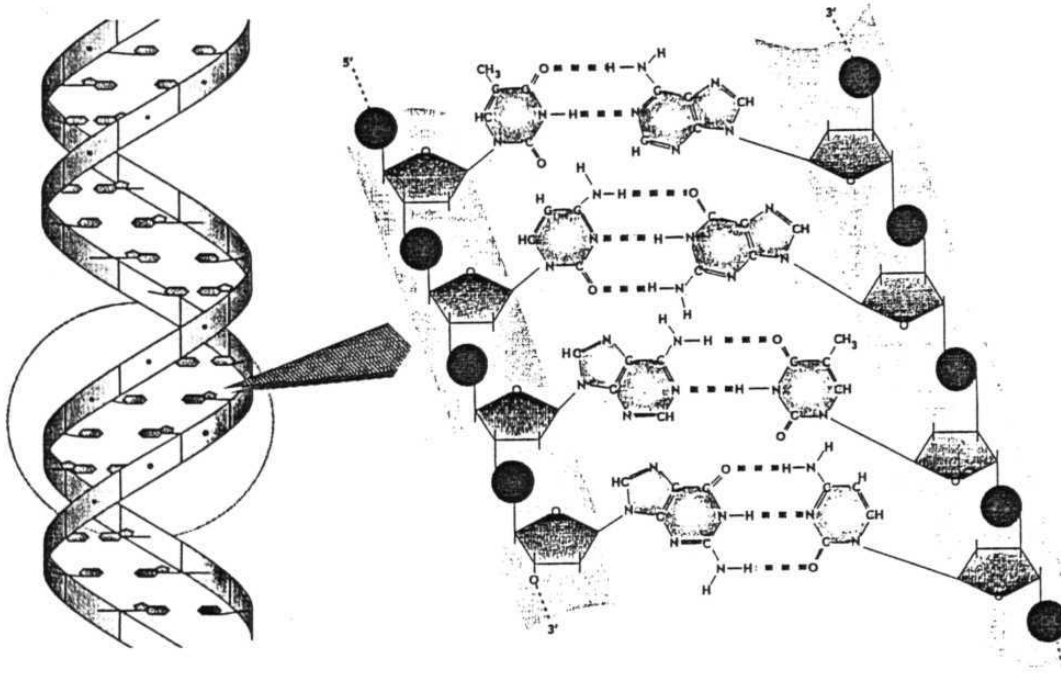


**Fig. 1.1.** Representation of the structure of B-DNA

the pyrimidines via the  $N_1$ . The  $C_3'$  hydroxyl of one nucleotidic unit is linked to the  $C_5'$  phosphate of the adjacent nucleotide (phosphodiester bond). The direction of the polynucleotide is defined as running from the 5' to the 3' sugar carbons along the phosphodiester bond.

Watson and Crick showed in 1953, using X-ray diffraction data of hydrated DNA fibres<sup>1</sup>, that B-DNA, the most commonly encountered form, corresponds to a right-handed double-stranded helix. Two polynucleotide strands are bound together by H-bonds formed between the complementary

bases of each strand. The double strands are coiled around a common axis to form a right handed double helix. The two specific, complementary, hydrogen bonded, base-pairs are: adenine-thymine (A-T) and guanine-cytosine (G-C). These base-pairs are roughly planar, and stacked one above the other inside the helix, perpendicular to the helical axis. Successive base-pairs are separated by  $3.4 \text{ \AA}$  and rotate an average of  $36^\circ$  around the helical axis, so that the structure repeats itself after ten residues on each chain. The sugars linked *via* the  $C_1'$  carbon to the two complementary bases are not disposed symmetrically around the helical axis. This asymmetry induces the formation of two grooves of different sizes with almost the same depth but different widths (of  $11.7$  and  $5.7 \text{ \AA}$ ); they are called major and minor grooves, respectively (Fig. 1.2).

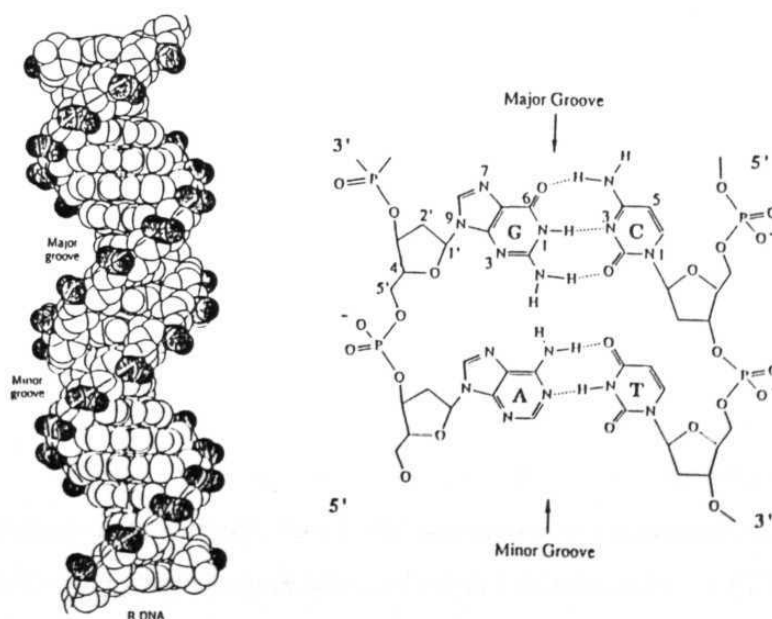
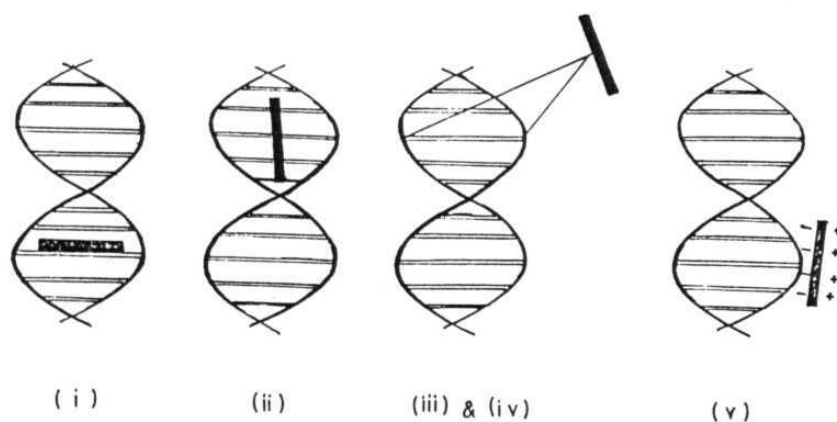


Fig. 1.2

### 1.1 Modes of drug-DNA interactions

A great variety of ligands (drugs) are known to bind DNA. The modes of interaction of these DNA-binding agents can be classified as follows (Fig. 1.3)

- ( i ) Intercalative interaction
- ( ii ) Non-intercalative groove binding
- ( iii ) Covalent interaction
- ( iv ) Interaction through coordination
- ( v ) Electrostatic interaction



**Fig. 1.3.** Schematic representation of various types interaction of drugs with DNA: ( i ) Intercalative interaction , (ii) Non-intercalative groove binding, ( iii ) Covalent interaction, ( iv ) Interaction through coordination and ( v ) Electrostatic interaction

If the ligand has an aromatic portion (normally corresponding at least to three fused six-membered rings), it can position itself between the base pairs, in a sandwich-like complex. This phenomenon, called intercalation<sup>2,3</sup>, was first described by Lerman<sup>4</sup> to explain the binding of aminoacridines to DNA. Intercalation increases the separation of adjacent base pairs and the resulting helix distortions are compensated by the adjustments in the sugar phosphate backbone, generally by an unwinding of the duplex. Association constants for intercalation are usually of the order of  $10^5$  to  $10^6 \text{ M}^{-1}$ .<sup>2</sup>

Surface binding takes place in minor or major groove, although minor groove binding is more common for small molecules.<sup>5,6</sup> The electrostatic potential, the pattern of hydrogen accepting/donating groups and the narrowness of the minor groove are three characteristic factors which are different for GC and AT base pairs, and are responsible for differential groove binding by various drugs. The presence, in the minor groove, of the N-2 amine group on guanine (in GC base pairs) is also an important factor in orienting the site of binding.

Covalent interaction occurs with the formation of covalent bond between the nitrogen atom/s in the bases of DNA and the drug.<sup>7,8</sup> Similarly, coordinative interaction occurs between the base nitrogens and the metal ion present on the drug.<sup>9</sup>

The external binding mode is due, mostly, to the electrostatic interaction of cations with the negatively charged phosphate backbone present at the periphery of the double helix.<sup>10</sup>

Intercalation is generally brought by the  $\pi$ - $\pi$  interaction between the molecule and the aromatic heterocyclic bases of DNA. Ethidium bromide

(Fig. 1.4) is the classical example for DNA intercalator.<sup>3</sup> Other examples for DNA intercalating agents include daunomycin, adriamycin etc.<sup>11</sup>

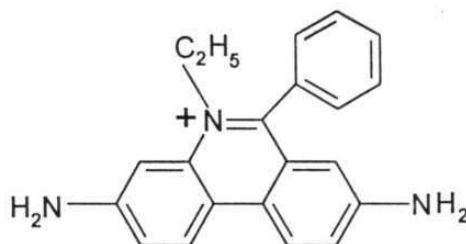


**Fig. 1.4**

Netropsin (Fig. 1.5) is a well known example which binds in the minor groove of DNA.<sup>5</sup> Distamycin A is another familiar example of a groove binding agent.

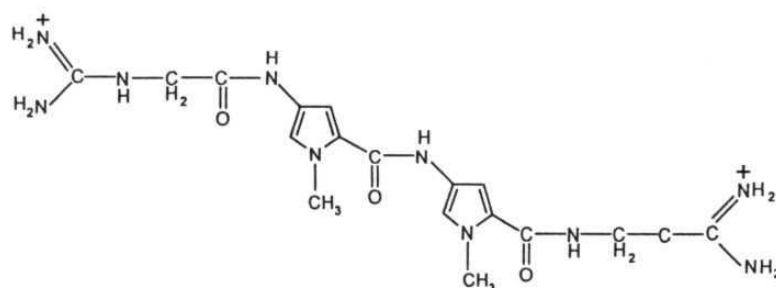


**Fig. 1.5**

An example for the major groove binding agent is  $\text{Ru}(\text{TMP})_3$  (TMP = 3,4,7,8-tetramehtyl 1,10-phenanthroline).<sup>6</sup> Drugs which interact through covalent bond formation are less common. Chlorambucil is a bi-functional alkylating

agent of DNA<sup>7</sup> and pyrrolo-(1,4)-benzodiazepines interacts with DNA *via* the covalent bond formation.<sup>8</sup> One among the early examples of drugs which coordinatively interact with DNA is that of the now well-known anticancer agent  $\text{cis-}[\text{Pt}(\text{NH}_3)_2\text{Cl}_2]^{2+}$  (cis-platin, Fig. 1.6(a)).<sup>9</sup> At a molecular level, the inhibition of cell replication is brought out by the coordination of DNA on N<sub>7</sub> and O<sub>6</sub> sites of guanine (Fig. 1.6 (b)) by means of the two labile chlorides of the molecule. The distance between the two chloride atoms (3.4 Å) is the key factor in the coordination of this drug with DNA. Recently, many more platinum complexes have been reported for their coordinative interaction with DNA.<sup>12</sup>

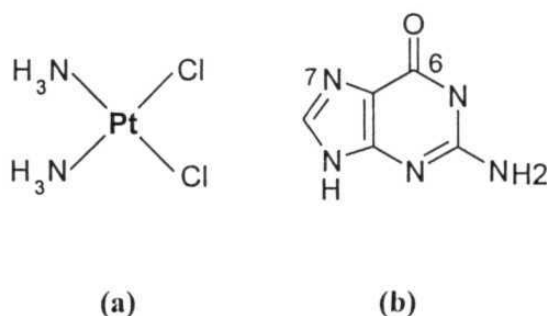


**Fig. 1.6**

Several biochemical, spectroscopic and physical techniques are being used to monitor the DNA-drug interaction.<sup>13</sup> Those relevant to the present study are briefly discussed here.

Absorption and luminescence spectroscopic methods are well exploited for this purpose. Hypochromicity in absorption, appearance of isosbestic point/s, red-shifts in the absorption maxima and luminescence

enhancement for the drug in the presence of DNA are all special characteristic features of interaction. The different modes of interaction of the  $\Delta$  and  $\Lambda$  isomers of a given metal complex with DNA can be studied not only by the above techniques but also by the circular dichroism spectroscopy. Study of emission life-times of the drug in the presence of DNA and in its absence has the potential to provide clearer details of binding. An increase in emission life-time of the drug is generally observed in the bound state. On the other hand, better understanding of the mode of binding, viz: intercalation/surface binding, can be achieved by monitoring the life-time quenching in the presence of various quenchers.

The physical properties of DNA considerably change when it is bound with the drug molecule. For example, intercalation of the drug between the adjacent base pairs leads to an increase in the viscosity of DNA as a consequence of an increase in the contour length of DNA. Binding mode of the drug can be studied by measuring the viscosity of DNA in the presence of drug.

Double-stranded DNA melts at a specific temperature and becomes single strand; this melting can be monitored by the change in absorbance at 260 nm. Intercalation of the drug between the adjacent base pairs stabilizes the DNA and, an increase in melting temperature of DNA would be observed.

Electrochemistry is a powerful technique for the study of drug-DNA interactions but, it has rarely been used for this purpose. Results of cyclic/differential-pulse voltammetric experiments (e.g. change in the current and/or shift in the redox potential of the drug in the presence of DNA) can be

utilized to estimate the affinity constant for binding and the number of drug molecules bound per nucleotide.

In the Watson-Crick structure of DNA, the bases are in close van der Waal's contact. In order to accommodate the drug between the bases during the intercalation process, an untwisting in the double helix occurs to provide space of suitable depth between the layers. Topoisomerase assay helps to estimate this unwinding angle.

Equilibrium dialysis can also be used for the estimation of binding affinity of the drug with DNA.

NMR spectroscopy can be conveniently employed to study the structure and dynamics of DNA-drug complex and also to discern the binding modes of drugs with oligonucleotides. ESR spectroscopy can be used to analyze reactive species responsible for DNA damage generated from the drug.

In the present study, absorption, luminescence, thermal denaturation, topoisomerase assay, viscometry, ESR and electrochemical techniques have been employed to monitor the drug-DNA interactions.

## **1.2 DNA-binding by metal complexes**

Studies on DNA-drug interaction are important for several reasons. For example, design of various therapeutic drugs including antitumour agents can be achieved by a better understanding of this interaction. DNA intercalators, such as adriamycin and daunomycin and also complexes such as cis-platin are strongly mutagenic in nature which stop the replication and transcription of the DNA resulting in promising chemotherapeutic activity.<sup>14</sup>

---

In addition, strongly intercalating metal complexes can act as luminescent markers for DNA.<sup>15</sup> Proflavine and ethidium have been used as probes of nucleic acid structure.<sup>16</sup> Designing drugs for DNA mapping and DNA footprinting is important in the context of understanding the interaction of sequence specific DNA binding proteins/molecules. Redox active metalintercalators have been successfully employed to “foot-print” the DNA binding proteins or non-protein molecules.<sup>17</sup> Recently, DNA photo-cleaving metal complexes are shown to be promising DNA footprinting agents.<sup>18,19</sup> Studies on DNA-ligand interactions are also important in the context of DNA mediated electron transfer reactions.<sup>20</sup> Photodynamic therapy is a new modality for the treatment of cancer<sup>21</sup> and current research in this field is also concerned with the design of molecules which potentially bind DNA and cleave the duplex under illumination with visible light.

Salient features of some of the above applications involving drug-DNA interactions will be discussed next. In doing so, special reference will be made of those applications and examples which bear relevance to the present study.

Double stranded DNA exists in three main forms: right handed A and B forms and the left handed Z form.<sup>22</sup> On the other hand, tris-chelated metal complexes are known to exist in two enantiomeric forms:  $\Delta$  and  $\Lambda$ . Enantioselective binding of DNA by metal complexes has now been well documented in the literature.<sup>23-27,31-33,37,40</sup> A few important systems are discussed below.

In 1982, it was shown that  $[\text{Zn}(\text{phen})_3]^{2+}$  (phen = 1, 10 - phenanthroline) binds to DNA in an enantioselective manner.<sup>23</sup> The  $\Delta$

enantiomer of  $[\text{Zn}(\text{phen})_3]^{2+}$  selectively intercalates into the right handed B form DNA, whereas the  $\Lambda$ - enantiomer does not intercalate. In the same manner  $\Delta$  enantiomer of  $[\text{Ru}(\text{phen})_3]^{2+}$  (Fig. 1.7 (a)) binds to the B form DNA with a higher affinity than the corresponding  $\Lambda$  enantiomer.<sup>24</sup>

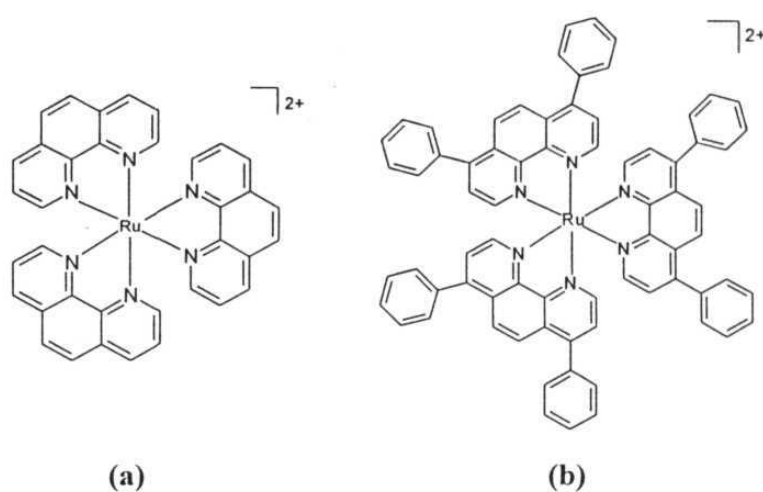


**Fig. 1.7**

In an elegant early study, Kumar et al<sup>25</sup> have shown that  $[\text{Ru}(\text{DIP})_3]^{2+}$  (DIP = 4,7 diphenyl 1,10-phenanthroline) (Fig. 1.7 (b)) also binds to DNA in a manner analogous to  $[\text{Ru}(\text{phen})_3]^{2+}$ . They have demonstrated, in this study, that the emission intensity increases in the case of  $[\text{Ru}(\text{phen})_3]^{2+}$  and  $[\text{Ru}(\text{DIP})_3]^{2+}$  with addition of DNA while, no detectable change in emission intensity could be observed when  $[\text{Ru}(\text{bpy})_3]^{2+}$  (bpy = 2, 2'-bipyridyl) was

employed. It has also been established that  $\Delta$ -[Ru(DIP)<sub>3</sub>]<sup>2+</sup> descriptively binds to the right handed B form DNA *via* intercalation whereas  $\Lambda$ -isomer binds electrostatically.

In an interesting study, Pyle et al<sup>26</sup> have explored the interaction of mixed ligand complexes of ruthenium(II) with B-DNA using a variety of biophysical and spectroscopic methods. The ligands employed here were bpy, phen and phenanthrenequinonediimine (phi). The complex [Ru(bpy)<sub>2</sub>(phi)]<sup>2+</sup> (Fig. 1.8) intercalates into the DNA base pair with the binding constant  $K_b = 48.0 \times 10^3 \text{ M}^{-1}$  and with a site size of 4 base pairs. On the other hand, binding constant for [Ru(phen)<sub>3</sub>]<sup>2+</sup>, under similar experimental conditions, is  $5.5 \times 10^3 \text{ M}^{-1}$ . It was suggested that both [Ru(phen)<sub>3</sub>]<sup>2+</sup> and [Ru(bpy)<sub>2</sub>(phi)]<sup>2+</sup> intercalate into the B-DNA.

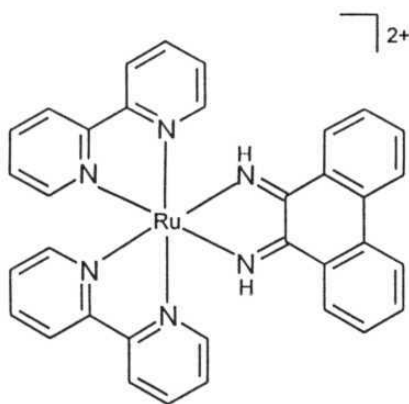


**Fig. 1.8**

The enantiomeric interaction of [Ru(phen)<sub>2</sub>(phi)]<sup>2+</sup> and [Ru(bpy)<sub>2</sub>(phi)]<sup>2+</sup> with DNA and polynucleotides has been investigated using absorption, emission and circular/linear dichroism methods. Both the enantiomers of

these two complexes bind to CT DNA as well as to the synthetic polynucleotides *via* intercalation. Results of circular dichroism studies show that these chiral complexes, upon binding to Z form poly[d(G-m<sup>5</sup>C)], transfer it into the B form of DNA.<sup>27a</sup> On the other hand, a reversible conversion of B form to Z form of CT DNA has been reported to be induced by [Cu(dmp)<sub>2</sub>]<sup>2+</sup> where dmp = 5,6-dimethyl-1,10-phenanthroline.<sup>27b</sup>

With a view to design shape selective DNA binding agents, Mei and Barton<sup>28</sup> have investigated the interaction of [Ru(TMP)<sub>3</sub>]<sup>2+</sup> with DNA (Fig. 1.9). In contrast to phen, the intercalation of TMP is inhibited by the methyl substitution on the periphery. This molecule selectively binds into surface of the A form of DNA; the shape of the molecule is too large to fit into groove of the B form helix.

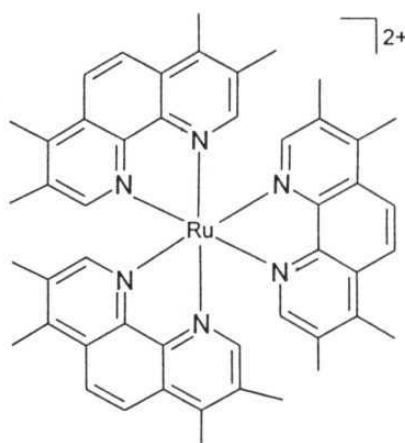


**Fig. 1.9**

Synthesis of a novel mixed-ligand complex  $[\text{Ru}(\text{bpy})_2(\text{dppz})]^{2+}$  (dppz = dipyrido[3,2-a:2',3'-c]phenazine), where dppz is a modified phen derived ligand has been reported, Fig. 1.10.<sup>29</sup>

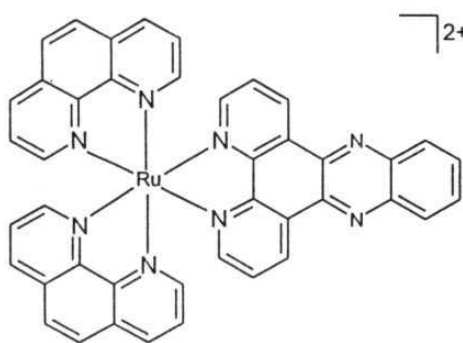


**Fig. 1.10**

Results of spectroscopic and electrochemical investigations have revealed that  $[\text{Ru}(\text{bpy})_2(\text{dppz})]^{2+}$  is made up of two electronically independent units: one behaving as a “ $[\text{Ru}(\text{bpy})_2]$ ” like chromophore and the other as an electron accepting unit, phenazine. In contrast to other ruthenium polypyridyl complexes,  $\text{rac-}[\text{Ru}(\text{bpy})_2(\text{dppz})]^{2+}$  binds to both B and Z forms of DNA through intercalation as evidenced by the steady state emission polarization and emission lifetime measurements. In an elegant experiment, Friedman et al<sup>30</sup> have shown that  $[\text{Ru}(\text{bpy})_2(\text{dppz})]^{2+}$  works as a molecular light switch for DNA.  $[\text{Ru}(\text{bpy})_2(\text{dppz})]^{2+}$  is non-luminescent in aqueous buffered solution but, the luminescence increases to  $> 10^4$  times in the presence of CT DNA or Z form of DNA to which the complex binds avidly ( $K_b = > 10^6 \text{ M}^{-1}$ ). Similar

light switch effect was noticed for  $[\text{Ru}(\text{phen})_2(\text{dppz})]^{2+}$  in the presence of DNA. The molecular light switch effect of  $[\text{Ru}(\text{bpy})_2(\text{dppz})]^{2+}$  and  $[\text{Ru}(\text{phen})_2(\text{dppz})]^{2+}$  upon intercalation to DNA has been attributed to the protection of phenazine nitrogen atoms interacting with water whereas, in the free complex, the excited state is quenched by water. The differential interaction of  $\Delta$  and  $\Lambda$ -enantiomers of  $[\text{Ru}(\text{phen})_2(\text{dppz})]^{2+}$  with DNA was also investigated using steady state as well as time resolved luminescence, linear dichroism and  $^1\text{H}$  and  $^{31}\text{P}$  NMR spectroscopies and by the viscosity measurements.<sup>31-33</sup>

In their efforts to develop novel DNA diagnostics, Barton and co-workers<sup>34</sup> have synthesized a series of mixed ligand ruthenium(II) complexes with phen and modified dppz as the ligands. None of the new derivatives showed ability to behave as good molecular light switches in the presence of DNA. All the complexes were found to be luminescent to some degree in aqueous solution in the absence of DNA. However, for a few complexes 20 - 300 times emission enhancement was observed upon binding with DNA.

More recently,  $[\text{Os}(\text{phen})_2(\text{dppz})]^{2+}$  has been reported as the first osmium containing DNA light switch.<sup>35</sup> No emission was reported upon exciting the complex at 480 nm in aqueous buffered solutions, but upon addition of DNA, a significant emission was observed at 738 nm. However, the emission enhancement was not as dramatic as that reported previously for the analogous ruthenium(II) complex. The very short lifetime of the osmium(II) complex in the presence of DNA, on the other hand, can serve in probing of water accessibility in picoseconds with a red wavelength emission.

In the mixed ligand complex  $[\text{Ru}(\text{phen})_2(\text{phehat})]^{2+}$  (Fig. 1.11, phehat = 1,10-phenanthroline[5,6-b]1,4,5,8,9,12-hexaazatriphenylene), planar aromatic ligand phehat intercalates ( $K_b = 2.5 \times 10^6 \text{ M}^{-1}$ ) into the adjacent base pairs of DNA.<sup>36</sup> This molecule is completely non-luminescent in water but shows a moderate light switch effect upon binding to DNA.

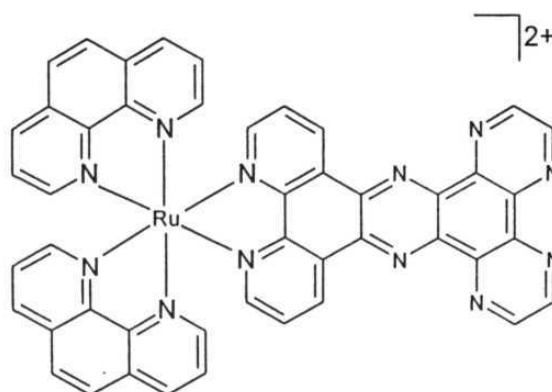
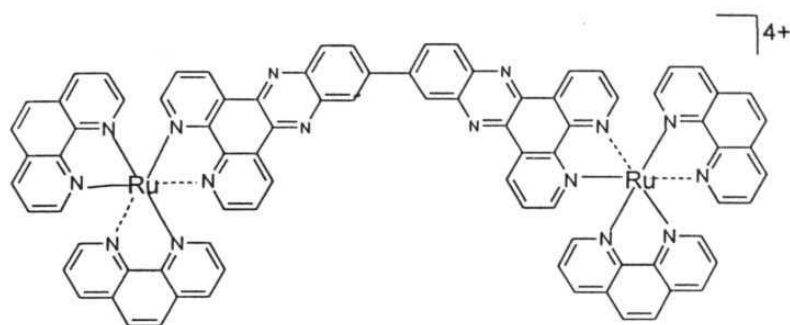
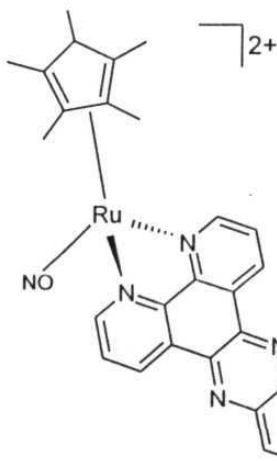


Fig. 1.11

Many interesting new type of ruthenium(II) complexes have been reported recently for probing the intricacies involved in DNA binding by metal complexes and also as spectroscopic probes for DNA. For example, Lincoln and Norden<sup>37</sup> have synthesized a dinuclear ruthenium(II) complex by connecting two dppz ligands together, (Fig. 1.12). This new complex is non-luminescent both in aqueous solution and in the presence of DNA, but it effectively quenches the luminescence of DNA-bound  $\Delta$ - $[\text{Ru}(\text{phen})_2(\text{dppz})]^{2+}$  by the displacement of the latter monomeric complex from the DNA groove. Both the  $\Delta\Delta$  and  $\Lambda\Lambda$  enantiomers of this new complex bind DNA with



A water soluble organometallic ruthenium(II)-dppz complex  $[\eta\text{-(C}_3\text{Me}_5\text{)}\text{Ru(NO)(dppz)}][\text{OTf}]_2$  (Fig. 1.13) has been reported recently. This molecule strongly binds to pLCS 972 DNA with a binding constant greater than  $10^6 \text{ M}^{-1}$ .<sup>38</sup>



**Fig. 1.13**

$[\text{Ru}(\text{bpy})_2(\text{ppz})]^{2+}$  (ppz = 4'7'-phenanthroline-5',6':2:3-pyrazine),  $[\text{Ru}(\text{bpy})_2(\text{dpp})]^{2+}$  (dpp = 2,3-di-2-pyridylpyrazine),  $[\text{Ru}(\text{bpy})_2(\text{qpy})]^{2+}$  (qpy = quaterpyridyl),  $[\text{Ru}(\text{bpy})_2(\text{Meppz}^+)]^{2+}$  and  $[\text{Ru}(\text{bpy})_2(\text{Me}_2\text{qpy}^{2+})]^{2+}$

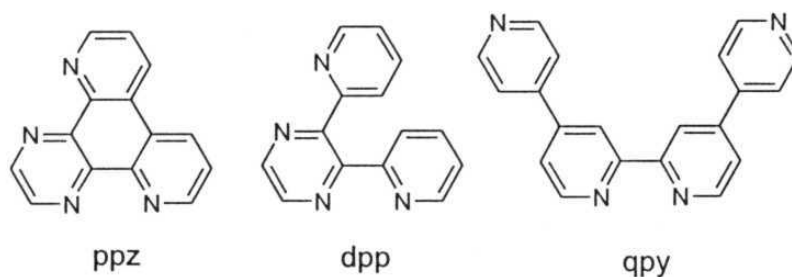


**Fig. 1.14**

(see Fig. 1.14 for structures of ppz, dpp and qpy) all bind to CT DNA with binding constants close to that of  $[\text{Ru}(\text{phen})_3]^{2+}$ .<sup>39</sup> Absorption and luminescence spectra of  $[\text{Ru}(\text{bpy})_2(\text{dpp})]^{2+}$  are not affected by the addition of DNA; binding constant could not be estimated for this complex.  $[\text{Ru}(\text{bpy})_2(\text{qpy})]^{2+}$  showed a hypochromicity in the MLCT band whereas, hyperchromicity was observed for  $[\text{Ru}(\text{bpy})_2(\text{Me}_2\text{qpy}^{2+})]^{4+}$  upon addition of DNA. This observation has been interpreted in terms of a unique mode of binding for  $[\text{Ru}(\text{bpy})_2(\text{Me}_2\text{qpy}^{2+})]^{4+}$ , involving electrostatic interaction of the positive charge on the 4' methyl group with a pair of DNA phosphate groove on either chain of the double-strand. Further studies using absorption, fluorescence, resonance Raman and emission polarization methods revealed that both  $\Delta$  and  $\Lambda$  enantiomers of  $[\text{Ru}(\text{bpy})_2(\text{ppz})]^{2+}$  bind into the major groove of B-DNA with partial intercalation of the ppz ligand.<sup>40</sup>

Lecomte et al<sup>41</sup> have reported a new complex shown in Fig. 1.15 that has two binding moieties which can interact with DNA *via* two different binding modes.

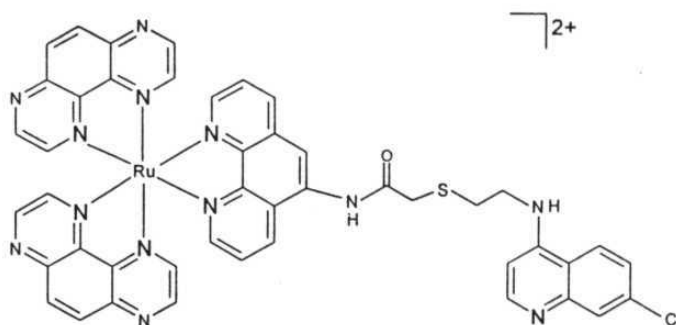


**Fig. 1.15**

A number of studies dealing with interaction of DNA with metal complexes having metal other than ruthenium have also been carried out.  $[\text{Cu}(\text{phen})_2]^+$  is a classic example.<sup>42</sup> This complex, in the presence of molecular oxygen and a reducing agent, cleaves DNA and it is used as an efficient foot printing agent. This particular aspect will be discussed in more detail in a later section of this chapter. In order to study the effect of the substitution on the phen ligand,  $[\text{Cu}(\text{bcp})_2]^+$  (bcp = 2,9-dimethyl-4,7-diphenyl-1,10-phenanthroline) was investigated.<sup>43</sup>  $[\text{Cu}(\text{bcp})_2]^+$  binds DNA and also shows a measurable luminescence signal upon addition of DNA to buffered aqueous solutions containing it. Interestingly, this complex binds to DNA in an aggregated manner at low  $[\text{DNA nucleotide phosphate}]/[\text{Cu}]$  ratio and as a monomeric complex at a high  $[\text{DNA nucleotide phosphate}]/[\text{Cu}]$  ratio. The complex was shown to bind DNA *via* major groove.  $[\text{Cu}(\text{dmp})_2]^+$

(dmp = 2,9-dimethyl-1,10-phenanthroline) has also been reported to show emission enhancement upon addition of DNA.<sup>43</sup>

A number of polypyridyl complexes containing metal ions such as rhodium, cobalt, nickel etc. have also been reported to bind DNA.<sup>55-59,62-64</sup> However, their utility is mainly concerned with the DNA cleavage effected upon chemical, electrochemical or photochemical initiation. These aspects will be discussed in the next Section.

### 1.3 DNA Cleavage

In recent years, a number of reports have appeared on chemical, photochemical and electrocatalytic DNA cleavage by metal complexes. Mainly, cobalt, ruthenium or rhodium complex mediated DNA cleavage has been well documented. In a majority of the cases, conversion of the supercoiled Form I to Form II (relaxed circular) and/or to Form III (relaxed linear) DNA (Fig. 1.16) has been reported while in a few cases, more detailed product analysis has been carried out.

#### 1.3.1 DNA photocleavage by ruthenium polypyridyl complexes

In an early report, Kelly et al<sup>44</sup> have shown that irradiation of  $[\text{Ru}(\text{phen})_3]^{2+}$  and  $[\text{Ru}(\text{bpy})_3]^{2+}$  in the presence of pBR 322 DNA for a short time (< 5min) produces open circular Form II DNA and, for longer time of exposure to light, the complex cleaves DNA into the linear form. The production of singlet molecular oxygen ( $^1\text{O}_2$ ) has been proposed to be the main reactive species in the observed DNA cleavage. Cleavage of pBR 322 DNA by  $[\text{Ru}(\text{bpy})_3]^{2+}$  in the presence of  $\text{K}_2\text{S}_2\text{O}_8$  under irradiation (400-500

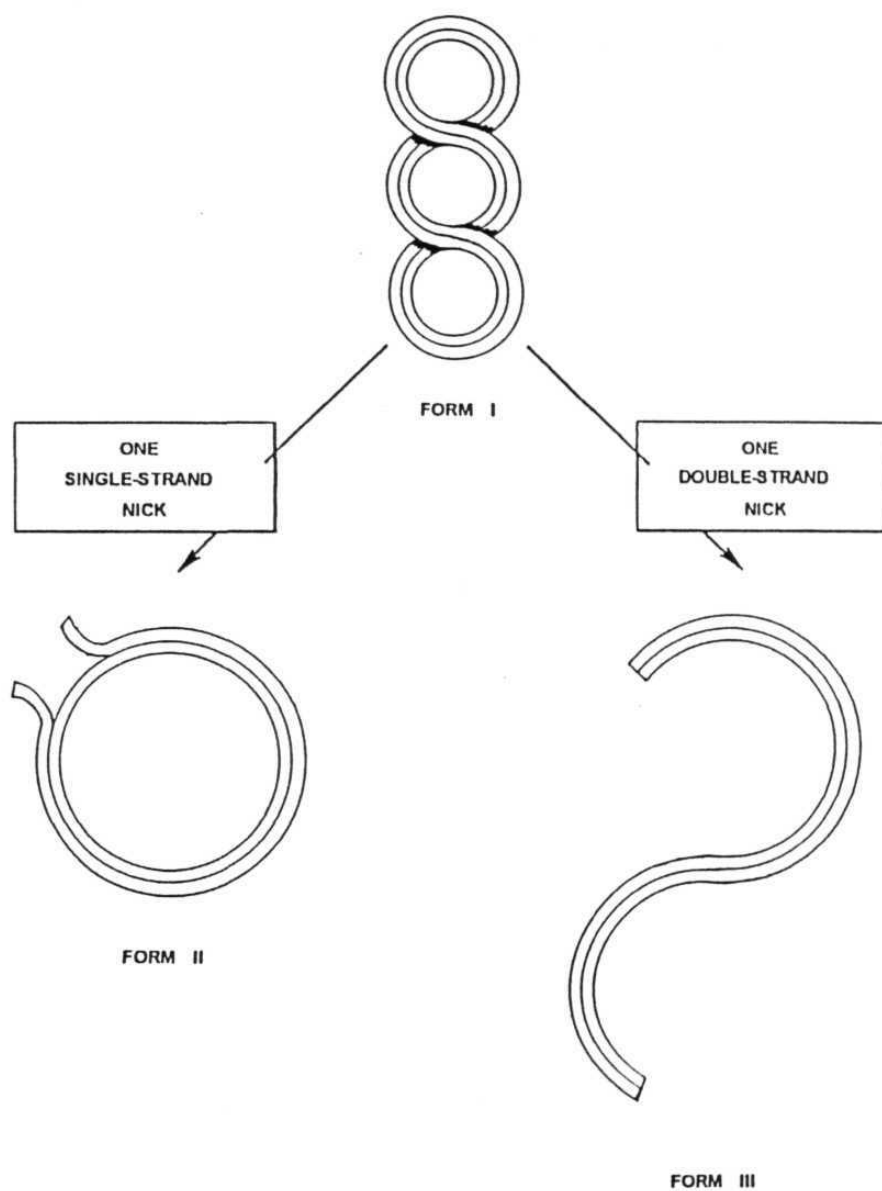


**Fig. 1.16.** Pictorial representation of the three forms of DNA: Form **I** (super coiled), Form **II** (open circular) and Form **III** (linear).

nm) has been reported to result in the generation of linear Form III DNA.<sup>45</sup> The damage on the DNA was shown to be mainly initiated by  $\text{SO}_4^{\bullet-}$ . Presence of  $\text{NaClO}_4$  or  $\text{MgCl}_2$  has been reported to reduce the nicking efficiency.

Basile and Barton<sup>46</sup> have further modified  $[\text{Ru}(\text{DIP})_3]^{2+}$  into a DNA cleaving macromolecule,  $[\text{Ru}(\text{DIP})_2(\text{macro})]^{2+}$ . This novel complex contains two arm like polyamine segments as shown in Fig. 1.17. In the presence of  $\text{Cu}^{2+}$ , this complex was shown to cleave the supercoiled DNA into the open circular and linear forms and the process was reported to be retarded in the presence of added  $\text{Zn}^{2+}$ ,  $\text{Cd}^{2+}$  or  $\text{Pb}^{2+}$ .<sup>47</sup> The DNA cleavage has been proposed to be mainly due to the hydrolysis of the phosphodiester linkages.

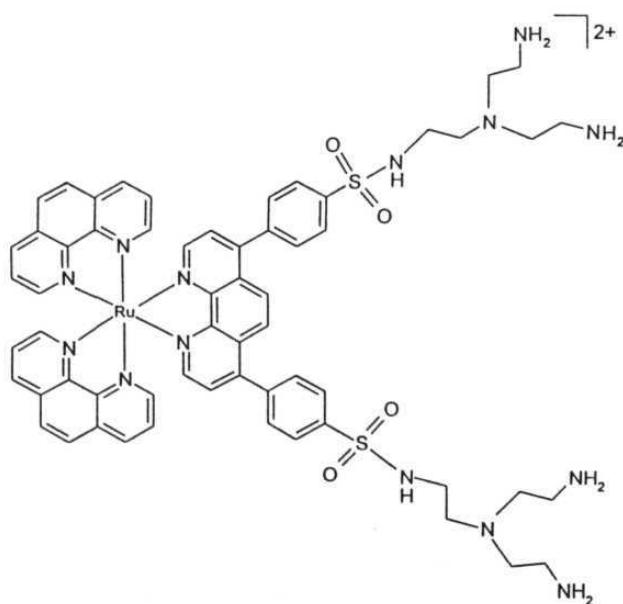
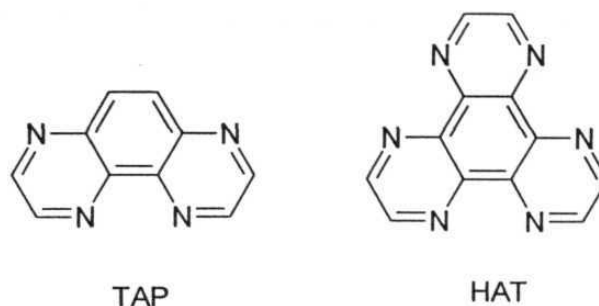


Fig. 1.17

**Fig. 1.18**

$[\text{Ru}(\text{TAP})_3]^{2+}$  (TAP = 1,4,5,8-tetraazaphenanthrene, Fig. 1.18) cleaves pBR 322 DNA into open circular form under irradiation at 488 nm.<sup>48</sup> Direct interaction of the excited state of  $[\text{Ru}(\text{TAP})_3]^{2+}$  with readily oxidizable guanine at the G-C center has been proposed to be involved in this DNA cleavage. HAT (1,4,5,8,12-hexaazatriphenylene) is a derivative of TAP (Fig. 1.18). Mixed-ligand complexes containing HAT and TAP are also reported to cleave DNA upon irradiation with visible light *via* the guanine oxidation mechanism.<sup>49,50</sup> Curiously,  $[\text{Ru}(\text{TAP})(\text{HAT})_2]^{2+}$  and  $[\text{Ru}(\text{HAT})_3]^{2+}$  photooxidize even adenine base of pdAT. In this regard, it should be noted that in contrast to  $[\text{Ru}(\text{phen})_3]^{2+}$  and  $[\text{Ru}(\text{bpy})_3]^{2+}$ , by and large, the emission of  $[\text{Ru}(\text{TAP})_3]^{2+}$ ,  $[\text{Ru}(\text{TAP})(\text{HAT})_2]^{2+}$  and  $[\text{Ru}(\text{HAT})_3]^{2+}$  were reported to be quenched by the addition of DNA. This quenching has been attributed to an electron transfer from the nucleobase to the highly oxidizing excited ruthenium complex.

Bimetallic complexes containing ruthenium and an other metal ion have also been reported to cleave DNA. For example,  $\Lambda$ - $[\text{Ru}(\text{bpy})_2(\text{ppz})\text{CuL}]^+$  (Fig. 1.19) cleaves pBR 322 DNA in the presence of

hydrogen peroxide and 3-mercaptopropionic acid in a enantiospecific manner.<sup>51</sup>

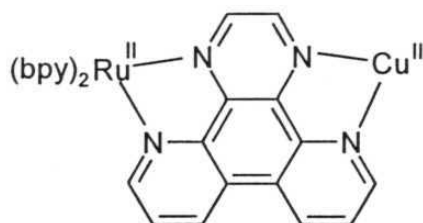


**Fig. 1.19**

Hirai et al<sup>52</sup> have synthesized  $[\text{Ru}(\text{smc})\text{Cl}_2]$  - a new photoactivated covalent binding DNA molecule (Fig. 1.20). This complex has been reported to bind DNA with an enhanced binding affinity in the presence of light than in its absence; a covalent binding of N<sub>7</sub> guanine with ruthenium has been proposed. Cleavage of pBR 322 DNA into the linear form was observed under irradiation in the presence of  $[\text{Ru}(\text{smc})_2\text{Cl}_2]$ .

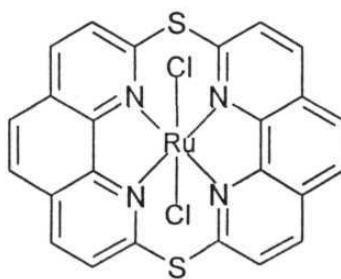


**Fig. 1.20**

Goulle et al<sup>53</sup> have reported a new ruthenium complex containing antileukemic alkaloid 2-bromoleptoclinidinone ligand (bld). The mixed

ligand complex  $[\text{Ru}(\text{bpy})_2(\text{bld})]^{2+}$  (Fig. 1.21) is non-emissive both in the absence and presence of DNA. Agarose gel electrophoresis experiments showed an increased streaking and retardation of DNA mobility in the presence of  $[\text{Ru}(\text{bpy})_2(\text{bld})]^{2+}$  under dark suggesting the binding of the complex with DNA. The complex photocleaves pBR 322 DNA into the open circular form under visible light irradiation.

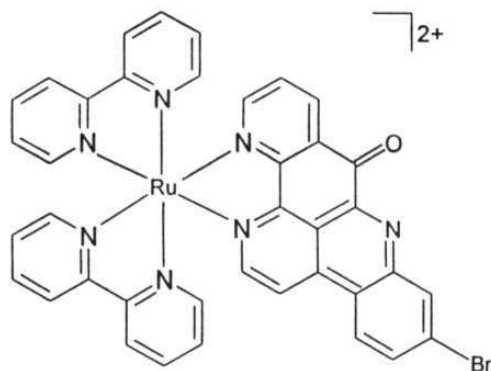


**Fig. 1.21**

### 1.3.2 Photonuclease activity of cobalt and rhodium complexes

The low spin  $d^6$  transition metals cobalt(III) and rhodium(III) are known to undergo photochemical reaction leading to ligand replacement or photoreduction of the metal.<sup>54</sup> Photoreduction of the metal ion has been implicated as an important step in the DNA cleavage exhibited by these complexes.

The vast majority of studies concerning the DNA cleavage by cobalt complexes have been inspired by the bleomycin chemistry. Bleomycin is an

anti-cancer glycopeptide that binds to specific sequences and cleaves DNA in the presence of molecular oxygen and ferrous ion.<sup>55</sup> On the other hand, metallo-bleomycins such as cobalt(III)-bleomycin efficiently cause single strand breaks in the supercoiled DNA under illumination with 366 nm light. This cleavage process is mainly driven by the photoreduction of cobalt(III) to cobalt(II).<sup>55c, 56</sup> No cleavage was observed with irradiation under visible light but, photosensitization using  $[\text{Ru}(\text{bpy})_3]^{2+}$  to activate Co(III)-bleomycin has been shown to be effective in cleaving DNA.<sup>57</sup>

Barton and Raphael<sup>58</sup> have investigated the photocleavage of supercoiled plasmid DNA with  $[\text{Co}(\text{phen})_3]^{3+}$ . This complex cleaves the col E1 DNA under irradiation at 254 nm with a concomitant photoreduction of cobalt(III). The cleavage was reportedly inhibited in the presence of dithiothreitol.  $[\text{Co}(\text{NH}_3)_6]^{3+}$  was found to cleave DNA more efficiently than  $[\text{Co}(\text{phen})_3]^{3+}$  under 325 nm irradiation.<sup>59</sup> A stereospecific photocleavage was evident when  $\Delta$  and  $\Lambda$  isomer of  $[\text{Co}(\text{DIP})_3]^{3+}$  was irradiated in the presence of DNA.<sup>59b</sup> Whereas the  $\Delta$  isomer cleaves the DNA efficiently, no appreciable cleavage is obtained in the case of  $\Lambda$ - $[\text{Co}(\text{DIP})_3]^{3+}$ .

$[\text{Co}(\text{cyclam})(\text{CH}_3)(\text{H}_2\text{O})]^{3+}$  (cyclam = 1,4,8,11-tetraazacyclotetradecane), upon photolysis, cleaves the supercoiled DNA into the open circular form.<sup>60</sup> The DNA damage has been reported to involve the photo-generated  $\cdot\text{CH}_3$ . Sargeson and co-workers have reported a series of Co(III) cage complexes.<sup>61</sup> A representative example is given in Fig. 1.22. This complex strongly binds to DNA through intercalation and cleaves the pUC 19 DNA under irradiation at 254 nm.

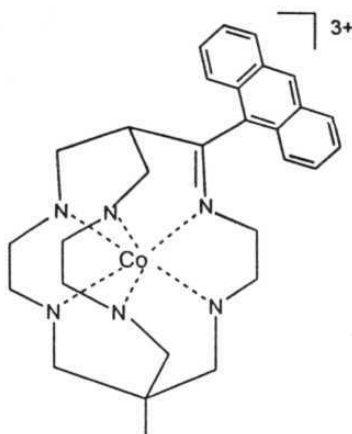


Fig. 1.22

Both  $[\text{Rh}(\text{phen})_2(\text{phi})]^{3+}$  and  $[\text{Rh}(\text{phi})_2(\text{bpy})]^{3+}$  bind avidly to DNA *via* intercalation and cleave DNA upon irradiation by 313 nm light.  $[\text{Rh}(\text{phen})_2(\text{phi})]^{3+}$  selectively binds through the major groove and inserts the phi ligand in between the base pairs.  $[\text{Rh}(\text{phi})_2(\text{bpy})]^{3+}$  binds DNA with a binding constant about  $10^7 \text{ M}^{-1}$ . The former complex has been reported<sup>62</sup> to cleave DNA in a sequence-selective manner whereas, a sequence-neutral cleavage was observed for  $[\text{Rh}(\text{phi})_2(\text{bpy})]^{3+}$ . A recent NMR study has provided some evidence in favor of enantioselective targeting of the 5'-CG-3' site by  $\Delta$ - $[\text{Rh}(\text{phen})_2(\text{phi})]^{3+}$ .<sup>63</sup>

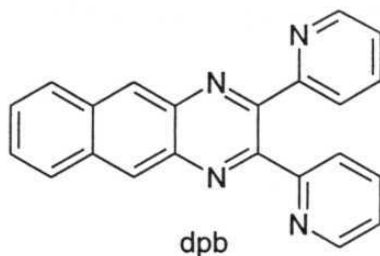
An oxidative DNA photodamage was observed due to the long range electron transfer initiated by irradiation of  $[\text{Rh}(\text{bpy})_2(\text{phi})]^{3+}$  tethered to a nucleic acid oligomer. Under irradiation at 365 nm, the cleavage specifically occurred at 5'-G site of 5'-GG-3' doublet at a distance of 34 Å away from

the intercalating phi. Irradiation at 313 nm resulted in cleavage at the binding site of the intercalator.<sup>20</sup>

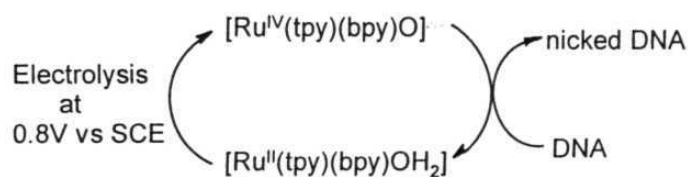
While both the  $\Delta$  and  $\Lambda$  isomers of  $[\text{Rh}(\text{en})_2(\text{phi})]^{3+}$  (en = ethylene diammine) avidly bind to DNA ( $K_b = 10^6 \text{ M}^{-1}$ ), only the  $\Delta$  isomer preferentially binds to GC rich regions of DNA and photocleaves it.<sup>64</sup>

### 1.3.3 Electrocatalytic DNA cleavage

Electrochemical studies are useful complements to spectroscopic methods for the study of DNA-drug interactions. Specifically, these methods are useful in investigations with weakly absorbing molecules and those complexes/drugs whose absorption spectra overlap with the spectrum of DNA. In an elegant study, Bard and co-workers<sup>65,66</sup> have shown the interaction of  $[\text{Co}(\text{phen})_3]^{3+}$  and  $[\text{Fe}(\text{phen})_3]^{2+}$  with DNA using cyclic voltammetric method. The change in the peak current and the shift in the redox potential of the complex in the presence of DNA were shown to be important for the determination of binding constant. The shift in the peak potential in the presence of DNA is due to the fact that one of redox species is bound more strongly than the other. The reduction in the peak current arises from the smaller diffusion coefficient of the bound complex than that of the free complex. Using the same method Carlson et al<sup>67</sup> have determined the binding constant of  $[\text{Ru}(\text{NH}_3)_4]_2(\text{dpp})^{4+}$  (dpp = 2-3-bis(2-bipyridyl)benzo(g)-quinoxaline, Fig. 1.23)

**Fig. 1.23**

Electrochemical DNA cleavage by  $[\text{Ru}^{\text{IV}}(\text{bpy})(\text{tpy})\text{O}]$ , has been reported.<sup>68</sup> The cleavage was actually initiated by the electrolysis of  $[\text{Ru}(\text{bpy})(\text{tpy})\text{OH}_2]^{2+}$  in the presence of DNA and was seen to be efficient at the stoichiometric concentration of the drug and DNA. Both  $[\text{Ru}(\text{phen})(\text{tpy})\text{OH}_2]^{2+}$  and  $[\text{Ru}(\text{tpy})(\text{tmen})\text{OH}_2]^{2+}$  (tmen = N,N,N',N'-tetramethyl ethylenediamine) were also reported to cleave DNA upon electrolysis of these complexes in the presence of DNA.<sup>69</sup>  $[\text{Ru}(\text{bpy})(\text{tpy})\text{OH}_2]^{2+}$  cleaves DNA more efficiently than  $[\text{Ru}(\text{phen})(\text{tpy})\text{OH}_2]^{2+}$  and in both cases, Form I DNA was converted to Form II. The following mechanism has been suggested.

**Fig. 1.24**

Interestingly,  $[\text{Ru}(\text{tpy})(\text{tmen})\text{OH}_2]^{2+}$  cleaves DNA into the linear Form III and, the same result was obtained during the chemical cleavage of DNA by  $[\text{Ru}^{\text{IV}}(\text{tpy})(\text{tmen})\text{O}_2]$ .

With a view to enhance the DNA binding affinity of this class of electrochemically induced DNA cleaving agents, one of the ligands was replaced by the planar intercalating dppz.  $[\text{Ru}(\text{dppz})(\text{tpy})\text{OH}_2]^{2+}$  strongly binds to DNA ( $K_b \geq 10^6 \text{ M}^{-1}$ ).<sup>70</sup> Efficient electrocatalytic cleavage of DNA occurs by  $[\text{Ru}^{\text{IV}}(\text{dppz})(\text{tpy})\text{O}]^{2+}$  upon electrolysis of the complex at 0.8 V.

New complexes containing tailor-made ligands such as tpt (tpt = 2,4,5-tripyridyltriazine) or tmen-AO (in which the well-known intercalator acridine orange has been tethered to tetramethyl ethylenediamine *via* a  $(\text{CH}_2)_n$  linker) also cleave DNA catalytically. Electrolysis of  $[\text{Ru}(\text{tpy})(\eta^2\text{-tpt})\text{OH}_2]^{2+}$  at 0.8 V results in a two electron oxidation to form  $[\text{Ru}^{\text{IV}}(\text{tpy})(\eta^2\text{-tpt})\text{O}]$  and

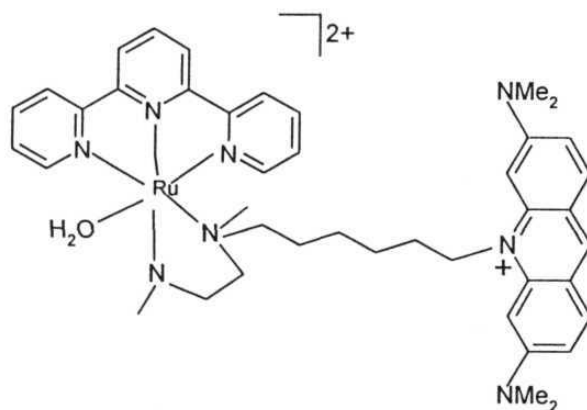
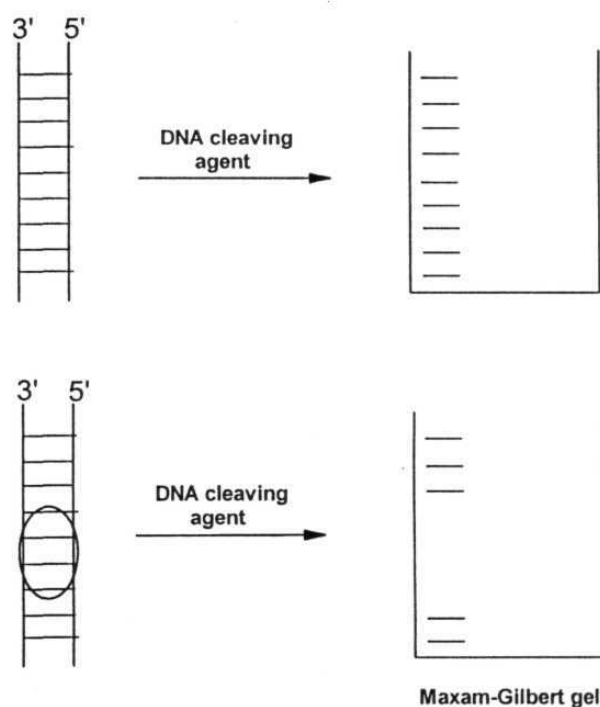


Fig. 1.25

this complex cleaves DNA. On the other hand,  $[\text{Ru}(\text{tpy})(\text{tmen-AO})\text{OH}_2]^{2+}$  (Fig. 1.25) efficiently cleaves the DNA at potentials as low as 0.5 V.<sup>71</sup>

### 1.3.4 DNA footprinting by metal complexes

Footprinting is one of the most powerful techniques in molecular biology for an understanding of molecular recognition and for visualizing the site-specific binding of proteins/smaller molecules to DNA.<sup>72</sup> A schematic illustrating the principles involved in DNA foot printing is shown in Fig. 1.26. Many DNA-cleaving metal complexes are being used as effective footprinting agents.<sup>73</sup> A few well-known systems will be described below.



**Fig. 1.26.** Schematic illustration of DNA footprinting methodology.

○ represents the protein/small molecule

Dervan and co-workers have reported an excellent footprinting reagent MPE-Fe(II) [methidiumpropyl-EDTA Fe(II)] (Fig. 1.27) which cleaves a restriction fragment of DNA in the presence of dithiothreitol.<sup>17,73</sup>

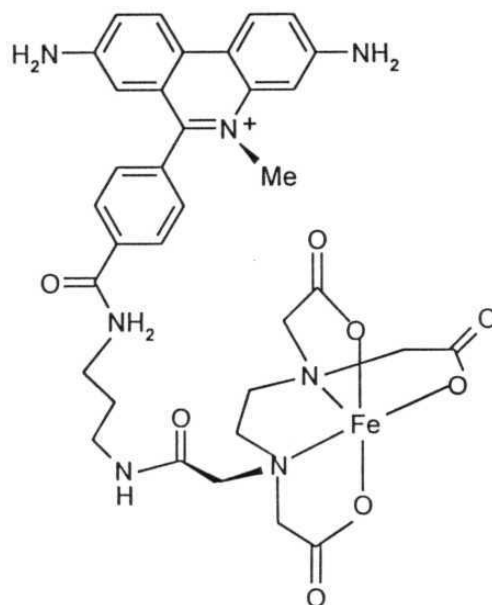


Fig. 1.27

Dervan's group has also come up with an improved artificial endonuclease by tethering a sequence specific DNA binding molecule (distamycin) to EDTA-Fe. Such a tethering resulted in the conversion of the sequence specific DNA binding molecule to a sequence specific DNA cleaving molecule.<sup>74</sup> The cleavage pattern with this endonuclease gives the exact binding locations, site size, and orientation of the sequence specific binding molecule on DNA.<sup>75</sup>

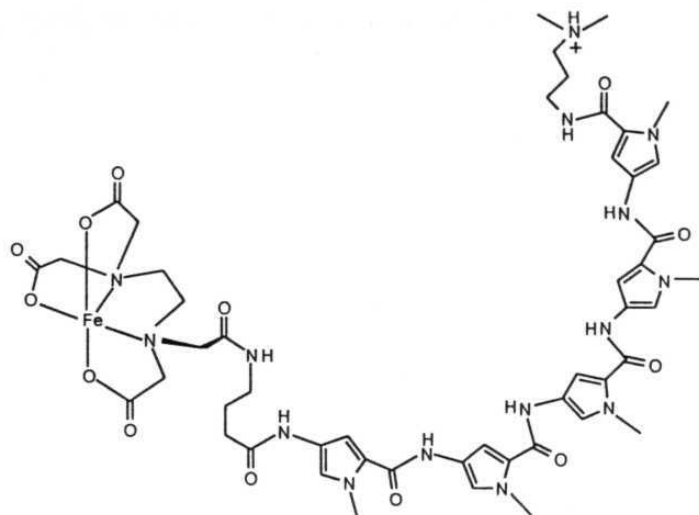
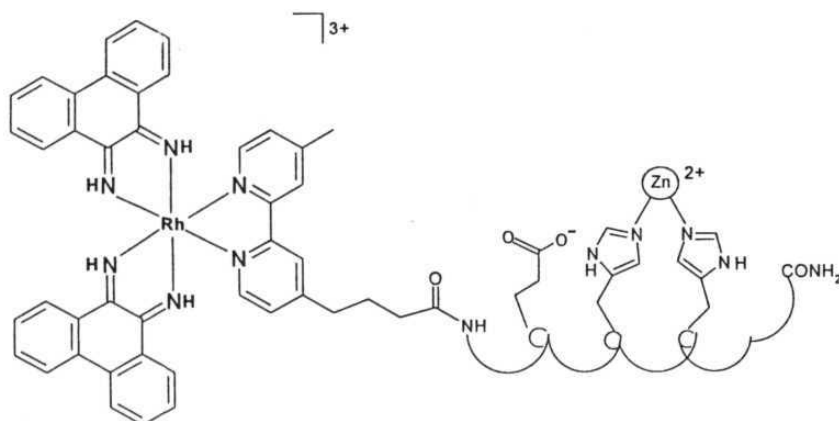


Fig. 1.28

EDTA-Fe(II) was also tethered to tetra, penta, and hexa (N-methylpyrrolicarboxamide) subunits.<sup>75</sup> Fig. 1.28 shows the structure of penta(N-methylpyrrolicarboxamide)-EDTA.Fe(II).

In an elegant study, Fitzsimons and Barton<sup>76</sup> have synthesized a 16-residue peptide tethered with  $[\text{Rh}(\text{phi})_2(\text{bpy})]^{3+}$  Fig 1.29. In the 7 and 11 positions of the tether are attached two histidines for zinc coordination. Cleavage of pBR 322, in the presence of  $[\text{Rh}(\text{phi})_2(\text{bpy})]^{3+}$  at stoichiometric Zn(II) coordination in the histidines, has been reported to produce both the single strand break (Form II) and double nick (Form III). Product analysis, carried out using high resolution electrophoresis techniques for the cleavage of pBR 322 and also for a 17-base-pair oligonucleotide, indicated that this metal-peptide conjugate combines the DNA-binding and reactive moieties for



**Fig. 1.29**

[Cu(phen)<sub>2</sub>]<sup>+</sup> has been shown to cleave DNA in the presence of H<sub>2</sub>O<sub>2</sub> and thiol;<sup>77</sup> this molecule was used to footprint many DNA binding proteins. Cleavage occurs only in A and B forms of DNA whereas, the Z form is completely resistant to cleavage.<sup>42,78</sup>

As delineated previously, combination of a metal complex and light is an attractive reagent for the cleavage of DNA. A few metal complexes have been shown to act as DNA photofootprinting agents.

$[\text{Co}(\text{DIP})_3]^{3+}$  (Fig. 1.30) damages DNA under irradiation and, the cleavage has been reported to involve photoreduction of the bound complex leading to the oxidative single strand nick at the binding site.<sup>18</sup>

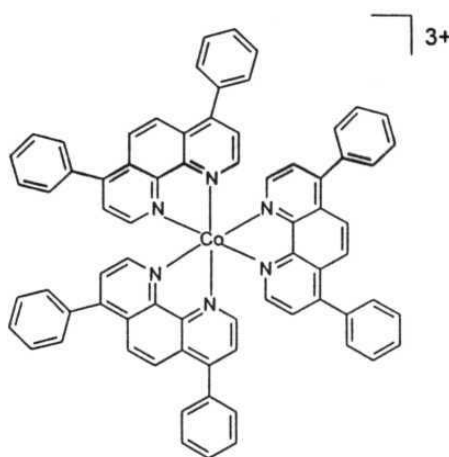


**Fig. 1.30**

$\Delta$ - $[\text{Co}(\text{DIP})_3]^{3+}$  cleaves right handed A and B forms of DNA enantiospecifically. Interestingly,  $\Lambda$ - $[\text{Co}(\text{DIP})_3]^{3+}$  binds to left handed Z form DNA and, upon irradiation at 315 nm effectively cleaves the left handed DNA site inserted in a right handed pBR 322 DNA. No cleavage was reported to have occurred when the Z segment was removed.<sup>79</sup>

Another excellent photofootprinting agent  $[\text{Rh}(\text{phi})_2(\text{bpy})]^{3+}$  the structure of which is shown in Fig. 1.31 has been developed by Uchida et al<sup>80</sup>

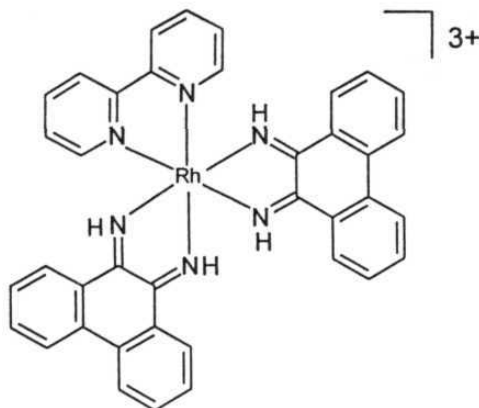


Fig. 1.31

This complex is especially useful for the footprinting of major groove binding proteins. It cleaves DNA in a sequence neutral manner under long-wavelength UV light irradiation and is useful in mapping precisely the binding location and site sizes of naturally occurring antitumour agent distamycin-A or large DNA major groove binding proteins.

Breiner et al<sup>19</sup> have developed an alternative approach to  $[\text{Fe}(\text{EDTA})]^{2+}$ -based foot printing agents. The tetraanionic complex  $[\text{Pt}_2(\text{pop})_4]^{4-}$  ( $\text{pop} = \text{P}_2\text{O}_5\text{H}_2^{2-}$ ) (Fig. 1.32) cleaves DNA in a sequence-neutral manner upon irradiation. The cleavage mechanism involving  $\text{OH}^\bullet$  and  $^1\text{O}_2$  was ruled out and a pathway involving the abstraction of hydrogen atom directly from DNA by the excited  $[\text{Pt}_2(\text{pop})_4]^{4-}$  was proposed. The foot printing of  $\lambda$  repressor protein binding on DNA was mapped using this complex. Footprinting pattern using  $[\text{Pt}_2(\text{pop})_4]^{4-}$  was found to be very similar to the one obtained using  $[\text{Fe}(\text{EDTA})_2]^{2+}$ .

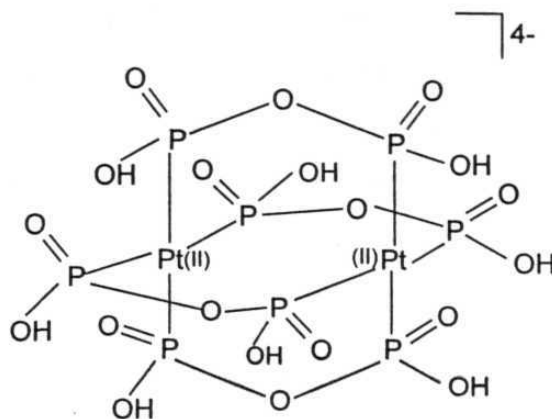


Fig. 1.32

Chapters 3, 4 and 5 of this thesis deal with the design, synthesis, DNA-binding and photocleavage characteristic of ruthenium, cobalt and nickel complexes containing modified phenanthroline ligands. The ligands were designed in such a way that while their architecture promotes DNA intercalation, their electronic structure promotes efficient photocleavage of DNA. Aspects related to the molecular light switching in the presence of DNA and redox switching of luminescence observed by a few of these new complexes will also be discussed in these Chapters.

#### 1.4 DNA photocleavage by porphyrins and diazoarenes

As mentioned earlier, this thesis also describes studies on DNA photocleavage by a class of porphyrin-based diad molecules and diazoarene chromophores. A brief introduction on these aspects is presented below.

The use of visible light as a therapeutic agent in clinical medicine is termed as phototherapy. The use of photoactivated drugs in the treatment of malignant tumors, destruction of arterial plaque, curing of psoriatic lesions, eradication of viral contaminants etc. is known as photodynamic therapy (PDT).<sup>21,81</sup> The technique of PDT in cancer therapy involves the intravenous injection of a photosensitizer (P), which over a period of time, is selectively retained by the neoplastic tissue. Subsequent irradiation with visible light using a laser generates  $^1\text{O}_2$  (or other cytotoxic species) within the tumour, ultimately leading to tumour regression and cell necrosis, Fig. 1.33.

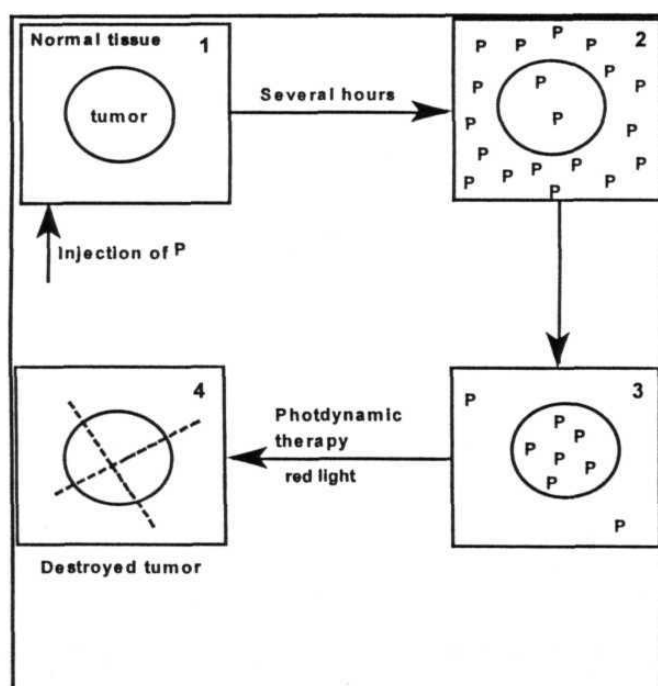


Fig. 1.33

An ideal photosensitizer for PDT should fulfill the following minimum criteria.

1. It should be single, nontoxic, stable compound of known chemical structure, which is retained with a high degree of selectivity in malignant tumors compared with the normal tissue.
2. It should have a strong absorption peak in the part of the spectrum where light penetrates the living tissue best and where the photon energy is still high enough to produce singlet oxygen (i.e. 600 to 900 nm).

Porphyrins possess most qualities that are expected in an ideal PDT photosensitizer. Indeed, porphyrins and related compounds are the best known PDT photosensitizers to date.<sup>21,81</sup> This section discusses some recent advances made in this field.

Among the first generation photosensitizers, hematoporphyrin derivative (HpD) and its commercial variant, photofrin II<sup>®</sup> have been used clinically.<sup>21,81</sup> HpD is complex mixture of hematoporphyrin (Hp), hydroxyethylvinyl deuteroporphyrin (Hvd) and protoporphyrin together with dimers and higher oligomers of these porphyrins joined with ether or ester linkages. Photofrin II<sup>®</sup> is a purified preparation of the active fraction of HpD. Despite the utility of photofrin II<sup>®</sup>, it has three severe disadvantages which are given below.

1. It is a complex and variable mixture of porphyrin oligomers linked with ether, ester or carbon-carbon linkages, which are not stable either during storage or after administration.

2. It has only a weak absorption peak in the relevant part of the spectrum at about 630 nm, but absorbs much more strongly at shorter wavelengths in the visible and near UV regions.
3. It is not very selective and causes skin photosensitivity.

It was therefore found desirable to develop new photosensitizers and, a plethora of new second-generation photosensitizers including modified phthalocyanines,<sup>82-85</sup> chlorins and bacteriochlorins,<sup>86-90</sup> purpurins,<sup>91</sup> benzoporphyrin derivatives,<sup>92,93</sup> expanded porphyrins,<sup>94-96</sup> and picket fence porphyrins<sup>97-99</sup> have been reported recently. However, many of these new generation photosensitizing drugs suffer from their inability to accumulate selectively in tumors, leading to lower levels of tumor necrosis.

One possible way to circumvent the problem of low accumulation of a given porphyrin-based drug in the cells is to equip the drug with an intracellular recognition element *viz.* a DNA or membrane binding agent. Thus, porphyrin conjugates endowed with oligonucleotide,<sup>100-103</sup> monoclonal antibody,<sup>104,105</sup> ellipticine,<sup>106-108</sup> or other intracellular recognition element<sup>109-112</sup> have been reported during the last several years. More recently, photonuclease activity of porphyrins which bind selectively to DNA owing to their linkage to either an intercalator<sup>113</sup> (e.g. acridone, phenothiazine), a cross-linking agent<sup>114</sup> (e.g. chlorambucil) or a minor groove binder<sup>115</sup> (e.g. ellipticine) have been reported. In the present study, the above concept has been extended to incorporate photoactive DNA binding agent in the hybrid porphyrins. First part of Chapter 6 in this thesis describes the photonuclease activity of conjugates derived from a union of a porphyrin and anthraquinone subunits.

The second part of Chapter 6 deals with DNA photocleavage by diazoarene species. In a majority of earlier studies dealing with DNA cleavage/photocleavage, ion, radical or oxygen-centered reactive species have been proposed to be responsible for cleaving DNA. During the course of the present investigations, it was realized that carbenes, which are known to be reactive towards a wide variety of organic and bioorganic substrates including proteins, have never been tested for their ability to cleave DNA.<sup>116,117</sup> This is all the more surprising considering the fact that the naturally occurring anti-tumor agents kinamycin and prekinamycin, probably derive their DNA cleaving ability from the diazo group present in them.<sup>118</sup> In the present study, carbene species have been generated *via* photochemical means by irradiating the readily available diazoarenes.

### 1.5 Summary

Recent literature related to DNA-binding DNA photocleavage by metal complexes as applicable to the subject matter of this thesis is presented in this chapter. Also presented is a brief introduction concerning DNA photocleavage by porphyrin and diazoarene chromophores.

This thesis is divided into seven chapters and a brief chapter-wise account follows.

**Chapter 1** gives a general introduction to the basic principles involved in the DNA-drug interaction. It includes a survey of the recent literature on DNA binding and photocleavage by metal complexes highlighting the importance

of these studies in various biochemical and biomedical applications. A brief introduction concerning DNA photocleavage by porphyrin and diazoarene chromophores is also included in this Chapter.

**Chapter 2** presents a listing of the chemicals, a general description of the synthetic procedures and the details of spectroscopic, electrochemical and biochemical techniques employed during the research work.

**Chapter 3** deals with the design, synthesis, characterization and DNA interactions of new mixed-ligand ruthenium(II) complexes incorporating a quinone-fused dipyrrophenazine ligand or its hydroquinone form. Also discussed in this chapter are the aspects related to redox switching of luminescence exhibited by this redox couple.

**Chapter 4** presents DNA binding, photonuclease activity and novel luminescence properties of a series of ruthenium(II) complexes containing a new ligand - 6,7-dicyanodipyridoquinoxaline.

**Chapter 5** discusses DNA binding and photocleavage by dipyrrophenazine complexes of cobalt(III) and nickel(II).

**Chapter 6** deals with the photonuclease activity of porphyrin-anthraquinone diads and diazoarene chromophores.

**Chapter 7** presents general conclusions based on the results obtained during this research work.

## 1.6 References

1. Watson, J. D.; Crick, F. H. *Nature* **1953**, 171, 737.
2. Neidle, S.; Abraham, Z. *CRC Crit. Rev. Biochem.* **1984**, 17, 73.

3. (a) Wang, AH-J. *Current Opinion in Structural Biology* **1992**, 2, 361.  
(b) Wang, J. C. *J. Mol. Biol.* **1974**, 89, 783.
4. Lerman, L. S. *J. Mol. Biol.* **1961**, 3, 18.
5. Kennard, O.; Huntern, W. *Angew. Chem. Int. Eng. Edn.* **1991**, 30, 1254.
6. Mei, H. Y.; Barton, J. K. *J. Am. Chem. Soc.* **1986**, 108, 7414.
7. Mattes, W. B.; Hartley, J. A.; Kohn, K. W. *Nucleic Acid Res.* **1986**, 14, 2971.
8. Hurley, L. H.; Petrusek, R. *Nature* **1979**, 282, 529.
9. Rosenberg, B.; Van Camp, L.; Trosko, J. E.; Mansour, V. H. *Nature* **1969**, 222, 385.
10. Marzilli, L. G. *Progress in Inorganic Chemistry* **1977**, 23, 255.
11. Pigram, W.; Fuller, W.; Hamilton, L. *Nature New Biol.* **1972**, 17, 235.  
(b) Tsou, K. C.; Yip, K. F. *Cancer Res.* **1976**, 36, 3367.
12. Lippard, S. J. *Acc. Chem. Res.* **1978**, 11, 211. (b) Keck, M. V.; Lippard, S. J. *J. Am. Chem. Soc.* **1992**, 114, 3386.
13. Long, E. C.; Barton, J. K. *Acc. Chem. Res.* **1990**, 23, 271.
14. Weidle, S. *Prog. Med. Chem.* **1979**, 16, 151.
15. Friedman, A. E.; Chambron, J. C.; Sauvage, J. P.; Turro, N. J.; Barton, J. K. *J. Am. Chem. Soc.* **1990**, 112, 4960.
16. Waring, M. *J. Mol. Biol.* **1970**, 54, 247. (b) Lawrence, J. J.; Daune, M. *Biochemistry* **1976**, 15, 3301.
17. (a) Hertzberg, R. P.; Dervan, P. B. *J. Am. Chem. Soc.* **1982**, 104, 313.  
(b) Van Dyke, M. W.; Hertzberg, R. P.; Dervan, P. B. *Proc. Natl. Acad.*

- Sci. U.S.A.* **1982**, 79, 5470. (c) Low, C. M. L.; Drew, H. R.; Waring, M. *J. Nucleic Acids Res.* **1984**, 12, 4865. (d) Dervan, P. B. *Science* **1986**, 232, 464. (e) Tullius, T. D.; Dombroski, B. A.; Churchill, M. E. A.; Kam, L. *Meth. Enzymol.* **1987**, 155, 537. (e) Pyle, A. M.; Barton, J. K. *Prog. Inorg. Chem.* **1990**, 38, 413.
18. Pyle, A. M.; Long, E. C.; Barton, J. K. *J. Am. Chem. Soc.* **1989**, 111, 4520.
19. Breiner, K. M.; Daugherty, M. A.; Oas, T. G.; Thorp, H. H. *J. Am. Chem. Soc.* **1995**, 117, 11673.
20. Hall, B.; Holmlin, R. E.; Barton, J. K. *Nature* **1996**, 382, 731.
21. *Photodynamic Therapy: Basic Principles and Clinical Application*; Henderson, B. W., Dougherty, T. J., Eds.; Marcel Dekker: New York, **1992**.
22. Wang, AH-J.; Quigley, G. J.; Kolpak, F. J.; Crawford, J. L.; van Boom, J. H.; van der Marel, G.; Rich, A. *Nature* **1979**, 282, 680.
23. Barton, J. K.; Dannenberg, J. J.; Raphael, A. L. *J. Am. Chem. Soc.* **1982**, 104, 4967.
24. Barton, J. K.; Danishefsky, A. T.; Goldberg, J. M. *J. Am. Chem. Soc.* **1984**, 106, 2172.
25. Kumar, C. V.; Barton, J. K.; Turro, N. J. *J. Am. Chem. Soc.* **1985**, 107, 5518.
26. Pyle, A. M.; Rehman, J. P.; Meshoyrer, R.; Kumar, C. V.; Turro, N. J.; Barton, J. K. *J. Am. Chem. Soc.* **1989**, 111, 3051.

27. Naing, K.; Takahashi, M.; Taniguchi, M.; Yamagishi, A. *Inorg. Chem.* **1995**, 34, 350. (b) Mahadevan, S.; Palaniandavar, M. *J. Chem. Soc., Chem. Commun.* **1996**, 2547.
28. Mei, H. Y.; Barton, J. K. *Proc. Natl. Acad. Sci. U. S. A.* **1988**, 85, 1339.
29. Amouyal, E.; Homsy, A.; Chambron, J. C.; Sauvage, J. P. *J. Chem. Soc., Dalton Trans.* **1990**, 1841.
30. Friedman, A. E.; Kumar, C. V.; Turro, N. J.; Barton, J. K. *Nucleic Acid Res.* **1991**, 19, 2595.
31. Hiort, C.; Per Lincoln.; Norden, B. *J. Am. Chem. Soc.* **1993**, 115, 3448.
32. Cynthia, M.; Dupureur.; Barton, J. K. *Inorg. Chem.* **1997**, 36, 33.
33. Haq, I.; Per Lincoln.; Suh, D.; Norden, B.; Chowdhry, B. Z.; Chaires, J. *B. J. Am. Chem. Soc.* **1995**, 117, 4788.
34. Hartshorn, R. M.; Barton, J. K. *J. Am. Chem. Soc.* **1992**, 114, 5919.
35. Holmlin, R. E.; Barton, J. K. *Inorg. Chem.* **1995**, 34, 7.
36. Moucheron, C.; Kirsch-DeMesmaeker, A.; Choua., S. *Inorg. Chem.* **1997**, 36, 584.
37. Per Lincoln.; Norden, B. *J. Chem.Soc., Chem Commun.* **1996**, 2145.
38. Schoch, T. K.; Hubbard, J. L.; Zoch, C. R.; Yi, G. B.; Sørile, M. *Inorg. Chem.* **1996**, 35, 4383.
39. Morgan, R. J.; Chatterjee, S.; Baker, A. D.; Strekas, T. C. *Inorg. Chem.* **1991**, 30, 2687.
40. Tysoe, S. A.; Morgan, R. J.; Baker, A. D.; Strekas, T. C. *J. Phys. Chem.* **1993**, 97, 1707.

41. Lecomte, J. P.; Kirsch-DeMesmaeker, A.; Demeunynck, M.; Lhomme, J. *J. Chem. Soc., Faraday Trans.* **1993**, 89, 3261.
42. (a) Sigman, D. S.; Graham, D. R.; D'Aurora, V.; Stern, A. M. *J. Biol. Chem.* **1979**, 254, 12269. (b) Spassky, A.; Sigman, D. S. *Biochemistry* **1985**, 24, 8050. (c) Sigman, D. S. *Acc. Chem. Res.* **1986**, 19, 180.
43. Tamilarasan, R.; McMillin, D. R. *Inorg. Chem.* **1990**, 29, 2798.
44. Kelly, J. M.; Tossi, A. B.; McConnel, D. J.; OhUigin, C. *Nucleic Acid Res.* **1985**, 13, 6017.
45. Aboul-Ennin, A.; Schulte-Frohlinde, D. *Photochem. Photobiol.* **1988**, 48, 27.
46. Basile, L. A.; Barton, J. K. *J. Am. Chem. Soc.* **1987**, 109, 7548.
47. Basile, L. A.; Raphaël, A. L.; Barton, J. K. *J. Am. Chem. Soc.* **1987**, 109, 7550.
48. Kelly, J. M.; McConnell, D. J.; OhUigin, C.; Tossi, A. B.; Kirsch-DeMesmaeker, A.; Masschelein, A.; Nasielski, J. *J. Chem. Soc., Chem. Commun.* **1987**, 1821.
49. Kirsch-Demesmaeker, A.; Orellana, G.; Barton, J. K.; Turro, N. J. *Photochem. Photobiol.* **1990**, 52, 461.
50. Lecomte, J. P.; Kirsch-Demesmaeker, A.; Feeney, M. M.; Kelly, J. M. *Inorg. Chem.* **1995**, 34, 6481.
51. Baker, A. D.; Morgan, R. J.; Strekas, T. C. *J. Chem. Soc., Chem. Commun.* **1992**, 1099.
52. Hirai, M.; Shinazuka, K.; Ogawa, S.; Sawai, H. *Chem. Lett.* **1996**, 1113.

53. Goulle, V.; Lehn, J. M.; Schoentjes, B.; Schmitz, F. J. *Helvetica Chimica Acta*. **1991**, 74, 1471.
54. Adamson, A.W. *Coord. Chem. Rev.* **1968**, 3, 169.
55. (a) Sausville, E. A.; Peisach, J.; Horwitz, S. B. *Biochem. Biophys. Res. Com.* **1976**, 73, 814. (b) Sausville, E. A.; Peisach, J.; Horwitz, S. B. *Biochemistry* **1978**, 17, 2740. (c) Stubbe, J.; Kozarich, J. W. *Chem. Rev.* **1987**, 87, 1107.
56. Chang, C. H.; Meares, C. F. *Biochemistry* **1982**, 21, 6332.
57. Subramanian, R.; Meares, C. F. *J. Am. Chem. Soc.* **1986**, 108, 6427.
58. Barton, J. K.; Raphael, A. L. *J. Am. Chem. Soc.* **1984**, 106, 2466.
59. (a) Fleisher, M. B.; Waterman, K. C.; Turro, N. J.; Barton, J. K. *Inorg. Chem.* **1986**, 25, 3549. (b) Barton, J. K.; Raphael, A. L. *J. Am. Chem. Soc.* **1984**, 106, 2466.
60. Riordan, C. G.; Wei, P. *J. Am. Chem. Soc.* **1994**, 116, 2189.
61. Sargeson, A. M. *Coord. Chem. Rev.* **1996**, 151, 89.
62. Sitlani, A.; Long, E. C.; Pyle, A. M.; Barton, J. K. *J. Am. Chem. Soc.* **1992**, 114, 2303.
63. David, S. S.; Barton, J. K. *J. Am. Chem. Soc.* **1992**, 115, 2954.
64. Shields, T. P.; Barton, J. K. *Biochemistry* **1995**, 34, 15037.
65. Carter, M. T.; Bard, A. J. *J. Am. Chem. Soc.* **1987**, 109, 7528.
66. Carter, M. T.; Rodriguez, M.; Bard, A. J. *J. Am. Chem. Soc.* **1989**, 111, 8901.

67. Carlson, D. L.; Huchital, D. H.; Mantilla, E. J.; Sheardy, R. D.; Murphy Jr, W. R. *J. Am. Chem. Soc.* **1993**, 115, 6424.
68. Grover, N.; Thorp, H. H. *J. Am. Chem. Soc.* **1991**, 113, 7030.
69. Grover, N.; Gupta, N.; Singh, P.; Thorp, H. H. *Inorg. Chem.* **1992**, 31, 2014.
70. Gupta, N.; Grover, N.; Neyhart, G. A.; Liang, W.; Singh, P.; Thorp, H. H. *Angew. Chem. Int. Ed. Engl.* **1992**, 31, 1048.
71. Gupta, N.; Grover, N.; Neyhart, G. A.; Singh, P.; Thorp, H. H. *Inorg. Chem.* **1993**, 32, 310.
72. Galas, D. J.; Schimitz, A. *Nucleic Acids Res.* **1978**, 5, 3157.
73. Hertzberg, R. P.; Dervan, P. B. *Biochemistry* **1984**, 23, 3934. (b) Schultz, P. G.; Taylor, J. S.; Dervan, P. B. *J. Am. Chem. Soc.* **1982**, 104, 6861.
74. Taylor, J. S.; Schultz, P. G.; Dervan, P. B. *Tetrahedron* **1984**, 40, 457.
75. Youngquist, R. S.; Dervan, P. B. *Proc. Natl. Acad. Sci. U.S.A.* **1985**, 82, 2565.
76. Fitzsimons, M. P.; Barton, J. K. *J. Am. Chem. Soc.* **1997**, 119, 3379.
77. Sigman, D. S. *Biochemistry* **1990**, 29, 9097.
78. Pope, L. E.; Sigman, D. S. *Proc. Natl. Acad. Sci. U. S. A.* **1984**, 81, 3.
79. Barton, J. K.; Raphael, A. L. *Proc. Natl. Acad. Sci. U. S. A.* **1985**, 82, 6460.
80. Uchida, K.; Pyle, A. M.; Morii, T.; Barton, J. K. *Nucleic Acid. Res.* **1989**, 17, 10259.

81. (a) Gomer, C. J.; Doiron, D. R.; Dunn, S.; Rucker, N.; Razum, N.; Fountain, S. *Photochem. Photobiol.* **1983**, 37S, S91. (b) Girotti, A. W. *Photochem. Photobiol.* **1983**, 38, 745. (d) Dolphin, D. *Can. J. Chem.* **1994**, 72, 1005. *Photodynamic Therapy: Basic Principles and Clinical Application*; Henderson, B. W., Dougherty, T. J., Eds.; Marcel Dekker: New York, **1992**. (f) Bonnet, R. *Chem. Soc. Rev.* **1995**, 19. (g) Morgan, A. R. *Curr. Med. Chem.*, **1995**, 2, 604.
82. Shopova, M.; Mantareva, V.; Krastev, K.; Hadjiolov, D.; Milev, A.; Spirov, K.; Jor, G.; Ricchelli, F. J. *Photochem. Photobiol., B. Biol.* **1992**, 16, 83.
83. Bishop, S. M.; Khoo, B. J.; MacRobert, A. J.; Simpson, M. S. C.; Phillips, D.; Beeby, A. *J. Chromatogr.* **1993**, 646, 345.
84. Boyle, B. W.; Leznoff, C. C.; van Lier, J. E. *Br. J. Cancer* **1993**, 67, 1177.
85. Segalla, A.; Milanesi, C.; Jori, G.; Capraro, H. -G.; Isele, U.; Schieweck, K. *Br. J. Cancer* **1994**, 69, 817.
86. Kostenich, G. A.; Zhuravkin, I. N.; Zhavrid, E. A. *J. Photochem. Photobiol. B. Biol.* **1994**, 22, 211.
87. Bonnett, R.; Benzie, R.; Grahn, M. F.; Salgado, A.; Valles, M. A. *Proc. SPIE* **1994**, 2078, 171.
88. Leach, M. W.; Higgins, R. J.; Autrey, S. A.; Boggan, J. E.; Lee, S. -J. H.; Smith, K. M. *Photochem. Photobiol.* **1993**, 58, 653.
89. Pandey, R. K.; Shiau, F. -Y.; Ramachandran, K.; Dougherty, T. J.; Smith, K. M. *J. Chem. Soc. Perkin Trans I* **1992**, 1377.

90. Richter, A. M.; Kelly, B.; Chow, J.; Liu, D. J.; Towers, G. M. N.; Dolphin, D.; Levy, J. G. *J. Natl. Cancer Inst.* **1987**, 79, 1327.
91. Morgan, A. R.; Garbo, G. M.; Keck, R. W.; Skalkos, D.; Selman, S. H. *Photochem. Photobiol.* **1990**, 6, 133.
92. Ritcher, A. M.; Watterfield, M. E.; Jain, A. K.; Allison, B.; Sternberg, E. D.; Dolphin, D.; Levy, J. G. *Br. J. Cancer* **1991**, 63, 87.
93. Hunt, D. W. C.; Jiang, J. -H.; Levy, G. J.; Kabn. A. H. *Photochem. Photobiol.* **1995**, 61, 417.
94. Vogel, E.; Kocher, M.; Schmickler, H.; Lex, J. *Angew. Chem., Int. Ed. Engl.* **1986**, 25, 197.
95. Leung, M.; Richert, C.; Gamarra, F.; Lumper, W.; Voge. E.; Jochanji, D.; Goetz, A. E. *Br. J. Cancer* **1993**, 68, 225.
96. Sessler, J. L.; Hemmi, G.; Mody, T. D.; Murai, T.; Burrell, A.; Young, S. W. *Acc. Chem. Res.* **1994**, 27, 43 and references therein.
97. Hegan, W. J.; Barber, D. C.; Whitten, D. G.; Kelly, M.; Albrecht, F.; Gibson, S. L.; Hilf, R. *Cancer Res.* **1988**, 48, 1148.
98. Barber, D. C.; Van Der Meid, K. R.; Gibson, S. L.; Hilf, R.; Whitten, D. G. *Cancer Res.* **1991**, 51, 1836.
99. Lawrence, D. S.; Gibson, S. L.; Nguyen, M. L.; Whittemore, K. R.; Whitten, D. G.; Ressel, H. *Photochem. Photobiol.* **1995**, 61, 90.
100. Bigey, P.; Pratviel, G.; Meunier, B. *J. Chem. Soc., Chem. Commun.* **1995**, 181.
101. Mastruzzo, L.; Woisard, A.; Ma, D. D. F.; Rizzarelli, E.; Favre, A.; Doan, T. L. *Photochem. Photobiol.* **1994**, 60, 316.

102. Le Doan, T. Praseuth, D.; Perrouault, L.; Chassignol, M.; Thuong, N. T.; Helene, C. *Bioconjugate Chem.* **1990**, 2, 108.
103. Fedorova, O. S.; Savitskii, A. P.; Shoikhet, K. G.; Ponomarev, G. V. *FEBS Lett.* **1990**, 259, 335.
104. Milgrom, L. R.; O'Neill, F. *Tetrahedron* **1995**, 51, 2137.
105. Harada, A.; Shiotsuki, K.; Fukushima, H.; Yamaguchi, H.; Kamachi, M. *Inorg. Chem.* **1995**, 34, 1070.
106. Ding, L.; Moghadam, G. E.; Cros, S.; Auclair, C.; Meunier, B. *J. Chem. Soc., Chem. Commun.* **1989**, 1711.
107. Moghadam, G. E.; Ding, L.; Tadj, F.; Meunier, B. *Tetrahedron* **1989**, 45, 2641.
108. Ding, L.; Moghadam, G. E.; Meunier, B. *Biochemistry* **1990**, 29, 7868.
109. Perreee-Fauvet, M.; Gresh, N. *Tetrahedron Lett.* **1995**, 36, 4227.
110. Mathews, S. E.; Pouton, C. W.; Threadgill, M. D. *J. Chem. Soc., Chem. Commun.* **1995**, 1809.
111. Herbelin, G. A.; Perreee-Fauvet, M.; Gaudemer, A.; Helissey, P.; Renault, S. G.; Gresh, N. *Tetrahedron Lett.* **1993**, 45, 7263.
112. Hashimoto, Y.; Lee, C. -S.; Shudo, K.; Okamoto, T. *Tetrahedron Lett.* **1983**, 24, 1523.
113. Mehta, G.; Sambaiah, T.; Maiya, B. G.; Sirish, M.; Chatterjee, D. *J. Chem. Soc. Perkin Trans. 1.* **1993**, 2667. (b) Mehta, G.; Sambaiah, T.; Maiya, B. G.; Sirish, M.; Dattagupta, A. *J. Chem. Soc. Perkin Trans. 1.* **1995**, 295. (c) Mehta, G.; Muthusamy, S.; Maiya, B. G.; Sirish, M. *J. Chem. Soc. Perkin Trans. 1.* **1996**, 2421.

114. Mehta, G.; Sambaiah, T.; Maiya, B. G.; Sirish, M. Dattagupta, A. *Tetrahedron Lett.* **1994**, 35, 4201.
115. Milder, S. J.; Ding, L.; Etemad-Moghadam, G.; Meunier, B.; Paillous, N. *J. Chem. Soc., Chem. Commun.* **1990**, 1131. (b) Sentagne, C.; Meunier, B.; Paillous, N. *J. Photochem. Photobiol B: Biol.* **1992**, 16, 47.
116. Kirmse, W. *Carbene Chemistry*, (vol I) 2nd edn., Academic Press, **1971**. (b) Jones, Jr., M.; Moss, R. A. *Carbenes*, (vol I, A volume in Reactive Intermediates in Organic Chemistry), Wiley-Interscience, **1973**.
117. Bayley, H.; Knowles, J. R. *Meth. Enzymol.* **1977**, 46, 69 (and references therein).
118. (a) Cone, M. C.; Hassan, A. M.; Gore, M. P.; Gould, S. J.; Borders, D. B.; Alluri, M. R. *J. Org. Chem.* **1994**, 59, 1923. (b) Gould, S. J.; Tamayo, N.; Melville, C. R.; Cone, M. C.; *J. Am. Chem. Soc.* **1994**, 116, 2207. (c) Mithani, S.; Weeratunga, G.; Taylor, N. J.; Dmitrienko, G. I. *J. Am. Chem. Soc.* **1994**, 116, 2209.

## CHAPTER 2

### *Materials and Methods*

#### **2.1 Introduction**

In this Chapter, a listing of all the materials employed at different stages of the investigation and procedures for purification of the utilized chemicals/solvents are given. Also given here is a brief description of the physicochemical and biochemical techniques employed in this study.

#### **2.2 Materials**

##### **2.2.1 Chemicals and biochemicals**

Ruthenium(III) chloride hydrate, ammonium hexafluorophosphate ( $\text{NH}_4\text{PF}_6$ ), tetrabutylammonium chloride hydrate (TBACl), tetrabutylammonium hexafluorophosphate ( $\text{TBAPF}_6$ ), diaminomaleonitrile, 1,2-diaminoanthraquinone, sodium dodecyl sulphate (SDS), 1,3-diphenylisobenzofuran (DPBF) were all obtained from Aldrich Chemical Co. (U. S. A).

1,10-phenanthroline monohydrate (phen), o-phenylenediamine, cobalt(III) chloride hexahydrate, nickel(II) chloride hexahydrate, sodium dithionite, 1,4-diazabicyclo[2.2.2]octane (DABCO), mannitol, cumene and cysteine were purchased from E. Merck (Mumbai, India).

Aluminium oxide (basic and neutral) for column chromatography was obtained from Acme Synthetic Chemicals (Mumbai, India).

Supercoiled DNA pBR 322 (cesium chloride purified) and DNA topoisomerase I (from wheat germ) were obtained from Bangalore Genei (Bangalore, India).

Agarose (low melt, 65 °C, molecular biology grade for DNA gels) and Hind III, a restriction enzyme were purchased from Bio-Rad (U. S. A)

Highly polymerized calf-thymus DNA (CT DNA), superoxide dismutase (SOD), N-(t-butyl)- $\alpha$ -phenyl nitron (PBN), ethidium bromide and bromophenol blue were procured from Sigma Chemical Co. (U. S. A)

Tris(hydroxymethyl)aminomethane (Tris), sucrose, sodium chloride, ethylenediamine tetraacetic acid disodium salt ( $\text{EDTA-Na}_2$ ), sodium hydrogen phosphate ( $\text{Na}_2\text{HPO}_4$ ) and sodium dihydrogen phosphate ( $\text{NaH}_2\text{PO}_4$ ) were of molecular biology grade, obtained from Sisco Research Laboratories (Mumbai, India).

The drying agents employed at various stages of purification procedures viz. anhydrous sodium sulphate, calcium chloride, calcium hydride, magnesium turnings and magnesium sulphate and the mineral acids such as hydrochloric acid, sulphuric acid and nitric acid were all of Analytical Reagent grade and obtained from either B. D. H. (Mumbai, India) or Ranbaxy (Mumbai, India). All other common chemicals were purchased from locally available sources.

The gases utilized in this study, nitrogen and oxygen, were obtained from India Oxygen Limited (Hyderabad, India). Nitrogen was further purified by using the pyrogallol and BASF catalyst before use. Chlorine gas was generated by following a standard procedure.<sup>1</sup> 1 g of  $\text{KMnO}_4$  was placed in a round bottom flask and 6.2 ml of HCl was added dropwise from a pressure-

equalising funnel. The evolving chlorine gas was allowed to pass through a Drechsel bottle containing water to remove hydrogen chloride and was then dried by means of another Drechsel bottle charged with concentrated sulphuric acid. The flask was shaken from time to time to complete the evolution of chlorine gas.

### 2.2.2 Solvents

The common solvents used during the research work were purified according to the standard procedures.<sup>1,2</sup>

Acetonitrile and methanol used for the spectroscopic and electrochemical studies were of spectroscopic grade from E. Merck (Mumbai, India). They were further purified by distilling over phosphorous pentoxide and calcium oxide, respectively.

Dimethylformamide (DMF) was obtained from E. Merck (Mumbai, India) and was purified using flash distillation over calcium hydride under vacuum.

Methylene chloride used for the spectroscopic and electrochemical studies was purified rigorously. The Laboratory Reagent grade solvent obtained from B. D. H (Mumbai, India) was washed twice from sulphuric acid, and then with water. This was followed by washing twice with sodium carbonate solution and water again. It was dried over anhydrous  $\text{CaCl}_2$ , and distilled from  $\text{CaH}_2$  before use. The other solvents used were acetone, ethanol and dimethylsulphoxide. They were purified according to the known procedures before use.<sup>1,2</sup>

$\text{CDCl}_3$  (99.8%) and  $\text{DMSO-d}_6$  (99.5%),  $\text{D}_2\text{O}$  (99.8%) and  $\text{CD}_3\text{CN}$  (99.5 %) were obtained from Aldrich Chemical Co. (U. S. A)

Water used for the biochemical studies was triply distilled using a quartz distillation set-up and then autoclaved before use.

## 2.3 Preparation of the starting materials

### 2.3.1 Preparation of 1,10-phenanthroline 5,6-dione (phen-dione)<sup>3</sup>

A round bottom flask containing 1.00 g of phen (5.04 mmol) and 5.95 g (50.0 mmol) of potassium bromide was placed in an ice bath. Concentrated sulfuric acid (20 ml) was added in small portions, and then was added 10 ml of concentrated nitric acid. The resulting solution was heated for 2 h. at 80-85 °C. It was cooled to room temperature and then was poured into 400 ml of water. The solution was neutralized with  $\text{NaHCO}_3$ , and then extracted with dichloromethane. Removal of dichloromethane gave 1,10-phenanthroline 5,6-dione as yellow needles. Yield: ~ 80%.

### 2.3.2 Preparation of dipyrido[3,2-a:2',3'-c]phenazine (dppz)<sup>4</sup>

A 0.5 g (2.4 mmol) sample of phen-dione and 0.5 g (4.6 mmol) of o-phenylenediamine were together refluxed in ethanol (50 ml) for 10 min. The solution was cooled to room temperature to yield golden yellow needles of dppz, which was suction filtered and recrystallised from aqueous ethanol. Yield: ~ 80%.

### 2.3.3 Preparation of $[\text{Co}(\text{phen})_2\text{Cl}_2]^+{}^5$

0.5 g ( 2.1 mmol) of  $\text{CoCl}_2 \cdot 6\text{H}_2\text{O}$ , 0.5 g (12.0 mmol) of  $\text{LiCl}$  and 0.9 g (4.5 mmol) of phen were dissolved in 50 ml of dry methanol under nitrogen. Gaseous  $\text{Cl}_2$  was then slowly introduced into this solution under

cooling for 30 min. The resulting crystals were filtered off and washed with methanol. Yield: ~ 75%.

#### 2.3.4 Preparation of $[\text{Ni}(\text{phen})_2\text{Cl}_2]$ <sup>6</sup>

$\text{NiCl}_2 \cdot 6\text{H}_2\text{O}$  (0.26 g, 1.1 mmol) and phen (0.40 g, 2 mmol) were dissolved in 20 ml water and the solution was evaporated to 5 ml. Acetone (20 ml) was added to this lilac solution which was then set aside in a closed vessel for 24 h. The crystals were filtered off, washed with acetone and dried under vacuum. Yield: ~ 65%.

#### 2.3.5 Preparation of $[\text{Ru}(\text{phen})_3]\text{Cl}_2$ <sup>7</sup>

Potassium aquopentachlororuthenate(III) (0.5 g, 1.3 mmol)<sup>7</sup> was dissolved in 50 ml of hot water containing one drop of 6 N HCl and a stoichiometric amount of phen was added slowly with stirring. The mixture was refluxed until a deep green solution resulted (10-20 min.). Hypophosphorous acid (1.2 ml of 30% solution) neutralized with NaOH (~ 3.5 ml of a 2 N solution) was added and the mixture was refluxed 15-30 min. until the color changed to deep orange-red. The mixture was filtered and 10 ml of 6 N HCl was added dropwise with stirring to the hot filtered solution. The crude product was recrystallized from hot water. Yield: ~ 70%.

#### 2.3.6 Preparation of $[\text{Ru}(\text{phen})\text{Cl}_4]^-$ <sup>8</sup>

To 10 ml of 1.0 N HCl was added 1.03 g (3.83 mmol) of  $\text{RuCl}_3 \cdot 3\text{H}_2\text{O}$  and 0.95 g of phenanthroline (20% excess over the equivalent). After stirring to dissolve the solids the container was stoppered, allowed to stand for several days and, the product isolated by filtration and washing with water. It was dried in vacuum over  $\text{P}_4\text{O}_{10}$ . Yields increased with time; isolation after seven days gave 70%.

### 2.3.7 Preparation of $[\text{Ru}(\text{phen})_2\text{Cl}_2]\cdot 2\text{H}_2\text{O}$ <sup>9</sup>

$\text{RuCl}_3\cdot 3\text{H}_2\text{O}$  (7.8 g, 29.8 mmol), phen (12 g, 60.0 mmol) and LiCl (8.4 g) dissolved in reagent grade dimethylformamide (50 ml) were heated at reflux for 8 h. The reaction mixture was stirred magnetically through this period. After the reaction mixture was cooled to room temperature, 250 ml of reagent grade acetone was added and the resultant solution cooled at 0 °C overnight. Filtering yielded a red to red-violet solution and a dark green-black microcrystalline product. The solid was washed three times with 25 ml portions of water followed by three 25 ml portions of diethyl ether, and then it was dried by suction. Yield: ~ 65%.

### 2.3.8 Preparation of $[\text{Ru}(\text{phen})_2(\text{dppz})](\text{PF}_6)_2\cdot 2\text{H}_2\text{O}$ <sup>10</sup>

A mixture of  $[\text{Ru}(\text{phen})_2\text{Cl}_2]\cdot 2\text{H}_2\text{O}$  (1.70 g, 3.0 mmol) and dipyrro phenazine (0.93 g, 3.2 mmol) in methanol-water (1 : 2 v/v; 380 ml) was refluxed for 4.5 h. The deep red solution was concentrated to 10% of its original volume, diluted with water (140 ml), boiled for 10 min, cooled in an ice-bath and filtered. The hexafluorophosphate salt of the complex was precipitated by the addition of 10%  $\text{NH}_4\text{PF}_6$  (30 ml) to the filtrate. Yield: ~ 75%.

## 2.4 Physical methods

The new compounds synthesized in this study were characterized by elemental analysis, FABMS, infrared, electronic absorption and emission, proton magnetic resonance, electron spin resonance, magnetic susceptibility and electrochemical methods.

The elemental analyses were done on a Perkin-Elmer Model 240 C - CHN analyzer.

The infrared spectra were recorded either on a Perkin-Elmer Model 1310 or on a Jasco Model 5300 FT-IR spectrophotometer. The spectrum of the solid samples were recorded by dispersing the samples in Nujol mull or as KBr pellets.

The UV-visible spectra were recorded with either on a Shimadzu model 160A or a Jasco model 7800 spectrophotometer. A matched pair of quartz cuvettes were employed.

Steady-state fluorescence spectra were recorded on a Jasco model FP-777 spectrofluorometer using 1 cm quartz cell. Detection of emission was done at right angle to the excitation wavelength. The excitation and emission slit widths employed were usually both 2 or 5 nm. For recording the emission spectra, optical densities of the samples were adjusted to  $\leq 0.2$  at the excitation wavelength. Emission quantum yields ( $\phi$ ) were estimated by integrating the areas under the fluorescence curves and by using the formula<sup>11</sup>

$$\phi_{\text{sample}} = \frac{A_{\text{sample}} \times O.D_{\text{standard}}}{A_{\text{standard}} \times O.D_{\text{sample}}} \times \phi_{\text{standard}} \quad \text{----- (2.1)}$$

where A is the area under the emission spectral curve and O.D is optical density of the compound at the excitation wavelength. The standards used for the fluorescence quantum yield measurements were  $[\text{Ru}(\text{phen})_3]^{2+}$  ( $\phi = 0.028$ )

in  $\text{CH}_3\text{CN}$ )<sup>12</sup> and 5,10,15,20-tetra(phenyl) porphyrin ( $\text{H}_2\text{TPP}$ ,  $\phi = 0.12$  in  $\text{CH}_2\text{Cl}_2$ ).<sup>13</sup>

The nuclear ( $^1\text{H}$  and  $^{13}\text{C}$ ) magnetic resonance spectra were recorded on a Bruker NR-200 AF-FT NMR spectrometer using  $\text{CDCl}_3$ ,  $\text{DMSO-d}_6$ ,  $\text{D}_2\text{O}/\text{CD}_3\text{CN}$  mixture or  $\text{CD}_3\text{CN}$  as the solvent. Tetramethylsilane (TMS) was the internal standard employed for recording the spectra.

The electron spin resonance (ESR) spectra were recorded on a JEOL model JM-FE 3X spectrometer. Diphenylpicrylhydrazide (DPPH) was used as the g-marker. For the spin trapping experiments using ESR, the solution, containing both the desired compound and spin trapping agent PBN, was taken in a flat quartz ESR tube and an on-line irradiation of the sample in the ESR cavity was carried out using 150 W PTI model A 1010 Xe arc lamp coupled with a PTI model LPS 2020 power supply. Appropriate filters were used to isolate the irradiation wavelength range. All the spectra were recorded at room temperature.

Fast atom bombardment mass spectra (FABMS) were recorded on a JEOL SX 102/DA-6000 mass spectrophotometer/data system using xenon (6 KV, 100 mA) as the FAB gas. The accelerating voltage was 10 KV and the spectra were recorded at room temperature. m-nitrobenzyl alcohol (NBA) was used as the matrix.

Cyclic and differential-pulse voltammetric experiments were carried out with a Princeton Applied Research (PAR) model 174A/175 polarographic analyzer/universal programmer or with a BAS model CV-27 potentiostat. Either  $\text{TBACl}$  or  $\text{TBAPF}_6$  (usually 0.1 M) was used as the supporting electrolyte. The cyclic voltammetric experiments were performed using a

standard three electrode, single compartment cell. A button platinum or glassy carbon working electrode, a platinum wire counter electrode and a saturated calomel reference electrode (SCE) were employed. Ferrocene was used as the internal standard in these experiments.. For the controlled potential electrolysis (Coulometry), a platinum wire gauze working electrode, a platinum flag counter electrode and an SCE reference electrode were employed. A H-type cell was employed for this purpose wherein the counter electrode and the working electrode were separated by a frit.

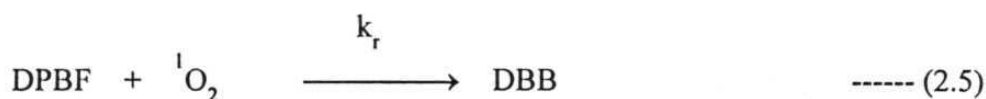
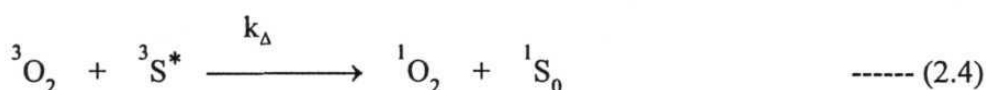
Room temperature magnetic susceptibility measurements were carried out on a 6612 CAIIN Research Magnetic Susceptibility system provided with an electrobalance model CAHN 1000. The magnetometer was calibrated with  $\text{Cu}(\text{SO}_4) \cdot 5\text{H}_2\text{O}$  and then cross checked against  $\text{HgCo}(\text{NCS})_4$ . Diamagnetic corrections were made using Pascal's constants.<sup>14</sup>

## 2.5 Singlet oxygen quantum yield ( $\phi_\Delta$ ) measurements

A 2.5 ml of DMF (saturated with AR grade molecular oxygen) solution containing  $1.0 \times 10^{-6}$  M of a given sensitizer and  $0.5 - 1.0 \times 10^{-4}$  M DPBF was taken in 1 cm path-length quartz cuvette and irradiated at the desired wavelength ( $500 \pm 10$  nm for ruthenium(II) complexes and  $550 \pm 10$  nm for the porphyrins). A 150 W Xe arc lamp (PTI Model A1010) coupled with a PTI Model S/N 1366 monochromator (10 nm band-pass) was used as the source of irradiation. It should be noted that sensitizer is the only chromophore that absorbs at this wavelength and DPBF, the singlet oxygen scavenger, does not absorb appreciably in this region. The solution was stirred during the irradiation period. The depletion of DPBF due to its

reactions with  $^1\text{O}_2$  was monitored at 410 nm spectrophotometrically. The total depletion of DPBF was restricted to 10 -15% of its original concentration and an average of five or six depletion rate runs were used for quantum yield measurements.

The mechanism of  $^1\text{O}_2$  production by the photosensitizers and the decay of it *via* reactions with DPBF are described below.



Here,  $I_{\text{abs}}$  is the intensity of the light absorbed,  $k_d$  is the rate of  $^1\text{O}_2$  production,  $k_r$  and  $k_q$  are the rates of chemical reaction and physical quenching of DPBF

with  $^1\text{O}_2$  respectively, and  $k_d$  is the solvent initiated  $^1\text{O}_2$  decay. (DBB = dibenzoylbenzene)

Thus,

$$\frac{d[^1\text{O}_2]}{dt} = I_{\text{abs}} \phi_{\Delta} \quad \text{----- (2.8)}$$

Equn. 2.9 can be obtained from equn. (2.5),

$$- \frac{d[\text{DPBF}]}{dt} = k_r [\text{DPBF}] [^1\text{O}_2] \quad \text{----- (2.9)}$$

and, from equns. (2.4), (2.5), (2.6) and (2.7), it follows that

$$\frac{d[^1\text{O}_2]}{dt} = I_{\text{abs}} \phi_{\Delta} - [^1\text{O}_2] (k_r [\text{DPBF}] + k_q [\text{DPBF}] + k_d) \quad \text{---(2.10)}$$

At steady state conditions,

$$\frac{d[^1\text{O}_2]}{dt} = 0 \quad \text{----- (2.11)}$$

Therefore, equn.(2.10) becomes

$$I_{\text{abs}} \phi_{\Delta} = [^1\text{O}_2] (k_r + k_q) [\text{DPBF}] + k_d \quad \text{----- (2.12)}$$

Rearranging, the above equation gives

$$[^1\text{O}_2] = \frac{I_{\text{abs}} \phi_{\Delta}}{k_d + (k_r + k_q) [\text{DPBF}]} \quad \text{-----}(2.13)$$

Substitution of equn. 2.13 into equn. 2.9, gives

$$-\frac{d[\text{DPBF}]}{dt} = I_{\text{abs}} \phi_{\Delta} \frac{k_r [\text{DPBF}]}{k_d + (k_r + k_q) [\text{DPBF}]} \quad \text{-----} (2.14)$$

Since, at low concentrations,  $k_q$  for DPBF is insignificant as compared to  $k_d$ <sup>15</sup> it can be assumed that  $(k_r + k_q) [\text{DPBF}] \ll k_d$  and thus equn. (2.14) becomes

$$-\frac{d[\text{DPBF}]}{dt} = \frac{I_{\text{abs}} \phi_{\Delta} k_r [\text{DPBF}]}{k_d} \quad \text{-----} (2.15)$$

Integration of equn. (2.15) gives,

$$-\ln \frac{[\text{DPBF}]_t}{[\text{DPBF}]_0} = \frac{I_{\text{abs}} \phi_{\Delta} k_r}{k_d} \times t \quad \text{-----} (2.16)$$

Thus, a plot of  $-\ln(A_t / A_0)$  ( $A$  is the absorbance of DPBF at 410 nm) versus time of irradiation,  $t$ , will give a straight line passing through the origin,

whose slope equals to  $I_{\text{abs}} \phi_{\Delta} k_r / k_d$ . By knowing  $k_r$ ,  $k_d$  and  $I_{\text{abs}}$ , the  $\phi_{\Delta}$  can be calculated. In this study, the values of  $k_r$  and  $k_d$  were taken to be  $1.1 \times 10^9 \text{ M}^{-1} \text{ s}^{-1}$  and  $1.40 \times 10^5 \text{ s}^{-1}$  respectively.<sup>16</sup>  $I_{\text{abs}}$  for a given photosensitizer was calculated from the slope by substituting the values of  $k_r$ ,  $k_d$  and  $\phi_{\Delta}$  of  $\text{H}_2\text{TPP}$  ( $\phi_{\Delta} = 0.60$ ) taken as the standard.

## 2.6 DNA - binding experiments

CT DNA was used for binding with the various drugs investigated during this work. It was purified by phenol extraction. The stock solution was made by dissolving CT DNA in appropriate buffers and kept overnight at 4 °C for complete dissolution. The concentration of CT DNA (nucleotide phosphate) was measured by using its known extinction coefficient at 260 nm ( $6600 \text{ M}^{-1} \text{ cm}^{-1}$ ).<sup>17</sup>

### 2.6.1 Thermal denaturation

Thermal denaturation experiments were performed using a Shimadzu model UV-160A spectrophotometer coupled with a temperature controller model TCC-240 A. The buffer used was 1mM phosphate, pH 7.0, 2 mM NaCl. The absorption at 260 nm for the CT DNA (160  $\mu\text{M}$  nucleotide phosphate) was continuously monitored at various temperatures. The melting temperature ( $T_m$ ) is defined as the temperature at which 50% of double strand becomes single stranded and  $\sigma_T$ , the curve width, is the temperature range between which 10% and 90% of the absorption increase occurs. The  $T_m$  of CT DNA in this buffer is  $60 \pm 1$  °C and  $\sigma_T$  is  $22 \pm 1$  °C under the experimental

conditions employed in this study. The  $T_m$  values of CT DNA in the presence of drugs at various [DNA nucleotide phosphate]/[drug] ratios were also obtained in a similar fashion described above upon adding equal concentration of the drug to both the reference and the sample cuvettes.

### 2.6.2 Absorption titration

Absorption titration experiments (Tris 5 mM, 50 mM NaCl, pH 7.0) were performed by using a fixed metal complex concentration to which increments of the stock DNA solutions (containing the same concentration of the metal complex) were added. Typical concentration of the metal complex used was 20-30  $\mu$ M and that of DNA ranged between 0 - 100 or more equivalents (base pairs). After the addition of DNA to metal complex, the resulting solution was allowed to equilibrate for 5 - 10 min. at 25 °C. The absorption readings (usually corresponding to the changes at maximum absorption) were noted. The data were then fit to the following equation to obtain the intrinsic binding constant  $K_b$ <sup>18</sup>

$$[\text{DNA}]/(\epsilon_a - \epsilon_f) = [\text{DNA}]/(\epsilon_b - \epsilon_f) + 1/K_b (\epsilon_b - \epsilon_f) \quad \text{-----}(2.17)$$

where  $\epsilon_a$ ,  $\epsilon_f$ , and  $\epsilon_b$  are the apparent, free and bound metal complex extinction coefficients, respectively. A plot of  $[\text{DNA}]/(\epsilon_a - \epsilon_f)$  Vs  $[\text{DNA}]$  gave a slope of  $1/(\epsilon_b - \epsilon_f)$  and a Y intercept equal to  $K_b/(\epsilon_b - \epsilon_f)$ ;  $K_b$  is the ratio of slope to Y intercept.

At times, the data were also fit to the following equation.<sup>19</sup>

$$C_b = 1/2 K (b - (b^2 - 2 K^2 C_t [\text{DNA}]/s)^{1/2}) \quad \text{----- (2.18a)}$$

$$b = 1 + K C_t + K [\text{DNA}]/2s \quad \text{----- (2.18b)}$$

where  $C_b$  is the concentration of the bound complex,  $K_b$  is the microscopic binding constant for each site,  $C_t$  is the total metal complex concentration and  $s$  is the site size in base pairs.

The values of  $K$  and  $s$  were obtained using an in-house non-linear least square analysis program or the MicroCal Origin soft-ware package both run on an IBM-compatible 486/pentium computer.

### 2.6.3 Viscometric titration

Viscometric titrations were performed with a Cannon-Ubbelohde viscometer. The viscometer was thermostated at  $25 \pm 0.5$  °C. The buffer used was 1.5 mM  $\text{Na}_2\text{HPO}_4$ , 0.5 mM  $\text{NaH}_2\text{PO}_4$ , 0.25 mM EDTA- $\text{Na}_2$ , pH 7.0. The DNA concentration was 300  $\mu\text{M}$  in base pairs. Titrations were carried out at a drug to DNA (base pairs) ratio of 0.0 to 0.1. Each titration was conducted without removing the DNA from the bulb of the viscometer. Drug was introduced in to the DNA solution using a Hamilton syringe fitted with a glass extender. Mixing of drug and DNA was done by bubbling thoroughly with nitrogen. Flow times were measured by a digital stop-watch. Flow times were measured at least three times, and were accepted if they agreed within 0.2 sec. Reduced specific viscosity was calculated according to Cohen and Eisenberg.<sup>20a</sup> Plots of  $\eta/\eta_0$  ( $\eta$  and  $\eta_0$  are the reduced specific viscosities of DNA in the presence and in the absence of drug) vs  $[\text{Drug}]/[\text{DNA}]$  were

constructed using the Microcal Origin program. Plots of  $\eta/\eta_0$  vs  $[\text{EtBr}]/[\text{DNA}]$  were found to be similar to those reported in the literature.<sup>20b</sup>

#### 2.6.4 Topoisomerase I assay

Topoisomerase I (Wheat germ) was used to convert supercoiled pBR 322 DNA to its relaxed state. Samples containing pBR 322 DNA (0.5  $\mu\text{g}$  in 20  $\mu\text{L}$  of the assay buffer containing 50 mM tris, 50 mM NaCl, 1 mM EDTA, 1 mM DTT and 100  $\mu\text{g}/\text{ml}$  nuclease free bovine serum albumin (BSA) and 1 mM  $\text{MgCl}_2$ , topoisomerase (2-3 units) and the drug were incubated for 30 min. at 37 °C. The reaction was stopped by the addition of 250 mM EDTA and 10% SDS. The samples were then electrophoresed in a 1% agarose gel for 5-6 h. The details of the electrophoresis experiments are described in the next Section. A control experiment was also carried out under the same experimental conditions without the addition of drug. The unwinding angle was determined from the plot of  $-\tau$  vs concentration of the bound drug, as described by equn. 2.19.<sup>21</sup>

$$\sigma = -20r_c(\Phi/360) = -r_c\Phi/18 \quad \text{----- (2.19)}$$

where  $\tau$  is the number of superhelical turns,  $\sigma$  superhelical density of the plasmid,  $r_c$  is the amount of drug bound per nucleotide when all the superhelices are removed and  $\Phi$  is the unwinding angle.

## **2.7 DNA photocleavage and agarose gel electrophoresis**

Electrophoresis through agarose is the standard method used to separate, identify or purify DNA fragments.<sup>22-25</sup> The technique is simple, rapid to perform and capable of resolving fragments of DNA that cannot be separated by other procedures such as density gradient centrifugation. The location of DNA within the gel can be determined directly by staining with low concentration of the fluorescent, intercalating dye ethidium bromide. Using this technique, bands containing as little as 1-10 ng of DNA can be detected by direct examination of the gel in the UV light.<sup>25</sup> Agarose gels are usually run in a horizontal configuration in an electric field of constant strength and direction. When an electric field is applied across the gel, DNA, which is negatively charged at neutral pH, migrates toward the anode. The intact supercoiled (Form I) DNA migrates faster than the single nicked (Form II) in the gel. This technique has been employed to identify the product/s of the DNA photocleavage which was carried out in this work.

### **2.7.1 Buffers used**

#### **2.7.1.1 Tris-acetate ethylenediaminetetraacetate (TAE) electrolyte buffer (50 X stock)**

A 48.4 g of tris base was dissolved in 100 ml of water. A 7.44 g of EDTA disodium salt was dissolved in 50 ml of water and the pH was adjusted to 8.0 using sodium hydroxide. This pH-adjusted EDTA solution was added to tris solution followed by the addition of 11.42 ml of glacial acetic acid. The volume was made up to 200 ml with water and the resulting buffer was stored at 4 °C.

#### **2.7.1.2 Sample buffer (6X)**

A 0.25% bromophenol blue in 40% sucrose/H<sub>2</sub>O was used as the sample buffer. This buffer was prepared by first dissolving a 2 g of sucrose in 3 ml of water and by then adding a 12.5 mg of bromophenol blue to this solution. The volume was made up to 5 ml. The resulting buffer was stored at 4 °C.

#### **2.7.2 Ethidium bromide stock solution (10 mg/ml)**

A 100 mg of ethidium was dissolved in 10 ml of water by stirring in dark for several hours. The resulting solution was stored in a brown bottle at the ambient temperature. A working concentration of 0.5 µg/ml was used for staining the gels after electrophoresis.

#### **2.7.3 Gel configuration and gel casting**

A horizontal slab gel electrophoresis chamber for submerged mini gels 3.5 X 7.5 or 6.0 X 7.5 inch polystyrene snaplock box obtained from Broviga Inc. (Chennai, India) was used to carry out the agarose gel electrophoresis. Platinum wire was used for each of the two electrodes that are glued in place with silicone rubber cement. A platform composed of four lantern slides glued together in a stack is cemented in the center of the box. A gel plate of 7 cm X 10 cm in size rests on this platform so that the gel is submerged just beneath the surface of the electrophoresis buffer. The standard TAE buffer is used for the electrophoresis. The details of gel casting are given below.

A 400 mg of low-melt (molecular biology grade) agarose was added to 50 ml of TAE buffer. The slurry was then heated on a boiling - water bath until the agarose dissolved completely. The solution was cooled to 50° C. Both ends of the gel mold was closed with a clean autoclaved tape and a small quantity of agarose solution was applied with a pipette along the edges of the gel mold so as to seal completely. Remaining warm agarose solution was poured onto the gel mold and immediately the comb was clamped into position near one end of the gel. The teeth of the comb formed the sample wells. Care was taken to see that at least 0.5-1.0 mm of agarose was left between the bottom of the teeth and the base of the gel, so that the sample wells are completely sealed. After 35-40 min. (by which time the gel was completely set), the comb and the autoclaved tape were removed carefully and the gel was mounted in the electrophoresis tank. A 200 ml of working buffer (TAE) was poured into the gel until the gel was covered to a depth of about 1 mm.

#### **2.7.4 Photolysis of pBR 322 DNA**

Photolysis experiments were carried out for pre-incubated (1 h.) samples of pBR 322 DNA (100  $\mu$ M nucleotide phosphate, 10  $\mu$ L) and the appropriate concentration of the drug placed in a quartz tube of 3 mm internal diameter. Tris-HCl buffer (pH 8.0) was the medium in the case of polypyridyl complexes and tris-HCl buffer (pH 8.0) containing not more than 5% dimethylformamide was used in the remaining cases. Irradiation of the samples were done using a Xe arc lamp (150 W, Photon Technology International) as the source. The required wavelength for the irradiation was

isolated from the source using a PTI Model S/N 1366 (10 nm band pass) monochromator. At times, photolysis was also carried out inside the sample chamber of a Jasco Model FP-777 spectrofluorometer with the slit width 5 nm. The temperature was maintained at 20 °C throughout irradiation. After irradiation, 2 µL of sample buffer was added and the contents were directly loaded onto a 0.7 % (w/v) agarose gel. The gel was run with standard TAE buffer pH 8.0 at 40 V for 4 h. after which it was stained with 0.5 µg/ml solution of ethidium bromide for 30 min. It was analyzed using the UVP gel documentation system GDS 2000 and was also directly photographed and developed. The DNA bands were read as integrated peak areas using the software package SW2000 version 2.

The percentage of cleavage (C) was calculated using the expression<sup>26</sup>

$$C = \frac{[\text{Form II}] + 2[\text{Form III}]}{[\text{Form I}] + [\text{Form II}] + 2[\text{Form III}]} \times 100 \quad \text{----- (2.20)}$$

## 2.8 General considerations

Care was taken to avoid the entry of direct, ambient light into the samples in all the spectroscopic and electrochemical experiments. Care was also taken to avoid the direct human contact of DNA and ethidium bromide solutions. All solutions containing ethidium bromide and other hazardous chemicals were decontaminated before disposal. Protective goggles, gloves and safety mask were used to minimize the exposure to obnoxious chemicals, ultraviolet light etc..

Unless otherwise specified, all the experiments were carried out at  $293 \pm 3$  K.

Standard error limits involved in various measurements (unless otherwise stated):

$\lambda_{\max}$ (absorption/fluorescence)	$\pm 1$ nm
$\log \epsilon$	$\pm 7\%$
$^1\text{H}$ NMR chemical shifts	$\pm 0.01$ ppm
$\phi_r$	$\pm 10\%$
$\phi_\Delta$	$\pm 10\%$
$E_{1/2}$	$\pm 0.03$ V
% DNA cleavage (C)	$\pm 8\%$

## 2.9 Summary

A brief account of various solvents and chemicals used during this work is given in this Chapter. Also given here is a description of spectroscopic as well as other physical and biochemical methods employed in this study.

## 2.10 References

1. *Vogel's text book of practical organic chemistry*; ELBS: England, 1989.

2. Perrin, D. D.; Armanego, W. L. F.; Perrin, D. R. *Purification of Laboratory Chemicals*; Pergamon: Oxford, 1986.
3. Yamada, M.; Tanaka, Y.; Yoshimoto, Y.; Kuroda, S.; Shimao, I. *Bull. Chem. Soc. Jpn.* **1992**, 65, 1006.
4. Dickeson, J. E.; Summers, L. A. *Aust. J. Chem.* **1970**, 23, 1023.
5. Vlcek, A. A.; *Inorg. Chem.* **1967**, 6, 1425.
6. Haris, C. M.; McKenzie, E. D. *Inorg. Nucl. Chem.* **1967**, 29, 1047.
7. Lin, C.-T.; Bottcher, W.; Chou, M.; Cruetz, C.; Sutin, M. *J. Am. Chem. Soc.* **1976**, 98, 6536.
8. Krause, R. A. *Inorg. Chim. Acta* **1977**, 22, 209.
9. Sullivan, B. P.; Salmon, D. J.; Meyer, T. J. *Inorg. Chem.* **1978**, 17, 3334.
10. Amouyal, E.; Homsy, A.; Chambron, J. C.; Sauvage, J. P. *J. Chem. Soc., Dalton Trans.* **1990**, 1841.
11. Austin, E.; Gouterman, M. *Bioinorg. Chem.* **1978**, 9, 281.
12. Juris, A.; Balzani, V.; Barigelletti, F.; Campagna, S.; Belser, P.; Zelewsky, A. V. *Coord. Chem. Rev.* **1988**, 84, 85.
13. Quimby, D. J.; Longo, F. R. *J. Am. Chem. Soc.* **1975**, 97, 5111.
14. Eranshaw, A. *Introduction to Magnetochemistry*, Academic press, London: 1968
15. Stevens, B.; Ors, J. A.; Christy, C. N. *J. Phy. Chem.* **1981**, 85, 210.
16. Reddi, E.; Jori, G.; Rodgers, M. A.; Spikes, J. D. *Photochem. Photobiol.* **1983**, 38, 639.
17. Reichmann, M.E.; Rice, S. A.; Thomas, C. A.; Doty, P. *J. Am. Chem. Soc.* **1954**, 76, 3047.

18. Wolfe, A.; Shimer, G. H.; Meehan, T. *Biochemistry* **1987**, 26, 6392.
19. Carter, M. T.; Rodrigues, M.; Bard, A. J. *J. Am. Chem. Soc.* **1989**, 111, 8901.
20. Cohen, G.; Eisenberg, H. *Biopolymers* **1969**, 8, 45. (b) Satyanarayana, S.; Dabrowiak, J. C.; Chaires, J. B. *Biochemistry* **1992**, 31, 9319.
21. Wang, J. C. *J. Mol. Biol.* **1974**, 89, 783.
22. Maniatis, T.; Fritsch, E. F.; Sambrook, J. *Molecular Cloning A Laboratory Manual*; CSH: New York, 1984.
23. Fisher, M. P.; Dingman, C. W. *Biochemistry* **1971**, 10, 895.
24. Ajay, C.; Borst, P. *Biochim. Biophys. Acta* **1972**, 269, 192.
25. Sugden, P. A. B.; Sambrook, J. *Biochemistry* **1973**, 12, 3055.
26. Kerwin, S. M. *Tetrahedron Lett.* **1994**, 35, 1023.



## CHAPTER 3

### *A New Metallointercalator Containing an Electroactive Dipyridophenazine Ligand: DNA Binding, Photonuclease Activity and Luminescence Properties*

#### 3.1 Introduction

As detailed in chapter 1, metal complexes of polypyridyl ligands are increasingly being employed in studies related to the development of DNA binding and cleaving agents for use in various biochemical and biomedical applications. In recent years, ligands derived from appropriate modification of 2,2'-bipyridyl (bpy) and 1,10-phenanthroline (phen) are being employed so as to suit the individual application.<sup>1-8</sup> Unique among the host of such modified ligands reported so far is dipyrido[3,2- $\alpha$ :2',3'-c]-phenazine (dppz) - a near-planar, hetero-aromatic entity obtained by fusing a phenazine subunit to bpy.<sup>9</sup> Metal-complexes containing dppz have found various applications which include, amongst the others, molecular light switching, DNA binding and cleavage and DNA-mediated electron transfer.<sup>3-8</sup> For example, complexes of the type  $[M(\text{phen})_2(\text{dppz})]^{2+}$  ( $M = \text{Ru}$  or  $\text{Os}$ ) have been shown, by Barton and co-workers, to act as selective 'molecular light switches' for DNA and in micellar solutions.<sup>3</sup> A number of studies have demonstrated that mixed-ligand complexes incorporating dppz are avid binders ( $K_b \cong 10^6 - 10^7 \text{ M}^{-1}$ ) of DNA.<sup>3-6</sup> While Thorp and co-workers<sup>5</sup> have demonstrated the electrochemically initiated cleavage of DNA by  $[\text{RuO}(\text{dppz})(\text{tpy})]^{2+}$  ( $\text{tpy} =$

terpyridine), others<sup>7</sup> have reported the photocleavage of DNA by dppz-complexes of ruthenium(II) and rhenium (I). These beneficial functions of the complexes containing dppz appear to be a consequence of the unique spectroscopic, redox and luminescence properties of this versatile ligand.

During the course of present investigations, we reasoned that further derivatization of dppz with suitable electron donating/withdrawing group(s) might not only accentuate DNA-binding and photocleavage efficiencies of the ensuing complexes but also serve to explore other interesting functional aspects associated therein. Quinone moiety was chosen for this purpose owing to the known DNA-binding ability and the rich redox chemistry of this ubiquitous electron-deficient functional group.<sup>10,11</sup> This chapter reports on the synthesis, characterization, DNA interaction and redox switching of the MLCT luminescence of a new mixed-ligand ruthenium(II) complex,  $[\text{Ru}(\text{phen})_2(\text{qdppz})]^{2+}$ , incorporating a quinone-fused dppz ligand (qddpz = naphtho[2,3-*a*]dipyrido[3,2-*h*:2',3'-*f*] phenazine-5,18-dione)

It should be noted here that while this study was in progress, synthesis and characterization of qdppz and a rhenium complex containing it ( $\text{Re}(\text{qdppz})(\text{CO})_3\text{Cl}$ ) have been reported by Lopez et al<sup>12</sup> but, that neither the DNA interaction nor the influence of redox chemistry on the luminescence properties of this rhenium complex was investigated in that study.

### 3. 2 Experimental details

1,10-phenanthroline-5,6-dione(phen-dione),<sup>13</sup>  $[\text{Ru}(\text{phen})_3]\text{Cl}_2$ <sup>14a</sup>,  $[\text{Ru}(\text{phen})_2\text{Cl}_2]$ <sup>14b</sup> and  $[\text{Ru}(\text{phen})_2(\text{dppz})]\text{Cl}_2$ <sup>9c</sup> were synthesized following the

reported procedures (see chapter 2). Synthesis of qdppz and its complex are described below, Fig. 3.1.

### 3.2.1 Synthesis of naphtho[2,3-a]dipyrido[3,2-h:2',3'-f] phenazine-5,18-dione, qdppz:

To a 250 ml ethanolic solution of phen-dione (0.21 g, 1 mM) was added a 0.22 g (1 mM) of 1,2-diamino anthraquinone and the resulting mixture was refluxed for 5 h. Evaporation of the solvent gave a greenish-brown residue which was taken up in 100 ml  $\text{CHCl}_3$  and warmed to ca. 50 °C during 0.5 h. The solution was cooled, filtered and a yellow precipitate was obtained upon addition of diethyl ether to the filtrate. The solids were filtered, washed with diethyl ether and vacuum dried. yield: 70%.

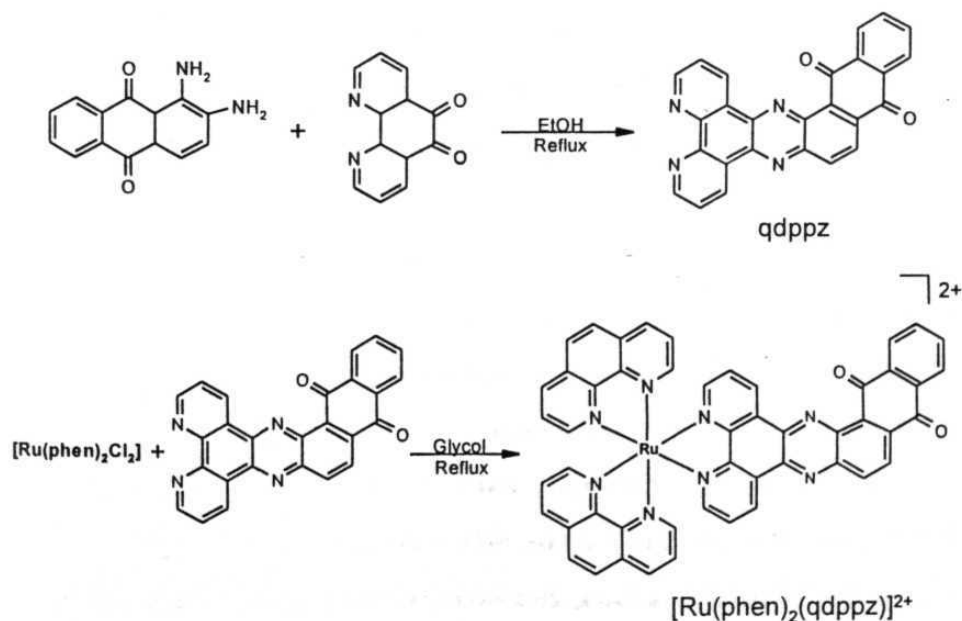


Fig. 3.1

Analytical data: Found: C, 73.02; H, 3.02; N, 12.35; Calcd. for  $C_{26}H_{12}N_4O_2$ : C, 73.73; H, 2.98; N, 12.59.

FABMS (m/z): 413,  $[M^+]$

IR (KBr): 1670, 1585, 1462  $cm^{-1}$ .

$^1H$  NMR ( $CDCl_3$ , 200 MHz, TMS)  $\delta$ , ppm: 9.85(d, 1H), 9.65(d, 1H), 9.35 (d, 2H), 8.71(dd, 2H), 8.32(q, 2H), 7.88(m, 4H).

**3.2.2 Synthesis of bis(1,10-phenanthroline) (naphtho[2,3-a]dipyrido[3,2-h:2',3'-f] phenazine-5,18-dione) ruthenium(II) hexafluorophosphate,  $[Ru(phen)_2(qdppz)](PF_6)_2$ :**

$Ru(phen)_2Cl_2$  (0.53 g, 1.0 mM) and  $qdppz$  (0.45 g, 1.1 mM) were refluxed in ethylene glycol (50 ml) for 12 h. The resulting solution was cooled to room temperature after which ca. 20 ml of water was added and the solution filtered. Addition of solid  $NH_4PF_6$  to the filtrate precipitated crude  $[Ru(phen)_2(qdppz)](PF_6)_2$  which was purified by repeated recrystallization by acetone-diethyl ether mixture. Yield: 80%.

Analytical data: Found: C, 50.86; H, 2.43; N, 9.22; Calcd. for  $C_{50}H_{32}N_8O_4P_2F_{12}Ru$ : C, 50.06; H, 2.49; N, 9.34.

FABMS (m/z): 1019,  $[M-PF_6]^+$ ; 874,  $[M-2PF_6]^+$ .

IR (KBr): 1670, 1589, 1427, 837  $cm^{-1}$ .

$^1H$  NMR ( $DMSO-d_6$ , 200 MHz, TMS)  $\delta$ , ppm: 9.5 (br, 2H), 8.81 (m, 6H), 8.41 (s, 4H), 8.32 (d, 2H), 8.23 (d, 4H), 8.10 (d, 4H), 7.82 (m, 6H).

$^{13}C$  NMR ( $CD_3CN/10\% D_2O$ , 200 MHz, TMS)  $\delta$ , ppm: 126.5, 128.6, 131.6, 137.5, 148.4, 153.7, 155.4, 182.8 & 183.5.

**3.2.3 Synthesis of bis(1,10-phenanthroline) (naphtho[2,3-a]dipyrido[3,2-h:2',3'-f] phenazine-5,18-dione) ruthenium(II) chloride,  $[\text{Ru}(\text{phen})_2(\text{qdppz})]\text{Cl}_2$ :**

The hexafluorophosphate salt obtained above was dissolved in minimum amount of acetone, and a saturated solution of tetrabutylammonium chloride in acetone was added dropwise until the precipitation was complete. The water-soluble chloride salt was filtered, washed thoroughly with acetone and vacuum dried. Recovery was about 90% of the theoretical yield.

Analytical data

IR (KBr): 1666, 1413  $\text{cm}^{-1}$ .

UV-visible ( $\text{H}_2\text{O}$ ):  $\lambda_{\text{max}}$ , nm (log  $\epsilon$ ) 439 (4.26), 400 (4.28), 278 (4.89), 263 (5.10).

**3.2.4 Synthesis of bis(1,10-phenanthroline) (5,18-dihydroxynaphtho[2,3-a]dipyrido[3,2-h:2',3'-f]phenazine)ruthenium(II),  $[\text{Ru}(\text{phen})_2(\text{hqdpz})]^{2+}$ :**

(a) **Chemical method:** The chloride or the hexafluorophosphate salt of this complex was obtained by the  $\text{Na}_2\text{S}_2\text{O}_4$  reduction of  $[\text{Ru}(\text{phen})_2(\text{qdppz})]\text{Cl}_2$  or  $[\text{Ru}(\text{phen})_2(\text{qdppz})](\text{PF}_6)_2$  in slightly basic ( $\text{pH} \approx 8.0$ ,  $\text{NaOH}$ ) aqueous or aqueous  $\text{CH}_3\text{CN}$  ( $\text{CH}_3\text{CN}/\text{H}_2\text{O}$  or  $\text{CD}_3\text{CN}/\text{D}_2\text{O}$ , 10:1 v/v) solutions.

(b) **Electrochemical method:** A  $1 \times 10^{-4}$  M of  $[\text{Ru}(\text{phen})_2(\text{qdppz})](\text{PF}_6)_2$  was subjected to exhaustive electrolysis under  $\text{N}_2$  atmosphere in aqueous  $\text{CH}_3\text{CN}$  (4-5%  $\text{H}_2\text{O}$ ) containing 0.1 M  $\text{TBAPF}_6$  at -0.5 V until the current value reached ca. < 1% of the initial value which took approximately 20 min. under our experimental conditions. Comparison of the total Coulombs passed

during the electrolysis with that of 1,4-benzoquinone ( $1 \times 10^{-4}$  M) revealed that reduction of  $[\text{Ru}(\text{phen})_2(\text{qdppz})]^{2+}$  involved  $1.9 \pm 0.2$  electrons. Aliquots of the solution containing the reduced species thus obtained were taken out under anaerobic conditions and the UV-visible as well as fluorescence spectra were measured using air-tight cuvettes. Bulk exhaustive re-oxidation was carried out in a manner similar to that adopted for the reductive electrolysis but, by holding the potential at +1.1 V. Reversibility of the redox cycle was checked by repeating the reduction and re-oxidation reactions for the same solution three to four times and by measuring the UV-visible and fluorescence spectra of the resulting sample each time. (note: at times, however, it was found necessary to add a base (NaOH; apparent pH of the solution  $\approx 8$ ), especially prior to the reoxidation, in order to avoid adsorption of a new, red-coloured species onto the surface of the electrode during the electrolysis)

Both  $[\text{Ru}(\text{phen})_2(\text{hqdpz})]\text{Cl}_2$  and  $[\text{Ru}(\text{phen})_2(\text{hqdpz})](\text{PF}_6)_2$  were found to be air-sensitive species and hence, the spectroscopic measurements (UV-visible ( $1 \times 10^{-5}$  M), fluorescence ( $1 \times 10^{-5}$ ) and  $^1\text{H}$  ( $\approx 2 \times 10^{-3}$  M) and  $^{13}\text{C}$  NMR ( $\approx 7 \times 10^{-3}$  M)) were conveniently done, strictly under an atmosphere of nitrogen, for their *in situ* preparations (inside the cuvette or the NMR tube) obtained by the addition of ca. 3 - 4 molar equivalents of  $\text{Na}_2\text{S}_2\text{O}_4$  to previously deaerated solutions of  $[\text{Ru}(\text{phen})_2(\text{qdppz})]^{2+}$ . In each case, the solution was kept aside in dark for ca. 45 - 60 min. with occasional shaking before the spectral measurements were made.

$^1\text{H}$  NMR ( $\text{CD}_3\text{CN}/10\% \text{D}_2\text{O}$ , 200 MHz, TMS)  $\delta$ , ppm: 8.72(m, 6H), 8.34(s, 6H), 8.33(s, 2H), 8.12(m, 4H), 7.80(m, 8H).

$^{13}\text{C}$  NMR ( $\text{CD}_3\text{CN}/10\% \text{D}_2\text{O}$ , 200 MHz, TMS)  $\delta$ , ppm: 128.1, 129.7, 132.7, 138.9, 149.8, 155.1, 156.5 & 157.6.

All the spectroscopic and electrochemical experiments leading to the characterization of the new complexes synthesized here were carried out as described in chapter 2. While the hexafluorophosphate salts of the complexes were employed for the luminescence measurements in non-aqueous solvents (rigorously dried  $\text{CHCl}_3$ ,  $\text{CH}_2\text{Cl}_2$ , dichloroethane and  $\text{CH}_3\text{CN}$ ) and aqueous  $\text{CH}_3\text{CN}$  (10%  $\text{H}_2\text{O}$ ) solutions, the corresponding chloride salts were used for measurements in aqueous, aqueous buffered (buffer A: 5 mM tris, pH 7.1, 50 mM NaCl), micellar (SDS, 0.1M) and CT DNA (up to 200  $\mu\text{M}$ ) solutions.

### 3.2.5 DNA binding and photocleavage studies

Buffer A was used for absorption titration, differential-pulse voltammetry and luminescence measurements. Buffer B (1 mM phosphate, pH 7.0, 2 mM NaCl) was used for thermal denaturation experiments. Buffer C (1.5 mM  $\text{Na}_2\text{HPO}_4$ , 0.5 mM  $\text{NaH}_2\text{PO}_4$ , 0.25 mM  $\text{Na}_2\text{EDTA}$ , pH = 7.0) was used for the viscometric titrations. The chloride salt of the complexes was used in studies with DNA.

DNA melting- ( [DNA nucleotide phosphate] = 175  $\mu\text{M}$ , [drug] = 0 - 7  $\mu\text{M}$ ) and absorption titration ([DNA base pairs] = 0 - 70  $\mu\text{M}$  for  $[\text{Ru}(\text{phen})_2(\text{qdppz})]^{2+}$  and 0 - 420  $\mu\text{M}$  for  $[\text{Ru}(\text{phen})_2(\text{hqdpz})]^{2+}$ , [drug] = 60  $\mu\text{M}$ ) experiments were carried out as described in Chapter 2. Differential-pulse voltammetric experiments (highly polished glassy carbon working

electrode, Pt-wire counter electrode and SCE reference electrode) were performed for 0.1 mM of the complex in the absence and in the presence of increasing amounts (0 - 3 mM) of CT DNA.

Absorbance and current values were recorded after each successive addition of DNA solution and equilibration (ca. 10 min.). Data obtained from both the absorption- and electrochemical titration experiments were analyzed using a procedure first developed by Bard and co-workers during their electrochemical studies on DNA interactions of metallopolyridyl complexes<sup>15</sup> and subsequently adopted by others for absorption titration experiments involving binding of DNA by ruthenium complexes containing dppz and other strongly intercalating ligands.<sup>16</sup> This treatment is valid for cases of noncooperative, nonspecific binding of a ligand to DNA and it involves fitting of the data to equn. 2.18 (see chapter 2). Use of equn. 2.18 rather than equn. 2.17 was deemed more appropriate here owing to the strong binding of the complexes investigated in this study.

Viscometric titrations were performed with a Cannon-Ubbelohde viscometer at  $25 \pm 1$  °C as described in chapter 2. Titrations were performed for  $[\text{Ru}(\text{phen})_3]^{2+}$ ,  $[\text{Ru}(\text{phen})_2(\text{qdppz})]^{2+}$ , ethidium bromide (EtBr) (3 - 40  $\mu\text{M}$ ) and for  $\text{Na}_2\text{S}_2\text{O}_4$  (9 - 120  $\mu\text{M}$ ) in the presence and absence of  $[\text{Ru}(\text{phen})_2(\text{hqdpz})]^{2+}$  (3 - 40  $\mu\text{M}$ ). The concentration of CT DNA used in these experiments was 300  $\mu\text{M}$  (base pairs).

For the gel electrophoresis experiments, supercoiled pBR 322 DNA (100  $\mu\text{M}$  in nucleotide phosphate) in tris-HCl buffer (pH = 8.0) was treated with an 10  $\mu\text{M}$  of the metal complex and the mixture was incubated for 1 h. in the dark. The samples were then analyzed by 0.8% agarose gel

electrophoresis (Tris-acetic acid- EDTA buffer, pH = 8.0) at 40 V for 5 h and further processed as described in chapter 2. Irradiation experiments were carried out by keeping the pre-incubated (dark, 1 h.) samples inside the sample chamber of a JASCO Model FP-777 spectrofluorimeter ( $\lambda_{\text{exc}} = 440 \pm 5$  nm; slit width = 5 nm).

In the experiments with the topoisomerase, samples of 0.5  $\mu\text{g}$  pBR 322 in 20  $\mu\text{l}$  of the assay buffer (50 mM Tris, 50 mM NaCl, 1 mM EDTA, 1 mM DTT and 100  $\mu\text{g}$  nuclease free BSA, 1 mM  $\text{MgCl}_2$ ), 2 - 3 units of topoisomerase and  $[\text{Ru}(\text{phen})_2(\text{qdppz})]^{2+}$  (1 - 9  $\mu\text{M}$ ) were used. The unwinding angle ( $\Phi$ ) was calculated as described in chapter 2. It should be noted here that the added ruthenium concentrations in this assay could be assumed to be totally bound based on the absorption titration data (*vide infra*). Two independent control experiments were also carried out under the same set of experimental conditions. In the first control, no drug was used and here, no Form I could be detected upon electrophoresis of the samples treated only with topoisomerase. In the other control where EtBr was used as the intercalator; the value of  $\Phi$  calculated was found to be nearly equal ( $26 \pm 4^\circ$ ) to that reported in the literature ( $24 \pm 2^\circ$ ).<sup>17b</sup>

### 3.3 Results and discussion

The 'untypical' electronic structure of dppz, which has been proposed<sup>18</sup> to impart to it features both of an  $\alpha, \alpha'$ -diimine chelate and of a 1,4-diazine moiety, together with the consequent structural and electronic features of the complexes derived from this versatile ligand seem to have made them attractive candidates for use in various applications.<sup>3-8</sup> In this

study, we have synthesized a dipyridophenazine ligand fused with a quinone moiety in an attempt to assess the effects due to this additional, electroactive component on the functions associated with the resulting metal-complexes.<sup>19</sup> Three important aspects of the mixed-ligand complexes  $[\text{Ru}(\text{phen})_2(\text{qdppz})]^{2+}$  and  $[\text{Ru}(\text{phen})_2(\text{hqdpz})]^{2+}$  which contain qdppz or its hydroquinone form as the 'active' ligand have been addressed in this Chapter: These are: (i) DNA binding (ii) DNA photocleavage and (iii) luminescence as well as redox-switching of luminescence. Before we take up these issues, it is instructive to examine the details concerning the synthesis and characterization of these new complexes in light of those of the other structurally and functionally similar systems reported previously.

### 3.3.1 Synthesis and chracterization

Synthesis of qdppz and  $[\text{Ru}(\text{phen})_2(\text{qdppz})]^{2+}$  are illustrated in Fig. 3.1 and the relevant details have been provided in the Experimental Section. Our procedure for the synthesis of qdppz is marginally different from that reported recently by Lopez et al.<sup>12</sup> Refluxing an ethanol solution containing readily accessible phen-dione and 1,2-diamino anthraquinone, subsequent work-up and purification by recrystallization gave the desired ligand in pure form.  $[\text{Ru}(\text{phen})_2(\text{qdppz})](\text{PF}_6)_2$  was prepared by condensing  $\text{Ru}(\text{phen})_2\text{Cl}_2$  and qdppz in refluxing ethylene glycol and addition of  $\text{NH}_4\text{PF}_6$ . This  $\text{PF}_6$  salt was converted to the water-soluble chloride salt,  $[\text{Ru}(\text{phen})_2(\text{qdppz})]\text{Cl}_2$ , by the standard procedure using TBACl. Each synthetic step involved here is straightforward and provides good yield of the desired product in pure form.

**Table. 3.1** UV-visible data

Compound	$\lambda_{\max}$ , nm (log $\epsilon$ )
qdppz <sup>a</sup>	259 (4.62), 281 (4.58), 392 (4.13) 410 (4.13)
dppz <sup>a</sup>	269 (4.73), 295 (4.28), 359 (4.06) 378 (4.07)
[Ru(phen) <sub>2</sub> (qdppz)] <sup>2+</sup> <sup>b</sup>	263 (5.09), 278 (4.92), 302 (sh) 388 (4.32), 438 (4.29)
[Ru(phen) <sub>2</sub> (dppz)] <sup>2+</sup> <sup>b</sup>	265 (5.11), 277 (sh), 360 (4.39) 369 (4.35), 443 (4.33)

a: In CH<sub>2</sub>Cl<sub>2</sub>b: In CH<sub>3</sub>CN

qdppz had been characterized earlier by UV-visible and infra-red methods<sup>12</sup> and, our data agree well with the reported data. Additional characterization of this ligand has been carried out in the present study by elemental analysis, FABMS, <sup>1</sup>H NMR and electrochemical methods (see Tables 3.1 and 3.2). These data are also consistent with the structure and integrity of the compound. The PF<sub>6</sub><sup>-</sup> salt of [Ru(phen)<sub>2</sub>(qdppz)]<sup>2+</sup> gave

satisfactory elemental analysis and it showed expected pattern in the FABMS spectrum. In addition, the peak positions and their intensities in the  $^1\text{H}$  and  $^{13}\text{C}$  NMR spectra of the complex gave sufficient evidence for its structure. The complex also showed the characteristic MLCT band at 438 nm and bands due to the intra-ligand transitions at 388 (qdppz) and 263 (phen) nm in the UV-visible spectrum (see Table 3.1). The spectra of phen, qdppz and  $[\text{Ru}(\text{phen})_2(\text{qdppz})](\text{PF}_6)_2$  given in Fig. 3.2 serve to illustrate this point.

The infra-red spectra of qdppz and  $[\text{Ru}(\text{phen})_2(\text{qdppz})]^{2+}$  both showed a peak at  $1670\text{ cm}^{-1}$  ascribable to the quinone-carbonyl stretching in each case thus confirming that chelation of qdppz to ruthenium has not affected the quinone part of this ligand. The well-defined cyclic voltammetric responses ( $i_p$  vs.  $v^{1/2} = \text{constant}$  where  $i_p$  is the peak current and  $v$  is the scan rate,  $i_{pa}/i_{pc} = 0.9 - 1.0$  where  $i_{pa}$  and  $i_{pc}$  refer to anodic and cathodic peak currents, respectively and  $\Delta E_p = 60 - 80\text{ mV}$  where  $E_p$  is the peak potential for these electron transfer processes<sup>20</sup>) seen at +1.36 and -0.37 V for the complex can be assigned to  $\text{Ru}^{\text{III}}/\text{Ru}^{\text{II}}$  and qdppz/qdppz $^{\cdot-}$  couples, respectively (see Table 3.2). The spectral and redox characteristics of  $[\text{Ru}(\text{phen})_2(\text{qdppz})]\text{Cl}_2$  were found to be essentially similar to those described above for the  $\text{PF}_6$  salt.

$[\text{Ru}(\text{phen})_2(\text{hqdpz})]^{2+}$  could be obtained by the reduction of  $[\text{Ru}(\text{phen})_2(\text{qdppz})]^{2+}$  with  $\text{Na}_2\text{S}_2\text{O}_4$  and the process could be reversed to get back the quinone-form by  $\text{Ce}(\text{NH}_4)_2(\text{NO}_3)_6$ . Electrochemical and fluorescence methods have provided further support for the reversible nature of this quinone/hydroquinone redox reaction and this aspect will be addressed in a later section of this Chapter. The reduced complex obtained *via* the chemical

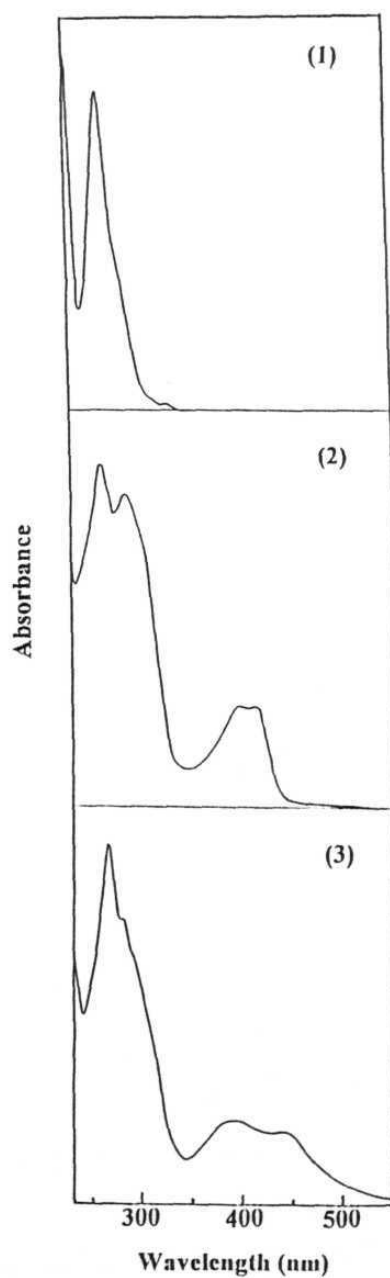


**Fig. 3.2.** UV-visible spectra of phen (1) in  $\text{CH}_2\text{Cl}_2$  and of, qdppz (2) and  $[\text{Ru}(\text{phen})_2(\text{qdppz})]^{2+}$  (3) both in  $\text{CH}_3\text{CN}$ .

means could be characterized by UV-visible, NMR and electrochemical methods. In particular, and as illustrated in Fig. 3.3, the

**Table. 3.2** Cyclic voltammetric data

Compound	Potential, V vs SCE	
	$E_{1/2 \text{ red}}^a$	$E_{1/2 \text{ ox}}^b$
qdppz	-0.46, -1.48	-
phen	-1.92	-
dppz	-1.46	-
$[\text{Ru}(\text{phen})_2(\text{qdppz})]^{2+}$	-0.37, -1.27, -1.49	+1.36
$[\text{Ru}(\text{phen})_3]^{2+}$	-1.28, -1.44, -1.71	+1.26
$[\text{Ru}(\text{phen})_2(\text{dppz})]^{2+}$	-0.87, -1.30, -1.52	+1.33

a: In DMF, 0.1 M TBAPF<sub>6</sub>

b: In CH<sub>3</sub>CN, 0.1 M TBAPF<sub>6</sub>

complex shows only the MLCT band (442 nm) at  $\lambda > 350$  nm, with the quinone  $\pi$ - $\pi^*$  transition (388 nm) of its precursor  $[\text{Ru}(\text{phen})_2(\text{qdppz})]^{2+}$  having clearly disappeared from the UV-visible spectrum. Equally important is the appearance of a pair of <sup>13</sup>C NMR signals at 156.5 and 157.6 ppm ascribable to the phenolic carbon atoms of the complex in place of those due to quinone-carbon atoms on  $[\text{Ru}(\text{phen})_2(\text{qdppz})]^{2+}$  (182.8 and 183.5 ppm).

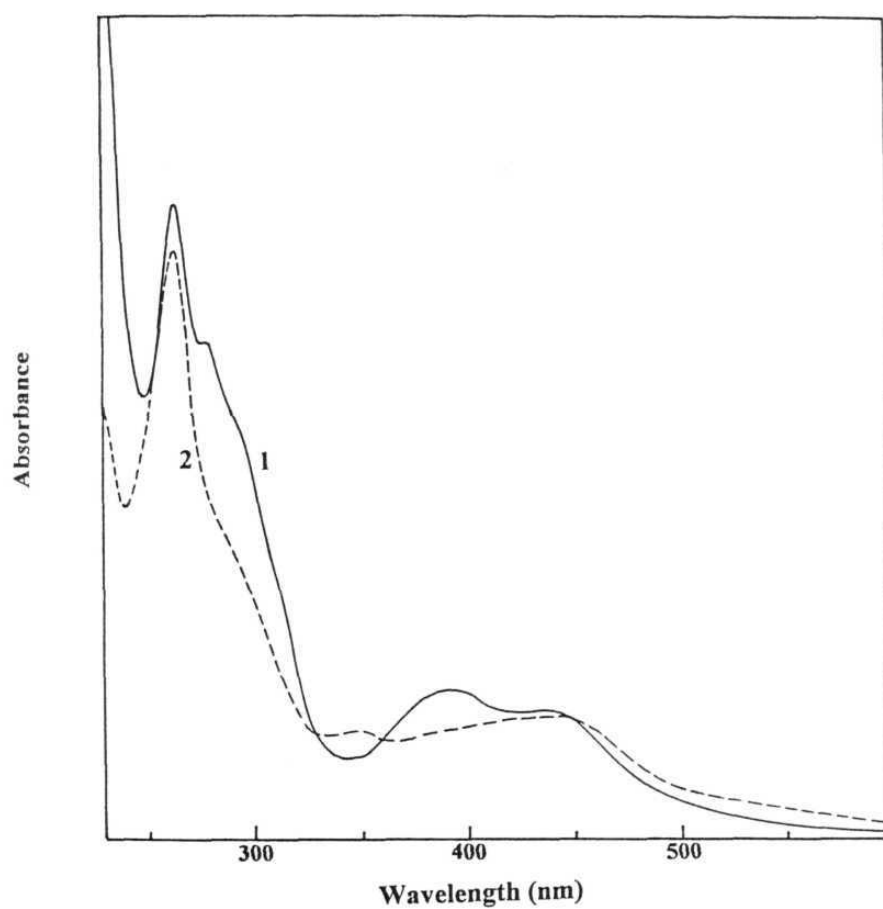


Fig.3.3. UV-visible spectra of  $[\text{Ru}(\text{phen})_2(\text{qdppz})]^{2+}$  (1) and  $[\text{Ru}(\text{phen})_2(\text{hqdpz})]^{2+}$  (2) in  $\text{CH}_3\text{CN}/\text{H}_2\text{O}$  (10:1, v/v). The reduced complex has been obtained by the dithionite reduction of  $[\text{Ru}(\text{phen})_2(\text{qdppz})]^{2+}$ .

As far as the UV-visible features of  $[\text{Ru}(\text{phen})_2(\text{hqdpz})]^{2+}$  are concerned, it is interesting to note that  $[\text{Ru}(\text{phen})_2(\text{DPPN})]^{2+}$  where DPPN is benzo[i]dipyrido [3,2-*a*:2',3'-*c*]phenazine, has been reported to show a transition at 391 nm that is ascribable to the  $\pi$ - $\pi^*$  transition of the 'benzene-fused phenazine' moiety<sup>3d, 7b</sup>. However, such a transition is not apparent in the spectrum of  $[\text{Ru}(\text{phen})_2(\text{hqdpz})]^{2+}$  incorporating the 'naphthalene-fused phenazine' ligand. It is possible that the this intraligand  $\pi$ - $\pi^*$  transition is broad and red-shifted and that there is an overlap of this band with the MLCT band. In fact,  $[\text{Ni}(\text{phen})_2(\text{hqdpz})]^{2+}$  (obtained by dithionite reduction of the corresponding quinone complex) shows broad absorption between 300 - 400 nm.<sup>21</sup>

### 3.3.2 DNA-binding

Initially, interaction of  $[\text{Ru}(\text{phen})_2(\text{qdppz})]\text{Cl}_2$  with DNA was monitored by absorption titration (MLCT band) and thermal denaturation (monitoring  $\Lambda_{260}$  of DNA) methods. In the presence of increasing amounts of CT DNA the complex showed bathochromic shift ( $4 \pm 1$  nm) and hypsochromism ( $75 \pm 3$  %) in the UV-visible spectrum (see Fig. 3.4) and increased values (at  $[\text{DNA nucleotide phosphate}]/[\text{Ru}] = 25$ ) of both the DNA melting temperature ( $\Delta T_m = 6 \pm 1$  °C) and the curve width ( $\Delta \sigma_T = 4 \pm 1$  °C) in the thermal denaturation experiments.  $T_m$  and  $\sigma_T$  values increased with increasing addition of the metal complex as expected. These observations are reminiscent of those reported earlier for various metallointercalators<sup>22</sup> and suggest that  $[\text{Ru}(\text{phen})_2(\text{qdppz})]\text{Cl}_2$  binds strongly to DNA by an intercalative mode. It should be noted here that absorption saturation was evident even at

$[\text{Drug}]/[\text{DNA}] = 1$  (see Fig. 3.4) suggesting essentially stoichiometric binding. The binding data could not be satisfactorily fit either to equn 2.17 or to the McGhee and von Hippel equation<sup>23</sup> with and without incorporating the cooperativity parameters as is true for  $[[\text{Ru}(\text{NH}_3)_4]_2(\text{dpb})]^{4+}$ .<sup>16</sup> On the other hand, the best fit of the binding data to equn. 2.18 gave a values of  $0.27 \pm 0.04$  and  $(1 \pm 0.3) \times 10^6 \text{ M}^{-1}$  for  $s$  and  $K_b$ , respectively. Thus, accurate determination of the DNA binding constant could not be made for  $[\text{Ru}(\text{phen})_2(\text{qdppz})]^{2+}$ . This is true for the majority of previously studied dppz complexes.<sup>3,4,6, 16,23</sup> Thus, the near-stoichiometric binding with DNA observed even at micromolar concentrations suggests that the  $K_b$  should be  $> 10^6 \text{ M}^{-1}$  for this complex.

It is of interest to know which ligand between the available two on  $[\text{Ru}(\text{phen})_2(\text{qdppz})]^{2+}$ , i. e. phen or qdppz, intercalates with DNA. In this regard, it may be noted that the strength of DNA binding by  $[\text{Ru}(\text{phen})_2(\text{qdppz})]^{2+}$  reported here is higher than that by  $[\text{Ru}(\text{phen})_3]^{2+}$  but, it is in the same range as that for the Os(II), Ru(II), Ni(II) and Co(III) complexes containing dppz (or modified dppz).<sup>3-8</sup> Although this observation argues in favour of an interaction of the bound-qdppz with DNA, we note that it is only an indirect evidence. This is mostly because the UV-visible method employed here for the estimation of the binding constant does not monitor exclusive properties of the individual ligands on  $[\text{Ru}(\text{phen})_2(\text{qdppz})]^{2+}$ . We adduce direct evidence for the intercalation of bound-qdppz with DNA by the application of viscometric, topoisomerase assay and electrochemical methods. Intercalation of a ligand to DNA is known to cause a significant increase in the viscosity of a DNA solution due to an increase in

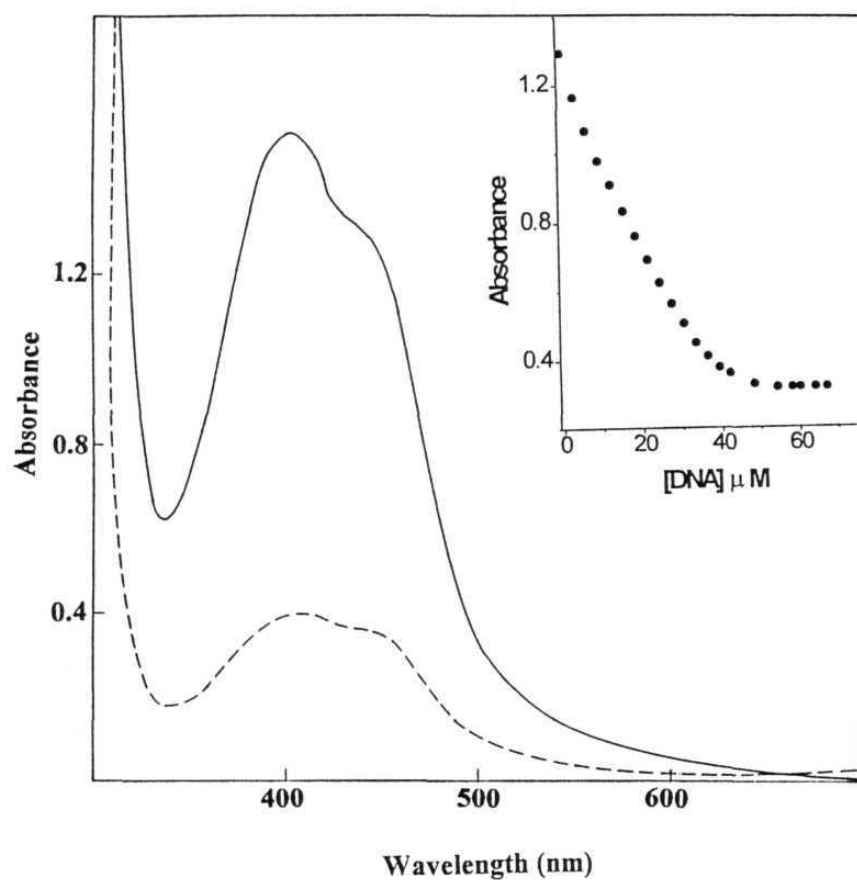


**Fig. 3.4.** UV-visible spectra of  $[\text{Ru}(\text{phen})_2(\text{qdppz})]^{2+}$  (60  $\mu\text{M}$ ) in the absence (—) and presence (---) of CT DNA (max. 70  $\mu\text{M}$  base pairs, buffer A). Inset: Plot of the absorption titration data at 440 nm, demonstrating the saturation of binding of  $[\text{Ru}(\text{phen})_2(\text{qdppz})]^{2+}$  to CT DNA.

the separation of the base pairs at the intercalation site and, hence, an increase in the overall DNA molecular length. In contrast, a ligand that binds in the DNA-grooves causes a less pronounced change (positive or negative) or no change in the viscosity of a DNA solution.<sup>24</sup> The effects of  $[\text{Ru}(\text{phen})_2(\text{qdppz})]^{2+}$ ,  $[\text{Ru}(\text{phen})_2(\text{hqdpzz})]^{2+}$  and  $[\text{Ru}(\text{phen})_3]^{2+}$  on the viscosity of CT DNA solution were studied in order to assess the binding mode of these complexes with DNA. Plots of  $\eta/\eta_0$  vs.  $[\text{drug}]/[\text{DNA}]$  are shown in Fig. 3.5. As seen in this figure, while  $[\text{Ru}(\text{phen})_3]^{2+}$  does not affect the DNA viscosity as previously reported,<sup>22</sup> there is a positive change of viscosity with increasing addition of the complex for  $[\text{Ru}(\text{phen})_2(\text{qdppz})]^{2+}$  suggesting intercalation.<sup>22</sup> On the other hand, significant negative change in the viscosity of DNA is noticed for  $[\text{Ru}(\text{phen})_2(\text{hqdpzz})]^{2+}$  that is generated *in situ* in the viscometric cell by the dithionite reduction of  $[\text{Ru}(\text{phen})_2(\text{qdppz})]^{2+}$  ( $[\text{Ru}(\text{phen})_2(\text{qdppz})]^{2+}/\text{Na}_2\text{S}_2\text{O}_4 = 1/3$ , mole/mole). However, it should be noted that, as such, addition of dithionite alone to DNA solutions results in negative changes in the viscosity. A mixture of  $\text{Na}_2\text{S}_2\text{O}_4$  and  $\text{Na}_2\text{SO}_4$  also effected negative changes in the DNA viscosity in a similar fashion to that noted for  $\text{Na}_2\text{S}_2\text{O}_4$  alone in Fig. 3.5 (note: addition of salts is known to influence the viscosity of DNA<sup>25</sup>). Thus, the 'net' viscosity change observed for  $[\text{Ru}(\text{phen})_2(\text{hqdpzz})]^{2+}$  is similar to that exhibited by  $[\text{Ru}(\text{phen})_3]^{2+}$  as illustrated in Fig. 3.5.

Apart from the viscosity measurements, experiments involving the DNA topoisomerase assay have also provided a measure of intercalative binding by  $[\text{Ru}(\text{phen})_2(\text{qdppz})]^{2+}$ . The extent of DNA helix unwinding by a non-covalently bound species may be quantitated by examining the change in

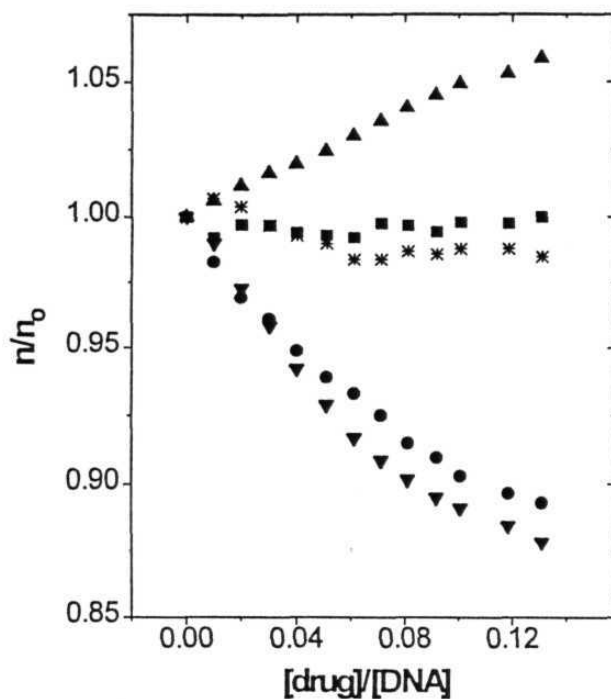


**Fig. 3.5.** Results of viscometric titrations carried out for CT DNA (300  $\mu\text{M}$  in base pairs, Buffer C) in the presence of ( $\blacktriangle$ )  $[\text{Ru}(\text{phen})_2(\text{qdppz})]^{2+}$  (3 - 40  $\mu\text{M}$ ), ( $\blacksquare$ )  $[\text{Ru}(\text{phen})_3]^{2+}$  (3 - 40  $\mu\text{M}$ ), ( $\bullet$ )  $\text{Na}_2\text{S}_2\text{O}_4$  (9 - 120  $\mu\text{M}$ ) and ( $\blacktriangledown$ )  $\text{Na}_2\text{S}_2\text{O}_4$  (9 - 120  $\mu\text{M}$ ) +  $[\text{Ru}(\text{phen})_2(\text{qdppz})]^{2+}$  (3 - 40  $\mu\text{M}$ ). Plot marked with \* is obtained by subtracting data of  $\text{Na}_2\text{S}_2\text{O}_4$  alone from that of  $\text{Na}_2\text{S}_2\text{O}_4$  +  $[\text{Ru}(\text{phen})_2(\text{qdppz})]^{2+}$ .

the superhelical density in a plasmid after relaxation of the plasmid in the presence of bound complex with topoisomerase I.<sup>17b</sup> Figure 3.6 shows the unwinding of pBR 322 DNA by  $[\text{Ru}(\text{phen})_2(\text{qdppz})]^{2+}$  following incubation with topoisomerase I in the presence of increasing amounts of the ruthenium complex. An unwinding angle of  $34 \pm 10^\circ$  per ruthenium bound is obtained for  $[\text{Ru}(\text{phen})_2(\text{qdppz})]^{2+}$ . This value is consistent with those observed for other strongly intercalating ruthenium complexes such as  $[\text{Ru}(\text{bpy})_2(\text{phi})]^{2+}$  ( $\text{phi}$  = 9, 10 - phenanthrenequinonediimine)<sup>26</sup> and  $[\text{Ru}(\text{bpy})_2(\text{dppz})]^{2+}$ .<sup>3e</sup> On the other hand, topoisomerase assay carried out in presence of the reduced complex  $[\text{Ru}(\text{phen})_2(\text{hqdpz})]^{2+}$  gave a lower value for the unwinding angle ( $16 \pm 7^\circ$ ) per bound ruthenium, as expected.

Electrochemical methods, although can be easily adopted to monitor the DNA interaction by small molecules, have rarely been employed for this purpose in the case of metallopolyridyls.<sup>5,6,15,27</sup> Differential-pulse voltammetric method has been employed in the present study to monitor the DNA-binding by  $[\text{Ru}(\text{phen})_2(\text{qdppz})]^{2+}$ . In buffer A, ruthenium-bound qdppz could be reduced at  $-0.16 \text{ V}$  - a potential that is well within the solvent discharge limit and far away from the peaks due to  $\text{Ru}^{\text{III}}/\text{Ru}^{\text{II}}$ ,  $\text{Ru}^{\text{II}}/\text{Ru}^{\text{I}}$  or  $\text{phen}/\text{phen}^-$  redox couples. Coulometric studies revealed that this electrode process involves a  $2e^-(2\text{H}^+)$  transfer (see Experimental Section) and generates  $[\text{Ru}(\text{phen})_2(\text{hqdpz})]^{2+}$  (*vide infra*). Successive additions of CT DNA to a solution of  $[\text{Ru}(\text{phen})_2(\text{qdppz})]^{2+}$  resulted in diminution of the peak current (maximum:  $40 \pm 5 \%$ ) and cathodic shifts in the peak potential (maximum:  $33 \pm 2 \text{ mV}$ ) in the differential-pulse voltammograms as shown in Fig. 3.7. While the decrease in peak current is in conformity with the proposal that



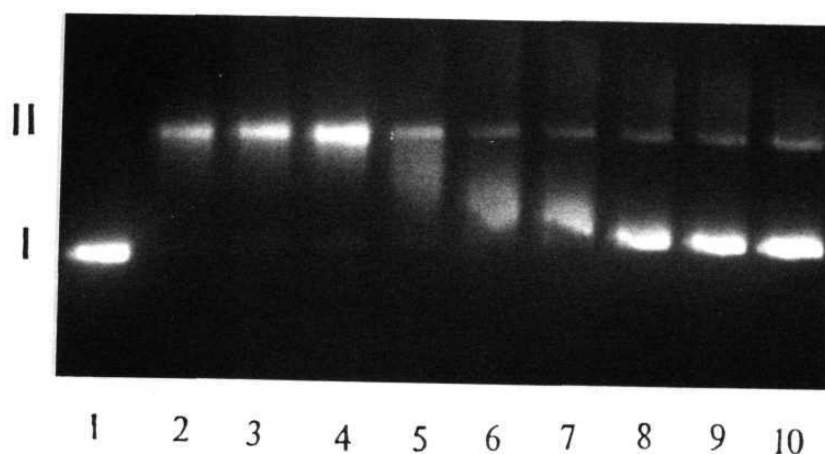


**Fig. 3.6** Agarose gel showing the unwinding of pBR 322 by  $[\text{Ru}(\text{phen})_2(\text{qdppz})]^{2+}$  after incubation with topoisomerase I in the presence of increasing amounts of ruthenium complex. While Lane 1 is pBR 322 control (without incubation), Lane 2 shows DNA after incubation with topoisomerase in the absence of the complex. Lanes 3 - 10 show the topoisomers after incubation of DNA, topoisomerase and 1.1, 2.2, 3.3, 4.4, 5.5, 6.6, 8 and 9  $\mu\text{M}$  of  $[\text{Ru}(\text{phen})_2(\text{qdppz})]^{2+}$ , respectively.

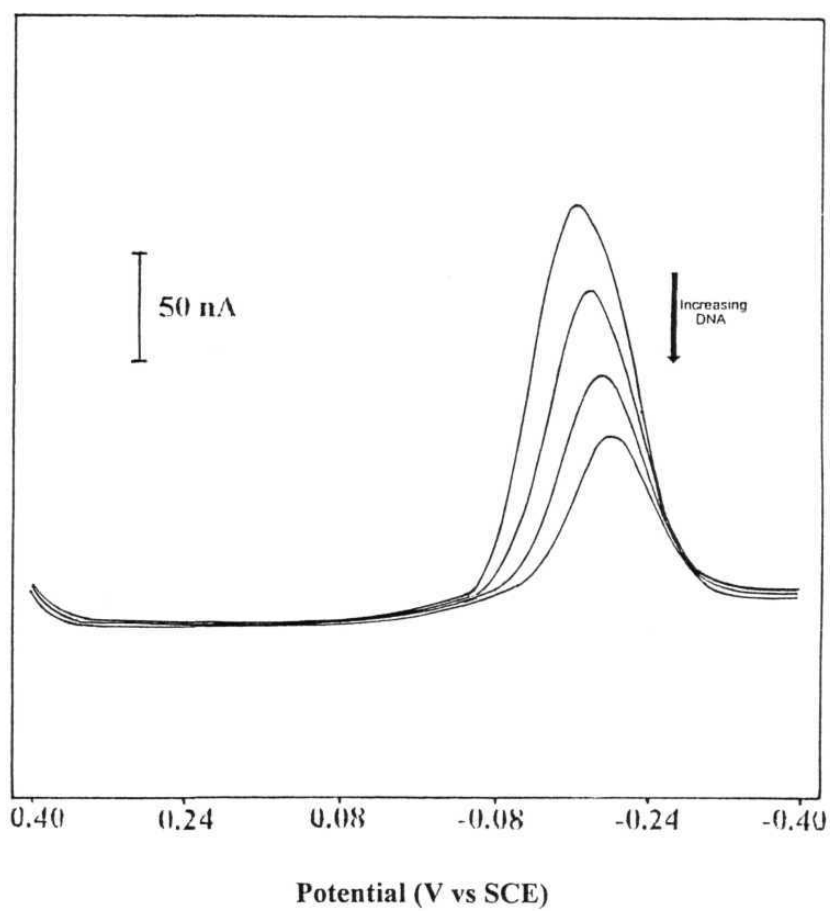


**Fig. 3.7.** Differential-pulse voltammograms (scan rate = 10 mV/s; modulation amplitude = 10 mV PP) of  $[\text{Ru}(\text{phen})_2(\text{qdppz})]^{2+}$  (0.1 mM, buffer A) in the absence (top) and in the presence of increasing amounts of CT DNA (0.3, 0.9 and 3.0 (bottom) mM, respectively).

ruthenium-bound qdppz intercalates with DNA,<sup>5,6,15,27</sup> the cathodic shift of the peak potential observed here merits further discussion.

It has been previously shown that binding of the metal complex to DNA can bring about a shift in the redox potential if one redox state is more strongly bound than the other.<sup>15</sup> The change in the binding constant can be determined according to equn. 3.1.

$$E_0^b - E_0^f = (RT/nF) \log (K_{\text{red}}/K_{\text{ox}}) \quad \text{----- (3.1)}$$

Here,  $E_0^b$  and  $E_0^f$  are the thermodynamic redox potentials for the bound and free complexes, respectively,  $n$  is the number of electrons transferred,  $K_{\text{red}}/K_{\text{ox}}$  is the ratio of binding constants for the reduced and oxidized species and, other parameters have their usual meaning. Substitution of appropriate values to suit the electrochemistry of  $[\text{Ru}(\text{phen})_2(\text{qdppz})]^{2+}$  and from a limiting shift of 33 mV, we calculate that  $K[\text{Ru}(\text{phen})_2(\text{qdppz})]^{2+}/K[\text{Ru}(\text{phen})_2(\text{hqdpz})]^{2+}$  is  $\approx 12.6$ . Note here that  $n = 2$  for the reduction of  $[\text{Ru}(\text{phen})_2(\text{qdppz})]^{2+}$  in aqueous solutions and that the electrode process (*and not the overall electrochemical reaction*) was found to be not strictly reversible and diffusion controlled during the cyclic voltammetric experiments in buffer B ( $E_p - E_a = 50 - 130$  mV and  $i_{pc}/\nu^{1/2}$  is not a constant with respect to scan rates ( $\nu$ ) ranging between 50 - 500 mV/s). However, a tendency towards reversibility was noticed in the presence of DNA. In any case, we note that these electrochemical results do not have any significant effect on the value of the ratio of binding constants. Thus, the reduced species binds to DNA less

strongly than  $[\text{Ru}(\text{phen})_2(\text{qdppz})]^{2+}$  and, this result is in agreement with the known intercalative ability of the quinone moiety.<sup>10,11</sup>

Results of absorption titration experiments carried out with the reduced complex also suggest the same.  $[\text{Ru}(\text{phen})_2(\text{hqdpz})]^{2+}$  (buffer A,  $\text{Na}_2\text{S}_2\text{O}_4$ ) showed bathochromic shifts (maximum:  $4 \pm 1$  nm) and hypsochromism (maximum:  $25 \pm 3$  %) during the UV-visible titration with DNA. The estimated (equn. 2.18) value of  $K_b$  is only  $(1 \pm 0.2) \times 10^5 \text{ M}^{-1}$  ( $s = 0.8 \pm 0.1$ ) as against the strong binding exhibited by  $[\text{Ru}(\text{phen})_2(\text{qdppz})]^{2+}$ . Note here that  $K_b$  for  $[\text{Ru}(\text{phen})_2(\text{hqdpz})]^{2+}$  obtained by the UV-visible methods is nearly equal to that predicted on the basis of electrochemical redox potential data using equn. 3.1 (i. e.  $10^6 / 12.6 = 8 \times 10^4 \text{ M}^{-1}$ ).

### 3.3.3 DNA Photocleavage

Control runs in the agarose gel electrophoresis experiments have suggested that untreated plasmid pBR 322 DNA does not show any perceptible cleavage in the dark and even upon irradiation by  $440 \pm 5$  nm light for 2 h. (Lanes 1 and 2, Fig. 3.8). Similarly, DNA nicking was not observed for the plasmid treated with  $[\text{Ru}(\text{phen})_2(\text{qdppz})]\text{Cl}_2$  in the dark run (Lane 3). On the other hand, irradiation of DNA in the presence of the complex for 25 min. caused complete conversion of the supercoiled form (Form I) generating the relaxed circular DNA (Form II) under similar experimental conditions (Lane 4). The reduced complex, obtained from dithionite reduction of  $[\text{Ru}(\text{phen})_2(\text{qdppz})]\text{Cl}_2$ , was also seen to cleave DNA albeit, with less efficiency (see Lanes 4 and 5). To sum up, these results demonstrate that the DNA photocleavage efficiencies of the two new complexes follow a trend

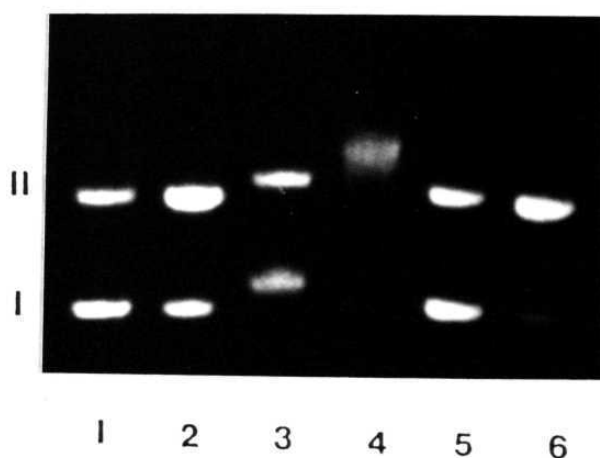


**Fig. 3.8.** Light-induced nuclease activity of  $[\text{Ru}(\text{phen})_2(\text{qdppz})]^{2+}$  and  $[\text{Ru}(\text{phen})_2(\text{hqdpz})]^{2+}$ . Dark and light ( $440 \pm 5 \text{ nm}$ ) experiments: Lanes 1 and 2, untreated pBR 322 ( $100 \mu\text{M}$  in nucleotide phosphate) in dark and upon irradiation (2 h.); Lanes 3 and 4, pBR 322 +  $[\text{Ru}(\text{phen})_2(\text{qdppz})]^{2+}$  ( $10 \mu\text{M}$ ) in dark and upon irradiation for 25 min.; Lanes 5 and 6, pBR 322 +  $[\text{Ru}(\text{phen})_2(\text{hqdpz})]^{2+}$  ( $10 \mu\text{M}$ ) in dark and upon irradiation for 25 min.

that is not only consistent with their DNA-binding abilities but also with the known capabilities of other previously reported complexes containing the parent ligand dppz.<sup>3-8</sup>

Additional evidence for the efficient DNA photoniccking of  $[\text{Ru}(\text{phen})_2(\text{qdppz})]^{2+}$  and  $[\text{Ru}(\text{phen})_2(\text{hqdpz})]^{2+}$  comes from a comparison of their DNA photocleavage abilities with those of the related complexes  $[\text{Ru}(\text{phen})_3]^{2+}$  and  $[\text{Ru}(\text{phen})_2(\text{dppz})]^{2+}$ . Under comparable experimental conditions, DNA nicking efficiencies of these complexes were seen to roughly follow the trend:  $[\text{Ru}(\text{phen})_3]\text{Cl}_2 \ll [\text{Ru}(\text{phen})_2(\text{hqdpz})]\text{Cl}_2 \leq [\text{Ru}(\text{phen})_2(\text{dppz})]\text{Cl}_2 < [\text{Ru}(\text{phen})_2(\text{qdppz})]\text{Cl}_2$ . This observed differences in the DNA photocleavage efficiencies of these complexes do not seem to arise from differences in the light absorption abilities since, their molar extinction coefficients at 440 nm are found to be close to each other ( $\log \epsilon = 4.3 \pm 0.2$ ).

As far as the mechanism of DNA photocleavage by these complexes are concerned, photocleavage by  $[\text{Ru}(\text{phen})_3]\text{Cl}_2$  has been reported<sup>28</sup> to involve  $^1\text{O}_2$  - based mechanism and, to a large extent, that by  $[\text{Ru}(\text{phen})_2(\text{dppz})]\text{Cl}_2$  is also expected to involve oxygen-centred reactive species including  $^1\text{O}_2$  (excited state of this complex was seen to generate  $^1\text{O}_2$  in DMF as evidenced by the decrease of absorbance due to 1,3-diphenylisobenzofuran). Indeed, photoinduced DNA cleavage by  $[\text{Ru}(\text{bpy})_2(\text{dppz})]^{2+}$  has been reported to occur via a Type II mechanism.<sup>7a</sup> On the other hand, nature of the reactive intermediates as well as the mechanism of their action involved in the efficient DNA photocleavage by the two new complexes synthesized in this study have not been explored in detail so far. However, careful experiments with various 'inhibitors' suggested that  $\text{N}_2$ ,

DABCO, D<sub>2</sub>O, mannitol, dimethyl sulfoxide and super-oxide dismutase (SOD) did not affect the DNA-nicking efficiency of [Ru(phen)<sub>2</sub>(qdppz)]<sup>2+</sup> suggesting that none of the reactive oxygen species (<sup>1</sup>O<sub>2</sub>, OH• or O<sub>2</sub><sup>•-</sup>) play a significant role in the cleavage mechanism (see Fig. 3.9). This situation is unlike the case with OH•-mediated DNA cleavage by [(η<sup>5</sup>-C<sub>5</sub>Me<sub>5</sub>)Ru(NO)(dppz)]<sup>2+7b</sup> but, quite similar to that reported recently for [Re(dppz)(CO)<sub>3</sub>(py)]<sup>+</sup> (py = pyridine)<sup>7c</sup>, indicating the possibility of photoinduced DNA cleavage by [Ru(phen)<sub>2</sub>(qdppz)]<sup>2+</sup> *via* a direct oxidation of the biopolymer. In this regard, it is interesting to note that whereas excitation of [Ru(phen)<sub>2</sub>(hqdpz)]<sup>2+</sup> at 440 nm can activate only the MLCT state, that of [Ru(phen)<sub>2</sub>(qdppz)]<sup>2+</sup> can, in principle, activate both its MLCT and localized quinone (π-π\*) states owing to a partial overlap of the corresponding absorption bands (see Fig. 3.2). While irradiation into the MLCT band of [Ru(phen)<sub>2</sub>(qdppz)]<sup>2+</sup> can generate a species containing oxidized ruthenium and reduced qdppz (1 e<sup>-</sup> transfer), direct excitation of the bound-qdppz is expected to provide the triplet quinone. Both these quinone-based, transient species are known to be potent DNA cleaving agents capable of reacting with the duplex *via* various mechanisms including hydrogen abstraction, electron transfer etc.<sup>10</sup>

### 3.3.4 Luminescence Studies

Here, we first present results on individual luminescence characteristics of the oxidized and the reduced species and then briefly discuss on the redox-reversibility aspect associated with their photoluminescence.

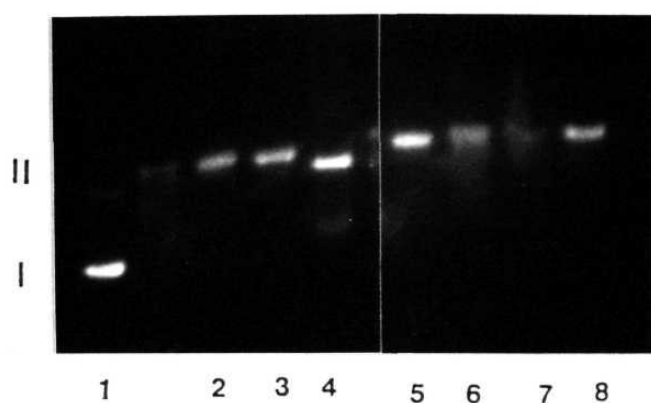


**Fig. 3.9.** Photograph showing effects of 'inhibitors' on the nuclease activity of  $[\text{Ru}(\text{phen})_2(\text{qdppz})]^{2+}$ . All the samples were irradiated for 25 min. at 440 nm after incubation for 1 h. : Lane 1: control pBR 322 DNA (100  $\mu\text{M}$  nucleotide phosphate), Lane 2: DNA +  $[\text{Ru}(\text{phen})_2(\text{qdppz})]^{2+}$  (10  $\mu\text{M}$ ); Lane 3: DNA + Ru in  $\text{N}_2$  atmosphere; Lane 4: DNA + Ru in  $\text{D}_2\text{O}$ ; Lane 5-8: DNA + Ru + DABCO (20 mM), mannitol (100 mM), DMSO (1 M) or SOD (20  $\mu\text{g/ml}$ ), respectively.

$[\text{Ru}(\text{phen})_2(\text{qdppz})]^{2+}$  was found to be weakly luminescent ( $\phi \leq 10^{-4}$ ) in rigorously dried  $\text{CHCl}_3$ ,  $\text{CH}_2\text{Cl}_2$ , dichloroethane and  $\text{CH}_3\text{CN}$  and to be essentially non-luminescent in buffer A, aqueous  $\text{CH}_3\text{CN}$  (10%  $\text{H}_2\text{O}$ ) and micellar solutions. The weak luminescence observed for the complex in non-aqueous solvents can be rationalized in terms of an intramolecular photoinduced electron transfer (PET) quenching of its MLCT state by the appended quinone fragment as was the case with  $\text{Re}(\text{qdppz})(\text{CO})_3\text{Cl}$ <sup>12</sup> or  $[\text{Ru}(\text{bpy})_2(\text{bpy-BQ})]^{2+}$  - a covalently-linked, Ru(II) complex-benzoquinone system reported previously.<sup>29</sup> An additional process involving the sensitivity of the excited state to quenching by water and the subsequent increase in the non-radiative decay rate seems to be responsible for the total lack of emission observed for the complex in the aqueous environments. Indeed, in aqueous solutions, excited state of  $[\text{Ru}(\text{phen})_2(\text{dppz})]^{2+}$  has been reported to be highly quenched due to proton transfer from the solvent to the dipyridophenazine ligand.<sup>3,6,30</sup>

$[\text{Ru}(\text{phen})_2(\text{hqdpz})]^{2+}$ , as obtained by *in situ* dithionite reduction, was found to be essentially non-luminescent in aqueous solutions with or without buffer A as was the case with its oxidized form. However, the complex showed its MLCT luminescence ( $\lambda_{\text{em}}^{\text{max}} = 601 \text{ nm}$ , but its intra-ligand character cannot be entirely ruled out) in micellar and aqueous  $\text{CH}_3\text{CN}$  solutions with the quantum yields of approximately 0.002 and 0.01, respectively (Fig. 3.10). We believe that the PET reaction, which has been proposed above for the quinone-containing complex, does not operate in this hydroquinone-containing complex. Thus, the lack of luminescence observed in water and in aqueous buffered solutions can be explained solely on the

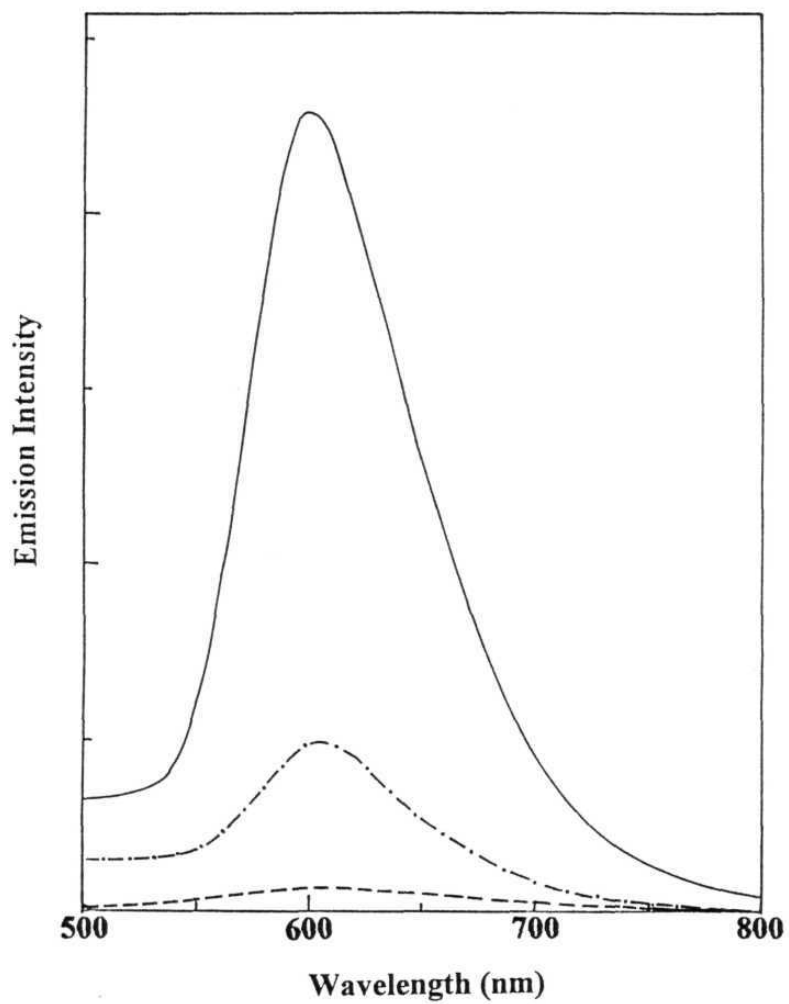


**Fig. 3.10.** Luminescence spectra ( $\lambda_{\text{exc}} = 440 \text{ nm}$ ) of  $10 \text{ } \mu\text{M}$   $[\text{Ru}(\text{phen})_2(\text{hqdpzz})]^{2+}$  (obtained by dithionite reduction of  $[\text{Ru}(\text{phen})_2(\text{qdpzz})]^{2+}$ ) in water (— — —),  $0.1 \text{ M}$  SDS (— · — · —) and  $\text{CH}_3\text{CN}/\text{H}_2\text{O}$  (10:1, v/v) (—).

basis of a proton transfer quenching of the excited state of the complex. A 'partial recovery' occurs in SDS solutions where the complex can, in principle, reside in a more hydrophobic micellar environment and the dipyridophenazine ligand protected from water.<sup>3,6,30</sup> There is a further enhancement of luminescence in aqueous CH<sub>3</sub>CN solutions due to less water present in solution and the complex becomes moderately luminescent.

Interestingly, both [Ru(phen)<sub>2</sub>(qdppz)]<sup>2+</sup> and [Ru(phen)<sub>2</sub>(hqdppz)]<sup>2+</sup> remain essentially non-luminescent in the presence of DNA. While the lack of luminescence for the oxidized form can be due, in most part, to an intramolecular electron transfer quenching, that by the reduced complex is quite curious and, moreover, is in stark contrast with the luminescence characteristics of [Ru(phen)<sub>2</sub>(dppz)]<sup>2+</sup> in the presence of DNA. The strong binding of [Ru(phen)<sub>2</sub>(dppz)]<sup>2+</sup> to DNA has been reported to give rise to the so-called 'molecular light switch effect' where the nearly undetectable emission from the MLCT excited state in water becomes strongly enhanced upon binding, assigned to intercalation of the planar dppz ligand between the base pairs of DNA.<sup>3</sup> The apparent lack of emission from [Ru(phen)<sub>2</sub>(hqdppz)]<sup>2+</sup> in the presence of DNA thus clearly indicates that the dipyridophenazine part of hqdppz is residing in a hydrophilic environment. This is possible if either this hydroquinone ligand is not a good intercalator or the complex is intercalating through its phen ligand. Both of these suppositions are consistent with the DNA binding characteristics (*vide supra*) of [Ru(phen)<sub>2</sub>(hqdppz)]<sup>2+</sup> as probed by absorption titration, viscometry, differential pulse voltammetry and topoisomerase assay.

The emission characteristics of the redox couple  $[\text{Ru}(\text{phen})_2(\text{qdppz})]^{2+} / [\text{Ru}(\text{phen})_2(\text{hqdpz})]^{2+}$  in various media described above suggest that there exists a distinct possibility of demonstrating the redox switching of luminescence in aqueous  $\text{CH}_3\text{CN}$  and SDS solutions. Cyclic- and differential pulse- voltammetric experiments carried out with  $[\text{Ru}(\text{phen})_2(\text{qdppz})](\text{PF}_6)_2$  in 0.1 M SDS solutions gave ill-defined current-voltage curves (due to adsorption of the electroactive species on the electrode surface) but, a reversible reduction was achievable at -0.26 V in aqueous  $\text{CH}_3\text{CN}$  (4-5%  $\text{H}_2\text{O}$ ) containing 0.1 M  $\text{TBAPF}_6$ . Exhaustive coulometric reduction of the complex conducted in deaerated, aqueous  $\text{CH}_3\text{CN}$  at -0.5 V generated  $[\text{Ru}(\text{phen})_2(\text{hqdpz})](\text{PF}_6)_2$  as identified by its UV-visible spectrum which is indistinguishable from that obtained by the dithionite method (see Fig. 3.3). The solution containing this reduced complex showed an oxidation wave at +0.92 V and, the bulk exhaustive coulometry conducted at +1.1 V was seen to regenerate  $[\text{Ru}(\text{phen})_2(\text{qdppz})]^{2+}$ . The redox-cycle was repeated three to four times with < 5% loss of the material. In addition, and as illustrated in Fig. 3.11, while the quinone form  $[\text{Ru}(\text{phen})_2(\text{qdppz})]^{2+}$  was found to be almost non-luminescent, the electrochemically generated hydroquinone form  $[\text{Ru}(\text{phen})_2(\text{hqdpz})]^{2+}$  showed the MLCT luminescence at 601 nm with the quantum yield of 0.02. The  $\phi$  is higher in this case than that observed for the complex obtained *via* the dithionite reduction due to less water content present in the utilized  $\text{CH}_3\text{CN}$  solution which is only 4-5% as against a 10% used during the chemical reduction. Indeed, quenching of luminescence was noticeable upon addition of more water to this electrolytic solution. In any case, the couple  $[\text{Ru}(\text{phen})_2(\text{qdppz})]^{2+} /$

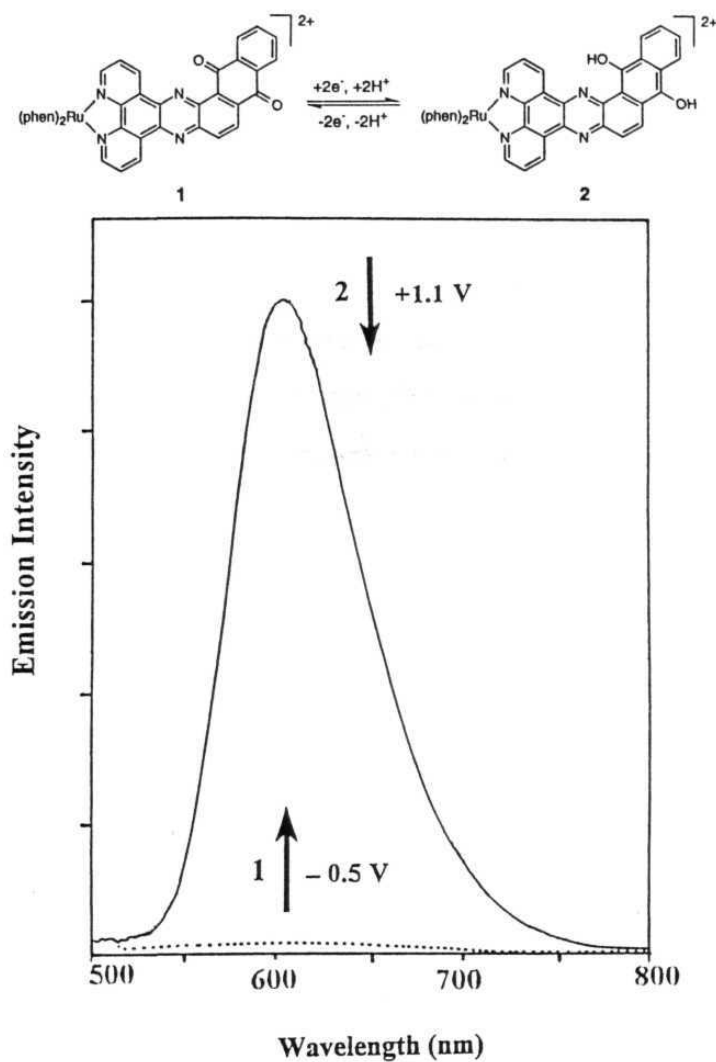


**Fig. 3.11.** Luminescence spectra ( $\text{CH}_3\text{CN}/5\% \text{H}_2\text{O}$ ,  $0.1 \text{ M TBAPF}_6$ ,  $\lambda_{\text{exc}} = 440 \text{ nm}$ ) of  $[\text{Ru}(\text{phen})_2(\text{qdppz})]^{2+}$  (1) and  $[\text{Ru}(\text{phen})_2(\text{hqdpzz})]^{2+}$  (2) as obtained by exhaustive electrolyses at the indicated potentials in each case. The arrows refer to the reversible changes observed upon electrochemical interconversion of these complexes.

$[\text{Ru}(\text{phen})_2(\text{hqdpz})]^{2+}$ , which combines an electroactive component with a light-emitting centre, represents a redox-activated luminescence on/off switching device with its function being similar to that exhibited by  $[\text{Ru}(\text{bpy})_2(\text{bpy-BQ})]^{2+}$  mentioned above.<sup>29</sup>

### 3.4 Summary

In summary, the new ruthenium(II) complex  $[\text{Ru}(\text{phen})_2(\text{qdppz})]^{2+}$  endowed with a novel, quinone-fused, dipyrrophenazine ligand is not only an avid binder of DNA but also an efficient photocleaving agent of the plasmid. On the other hand, the corresponding reduced species,  $[\text{Ru}(\text{phen})_2(\text{hqdpz})]^{2+}$ , also binds and photocleaves DNA albeit with less efficiency. These facts together with the finding that the redox couple  $[\text{Ru}(\text{phen})_2(\text{qdppz})]^{2+}/[\text{Ru}(\text{phen})_2(\text{hqdpz})]^{2+}$  represents an 'electro-photoswitch' testify to the importance of quinone/hydroquinone moieties<sup>31</sup> present on these complexes and further suggest that they are useful in the design of photonucleases and molecule-based, electronic devices.

### 3.5 References

1. See, for example (and references therein) (a) Mesmaeker, A. K. -D.; Lecomte, J. -P.; Kelly, J. M. *Topics in Current Chem.* **1996**, 177, 25. (b) Norden, B.; Lincoln, P.; Akerman, B.; Tuite, E. In "*Metal ions in biological systems: Probing of nucleic acids by metal ion complexes of small molecules*", Sigel, A.; Sigel, H., Eds.; Marcel Dekker: New York, **1996**, Vol. 33, pp: 177-252. (c) Roundhill, D. M. *Photochemistry and Photophysics of metal Complexes*; Plenum Press: New York, **1994**; pp

- 165 - 210. (d) Sigman, D. S.; Mazumder, A.; Perrin, D. M. *Chem. Rev.* **1993**, 93, 2295. (e) Murphy, C. J.; Barton, J. K. *Methods Enzymol.* **1993**, 226, 576. (f) Kalyanasundaram, K. *Photochemistry of Polypyridine and Porphyrin Complexes*, Academic Press: London, **1992**. (g) Turro, N. J.; Barton, J. K.; Tamalia, D. A. *Acc. Chem. Res.* **1991**, 24, 332. (h) Wilner, I.; Wilner, B. *Topics in Current Chem.* **1991**, 159, 153 - 218 (i) Balzani, V.; Scandola, F. *Supramolecular Photochemistry*, Ellis Horwood: Chichester, **1991**. (j) Pyle, A. M.; Barton, J. K. *Prog. Inorg. Chem.* **1990**, 38, 413. (k) Meyer, T. J. *Acc. Chem. Res.*, **1989**, 22, 163. (l) *Metal-DNA Chemistry* (ACS Symposium Series 402), Tullis, T.D., Ed.; American Chemical Chemistry: Washington, DC, **1989**. (m) *Photochemical Energy Conversion*, Norris, J.; Meisel, D.; Eds.; Elsevier: New York, **1989**. (n) *Supramolecular Photochemistry* (Nato ASI Series C214), Balzani, V.; Ed.; Reidel Publishing Company: Dordrecht, The Netherlands, **1987**. (o) Sigman, D. S. *Acc. Chem. Res.* **1986**, 19, 180. (p) Barton, J. K. *Science* **1986**, 233, 727.
2. For recent examples, see: (a) Hung, C. -Y.; Wang, T. -L.; Jang, Y.; Kim, W. Y.; Schmehl, R. H.; Thummel, R. P. *Inorg. Chem.* **1996**, 35, 5953. (b) Luo, Y.; Potvin, P. G.; Tse, Y. -H.; Lever, A. B. P. *Inorg. Chem.* **1996**, 35, 5445. (c) Kelso, L. S.; Reitsma, D. A.; Keene, F. R. *Inorg. Chem.* **1996**, 35, 5144. (d) Serroni, S.; Campagna, S.; Denti, G.; Keyes, T. E.; Vos, J. G. *Inorg. Chem.* **1996**, 35, 4513. (e) Vogler, L. M.; Brewer, K. J. *Inorg. Chem.* **1996**, 35, 818. (f) Alsfasser, R.; van Eldik, R. *Inorg. Chem.* **1996**, 35, 628. (g) Shreder, K.; Harriman, A.;

- Iverson, B. L. *J. Am. Chem. Soc.* **1996**, 118, 3192. (h) Constable, E. C.; Harverson, P.; Oberholzer, M. *J. Chem. Soc., Chem. Commun.*, **1996**, 1821. (i) Harriman, A.; Ziessel, R. *J. Chem. Soc., Chem. Commun.*, **1996**, 1707. (j) Jacquet, L.; Kelly, J. M.; Mesmaeker, K. -D. *J. Chem. Soc. Chem. Commun.*, **1995**, 913. (k) Beer, P. D.; Dent, S. W.; Wear, T. J. *J. Chem. Soc., Dalton Trans.*, **1996**, 2341.
3. (a) Holmlin, R. E.; Barton, J. K. *Inorg. Chem.* **1995**, 34, 7. (b) Turro, C.; Bossman, S. H.; Jenkins, Y.; Barton, J. K.; Turro, N. J. *J. Am. Chem. Soc.* **1995**, 117, 9026. (c) Dupureur, C. M.; Barton, J. K. *J. Am. Chem. Soc.* **1994**, 116, 10286. (d) Hartshorn, R. M.; Barton, J. K. *J. Am. Chem. Soc.* **1992**, 114, 5919. (e) Jenkins, Y.; Friedman, A. E.; Turro, N. J.; Barton, J. K. *Biochemistry* **1992**, 31, 10809. (f) Friedman, A. E.; Kumar, C. V.; Turro, N. J.; Barton, J. K. *Nucl. Acid Res.* **1991**, 19, 2595. (g) Friedman, A. E.; Chambron, J. C.; Sauvage, J. P.; Turro, N. J.; Barton, J. K. *J. Am. Chem. Soc.* **1990**, 112, 4960.
4. (a) Bogler, J.; Gourdon, A.; Ishow, E.; Launay, J. -P. *Inorg. Chem.*, **1996**, 35, 2937. (b) Lincoln, B.; Broo, A.; Norden, B. *J. Am. Chem. Soc.* **1996**, 118, 2644. (c) Lincoln, P.; Norden, B. *J. Chem. Soc. Chem. Commun.* **1996**, 2145. (d) Stoeffler, H. D.; Thornton, N. B.; Temkin, S. L.; Schanze, K. S. *J. Am. Chem. Soc.* **1995**, 117, 7119. (e) Haq, I.; Linclon, P.; Suh, D.; Norden, B.; Chowdhry, B. Z.; Chaires, J. B. *J. Am. Chem. Soc.* **1995**, 117, 4788. (f) Yam, V. W.-W.; Lo, K. K.-W.; Cheung, K.-K.; Kong, R. Y.-C. *J. Chem. Soc. Chem. Commun.* **1995**, 1191. (g) Maggini, M.; Dono, A.; Scorrano, G.; Prato, M. *J. Chem. Soc., Chem. Commun.*, **1995**, 845. (h) Hiort, C. H.; Lincoln, P.; Norden,

- B. *J. Am. Chem. Soc.* **1993**, 115, 3448. (i) Eriksson, M.; Leijon, M.; Hirot, C.; Norden, B.; Graslund, A. *Biochemistry* **1994**, 33, 5031.
5. Gupta, N.; Grover, N.; Neyhart, G. A.; Liang, W.; Singh, P.; Thorp, H. H. *Angew. Chem. Int. Ed. Engl.* **1992**, 31, 1048.
  6. Olson, E. J. C.; Hu, D.; Hormann, A.; Jonkman, A. M.; Arkin, M. R.; Stemp, E. D. A.; Barton, J. K.; Barbara, P. F. *J. Am. Chem. Soc.* **1997**, 119, 11458.
  7. (a) Sentagne, C.; Chambron, J.-C., Sauvage, J. P.; Paillous, N. *J. Photochem. Photobiol. B: Biol.* **1994**, 26, 165. (b) Schoch, K.; Hubbard, J. L.; Zoch, C. R.; Yi, G. -B.; Sorlie, M. *Inorg. Chem.* **1996**, 35, 4383. (c) Yam, V. W.-W.; Lo, K. K.-W.; Cheung, K.-K.; Kong, R. Y.-C. *J. Chem. Soc. Dalton Trans.*, **1997**, 2067.
  8. (a) Arkin, R.; Stemp, E. D. A.; Turro, C.; Turro, N. J.; Barton, J. K. *J. Am. Chem. Soc.*, **1996**, 118, 2267. (b) Stemp, E. D. A.; Arkin, M. R.; Barton, J. K. *J. Am. Chem. Soc.* **1995**, 117, 2375. (c) Murphy, C. J.; Arkin, M. R.; Ghatlia, N. D.; Bossman, S. H.; Turro, N. J.; Barton, J. K. *Proc. Natl. Acad. Sci. USA.* **1994**, 91, 5315. (d) Murphy, C. J.; Arkin, M. R.; Jenkins, Y.; Ghatlia, N. D.; Bossman, S. H.; Turro, N. J.; Barton, J. K. *Science* **1993**, 262, 1025.
  9. (a) Dickenson, J. E.; Summers, L. A. *Aust. J. Chem.* **1970**, 23, 1023. (b) Chambron, J. -C.; Sauvage, J. -P.; Amouyal, E.; Koffi, P. *Nouv. J. Chem.* **1985**, 9, 527. (c) Amouyal, E.; Homsy, A.; Chambron, J. -C.; Sauvage, J. -P. *J. Chem. Soc. Dalton Trans* **1990**, 1841. (d) Chambron, J.-C.; Sauvage, J.-P. *Chem. Phys. Lett.* **1991**, 182, 603.

10. Breslin, D. T.; Coury, J. E.; Anderson, J. R.; Mcfail-Isom, L.; Kan, Y.; Williams, L. D.; Bottomley, L. A.; Schuster, G. B. *J. Am. Chem. Soc.* **1997**, 119, 5043 (and references therein). (b) Koch, T.; Ropp, J. D.; Sligar, S. D.; Schuster, G. B. *Photochem. Photobiol.* **1993**, 58, 554.
11. Bhattacharya, S.; Mandal, S. S. *J. Chem. Soc. Chem. Commun.* **1996**, 1515
12. Lopez, R. B.; Loeb, B. L.; Boussie, T.; Meyer, T. J. *Tetrahedron Lett.*, **1996**, 37, 5437.
13. Yamada, M.; Tanaka, Y.; Yoshimoto, Y.; Kuroda, S.; Shimao, I. *Bull. Chem. Soc. Jpn.* **1992**, 65, 1006.
14. (a) Lin, C.-T.; Bottcher, W.; Chou, M.; Cruetz, C.; Sutin, M. *J. Am. Chem. Soc.* **1976**, 98, 6536. (b) Sullivan, B. P.; Salmon, D. J.; Meyer, T. J. *Inorg. Chem.* **1978**, 17, 3334
15. (a) Carter, M. T.; Bard, A. J. *J. Am. Chem. Soc.* **1987**, 109, 7528. (b) Carter, M. T.; Rodriguez, M.; Bard, A. J. *J. Am. Chem. Soc.* **1989**, 111, 8901. (c) Carter, M. T.; Bard, A. J. *Bioconjugate Chem.* **1990**, 1, 257.
16. Carlson, D. L.; Hutchital, D. H.; Mantilla, E. J.; Sheardy, R. D.; Murphy Jr., W. R. *J. Am. Chem. Soc.*, **1993**, 115, 6424.
17. (a) Keller, W. *Proc. Natl. Acad. Sci. U.S.A.*, **1975**, 72, 4876. (b) Wang, J. C. *J. Mol. Biol.* **1974**, 89, 783.
18. (a) Ackermann, M. N.; Interrante, L. V. *Inorg. Chem.* **1984**, 23, 3904. (b) Fees, J.; Kaim, W.; Moscherosch, M.; Matheis, W.; Klima, J.; Krejcik, M.; Zalis, S. *Inorg. Chem.* **1993**, 32, 166.
19. Yam, V. W.-W.; Lee, V. W.-M.; Ke, F.; Siu, K.-M. *Inorg. Chem.*, **1997**, 36, 2124.

20. Nicholson, R. S. ; Shain, I. *Anal. Chem.* **1964**, 36, 706.
21. Eswaramoorthy, K.; Maiya, B. G. (*unpublished results*).
22. (a) Barton, J. K. *Acc. Chem. Res.* 1990, 23, 271. (b) Satyanarayana, S.; Dabrowiak, J. C.; Chaires, J. B. *Biochemistry*, **1992**, 31, 9319. (c) Neyhart, G. A.; Grover, N.; Smith, S. R.; Kalsbeck, W. A.; Fairley, T. A.; Cory, M.; Thorp, H. H. *J. Am. Chem. Soc.* **1993**, 115, 4423.
23. McGhee, J. D.; von Hippel, P. H. *J. Mol. Biol.* **1974**, 86, 469.
24. (a) Lerman, L. S. *J. Mol. Biol.* **1961**, 3, 18. (b) Neyhart, G. A.; Grover, N.; Smith, S. R.; Kalsbeck, W. A.; Fairley, T. A.; Cory, M.; Thorp, H. H. *J. Am. Chem. Soc.*, **1993**, 115, 4423.
25. see, for example: (a) Ref. 33(a). (b) Cavalieri, L. F.; Rosoff, M.; Rosenberg, B. H. *J. Am. Chem. Soc.* **1956**, 78, 5239. (c) Cory, M.; McKee, D. D.; Kagan, J.; Henty, D. W.; Miller, J. A. *J. Am. Chem. Soc.* **1985**, 107, 2528.
26. (a) Pyle, A. M.; Rehmann, J. P.; Meshoyeer, R.; Kumar, C. V.; Turro, N. J.; Barton, J. K. *J. Am. Chem. Soc.* **1989**, 111, 3051.
27. Grover, N.; Gupta, N.; Singh, P.; Thorp, H. H. *Inorg. Chem.*, **1992**, 31, 2014.
28. (a) Kelly, J. M.; Tossi, A. B.; McConnell, D. J.; OhUigin, C. *Nucl. Acid. Res.* **1985**, 13, 6017. (b) Mei, H.-Y.; Barton, J. K. *Proc. Natl. Acad. Sci. USA* **1988**, 85, 1339.
29. Goulle, V.; Harriman, A.; Lehn, J. -M. *J. Chem. Soc., Chem. Commun.*, **1993**, 1034.
30. Nair, R. B.; Cullum, B. M.; Murphy, C. J. *Inorg. Chem.*, **1997**, 36, 962

31. (a) Ref. 12. (b) Treadway, J. A.; Loeb, B.; Lopez, R.; Anderson, P. A.; Keene, F. R.; Meyer, T. J. *Inorg. Chem.* **1996**, 35, 2242.

## CHAPTER 4

### *DNA Binding, Photonuclease Activity and Luminescence Properties of a Series of Ruthenium(II) Complexes Containing 6,7-Dicyano-dipyridoquinoxaline*

#### 4.1 Introduction

In the previous Chapter, results of DNA binding, DNA photocleavage and novel luminescence properties of the redox couple  $[\text{Ru}(\text{phen})_2(\text{qdppz})]^{2+}/[\text{Ru}(\text{phen})_2(\text{hqdpz})]^{2+}$  were presented. However, owing to the efficient PET occurring in the oxidized form and the relative weak DNA-binding by the reduced form, it was not possible to observe any 'molecular light switching' effect by either of these complexes in the presence of DNA. In addition, the near-stoichiometric binding of  $[\text{Ru}(\text{phen})_2(\text{qdppz})]^{2+}$  precluded the estimation of meaningful binding constant for this complex with DNA. In order to circumvent these problems, a new ligand viz: 6,7-dicyanodipyridoquinoxaline (dicnq) has been designed by us. This ligand, while retaining the basic 'dppz' structure, also possesses strongly electron withdrawing cyano groups in its architecture. These features are expected to assist dicnq not only in binding strongly with DNA but also make it easy to reduce as in the case with the quinone ligand. In this Chapter, results of DNA binding, photocleavage and 'molecular light switching' aspects of  $([\text{Ru}(\text{phen})_2(\text{dicnq})]^{2+})$ ,  $[\text{Ru}(\text{phen})(\text{dicnq})_2]^{2+}$  and  $[\text{Ru}(\text{dicnq})_3]^{2+}$  will be discussed.

## 4.2 Experimental details

1,10-phenanthroline-5,6-dione (phen-dione),<sup>1</sup>  $[\text{Ru}(\text{phen})_3]\text{Cl}_2$ ,<sup>2</sup>  $[\text{Ru}(\text{phen})_2\text{Cl}_2]$ <sup>3</sup> and  $[\text{Ru}(\text{phen})\text{Cl}_4]^-$ <sup>4</sup> were synthesized following the reported procedures (see Chapter 2). Synthesis of dicnq and its complexes are described below.

### 4.2.1 Synthesis of 6,7-dicyanodipyridoquinoxaline (dicnq):

This ligand was synthesised (Fig. 4.1) by refluxing phen-dione (105 mg, 0.5 mM) and diaminomaleonitrile (108 mg, 1.0 mM) in ethanol for 45 min. under a nitrogen atmosphere. The solution was cooled to room temperature and the product obtained as brownish yellow needles. It was filtered, washed with cold ethanol and suction dried. Yield: ~ 80%.

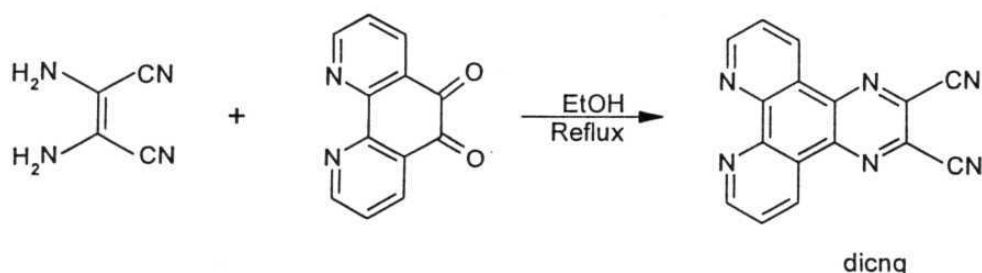


**Fig. 4.1**

Analytical data: Found: C, 67.98; H, 2.19; N, 29.37. Calcd. for  $\text{C}_{16}\text{H}_6\text{N}_6$ : C, 68.08; H, 2.14; N, 29.77.

FABMS (m/z): 283,  $[\text{M}^+]$ .

IR (KBr): 742, 1373, 1504, 1583, 2239, 2337  $\text{cm}^{-1}$ .

$^1\text{H}$  NMR (DMSO- $d_6$ , 200 MHz, TMS)  $\delta$ , ppm: 9.38( m, 4H), 8.04(q, 2H)

Synthesis of the mixed-ligand and tris- complexes containing dicnq are illustrated in Fig. 4.2.

#### 4.2.2 Synthesis of $[\text{Ru}(\text{phen})_2(\text{dicnq})](\text{PF}_6)_2 \cdot 2\text{H}_2\text{O}$ :

$\text{Ru}(\text{phen})_2\text{Cl}_2$  (100 mg, 0.2 mM) and dicnq (62 mg, 0.22 mM) were added to a 100 ml round bottom flask containing 60 ml of (1:1) methanol-water. The suspension was heated to reflux for 2 h. The brownish-red solution was allowed to cool to room temperature and stored at 0 °C for 1 h. A saturated aqueous  $\text{NH}_4\text{PF}_6$  was added to this solution to precipitate the complex as its  $\text{PF}_6$  salt which was filtered and vacuum dried. Yield: ~ 85%.

Analytical data: Found: C, 46.00; H, 2.29; N, 12.96. Calcd. for  $\text{C}_{40}\text{H}_{26}\text{N}_{10}\text{O}_2$  : C, 44.92; H, 2.45; N, 13.10.

FABMS (m/z): 889,  $[\text{M}-\text{PF}_6]^+$ ; 743,  $[\text{M}-2\text{PF}_6]^+$ .

IR (KBr): 715, 837, 1373, 1427, 1554, 2229, 3408, 3641  $\text{cm}^{-1}$

$^1\text{H}$  NMR (DMSO- $d_6$ , 200 MHz, TMS)  $\delta$ , ppm: 8.80(dd, 4H), 8.40(s, 4H), 8.21(m, 2H), 8.05(dd, 4H), 7.94(m, 2H), 7.80(m, 4H).

#### 4.2.3 $[\text{Ru}(\text{phen})(\text{dicnq})_2](\text{PF}_6)_2 \cdot 2\text{H}_2\text{O}$ :

This complex was prepared starting from  $\text{Ru}(\text{phen})\text{Cl}_4$  (150 mg, 0.35 mM) and dicnq (110 mg, 0.4 mM) in a manner analogous to that adopted for the synthesis of  $[\text{Ru}(\text{phen})(\text{dicnq})_2](\text{PF}_6)_2$ . Yield: ~ 70%.

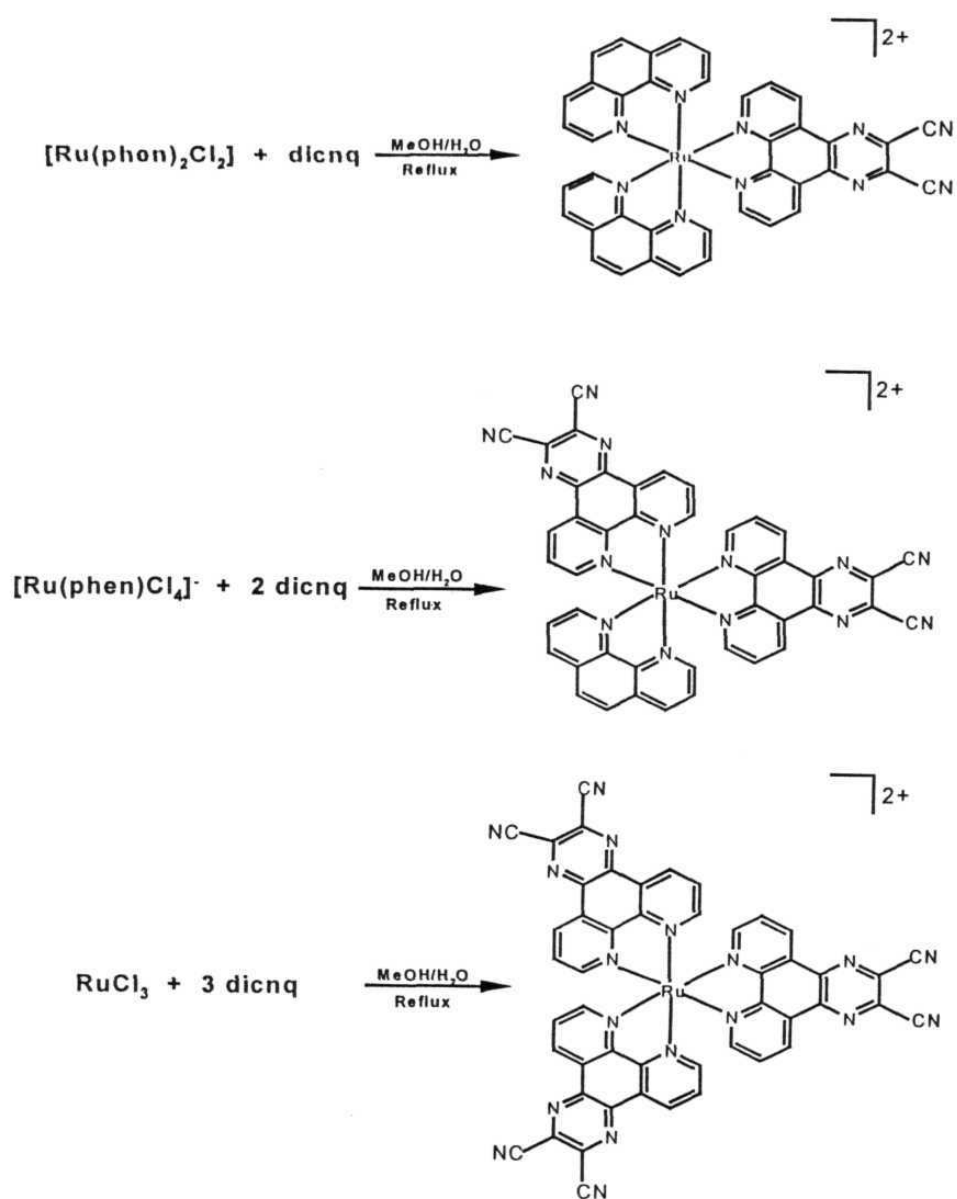


Fig. 4.2

Analytical data: Found: C, 45.12; H, 2.04; N, 16.68. Calcd. for  $C_{44}H_{24}N_{14}O_2$  : C, 45.11; H, 2.07; N, 16.74.

FABMS (m/z): 991,  $[M-PF_6]^+$ ; 845,  $[M-2PF_6]^+$ .

IR (KBr): 725, 841, 1371, 1429, 1554, 2237, 3645  $cm^{-1}$ .

$^1H$  NMR (DMSO- $d_6$ , 200 MHz, TMS)  $\delta$ , ppm: 9.48(dd, 4H), 8.80(dd, 2H), 8.41(s, 2H), 8.28(m, 2H), 8.19(dd, 4H), 7.94(dd, 4H), 7.79(m, 2H).

#### 4.2.4 $[Ru(dicnq)_3](PF_6)_2 \cdot 2H_2O$ :

Hydrated ruthenium trichloride (150 mg, 0.7 mM) and dicnq (595 mg, 2.1 mM) were refluxed in 40 ml of 1:1 methanol - water mixture for 4 h. The resulting solution was allowed to cool to room temperature and filtered. Saturated aqueous solution of  $NH_4PF_6$  was added to the red colored filtrate to precipitate the product which was filtered and vacuum dried. Yield: ~ 70%.

Analytical data: Found: C, 45.57; H, 1.64; N, 19.05. Calcd. for  $C_{48}H_{22}N_{18}O_2$ : C, 45.26; H, 1.74; N, 19.79.

FABMS (m/z): 1093,  $[M-PF_6]^+$ ; 948,  $[M-2PF_6]^+$ .

IR (KBr): 841, 1371, 1448, 1662, 3640, 2361, 2212  $cm^{-1}$ .

$^1H$  NMR (DMSO- $d_6$ , 200 MHz, TMS)  $\delta$ , ppm: 9.51, 9.42 (dd, 2H), 8.40(dd, 2H), 8.01(m, 2H).

The chloride salts of the above complexes were obtained by dissolving them in minimum amount of acetone and by precipitating by the addition of a saturated solution of TBACl in acetone.

All the spectroscopic and electrochemical experiments leading to the characterization of the new complexes synthesized here were carried out as

described in Chapter 2. While the hexafluorophosphate salts of the complexes were employed for the luminescence measurements in non-aqueous solvents, the corresponding chloride salts were used for measurements in aqueous and aqueous buffered (buffer A: 5 mM tris, pH 7.1, 50 mM NaCl) solutions.

#### **4.2.5 DNA binding and Photocleavage Studies**

Buffer A was used for absorption titration experiments and luminescence measurements. Buffer B (1 mM phosphate, pH 7.0, 2 mM NaCl) was used for thermal denaturation experiments. The chloride salts of the complexes were used in studies with DNA.

DNA melting- ( [DNA nucleotide phosphate] = 170  $\mu$ M, [drug] = 0 - 7  $\mu$ M) and absorption titration ( [drug] = 30  $\mu$ M and [DNA base pairs] = 0 - 200  $\mu$ M) experiments were carried out as described in Chapter 2.

Absorbance values were recorded after each successive addition of DNA solution and equilibration (ca. 10 min.). Data obtained from the absorption titration experiments were analyzed by using equation 2.17:

Gel electrophoresis experiments were carried out as described in Chapters 2 and 3. Samples (pre-incubated in dark, 1h.) were irradiated at 440  $\pm$  5 nm.

### **4.3 Results and discussion**

#### **4.3.1 Synthesis**

The new ligand dicnq was synthesised by the condensation of phen-dione with diaminomaleonitrile in ethanol in a manner similar to that reported

for the preparation of dppz.<sup>5</sup> The condensation went on smoothly providing the pure sample in 85% yield.

All the ruthenium(II) complexes containing dicnq were synthesised by refluxing dicnq with the appropriate mole ratios of the precursor starting materials in methanol-water mixture and precipitating as their PF<sub>6</sub> salts. The yields were satisfactory in each case. The corresponding chloride salts were prepared with ease by a standard method.

#### 4.3.2. Spectral and electrochemical characterization of dicnq and its complexes

The new ligand and its complexes have been characterised by elemental analysis, <sup>1</sup>H NMR, and FABMS methods. While dicnq showed a base-peak at  $m/z = 283$  (M<sup>+</sup>) in the mass spectrum, providing evidence for its integrity, the peaks due to both [M-PF<sub>6</sub>]<sup>+</sup> and [M-2PF<sub>6</sub>]<sup>+</sup> were seen in the spectra for each of the complexes typical of PF<sub>6</sub> salts of ruthenium(II) polypyridyl complexes.<sup>6</sup>

IR spectra of dicnq shows the CN stretching frequency at 2239 cm<sup>-1</sup>. The corresponding peak appears at 2229, 2237 and 2212 cm<sup>-1</sup> for [Ru(phen)<sub>2</sub>(dicnq)]<sup>2+</sup>, [Ru(phen)(dicnq)<sub>2</sub>]<sup>2+</sup> and [Ru(dicnq)<sub>3</sub>]<sup>2+</sup>, respectively.

<sup>1</sup>H NMR spectrum of dicnq is illustrated in Fig. 4.3(a). The spectrum is characteristic of the structure of this ligand and can be analyzed based on the positions and the integrated intensities of the resonance peaks. As seen in this Figure, while the H-C(4) and the H-C(2) aromatic protons appear as multiplets around 9.38 ppm, the resonance due to H-C(3) appears as a quartet at 8.04 ppm. In comparison, the H-C(4), H-C(2) and H-C(3) protons of phen

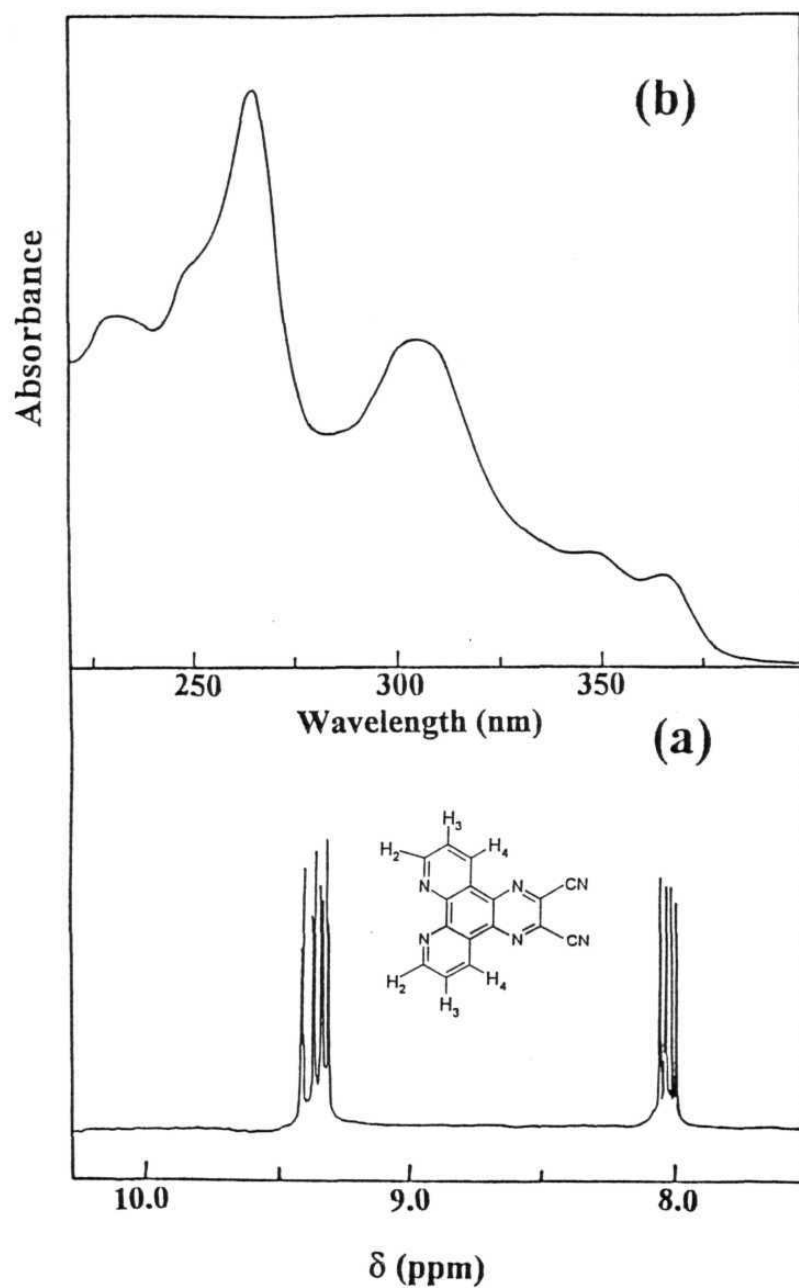


**Fig. 4.3.** (a)  $^1\text{H}$  NMR spectrum of dicnq in  $\text{CDCl}_3$ . (b) UV-visible spectrum of dicnq in  $\text{CH}_3\text{CN}$ .

are located at 9.11 (doublet of doublet), 8.51 (doublet of doublet) and 7.78 (quartet) ppm, respectively. The observed downfield shifts for these protons on dicnq in comparison with the corresponding protons on phen are consistent with the electron withdrawing nature of the cyano groups. Fig. 4.4 compares the  $^1\text{H}$  NMR spectra of  $[\text{Ru}(\text{phen})_2(\text{dicnq})]^{2+}$ ,  $[\text{Ru}(\text{phen})(\text{dicnq})_2]^{2+}$  and  $[\text{Ru}(\text{dicnq})_3]^{2+}$  with the spectrum of  $[\text{Ru}(\text{phen})_3]^{2+}$ . In these spectra, the resonances due to the protons of both phen and dicnq are seen to be considerably shifted to the down field region indicating complexation. In addition, there is a progressive decrease in the intensity of the peaks due to phen concomitant with an increase in the intensity of peaks due to dicnq as one moves from  $[\text{Ru}(\text{phen})_3]^{2+}$  to  $[\text{Ru}(\text{phen})_2(\text{dicnq})]^{2+}$ ,  $[\text{Ru}(\text{phen})(\text{dicnq})_2]^{2+}$  and  $[\text{Ru}(\text{dicnq})_3]^{2+}$  in that order.

The results of the cyclic voltammetric experiments carried out with dicnq and its ruthenium(II) complexes are compared with the electrochemical data of free phen and  $[\text{Ru}(\text{phen})_3]^{2+}$  in Table 4. 1. In DMF containing 0.1 M  $\text{TBAPF}_6$ , uncomplexed dicnq shows a well defined, reversible, one electron reduction wave (Fig. 4.5) at  $-0.66$  V vs SCE. Reduction wave for the complexed dicnq in  $[\text{Ru}(\text{phen})_2(\text{dicnq})]^{2+}$  occurs at  $-0.83$  V (reversible, one-electron transfer) followed by the successive phen reductions at  $-1.29$  and  $-1.48$  V in DMF, 0.1 M  $\text{TBAPF}_6$  (Fig. 4.6). It is interesting that electron addition to the complexed dicnq in this complex is more difficult than it is to the free ligand itself. This is unlike the case with either dppz or qdppz both of which are reduced relatively easily in  $[\text{Ru}(\text{phen})_2(\text{dppz})]^{2+}$  or  $[\text{Ru}(\text{phen})_2(\text{qdppz})]^{2+}$  compared to the respective free ligands (compare data in Table 3.2). On the other hand, reduction of both the dicnq ligands on

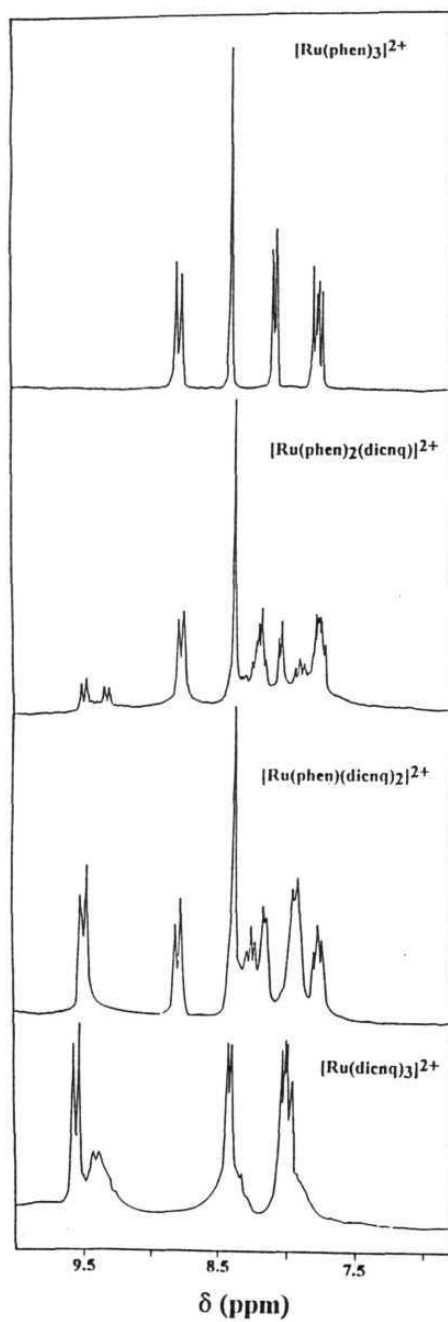
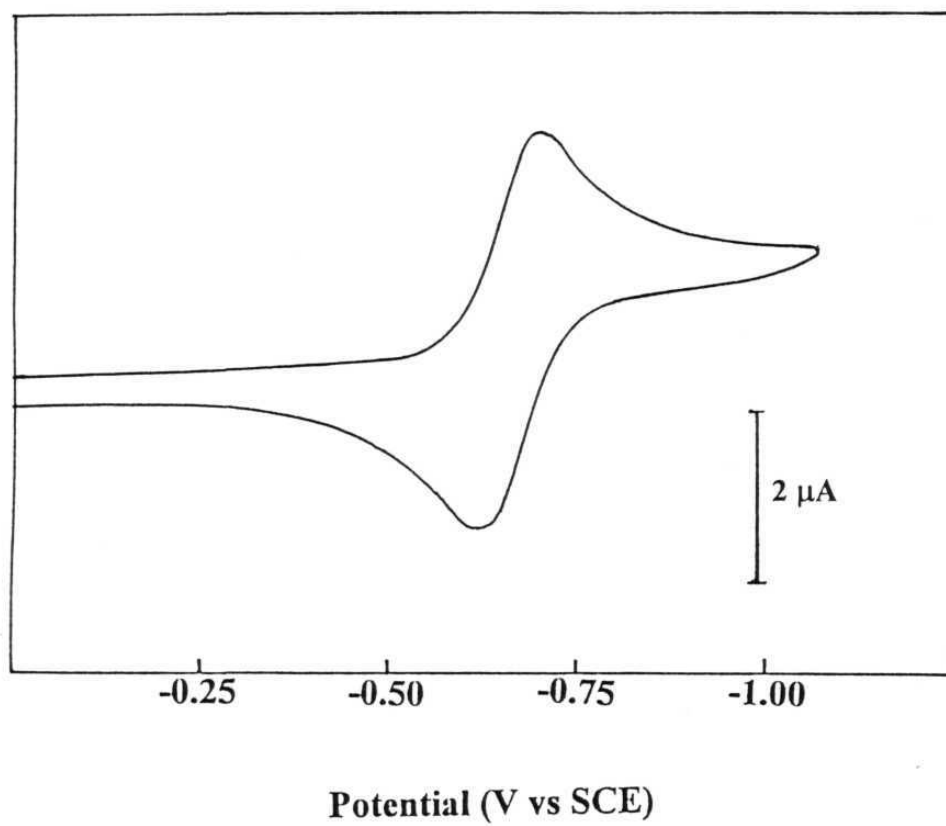


Fig. 4.4.  $^1\text{H}$  NMR spectra of  $[\text{Ru}(\text{phen})_3]^{2+}$ ,  $[\text{Ru}(\text{phen})_2(\text{dicnq})]^{2+}$ ,  $[\text{Ru}(\text{phen})(\text{dicnq})_2]^{2+}$  and  $[\text{Ru}(\text{dicnq})_3]^{2+}$  in  $\text{DMSO}-d_6$ .

**Table 4.1** Redox potential data of dicnq and its complexes

Compound	Potential, V vs SCE	
	$E_{1/2 \text{ red}}^a$	$E_{1/2 \text{ ox}}^b$
phen	-1.92	-
dicnq	-0.66	-
$[\text{Ru}(\text{phen})_3]^{2+}$	-1.28, -1.44, -1.71	+1.26
$[\text{Ru}(\text{phen})_2(\text{dicnq})]^{2+}$	-0.83, -1.29, -1.48	+1.33
$[\text{Ru}(\text{phen})(\text{dicnq})_2]^{2+}$	-0.51, -1.34	+1.41
$[\text{Ru}(\text{dicnq})_3]^{2+}$	-0.47	+1.51

a: In DMF, 0.1 M TBAPF<sub>6</sub>b: In CH<sub>3</sub>CN, 0.1 M TBAPF<sub>6</sub>



**Fig. 4.5.** Cyclic voltammogram (scan rate,  $100 \text{ mV s}^{-1}$ ) of dicnq in DMF, 0.1 M TBAPF<sub>6</sub>.

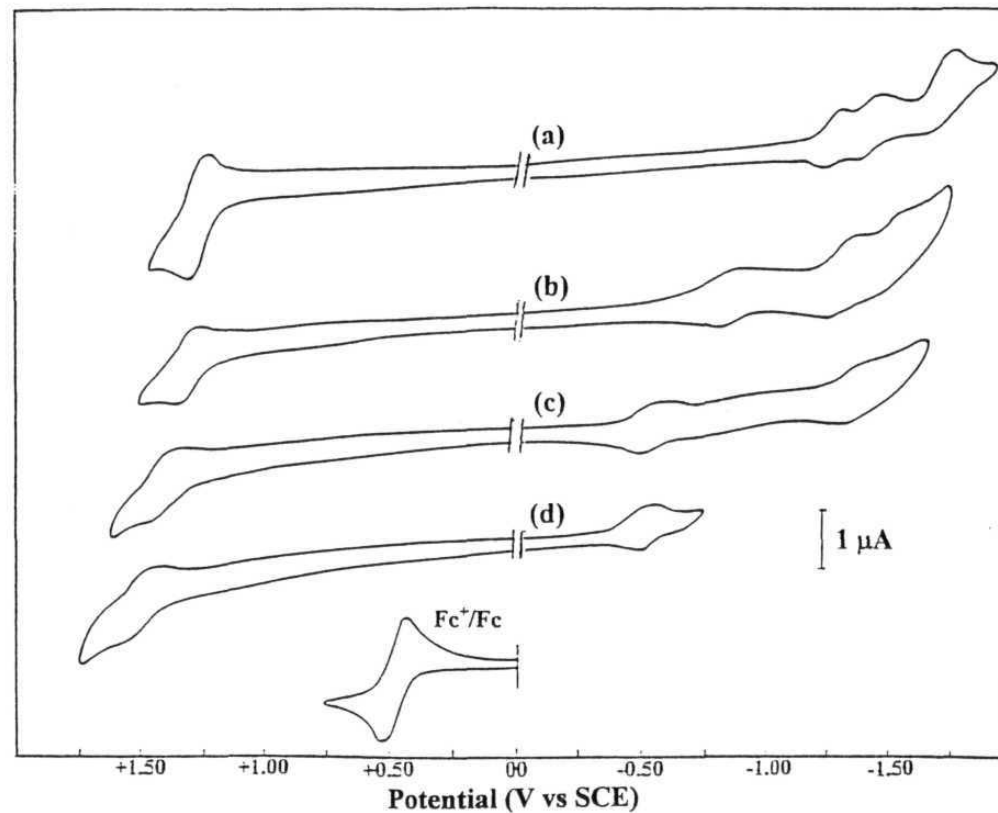


**Fig. 4.6.** Cyclic Voltammograms (scan rate,  $100 \text{ mV s}^{-1}$ ) of (a)  $[\text{Ru}(\text{phen})_2(\text{dicnq})]^{2+}$ , (b)  $[\text{Ru}(\text{phen})(\text{dicnq})_2]^{2+}$  and (c)  $[\text{Ru}(\text{dicnq})_3]^{2+}$ . Oxidation in  $\text{CH}_3\text{CN}$ ,  $0.1\text{M TBAPF}_6$  and reduction in  $\text{DMF}$ ,  $0.1 \text{ M TBAPF}_6$ . ( $\text{Fc}$  = Ferrocene)

$[\text{Ru}(\text{phen})(\text{dicnq})_2]^{2+}$  occurs at  $-0.51$  V followed by the reduction of phen at  $-1.34$  V. Electron addition to all the three dicnq ligands in  $[\text{Ru}(\text{dicnq})_3]^{2+}$  occurs at  $-0.47$  V. Thus, in these latter two complexes, reduction of the complexed dicnq is facile than the free ligand. Indeed, the relative ease of reduction of the bound dicnq follows the order  $[\text{Ru}(\text{phen})_2(\text{dicnq})]^{2+} > [\text{Ru}(\text{phen})(\text{dicnq})_2]^{2+} > [\text{Ru}(\text{dicnq})_3]^{2+}$ .

These results suggest that  $\pi^*$  orbital of dicnq lies lower than that of phen and probably, that the added electron is delocalized on the  $\pi^*$  levels of dicnq equally rather than on only one ligand in  $[\text{Ru}(\text{phen})(\text{dicnq})_2]^{2+}$  and  $[\text{Ru}(\text{dicnq})_3]^{2+}$ .<sup>7</sup> This latter supposition is not in line with DeArmond's<sup>8</sup> argument that the electron is localized in the  $\pi^*$  levels of one ligand rather than delocalized over the whole ligand  $\pi$ -system in  $[\text{Ru}(\text{bpy})_3]^{2+}$ . However, it is consistent with the electrochemical data on  $[\text{Ru}(\text{dppz})_3]^{2+}$  for which reduction of all the three complexed dppz ligands has been reported to occur at the same potential.<sup>7a</sup>

Electrochemical oxidation of the ruthenium polypyridyl complexes are known to involve metal  $\pi(t_{2g})$  orbital.<sup>9</sup> Oxidation of ruthenium center in  $[\text{Ru}(\text{phen})_2(\text{dicnq})]^{2+}$ ,  $[\text{Ru}(\text{phen})(\text{dicnq})_2]^{2+}$  and  $[\text{Ru}(\text{dicnq})_3]^{2+}$  occurs at  $+1.33$ ,  $+1.41$  and  $+1.51$  V, respectively in  $\text{CH}_3\text{CN}$ ,  $0.1$  M  $\text{TBAPF}_6$ . Thus, electron abstraction from the metal center is more difficult in these complexes than that from  $[\text{Ru}(\text{phen})_3]^{2+}$  ( $1.26$  V), due to the presence of electron withdrawing nature of cyano groups on dicnq. Interestingly, the sequential substitution of phen in  $[\text{Ru}(\text{phen})_3]^{2+}$  with dicnq increases the oxidation potential of ruthenium steadily resulting in an overall anodic shift of  $0.25$  V for the oxidation of  $[\text{Ru}(\text{dicnq})_3]^{2+}$  compared to  $[\text{Ru}(\text{phen})_3]^{2+}$ . Such monotonic

increase in the metal-centered oxidations with the number of electron-withdrawing ligands in metallopolypyridyls has been well-documented in the literature.<sup>10</sup>

UV-visible data of dicnq and its ruthenium(II) complexes in CH<sub>3</sub>CN are summarized in Table 4. 2. The absorption spectrum of dicnq (Fig. 4.3(b)) shows bands in the 220-400 nm region with the most intense band being located at 265 nm. These bands can be assigned to  $\pi-\pi^*$  transitions. The presence of an intense peak at 265 nm for dicnq is similar to that at the same wavelength for phen. On the other hand, the additional peaks appearing at 305, 347, and 365 nm in the spectrum of dicnq indicate that the corresponding transitions could arise from the quinoxaline portion of this ligand.<sup>10a</sup>

In the UV-visible spectra of the three complexes (Fig. 4.7), the ultraviolet region of the absorption shows intense bands arising from the  $\pi-\pi^*$  transitions of the ligands coordinated to the metal center. While both [Ru(dicnq)<sub>3</sub>]<sup>2+</sup> and [Ru(phen)<sub>3</sub>]<sup>2+</sup> show intense, ligand-centred  $\pi-\pi^*$  transitions at 266 and 263 nm, respectively, the former complex additionally displays sharp transitions at 302 and 384 nm. Thus, both phen and dicnq absorb at around 266 nm and, the bands at 302 and 384 nm are ascribable exclusively to transitions involving dicnq. Accordingly, in the mixed ligand complexes, [Ru(phen)<sub>2</sub>(dicnq)]<sup>2+</sup> and [Ru(phen)(dicnq)<sub>2</sub>]<sup>2+</sup>, the ultraviolet region is dominated by the  $\pi-\pi^*$  transitions due to both phen (263/264 nm) and dicnq (263/264 and 292/300 nm). It is interesting to note that the ratio of the absorbance at ~ 266 nm to that at ~ 300 nm decreases with increasing number of dicnq ligands on the complex as  $3.7 > 2.2 > 1.7$  for

**Table 4.2** UV-visible and emission data of dicnq and its complexes in CH<sub>3</sub>CN

Compound	Absorption	Emission	
	$\lambda_{\text{max}}$ , nm (log $\epsilon$ )	$\lambda_{\text{em}}$ , nm	$\phi_{\text{em}}$
dicnq	231 (4.43), 249 (sh), 265 (4.64) 305(4.40), 347 (3.93), 365 (3.83)	-	-
[Ru(phen) <sub>2</sub> (dicnq)] <sup>2+</sup>	263 (5.12), 292 (4.64), 349 (4.15) 362 (4.18), 445 (4.33)	616	0.012
[Ru(phen)(dicnq) <sub>2</sub> ] <sup>2+</sup>	264 (5.15), 300 (4.80), 346 (4.24) 441 (4.31)	613	0.003
[Ru(dicnq) <sub>3</sub> ] <sup>2+</sup>	266 (5.13), 302 (4.88), 384 (4.34) 452 (4.29)	-	-
[Ru(phen) <sub>3</sub> ] <sup>2+</sup>	263 (5.07), 422 (4.25), 446 (4.28)	596	0.028

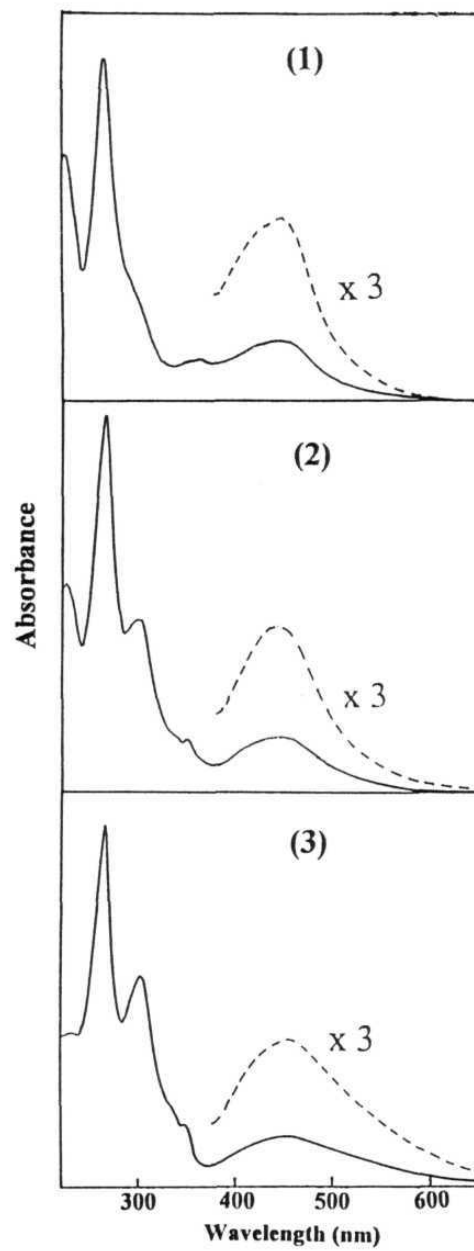


**Fig. 4.7.** UV-visible spectra of (1)  $[\text{Ru}(\text{phen})_2(\text{dicnq})]^{2+}$ , (2)  $[\text{Ru}(\text{phen})_2(\text{dicnq})]^{2+}$  and (3)  $[\text{Ru}(\text{dicnq})_3]^{2+}$  in  $\text{CH}_3\text{CN}$ .

$[\text{Ru}(\text{phen})_2(\text{dicnq})]^{2+}$ ,  $[\text{Ru}(\text{phen})(\text{dicnq})_2]^{2+}$  and  $[\text{Ru}(\text{dicnq})_3]^{2+}$ , respectively. (compare the corresponding  $\epsilon$  values in Table 4.2)

Visible region of the spectra of these complexes is characterized by the presence of broad  $d\pi-\pi^*$  MLCT transition (see Fig. 4.7, dashed lines). The MLCT transitions of  $[\text{Ru}(\text{phen})_2(\text{dicnq})]^{2+}$ ,  $[\text{Ru}(\text{phen})(\text{dicnq})_2]^{2+}$  and  $[\text{Ru}(\text{dicnq})_3]^{2+}$  are located at 445, 441 and 452 nm respectively, close to that of  $[\text{Ru}(\text{phen})_3]^{2+}$  (446 nm). Thus, although the electrochemical data suggest that the  $\pi^*$  orbital of dicnq lies lower than the phen  $\pi^*$  (vide supra), we believe that the MLCT absorptions of the new complexes investigated here could probably result from an overlap of  $\text{Ru}(d\pi) \rightarrow \text{dicnq}(\pi^*)$  and  $\text{Ru}(d\pi) \rightarrow \text{phen}(\pi^*)$  transitions as is the case with various mixed-ligand complexes of the type  $[\text{Ru}(\text{LL})_n(\text{LL}')_{3-n}]^{2+}$  where LL = bpy or phen and LL' is a heterocyclic ligand other than bpy/phen.<sup>11</sup>

Excitation of these complexes at 440 nm gave luminescence spectra in  $\text{CH}_3\text{CN}$  that are shown in Fig. 4.8. The relevant data are summarized in Table 4.2. Inspection of Fig. 4.8 and Table 4.2 reveals that while the mono- and bis- dicnq complexes are moderately luminescent with their emission maxima appearing at 616 and 613 nm respectively, the tris-dicnq complex is totally nonemissive in nature. The band maxima of these dicnq complexes are red shifted in comparison with that of  $[\text{Ru}(\text{phen})_3]^{2+}$  under the similar experimental conditions of solvent and excitation wavelength. This situation is quite similar to that of  $[\text{Ru}(\text{phen})_2(\text{dppz})]^{2+}$  which has been reported to have its  $^3\text{MLCT}$  emission band maximum located at 618 nm in  $\text{CH}_3\text{CN}$ .<sup>12</sup> Based, mainly, on the results of excited state absorption and resonance Raman spectroscopies,  $[\text{Ru}(\text{phen})_2(\text{dppz})]^{2+}$  and its *cousin*  $[\text{Ru}(\text{bpy})_2(\text{dppz})]^{2+}$  have

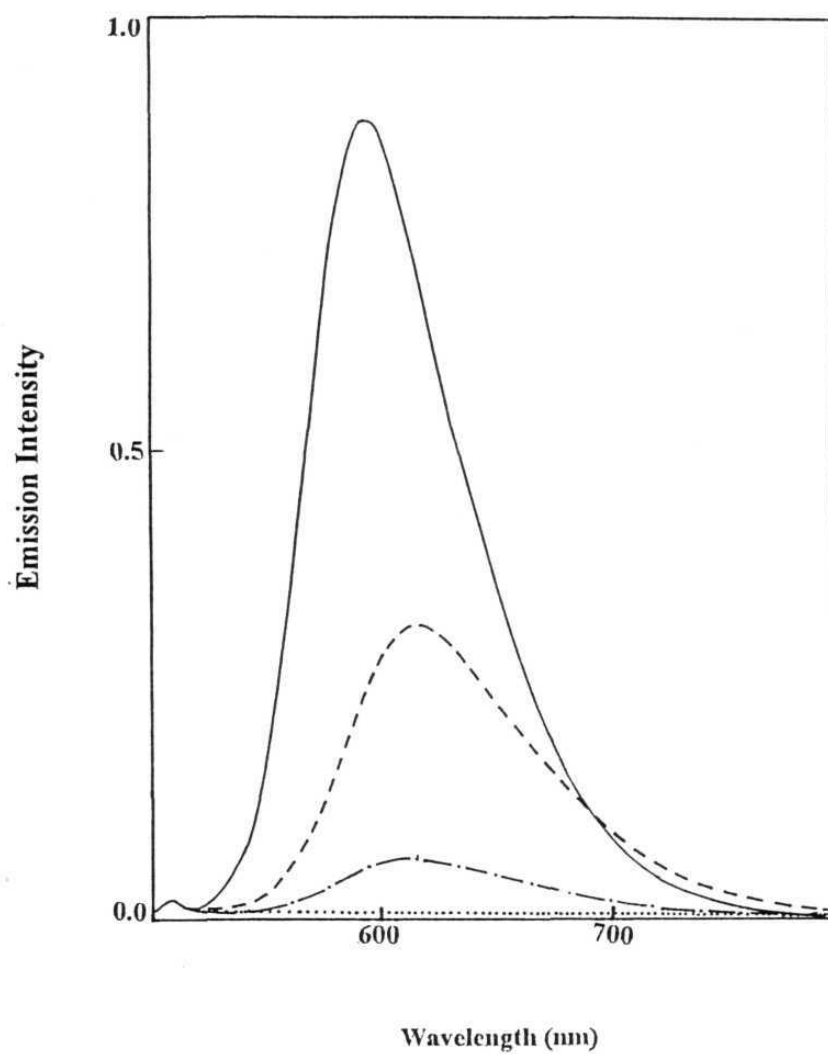
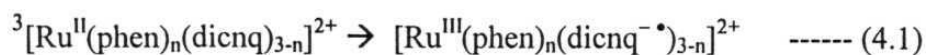


**Fig. 4.8.** Luminescence spectra of equi-absorbing (O. D = 0.2)  $[\text{Ru}(\text{phen})_3]^{2+}$  (—),  $[\text{Ru}(\text{phen})_2(\text{dicnq})]^{2+}$  (---),  $[\text{Ru}(\text{phen})(\text{dicnq})_2]^{2+}$  (- · - · -) and  $[\text{Ru}(\text{dicnq})_3]^{2+}$  (·····) in  $\text{CH}_3\text{CN}$  ( $\lambda_{\text{exc}} = 440 \text{ nm}$ ).

been reported to have their MLCT states localized on the electron withdrawing dipyridophenazine ligand.<sup>13</sup> It is reasonable to expect that the MLCT states of  $[\text{Ru}(\text{phen})_2(\text{dicnq})]^{2+}$  and  $[\text{Ru}(\text{phen})(\text{dicnq})_2]^{2+}$  are also localized mainly on dicnq. However, confirmation of this proposal awaits the excited state absorption data on these complexes.

Data given in Table 4.2 also reveals that the emission quantum yields of the complexes investigated here are lower than that  $\text{Ru}(\text{phen})_3^{2+}$  and vary as  $\text{Ru}(\text{phen})_3^{2+} > [\text{Ru}(\text{phen})_2(\text{dicnq})]^{2+} > [\text{Ru}(\text{phen})(\text{dicnq})_2]^{2+} \gg \text{Ru}(\text{dicnq})_3^{2+}$ . A variety of excited state processes including enhanced internal conversion and intersystem crossing, ion-association, excitation energy transfer (EET), photoinduced electron transfer (PET) etc. can be thought of to be operative in the quenching of emission observed for the complexes. Amongst these, the possibility of an intramolecular PET from the ruthenium center to the easily reducible dicnq ligand (equn. 4.1) is discussed here. A rough estimate of free energies ( $\Delta G$ ) for the PET reactions depicted in equn 4. 1 can be made using equn. 4.2.



$$\Delta G = E_{1/2}(\text{ox}) - E_{1/2}(\text{red}) - E_{0-0} \quad \text{----- (4.2)}$$

where  $E_{1/2}(\text{ox})$  and  $E_{1/2}(\text{red})$  are the oxidation and reduction potentials (see Table 4.1) of the donor and acceptor, respectively and  $E_{0-0}$  is the energy of the  $^3\text{MLCT}$  state of each complex. These calculations reveal that the  $\Delta G$  values for  $[\text{Ru}(\text{phen})_2(\text{dicnq})]^{2+}$  and  $[\text{Ru}(\text{phen})(\text{dicnq})_2]^{2+}$  are approximately 0.15, and -0.10 eV, respectively. Assuming that the  $E_{0-0}$  of  $[\text{Ru}(\text{dicnq})_3]^{2+}$  is

similar to that of  $[\text{Ru}(\text{phen})(\text{dicnq})_2]^{2+}$ , the value of  $\Delta G$  for an intramolecular PET for this complex can be estimated to be  $\sim -0.04$  eV. Thus, an intramolecular PET of the type given in equn. 4.1 is, in principle, possible in at least two of these complexes but, it is only moderate unlike the case with  $[\text{Ru}(\text{phen})_2(\text{qdppz})]^{2+}$  discussed in the previous chapter. In addition, we note here that it is not generally correct to consider exclusively a PET-based mechanism relying only on the thermodynamic criteria. Therefore, it is reasonable to expect that a PET based mechanism does contribute to the excited state decay of these donor-acceptor type complexes. As stated earlier, other intramolecular processes including an increase in the non-radiative emission rate of the  $^3\text{MLCT}$  state as reported for  $[\text{Ru}(\text{tap})_3]^{2+}$  (tap = 1,4,5,8-tetraazaphenanthrene) and even  $[\text{Ru}(\text{phen})_2(\text{dppz})]^{2+}$  in polar, aprotic solvents can not be ruled altogether.<sup>14</sup>

#### 4.4 DNA binding

Binding of the three new complexes synthesized in this study with CT DNA has been monitored by thermal denaturation, absorption titration and luminescence methods. These results are summarized in this Section which also discusses on aspects related to the ability of these complexes to act as “molecular light switches” for DNA.

CT DNA was seen to melt at  $60 \pm 1^\circ \text{C}$  (2 mM NaCl, 1mM phosphate) in the absence of any added complex. The  $T_m$  of DNA is increased by 5 and 3  $^\circ\text{C}$  in the presence of  $[\text{Ru}(\text{phen})_2(\text{dicnq})]^{2+}$  and  $[\text{Ru}(\text{phen})(\text{dicnq})_2]^{2+}$  (at  $[\text{DNA nucleotide phosphate}] / [\text{complex}] = 25$ ), respectively. The increase in the melting temperature of DNA can be interpreted in terms of the

stabilisation that results from the intercalation of these metal complexes with DNA.<sup>15</sup>  $[\text{Ru}(\text{dicnq})_3]^{2+}$  has no effect on the melting temperature of the DNA. Thus, it is likely that while  $[\text{Ru}(\text{phen})_2(\text{dicnq})]^{2+}$  and  $[\text{Ru}(\text{phen})(\text{dicnq})_2]^{2+}$  bind with DNA *via* intercalation,  $[\text{Ru}(\text{dicnq})_3]^{2+}$  may interact with the duplex through the minor groove or other, as yet unidentified, mode/s of binding.<sup>15</sup> The absorption titration data also seem to suggest the same.

$[\text{Ru}(\text{phen})_2(\text{dicnq})]^{2+}$  and  $[\text{Ru}(\text{phen})(\text{dicnq})_2]^{2+}$  showed the presence of isosbestic point/s, hypochromicity and red-shifted absorption maxima during the absorption titration experiments with CT DNA as illustrated for  $[\text{Ru}(\text{phen})(\text{dicnq})_2]^{2+}$  in Fig. 4.9. As seen in this Figure, presence of an isosbestic point at 477 nm and decrease in absorbance are noticed for the complex upon successive additions of CT DNA. Data from the absorption titration were fit to equn. 2.17 to give the binding constant  $K_b = (4.0 \pm 0.5) \times 10^4 \text{ M}^{-1}$  for this complex. In a similar set of experiments,  $[\text{Ru}(\text{phen})_2(\text{dicnq})]^{2+}$  and  $[\text{Ru}(\text{dicnq})_3]^{2+}$  both showed isosbestic points at 488 nm and, the binding constants were estimated to be  $(4.3 \pm 0.5) \times 10^4$  and  $(9.1 \pm 0.5) \times 10^3 \text{ M}^{-1}$ , respectively. The  $K_b$  values for all the three dicnq containing complexes are close to that of  $[\text{Ru}(\text{phen})_3]^{2+}$  but, are too low in comparison with the strong ( $K_b > 10^6 \text{ M}^{-1}$ ) DNA binding exhibited by  $[\text{Ru}(\text{phen})_2(\text{dppz})]^{2+}$  and  $[\text{Ru}(\text{phen})_2(\text{qdppz})]^{2+}$  described in the previous Chapter (see Table 4.3). Obviously, dicnq is not as an extended  $\pi$ -system as dppz is and, nor does its architecture contain a fused quinone moiety as in the case of qdppz.

It is interesting to note that the strength of DNA binding varies as  $[\text{Ru}(\text{phen})_2(\text{dicnq})]^{2+} \geq [\text{Ru}(\text{phen})(\text{dicnq})_2]^{2+} > [\text{Ru}(\text{dicnq})_3]^{2+}$ . The reasons

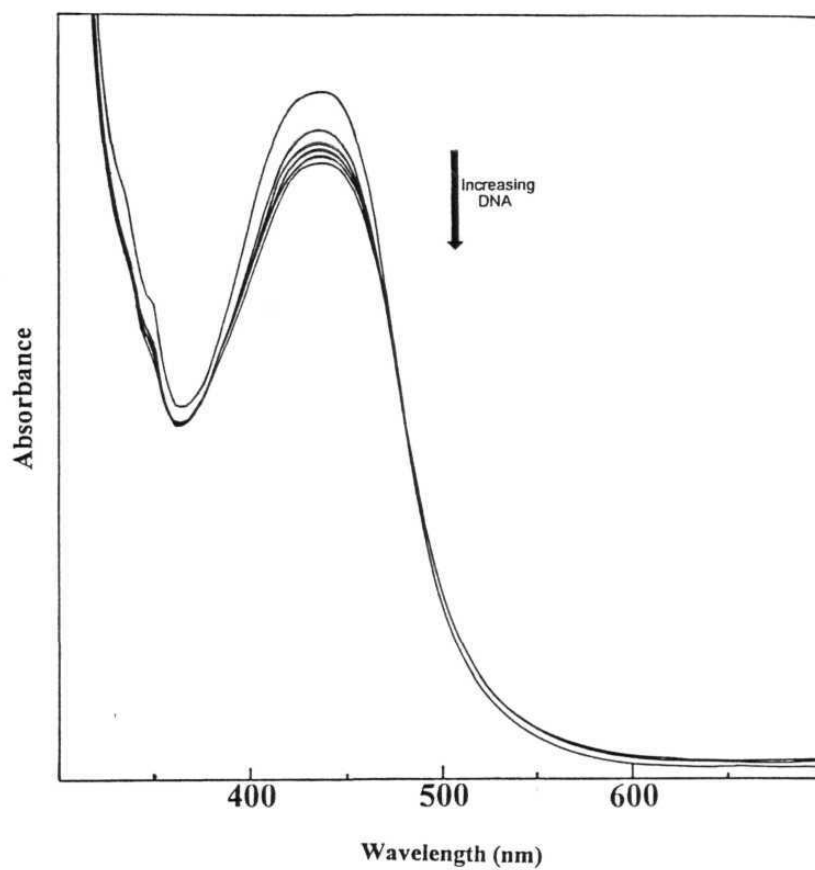


**Fig. 4.9.** UV-visible titration of  $[\text{Ru}(\text{phen})(\text{dicnq})_2]^{2+}$  with CT DNA in Bufl  
A.  $[\text{Ru}(\text{phen})(\text{dicnq})_2]^{2+} = 27 \mu\text{M}$ ;  $[\text{DNA base pairs}] = 0 - 100 \mu\text{M}$ .

**Table 4.3** Results of absorption titration ( $K_b$ ), thermal denaturation ( $T_m$ ) and luminescence studies carried out in the presence of DNA.

Compound	$K_b, M^{-1}$	$T_m, ^\circ C^a$	$I/I_0^b (R)$
DNA	-	60.0	-
$[Ru(phen)_2(dicnq)]^{2+}$	$4.30 \times 10^4$	65.0	15.9 (36)
$[Ru(phen)(dicnq)_2]^{2+}$	$4.01 \times 10^4$	63.5	8.3 (69)
$[Ru(dicnq)_3]^{2+}$	$9.10 \times 10^3$	60.0	-
$[Ru(phen)_3]^{2+}$	$7.88 \times 10^3$	68.0	2.0 (80)
$[Ru(phen)_2(dppz)]^{2+}$	$>10^7$	64.5	$>10^4$ (10)

a:  $[DNA \text{ nucleotide phosphate}]/[Drug] = 25$

b:  $I$  = Intensity of free complex,  $I_0$  = Intensity of the complex in the presence of DNA;  $R = [DNA \text{ nucleotide phosphate}]/[Drug]$

for the observed weak DNA binding by the tris-dicnq complex in comparison with the mixed-ligand complexes is not completely understood at present. As discussed above, it is possible that while  $[\text{Ru}(\text{phen})_2(\text{dicnq})]^{2+}$  and  $[\text{Ru}(\text{phen})(\text{dicnq})_2]^{2+}$  bind with DNA *via* intercalation, the tris-dicnq complex may interact with the duplex through a weak, non-intercalative mode of binding. In this regard, it should be noted that the presence of three dicnq ligands in  $[\text{Ru}(\text{dicnq})_3]^{2+}$  might sterically hinder the insertion of this ligand into the adjacent base pairs; the ancillary ligands might clash against the phosphate backbone. Effects such as net charge on the molecule, nature of the ligand, overall shape of the complex etc. are all known to influence the binding propensity of a given ruthenium complex with DNA.<sup>16</sup> Finally, the difference between the  $K_b$  values of  $[\text{Ru}(\text{phen})_2(\text{dicnq})]^{2+}$  and  $[\text{Ru}(\text{phen})(\text{dicnq})_2]^{2+}$  is only marginal and is within the experimental error. In these systems, based solely on the absorption titration data, it is difficult to ascertain whether it is phen or dicnq (or both!) that is intercalating with the DNA. Therefore, DNA interactions of these two complexes were also probed by the luminescence method; the results are described below.

Steady state emission spectra of 10  $\mu\text{M}$  solutions of  $[\text{Ru}(\text{phen})_2(\text{dicnq})]^{2+}$  and  $[\text{Ru}(\text{phen})(\text{dicnq})_2]^{2+}$  in tris buffer (5 mM Tris, 50 mM NaCl, pH 7.1) showed an increase in the emission intensity with successive addition of CT DNA. Fig. 4.10 illustrates this effect for these complexes along with that observed for  $[\text{Ru}(\text{phen})_3]^{2+}$  and  $[\text{Ru}(\text{phen})_2(\text{dppz})]^{2+}$ . As seen in this Figure, the spectral profile and the emission maximum are not markedly affected upon addition of DNA for each complex. Luminescence due to  $[\text{Ru}(\text{phen})_2(\text{dicnq})]^{2+}$  increases steadily with

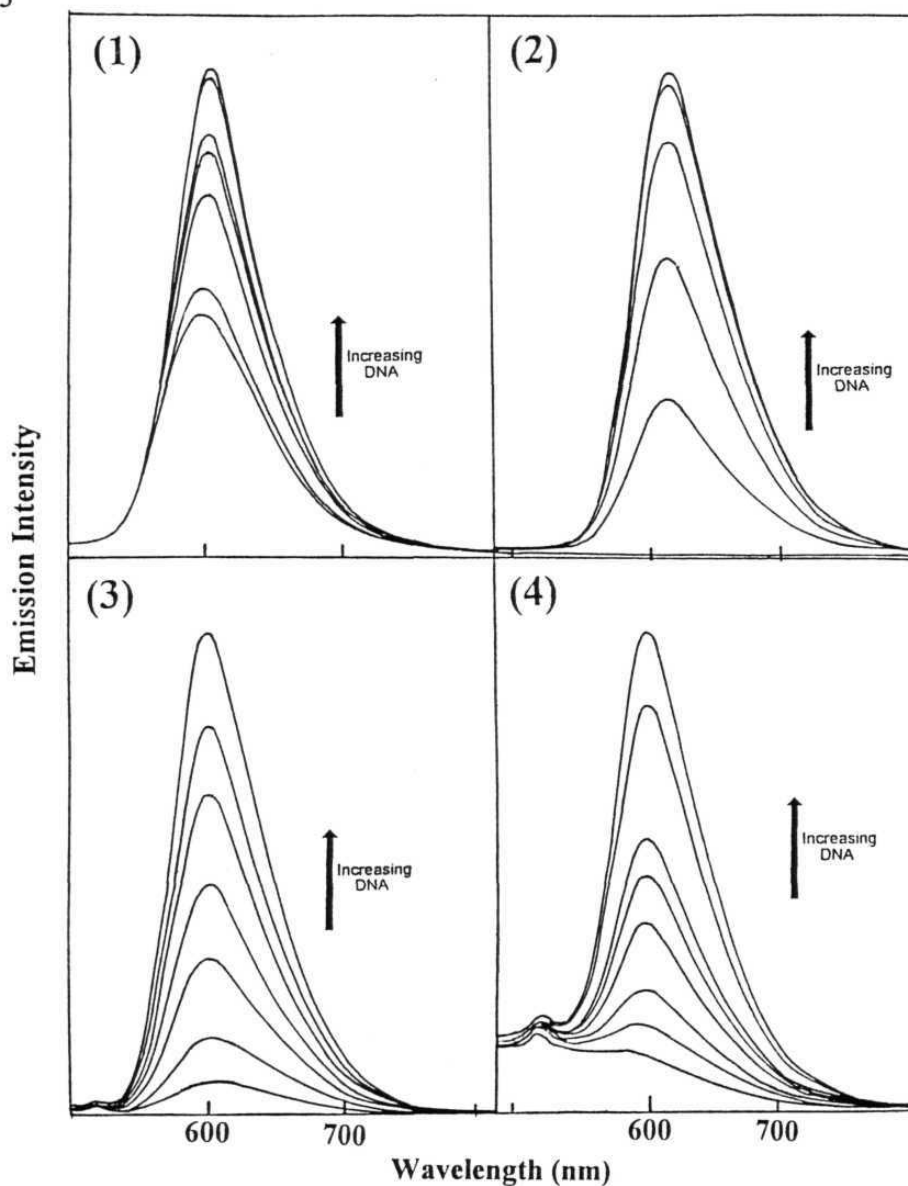


**Fig. 4.10.** Luminescence titration of the ruthenium(II) complexes with CT DNA in Buffer A. (1)  $[\text{Ru}(\text{phen})_3]^{2+}$ , (2)  $[\text{Ru}(\text{phen})_2(\text{dppz})]^{2+}$ , (3)  $[\text{Ru}(\text{phen})_2(\text{dicnq})]^{2+}$  and (4)  $[\text{Ru}(\text{phen})(\text{dicnq})_2]^{2+}$ . Concentration of the all the ruthenium complexes = 10  $\mu\text{M}$ , maximum DNA concentration (in nucleotide phosphate) used for (1), (2), (3) and (4) are 800, 100, 370 and 690  $\mu\text{M}$ , respectively.;  $\lambda_{\text{exc}} = 440 \text{ nm}$ .

increasing addition of CT DNA and reaches a maximum ( $\sim 16$  times, see Table 4.3 and Fig. 4.11) at [DNA nucleotide phosphate]/[Ru] ratio of 36. Further addition of DNA results in a slight decrease in the intensity of luminescence. In the case of  $[\text{Ru}(\text{phen})(\text{dicnq})_2]^{2+}$ , luminescence increases initially at low [DNA nucleotide phosphate]/[Ru] ratio but, reaches a plateau with the apparent enhancement factor of  $\sim 8$  at higher [DNA nucleotide phosphate]/[Ru] ratio.  $[\text{Ru}(\text{phen})_3]^{2+}$  also shows an intensity enhancement in the presence of DNA but, only moderately; the enhancement factor is only 2 for this complex even at [DNA nucleotide phosphate]/[Ru] ratio of  $\sim 80$  (see Fig. 4.11). On the other hand and as discussed in the previous Chapter,  $[\text{Ru}(\text{phen})_2(\text{dppz})]^{2+}$  shows a  $>10^4$  times enhancement of emission in the presence of DNA. In this case, emission enhancement has been ascribed to the protection of the imine nitrogen from attack by water and a consequent decrease in the non-radiative processes upon intercalation.<sup>17</sup> We believe that, dicnq being a quinoxaline ligand bearing imine nitrogens, the increase in emission intensity observed for  $[\text{Ru}(\text{phen})_2(\text{dicnq})]^{2+}$  and  $[\text{Ru}(\text{phen})(\text{dicnq})_2]^{2+}$  in the presence of DNA is also a consequence of a decrease in the non-radiative deactivation process of each excited complex due to the protection of dicnq ligand by intercalation.

Interestingly, although the DNA binding constants of  $[\text{Ru}(\text{phen})_2(\text{dicnq})]^{2+}$  and  $[\text{Ru}(\text{phen})(\text{dicnq})_2]^{2+}$  are close to each other (vide supra), the former complex shows relatively higher emission enhancement compared to the latter upon addition of DNA. The reasons for this is not immediately obvious but, it should be noted that there exists a second, non-

intercalating, spectator dicnq ligand on  $[\text{Ru}(\text{phen})(\text{dicnq})_2]^{2+}$  that is exposed to water. Thus, it is clear from these luminescence studies that dicnq is

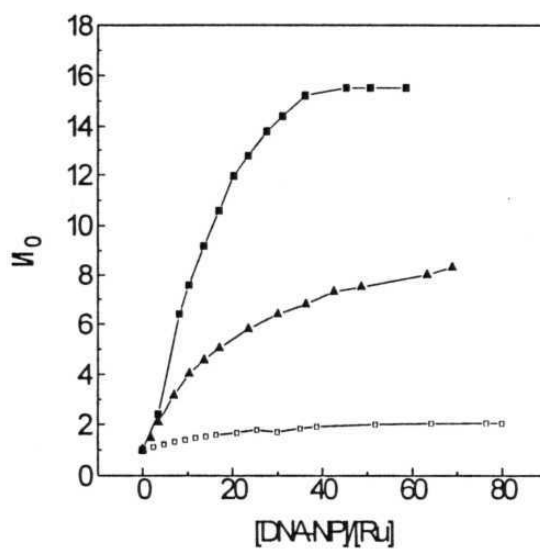


**Fig. 4.11.** Emission (I) due to 10  $\mu\text{M}$  solutions (buffer A) of  $[\text{Ru}(\text{phen})_2(\text{dicnq})]^{2+}$  (■),  $[\text{Ru}(\text{phen})(\text{dicnq})_2]^{2+}$  (▲) and  $[\text{Ru}(\text{dicnq})_3]^{2+}$  (□) versus increasing ratios of [DNA nucleotide phosphate]/[Ru].

involved in the DNA intercalation by  $[\text{Ru}(\text{phen})_2(\text{dicnq})]^{2+}$  and  $[\text{Ru}(\text{phen})(\text{dicnq})_2]^{2+}$  and that these complexes are moderately efficient molecular light switches for DNA.<sup>17</sup>

Finally, there was no emission enhancement for  $[\text{Ru}(\text{dicnq})_3]^{2+}$  in the presence of DNA. In this regard, it should be noted that  $[\text{Ru}(\text{dicnq})_3]^{2+}$  does not emit in both water and dry  $\text{CH}_3\text{CN}$  (or in dry  $\text{CH}_2\text{Cl}_2$ , for the  $\text{PF}_6$  salt),

which rules out the possibility of luminescence quenching *via* the attack of water at the quinoxaline nitrogens and the subsequent enhancement in the non-radiative decay. Instead, as suggested above, an intramolecular electron transfer involving the  $^3\text{MLCT}$  state and the ligand might explain the apparent non-emissive nature of this complex. This particular result additionally lends credence to the proposal made earlier that an intramolecular PET reaction is the major process in the decay of the excited states of  $\text{Ru}(\text{phen})_2(\text{dicnq})]^{2+}$  and  $[\text{Ru}(\text{phen})(\text{dicnq})_2]^{2+}$  as well.

#### 4.5 DNA photocleavage

Irradiation of samples containing pBR 322 DNA and each of these complexes were carried out as described in Chapter 2 and, the effects were monitored by the agarose gel electrophoresis method. Control experiments suggested that photolysis of untreated plasmid does not produce Form II from the native Form I upon irradiation of the sample at 440 nm for 20 min. In addition, both phen and dicnq (dissolved in 10% DMF) are not detectably active either in dark or upon irradiation. Fig. 4.12 shows gel electrophoresis pattern of the plasmid pBR 322 DNA in the presence of the three metal complexes (10  $\mu\text{M}$ ) investigated in this study. Lanes 1-3 refer to the dark experiments and Lanes 4-6 to the light experiments in this Figure. In the dark experiments, no DNA nicking was perceptible for the plasmid in the presence of each of these complexes. However, the strong interaction of  $[\text{Ru}(\text{phen})_2(\text{dicnq})]^{2+}$  with DNA can be seen from the increased streaking and retardation of DNA mobility.<sup>15b,18</sup> Whereas,  $[\text{Ru}(\text{phen})(\text{dicnq})_2]^{2+}$  and  $[\text{Ru}(\text{dicnq})_3]^{2+}$  show no such effect. In the light experiments,



$[\text{Ru}(\text{phen})_2(\text{dicnq})]^{2+}$  and  $[\text{Ru}(\text{phen})(\text{dicnq})_2]^{2+}$  cause single strand nicking with the conversion of Form I to Form II whereas,  $[\text{Ru}(\text{dicnq})_3]^{2+}$  shows no appreciable photocleavage. While the precise mechanism of the DNA cleavage by these complexes has not been explored and is still unknown, it is tempting to suggest, based on the absorption and luminescence results described above, that the DNA nicking ability of these complexes depends on their mode of binding with DNA.

#### 4.6 Summary

A series of ruthenium(II) complexes containing the new ligand dicnq have been synthesized and fully characterized by various physico-chemical techniques. Results of absorption and fluorescence titration, thermal denaturation and agarose gel electrophoresis experiments suggest that while both  $[\text{Ru}(\text{phen})_2(\text{dicnq})]^{2+}$  and  $[\text{Ru}(\text{phen})(\text{dicnq})_2]^{2+}$  bind to DNA *via* an intercalative mode, the tris- complex,  $[\text{Ru}(\text{dicnq})_3]^{2+}$ , on the other hand, binds to DNA only weakly and, the binding in this case may not involve intercalation. The DNA photocleavage efficiencies of the three complexes follow an order:  $[\text{Ru}(\text{phen})_2(\text{dicnq})]^{2+} > [\text{Ru}(\text{phen})(\text{dicnq})_2]^{2+} \gg [\text{Ru}(\text{dicnq})_3]^{2+}$ . Both  $[\text{Ru}(\text{phen})_2(\text{dicnq})]^{2+}$  and  $[\text{Ru}(\text{phen})(\text{dicnq})_2]^{2+}$  are luminescent in organic solvents but,  $[\text{Ru}(\text{dicnq})_3]^{2+}$  is totally non-luminescent. Finally, detailed luminescence studies have revealed that both  $[\text{Ru}(\text{phen})_2(\text{dicnq})]^{2+}$  and  $[\text{Ru}(\text{phen})(\text{dicnq})_2]^{2+}$  are moderately efficient molecular light switches in the presence of DNA.

#### 4.7 References

1. Yamada, M.; Tanaka, Y.; Yoshimoto, Y.; Kuroda, S.; Shimao, I. *Bull. Chem. Soc. Jpn.* **1992**, 65, 1006.
2. Lin, C.-T.; Bottcher, W.; Chou, M.; Cruetz, C.; Sutin, M. *J. Am. Chem. Soc.* **1976**, 98, 6536.
3. Sullivan, B. P.; Salmon, D. J.; Meyer, T. J. *Inorg. Chem.* **1978**, 17, 3334.
4. Krause, R. A. *Inorg. Chim. Acta* **1977**, 22, 209.
5. Dickeson, J. E.; Summers, L. A. *Aust. J. Chem.* **1970**, 23, 1023.
6. Didier, P.; Jacquet, L.; Mesmaeker, A. K.; Hueber, R.; van Dorsselaer, A. *Inorg. Chem.* **1992**, 31, 4803.
7. (a) Ackermann, M. N.; Interrante, L. V. *Inorg. Chem.* **1984**, 23, 3904.  
(b) Rillema, D. P.; Allen, G.; Meyer, T. J.; Conrad, D. *Inorg. Chem.* **1983**, 22, 1617.
8. DeArmond, M. K.; Carlin, C. M. *Coord. Chem. Rev.* **1981**, 36, 325.
9. Juris, A.; Balzani, V.; Barigelletti, F.; Campagna, S.; Belser, P.; von Zelewsky, A. *Coord. Chem. Rev.* **1988**, 84, 85.
10. (a) Rillema, D. P.; Taghdiri, D. G.; Jones, D. S.; Keller, C. D.; Worl, L. A.; Meyer, T. J.; Levy, H. A. *Inorg. Chem.* **1987**, 26, 578. (b) Black, E. J.; Huang, H.; High, S.; Starks, L.; Olson, M.; McGuire, M. E. *Inorg. Chem.* **1993**, 32, 5591. (c) Goss, C. A.; Abruna, H. D. *Inorg. Chem.* **1985**, 24, 4263.
11. (a) Juris, A.; Belser, P.; Barigelletti, F.; von Zelewsky, A.; Balzani, V. *Inorg. Chem.* **1986**, 25, 256. (b) Anderson, P. A.; Strouse, G. F.;

- Treadway, J. A.; Keene, F. R.; Meyer, T. J. *Inorg. Chem.* **1994**, 33, 3863. (c) Yam, W. V.; Lee, W. V.; Ke, F.; Siu, K. M. *Inorg. Chem.* **1997**, 36, 2124.
12. Hartshorn, R. M.; Barton, J. K. *J. Am. Chem. Soc.* **1992**, 114, 5919.
13. (a) Chambron, J. C.; Sauvage, J. P.; Amouyal, E.; Koffi, P. *New J. Chem.* **1985**, 9, 527. (b) Amouyal, E.; Homsy, A.; Chambron, J. C.; Sauvage, J. P. *J. Chem. Soc., Dalton Trans.* **1990**, 1841. (c) Fees, J.; Kaim, W.; Moscherosch, M.; Matheis, W.; Klima, J.; Krejcik, M.; Zalis, S. *Inorg. Chem.* **1993**, 32, 166. (d) Schoonover, J. R.; Bates, W. D.; Meyer, T. J. *Inorg. Chem.* **1995**, 34, 6421. (e) Olson, E. J. C.; Hu, D.; Hormann, A.; Jonkman, A. M.; Arkin, M. R.; Stemp, E. D. A.; Barton, J. K.; Barbara, P. F. *J. Am. Chem. Soc.* **1997**, 119, 11458.
14. (a) Masschelein, A.; Jacquet, L.; Mesmacker, A. K.; Nasielski, J. *Inorg. Chem.* **1990**, 29, 855. (b) Nair, R. B.; Cullum, B. M.; Murphy, C. J. *Inorg. Chem.* **1997**, 36, 962.
15. (a) Kelly, J. M.; Tossi, A. B.; McConnell, D. J.; OhUigin, C. *Nucleic Acids Res.* **1985**, 13, 6017. (b) Long, E. C.; Barton, J. K. *Acc. Chem. Res.* **1990**, 23, 273. (c) Satyanarayana, S.; Dabrowiak, J. C.; Chaires, J. B. *Biochemistry*, **1992**, 31, 9319. (d) Neyhart, G. A.; Grover, N.; Smith, S. R.; Kalsbeck, W. A.; Fairley, T. A.; Cory, M.; Thorp, H. H. *J. Am. Chem. Soc.* **1993**, 115, 4423.
16. (a) Mei, H. Y.; Barton, J. K. *Proc. Natl. Acad. Sci. USA.* **1988**, 85, 1339. (b) Morgan, R. J.; Chatterjee, S.; Baker, A. D.; Strekas, T. C. *Inorg. Chem.* **1991**, 30, 2687.

17. (a) Friedman, A. E.; Kumar, C. V.; Turro, N. J.; Barton, J. K. *Nucleic Acids Res.* **1991**, 19, 2595. (b) Hartshorn, R. M.; Barton, J. K. *Inorg. Chem.* **1992**, 114, 5919. (c) Turro, C.; Bossmann, S. H.; Jenkins, Y.; Barton, J. K.; Turro, N. J. *J. Am. Chem. Soc.* **1995**, 117, 9026. (d) Olson, E. J. C.; Hu, D.; Hormann, A. Jonkman, A. M.; Arkin, M. R.; Stemp, E. D. A.; Barton, J. K.; Barbara, P. F. *J. Am. Chem. Soc.* **1997**, 119, 11458. (e) Moucheron, C.; Mesmaeker, A. K.; Choua, S. *Inorg. Chem.* **1997**, 36, 584.
18. (a) Waring, M. J. *J. Mol. Biol.* **1966**, 54, 247. (b) Espejo, R. T.; Lebowitz, J. *Anal. Biochem.* **1976**, 72, 95. (c) Keck, M. V.; Lippard, S. J. *J. Am. Chem. Soc.* **1992**, 114, 3386. (d) Goulle, V.; Lehn, J. M.; Schoentjes, B.; Schmitz, F. J. *Helv. Chim. Acta* **1991**, 74, 1471.

## CHAPTER 5

*Dipyridophenazine Complexes of Cobalt(III) and Nickel(II): DNA-Binding and Photocleavage Studies***5.1 Introduction**

Both  $[\text{Ru}(\text{phen})_2(\text{dppz})]^{2+}$  and  $[\text{Ru}(\text{bpy})_2(\text{dppz})]^{2+}$  (phen = 1,10-phenanthroline and dppz = dipyrido[3,2-a:2',3'-c]phenazine) have been reported to be avid binders of DNA and more importantly, to be remarkable luminescent reporters of DNA structure.<sup>1</sup> In addition, it has been recently shown, by Barton and co-workers, that the application of mixed-ligand ruthenium(II) complexes of the type  $[\text{Ru}(\text{phen})_2(\text{LL}') ]^{2+}$  (LL' = a modified phenanthroline ligand belongs to the dppz family) permits variations in geometry, size, hydrophobicity and hydrogen-bonding ability of the complexes and allows a variation in the strength of their DNA binding and "light switching" ability.<sup>2</sup> These aspects of Ru-dppz complexes have been discussed in the previous Chapters. In addition, DNA binding and photocleavage as well as novel luminescence properties of mixed-ligand complexes containing modified dppz ligands have been discussed in Chapters 3 and 4.

During the course of this work, it occurred to us that notwithstanding the well-documented importance of dppz in DNA interactions of the complexes containing it, binding studies using such complexes having a metal ion other than ruthenium have attracted much less attention; exceptions being

recent reports on  $[\text{Os}(\text{phen})_2(\text{dppz})]^{2+}$  and  $[\text{Re}(\text{py})_2(\text{CO})_3\text{dppz}]^+$  (py = pyridine).<sup>3</sup> Moreover, only a few studies seem to have addressed DNA cleavage aspects of dppz-based complexes. For example, in an elegant study, Paillous and co-workers have shown that  $[\text{Ru}(\text{phen})_2(\text{dppz})]^{2+}$  photocleaves DNA *via* a Type II process.<sup>4</sup> Electrochemically initiated cleavage of DNA by  $[\text{Ru}(\text{O})(\text{tpy})\text{dppz}]^{2+}$  (tpy = terpyridine) has been reported recently.<sup>5</sup> Clearly, further studies using various  $[\text{M}(\text{phen})_2(\text{dppz})]^{n+}$  complexes are needed to evaluate the influence of metal-ion induced geometry, charge, spin-state, redox potential, etc. changes on the DNA binding and cleavage mechanisms in this important class of complexes as was the case with the previously reported metalloderivatives (M = Ru, Rh, Co, Cr, etc.) of phen or modified phen ligands.<sup>6,7</sup> Such studies are also needed to serve as complementary studies to those involving  $[\text{Ru}(\text{phen})_2(\text{LL}') ]^{2+}$  type complexes mentioned above. This Chapter reports on the synthesis, characterization, DNA binding, and photochemical DNA cleavage characteristics of  $[\text{M}(\text{phen})_2(\text{dppz})]^{n+}$  where M = Co(III) or Ni(II) and n = 3 or 2, respectively.

## 5.2 Experimental details

1,10-phenanthroline-5,6-dione (phen-dione),<sup>8</sup> dppz,<sup>9</sup>  $[\text{Co}(\text{phen})_2\text{Cl}_2] \cdot 3\text{H}_2\text{O}^{10a}$   $[\text{Co}(\text{phen})_3]\text{Cl}_2^{10b}$   $[\text{Ni}(\text{phen})_2\text{Cl}_2]^{11}$  and  $[\text{Ni}(\text{phen})_3]\text{Cl}_2^{11}$  were synthesized following the reported procedures (see Chapter 2). Synthesis of the hexafluorophosphate and chloride salts of  $[\text{Co}(\text{phen})_2(\text{dppz})]^{3+}$  and  $[\text{Ni}(\text{phen})_2(\text{dppz})]^{2+}$  are described below (see Fig. 5.1)

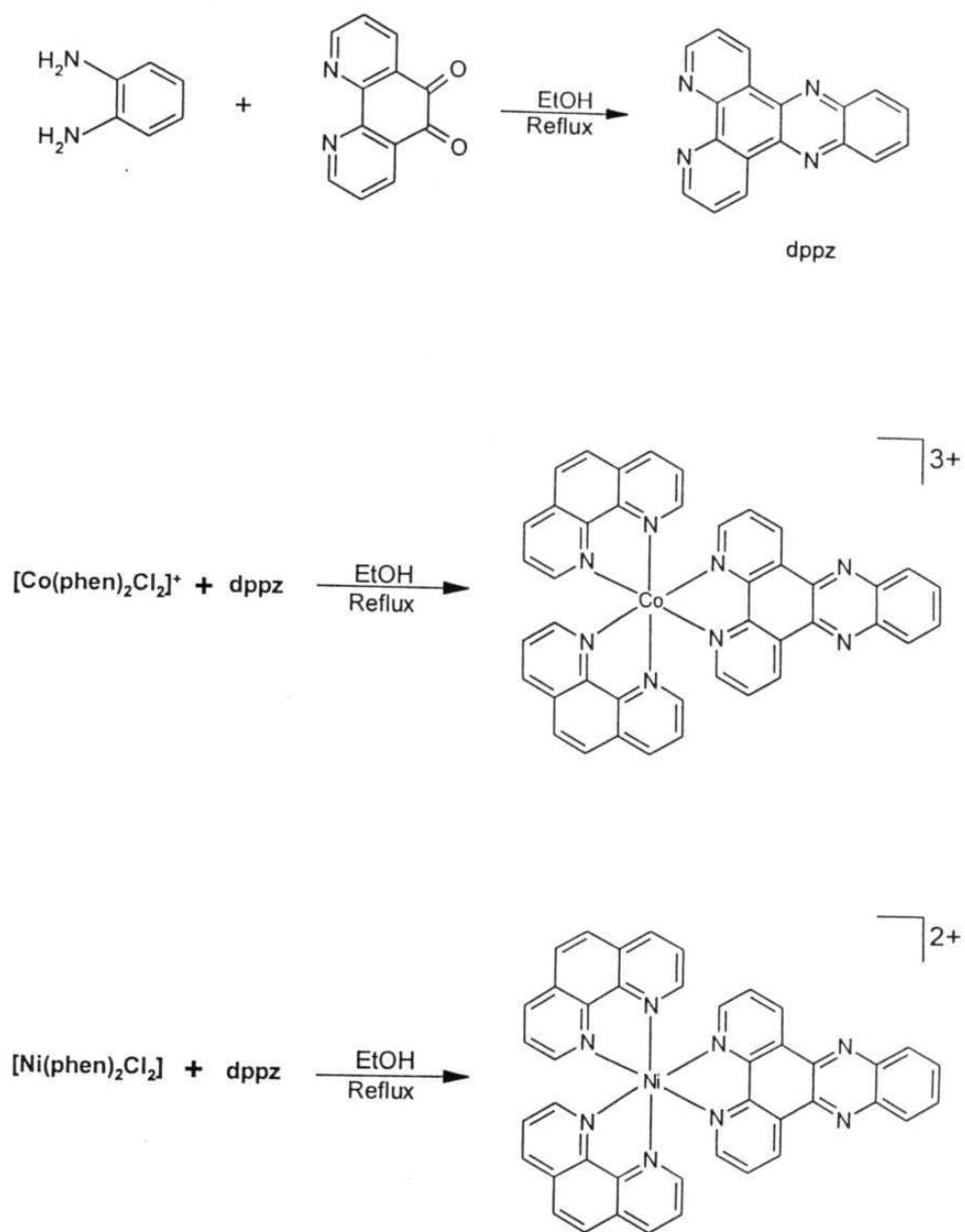


Fig. 5.1

### 5.2.1 Synthesis of $[\text{Co}(\text{phen})_2(\text{dppz})](\text{PF}_6)_3 \cdot 5\text{H}_2\text{O}$

To a 50 ml of ethanolic solution of  $[\text{Co}(\text{phen})_2\text{Cl}_2] \cdot 3\text{H}_2\text{O}$  (578 mg, 1.0 mM) was added 423 mg (1.5 mM) sample of dppz. The resulting solution was refluxed for 1 h. and further stirred for 4-5 h. under nitrogen. It was filtered, and the complex was precipitated upon addition of a saturated ethanolic solution of  $\text{NH}_4\text{PF}_6$ . The complex was filtered and further dried under vacuum before being recrystallized (acetone-ether). Yield: ~70%.

Analytical data: Found: C, 41.13; H, 2.95; N, 9.13. Calcd for  $\text{C}_{42}\text{H}_{34}\text{N}_8\text{O}_5\text{P}_3\text{F}_{18}\text{Co}$ : C, 41.74; H, 2.84; N, 9.27.

FABMS (m/z):  $[\text{M} - \text{PF}_6]^+$ , 991;  $[\text{M} - 2\text{PF}_6]$ , 846.

IR (KBr): 3400, 1608, 1523, 1506, 1433, 858 and  $715\text{ cm}^{-1}$ .

$^1\text{H}$  NMR ( $\text{DMSO-d}_6$ , 200 MHz, TMS)  $\delta$ , ppm: 9.95(dd, 2H), 9.21(d, 2H), 9.18(d, 2H), 8.59(m, 8H), 8.32(d, 4H), 8.00(m, 4H), 7.68(d, 4H).

### 5.2.2 Synthesis of $[\text{Ni}(\text{phen})_2(\text{dppz})](\text{PF}_6)_2 \cdot 4\text{H}_2\text{O}$

This complex was prepared, starting from  $[\text{Ni}(\text{phen})_2\text{Cl}_2]$  (490 mg, 1.0 mM) and dppz (423 mg, 1.5 mM) in a manner analogous to that described above for the cobalt complex. Yield: ~ 70%.

Analytical data: Found : C, 47.44; H, 3.22; N, 10.54. Calcd for  $\text{C}_{42}\text{H}_{34}\text{N}_8\text{O}_4\text{P}_2\text{F}_{12}\text{Ni}$ : C, 47.40; H, 3.21; N, 10.45.

FABMS (m/z):  $[\text{M} - \text{PF}_6]^+$ , 845;  $[\text{M} - \text{phen} - 2\text{PF}_6]^{2+}$ , 520.

IR (KBr): 3408, 1624, 1516, 1494, 1423, 848 and  $727\text{ cm}^{-1}$ .

$\mu_{\text{eff}}$  (solid,  $293 \pm 2\text{ K}$ ):  $3.16\ \mu_{\text{B}}$ .

Each hexafluorophosphate salt was dissolved in minimum amount of acetone and a saturated solution of TBACl in acetone was added dropwise until the precipitation was complete. The water-soluble chloride salts thus obtained were filtered, washed thoroughly with acetone and vacuum dried. Recovery was about 90% of the theoretical yield in each case.

All the spectroscopic and electrochemical experiments leading to the characterization of the new complexes synthesized here were carried out as outlined in Chapter 2.

For the spin trapping experiments using ESR, the solution (deaerated aqueous (1 %) CH<sub>3</sub>CN) containing [Co(phen)<sub>2</sub>(dppz)]<sup>3+</sup> (1 mM) and spin trapping agent PBN (20 mM) was taken in a flat quartz ESR tube and an on-line irradiation ( $\lambda > 350$  nm) of the sample in the ESR cavity was carried out as described in Chapter 2.

### 5.2.3 DNA binding and photocleavage studies

Buffer A (5 mM tris, pH 7.1, 50 mM NaCl) was used for absorption titration experiments and luminescence measurements. Buffer B (1 mM phosphate, pH 7.0, 2 mM NaCl) was used for thermal denaturation and differential-pulse voltammetric experiments. The chloride salt of the complexes was used in studies with DNA.

DNA melting- ( [DNA nucleotide phosphate] = 160  $\mu$ M, [drug] = 0 - 10  $\mu$ M) and absorption titration ( [DNA base pairs] = 0 - 40  $\mu$ M, [drug] = 15

$\mu\text{M}$ ) experiments were carried out as described in Chapter 2. Differential-pulse voltammetric experiments (highly polished glassy carbon working electrode, Pt-wire counter electrode and SCE reference electrode) were performed for 0.1 mM of the complex in the absence and in the presence of increasing amounts (0 - 3 mM) of CT DNA.

Absorbance values were recorded after each successive addition of DNA solution and equilibration (ca. 10 min.). Data obtained from the absorption titration experiments were analyzed as described in Chapter 2.

Gel electrophoresis experiments were also carried out as described in Chapter 2. Irradiation experiments were carried out by keeping the pre-incubated (dark, 1 h.) samples inside the sample chamber of a JASCO Model FP-777 spectrofluorometer ( $\lambda_{\text{exc}} = 350 \pm 5 \text{ nm}$ ; slit width = 5 nm).

## 5.3 Results and discussion

### 5.3.1 Synthesis and characterization

$[\text{Co}(\text{phen})_2(\text{dppz})]^{3+}$  and  $[\text{Ni}(\text{phen})_2(\text{dppz})]^{2+}$  were synthesized by the reaction of the corresponding dichloro complexes with dppz. Each new complex showed satisfactory elemental analysis, FABMS and IR data. While the  $d^6$ , diamagnetic cobalt complex was further characterized by its  $^1\text{H}$  NMR spectrum, the nickel complex, upon incorporating the diamagnetic correction, gave a  $\mu_{\text{eff}}$  of  $3.16 \mu_{\text{B}}$  consistent with the presence of a  $d^8$ , paramagnetic nickel(II) ion in it.<sup>11</sup>

### 5.3.2 UV-visible spectra

The UV-visible spectral data of dppz,  $[\text{Co}(\text{phen})_2(\text{dppz})]^{2+}$ ,  $[\text{Ni}(\text{phen})_2(\text{dppz})]^{2+}$  and, for comparison purposes,  $[\text{Ru}(\text{phen})_2(\text{dppz})]^{2+}$  are given in the Table. 5.1. UV-visible spectrum of the cobalt complex is illustrated in Fig. 5.2. The spectra (200-400 nm) of both the new complexes were seen to be dominated by bands due to the transitions involving phen and dppz ligands.<sup>12</sup> Absorption bands located at  $\sim 220$  and  $275$  nm for both the complexes arise from the  $\pi-\pi^*$  transitions of phen as well as dppz ligands. On the other hand, bands seen at  $348$ ,  $358$  &  $359$  and  $376$  &  $379$  nm in both  $[\text{Co}(\text{phen})_2(\text{dppz})]^{3+}$  and  $[\text{Ni}(\text{phen})_2(\text{dppz})]^{2+}$  can be assigned to  $\pi-\pi^*$  transitions of the metal-bound dppz. This interpretation is consistent with the spectral data of dppz,  $[\text{Ru}(\text{phen})_2(\text{dppz})]^{2+}$ <sup>1d</sup> and  $[\text{Ru}(\text{bpy})_2(\text{dppz})]^{2+}$ .<sup>1a</sup> It is also consistent with the interpretation of the spectral data of  $[\text{Ru}(\text{phen})_2(\text{qdppz})]^{2+}$  and  $[\text{Ru}(\text{phen})_2(\text{dicnq})]^{2+}$  (see Chapters 3 and 4).

### 5.3.3 Electrochemistry

The cyclic voltammetric data are summarized in the Table 5.2. The cyclic voltammogram of  $[\text{Co}(\text{phen})_2(\text{dppz})]^{3+}$  showed peaks at  $+0.40$ ,  $-0.95$ ,  $-1.17$ ,  $-1.70$  and  $-1.83$  V ( $\text{CH}_3\text{CN}$ ,  $0.1$  M  $\text{TBAPF}_6$ , vs SCE). Wave analysis suggested that while the peaks observed at  $+0.40$ ,  $-0.95$  and  $-1.17$  V represent diffusion-controlled, reversible/quasi-reversible, one electron transfer reactions (here  $i_p$  vs  $v^{1/2} = \text{constant}$  where  $i_p$  is the peak current and  $v$  is the scan rate,  $i_{pa}/i_{pc} = 0.9-1.0$  where  $i_{pa}$  and  $i_{pc}$  refers to anodic and cathodic peak potentials, respectively and  $\Delta E_p = 60-80$  mV where  $E_p$  is the peak potential),<sup>13</sup> those observed at  $-1.70$  and  $-1.83$  V are totally irreversible under identical

**Table 5.1** UV-visible data of dppz and its complexes in CH<sub>3</sub>CN

Compound	$\lambda_{\text{max}}$ , nm (log $\epsilon$ )
dppz	241 (4.49), 269 (4.73), 295 (4.28) 359 (4.05), 378 (4.06)
[Co(phen) <sub>2</sub> (dppz)] <sup>3+</sup>	220 (5.22), 282 (5.11), 330 (4.31) 348 (4.23), 359 (4.29), 377 (4.23)
[Ni(phen) <sub>2</sub> (dppz)] <sup>2+</sup>	226 (4.92), 273 (5.03), 325 (4.14) 348 (4.12), 358 (4.13), 376 (4.12)
[Ru(phen) <sub>2</sub> (dppz)] <sup>2+</sup>	265 (5.11), 277 (sh), 360 (4.39) 369 (4.35), 443 (4.33)

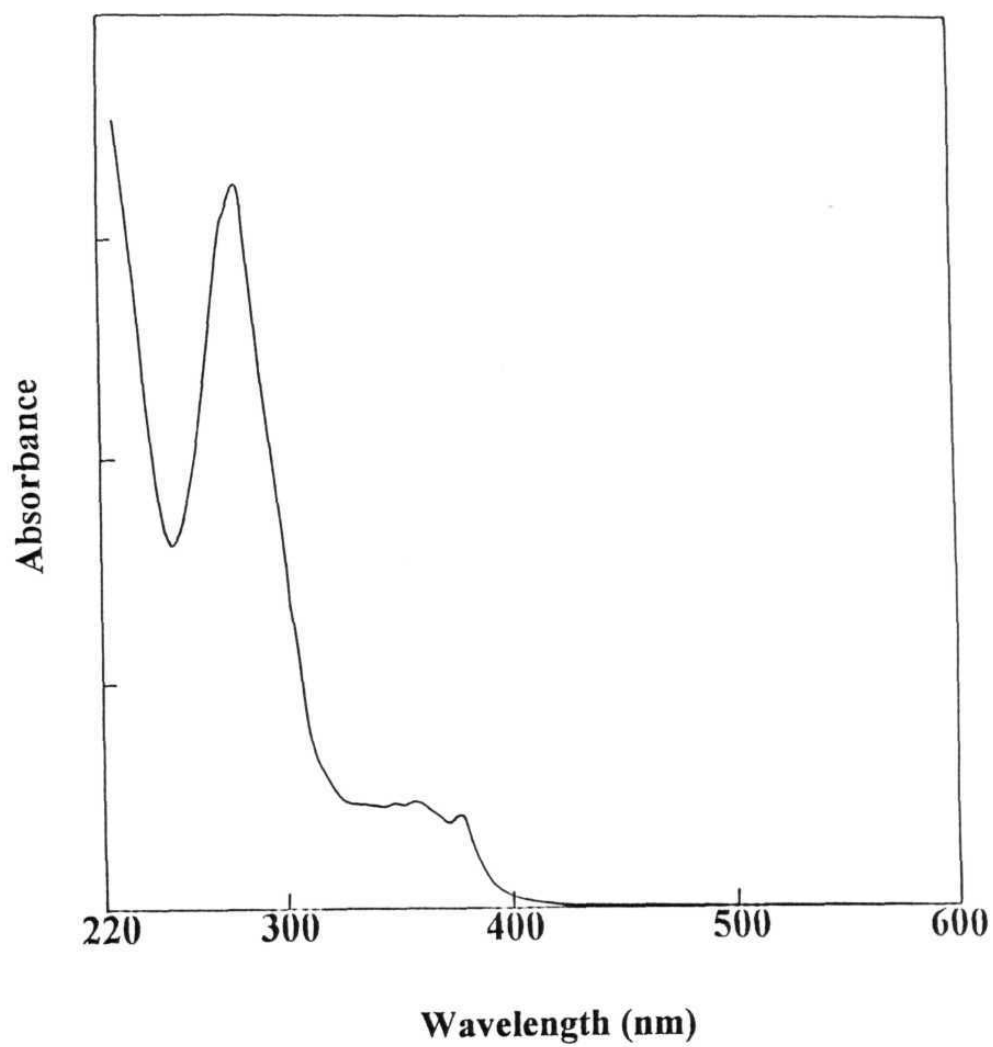


**Fig. 5.2.** UV-visible spectrum of  $[\text{Co}(\text{phen})_2(\text{dppz})]^{3+}$  in  $\text{CH}_3\text{CN}$ .

**Table 5.2** Cyclic voltammetric data of phen, dppz and their complexes in CH<sub>3</sub>CN, 0.1 M TBAPF<sub>6</sub>.

Compound	Potential, V vs SCE	
	Oxidation	Reduction
phen	-	-2.14
dppz	-	-1.22
phen-dione	-	-0.47
[Co(phen) <sub>2</sub> (dppz)] <sup>3+</sup>	+0.40	-0.95, -1.17, -1.70, -1.83
[Ni(phen) <sub>2</sub> (dppz)] <sup>2+</sup>	-	-0.99, -1.32, -1.46

experimental conditions. On the basis of the reported electrochemical data of  $[\text{Co}(\text{phen})_3]^{2+}$ <sup>14</sup> (+0.39, -0.96 V under our experimental conditions), the peak observed in the positive scan region for  $[\text{Co}(\text{phen})_2(\text{dppz})]^{3+}$  can be ascribed to the Co(III)/Co(II) redox couple and that observed at -0.95 V to the Co(II)/Co(I) couple. The peaks at -1.17, -1.70 and -1.83 V have been assigned to electron additions onto the Co(III)-bound dppz and phen ligands, respectively.<sup>12</sup> The ligands on  $[\text{Ni}(\text{phen})_2(\text{dppz})]^{2+}$  could be reduced at -1.29 and -1.72 V (dppz) and at -1.90 V (phen).

## 5.4 DNA binding studies

### 5.4.1 Absorption titration

Initial evidence for the binding of these complexes with DNA comes from the absorption titration experiments. Hypochromism and bathochromic shifts of the peak maxima in the UV-visible spectra of both  $[\text{Co}(\text{phen})_2(\text{dppz})]^{3+}$  and  $[\text{Ni}(\text{phen})_2(\text{dppz})]^{2+}$  were observed upon addition of increasing amounts of CT DNA to buffered solutions containing each of these complexes. As seen in the Fig. 5.3 (a), the lowest energy band of  $[\text{Ni}(\text{phen})_2(\text{dppz})]^{2+}$  (15  $\mu\text{M}$ ) shows a bathochromic shift of 7 nm in the presence of CT DNA (40  $\mu\text{M}$  in base pairs). The corresponding band in the cobalt complex, under similar experimental conditions, was seen to be red-shifted by 6 nm. Absorption titration curves with the absorbance being measured between 300 and 430 nm revealed that isosbestic points are present at 388 and 416 nm and at 385 nm and 414 nm for the nickel and cobalt complexes, respectively. These spectral changes are reminiscent of those

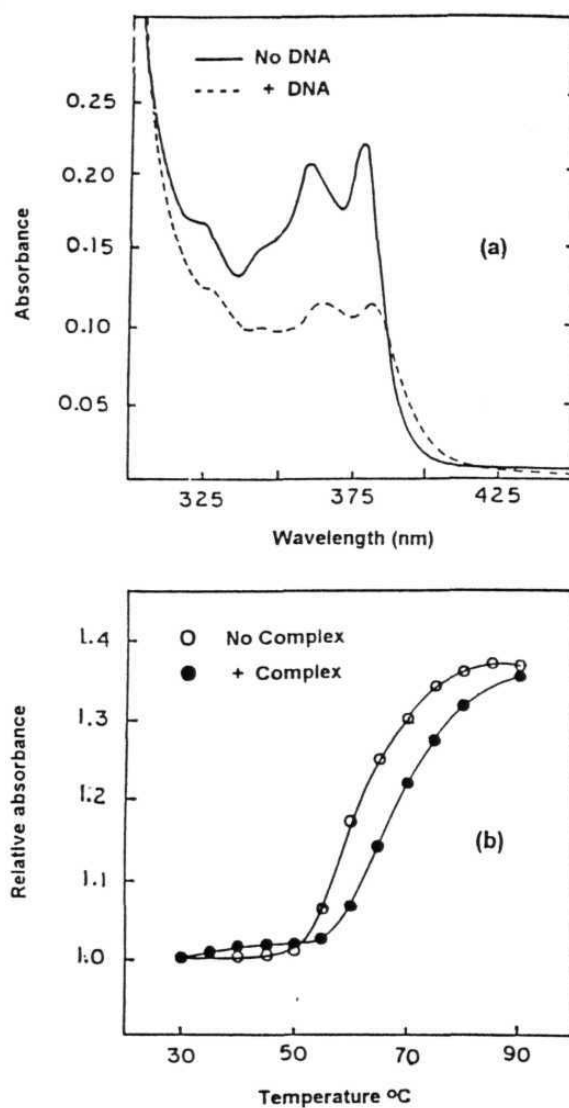


**Fig. 5.3.** (a) UV-visible spectra of  $[\text{Ni}(\text{phen})_2(\text{dppz})]^{2+}$  (15  $\mu\text{M}$ ) in the absence and in the presence of CT DNA (40  $\mu\text{M}$  base pairs). (b) Melting curves of CT DNA (160  $\mu\text{M}$  nucleotide phosphate) in the absence and in the presence of  $[\text{Co}(\text{phen})_2(\text{dppz})]^{3+}$  (8  $\mu\text{M}$ ).

reported for DNA interactions of several tris-chelated, mixed-ligand complexes containing phen and/or dppz including  $[\text{Ru}(\text{phen})_2(\text{dppz})]^{2+}$ .<sup>1</sup> The intrinsic binding constant  $K_b$ , which was obtained by monitoring the change in absorbance at 376 nm with increasing concentration of DNA is as high as  $(9 \pm 2) \times 10^5 \text{ M}^{-1}$  for both the complexes investigated in this study. It should be noted here that these  $K_b$  values can be taken only as the lower limit of the effective binding constants for these complexes because they bind too strongly even at micromolar concentrations of DNA as was the case with the previously studied dppz complexes.<sup>1</sup> Thus, although the two complexes investigated in the present study provide a good opportunity to compare directly the binding of isosteric intercalating species of +2 and +3 charge to DNA, such a comparison could not be made.

$[\text{Ru}(\text{bpy})_2(\text{dppz})]^{2+}$ ,  $[\text{Ru}(\text{phen})_2(\text{dppz})]^{2+}$ ,  $[\text{Os}(\text{phen})_2(\text{dppz})]^{2+}$  and  $[\text{Ru}(\text{H}_2\text{O})(\text{dppz})(\text{tpy})]^{2+}$  have all been reported to strongly bind to DNA ( $K_b \cong 10^6\text{-}10^7 \text{ M}^{-1}$ ) by an intercalative mode.<sup>1-5</sup> Results of various spectroscopic and biochemical studies have suggested that it is the dppz ligand that intercalates between the base pairs of DNA in these mixed ligand complexes. On the basis of the similarities in structures, absorption characteristics and apparent binding constants between the previously studied dppz complexes mentioned above and  $[\text{Co}(\text{phen})_2(\text{dppz})]^{3+}$  and  $[\text{Ni}(\text{phen})_2(\text{dppz})]^{2+}$ , it can be suggested that DNA binding by the latter complexes also involves an intercalation of dppz. This suggestion is further supported by thermal denaturation and differential pulse voltammetric experiments, the results of which are discussed below.

### 5.4.2 Thermal denaturation

Thermal denaturation experiments carried out on CT DNA in the absence of any added complex revealed that the  $T_m$  and  $\sigma_T$  values for the duplex are  $60 \pm 1$  and  $22 \pm 1$  °C, respectively, under our conditions (Fig. 5.3 (b)). Addition of  $[\text{Co}(\text{phen})_2(\text{dppz})]^{3+}$  or  $[\text{Ni}(\text{phen})_2(\text{dppz})]^{2+}$  ([DNA nucleotide phosphate]/[complex] = 20) increased  $T_m$  by  $8 \pm 1$  °C for the former and by  $6 \pm 1$  °C for the latter complex. ( $T_m$  and  $\sigma_T$  values increased with increasing addition of the metal complex as expected). By contrast, addition of either  $[\text{Co}(\text{phen})_3]^{3+}$  or  $[\text{Ni}(\text{phen})_3]^{2+}$  to DNA increased the  $T_m$  value by  $< 5$  °C. The  $\sigma_T$  values are  $24 \pm 1$  and  $26 \pm 1$  °C for  $[\text{Co}(\text{phen})_2(\text{dppz})]^{3+}$  and  $[\text{Ni}(\text{phen})_2(\text{dppz})]^{2+}$ , respectively.

### 5.4.3 Voltammetric studies

Differential-pulse voltammetric experiments were carried out with  $[\text{Co}(\text{phen})_3]^{3+}$  and  $[\text{Co}(\text{phen})_2(\text{dppz})]^{3+}$  in both the presence and the absence of CT DNA. Representative result is illustrated in Figure 5.4. As seen, there is a decrease in the peak current due to  $\text{Co}^{\text{III}}/\text{Co}^{\text{II}}$  redox couple ( $E_{1/2}(\text{Co}^{\text{III/II}}) = -0.02$  V vs SCE for both the complexes in 5mM tris, 50 mM NaCl, pH 7.0 buffer) in the presence of a 30 fold molar excess DNA (in comparison with the peak current in the same buffer). This decrease in the peak current is more pronounced for the dppz containing complex ( $\cong 75\%$ ) compared to that for the tris-phen complex ( $\cong 50\%$ ). Bard and co-workers<sup>15</sup> have previously shown that addition of DNA reduces the cyclic and differential-pulse voltammetric peak-currents of the  $\text{Co}^{\text{III/II}}$  couple for  $[\text{Co}(\text{phen})_3]^{3+}$  and have also estimated  $K_b$  to be  $(1.6 \pm 0.2) \times 10^4 \text{ M}^{-1}$  for this complex under experimental conditions

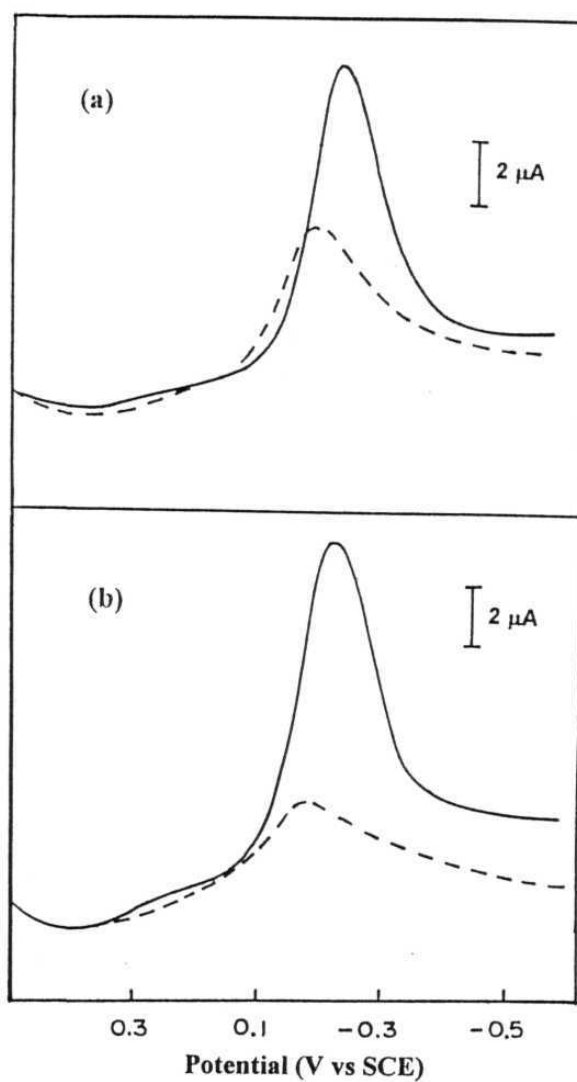


**Fig. 5.4.** (a) Differential-pulse voltammograms of  $0.1 \text{ mM } [\text{Co}(\text{phen})_3]^{3+}$  in the absence (—) and in the presence (---) of  $3 \text{ mM}$  (nucleotide phosphate) CT DNA. (b) Differential-pulse voltammograms of  $0.1 \text{ mM } [\text{Co}(\text{phen})_2(\text{dppz})]^{3+}$  in the absence (—) and in the presence (---) of  $3 \text{ mM}$  (nucleotide phosphate) CT DNA.

similar to those employed in this study.<sup>15b</sup> Our results are consistent with this data and, the pronounced reduction of the peak-current observed for  $[\text{Co}(\text{phen})_2(\text{dppz})]^{3+}$  can be explained if the affinity toward DNA is higher for this dppz containing complex than that for  $[\text{Co}(\text{phen})_3]^{3+}$ . Indeed, a rough estimate of  $K_b$  (using eqn. 2.18)<sup>15</sup> for the binding of  $[\text{Co}(\text{phen})_2(\text{dppz})]^{3+}$  with DNA by the differential-pulse voltammetric method is  $\cong 10^6 \text{ M}^{-1}$ , a value that is close to the one obtained by the absorption titration method.

### 5.5 Photocleavage of DNA

Photonuclease activity of both the nickel and cobalt complexes were investigated. Only  $[\text{Co}(\text{phen})_2(\text{dppz})]^{3+}$  was found to effect the photocleavage of the supercoiled pBR 322 DNA. Control experiments suggested that untreated DNA does not show any cleavage in the dark and even upon irradiation by a 350 nm light (Fig. 5.5, lanes 1 and 2). Similarly, DNA nicking was not observed for pBR 322 treated with  $[\text{Co}(\text{phen})_2(\text{dppz})]^{3+}$  in the dark experiments (Fig. 5.5, lane 3). On the other hand, irradiation of DNA in the presence of the complex for 20 min. caused the generation of relaxed circular DNA as shown in lane 4 of this Figure. Increasing the irradiation time to 60 min. resulted in further relaxation of the duplex only in the presence of the complex unaffected the untreated sample (compare lanes 2 and 5).

Interestingly, mobility change for pBR 322 is evident in the presence of  $[\text{Co}(\text{phen})_2(\text{dppz})]^{3+}$  as shown in this gel. Such a change in the mobility of DNA was also noticed when the nickel analogue was employed, but not when  $[\text{Co}(\text{phen})_3]^{3+}$  and  $[\text{Ni}(\text{phen})_3]^{2+}$  were employed in the gel electrophoresis experiments. It should be noted here that no change in the mobility has been

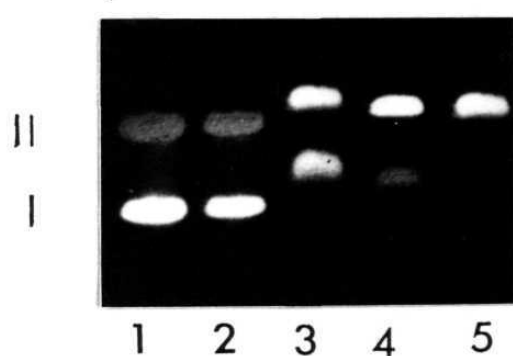


**Fig. 5.5.** Photograph showing the light-induced nuclease activity of  $[\text{Co}(\text{phen})_2(\text{dppz})]^{2+}$ . Dark and light experiments ( $\lambda_{\text{irr}} = 350 \text{ nm}$ ): Lanes 1 and 2: Untreated pBR 322 (100  $\mu\text{M}$  nucleotide phosphate) in the dark [55] and upon irradiation (60 min.) [52]; Lanes 3, 4 and 5: pBR 322 +  $[\text{Co}(\text{phen})_2(\text{dppz})]^{3+}$  (100  $\mu\text{M}$ ) in dark [46] and upon irradiation for 20 min. [66] and 60 min. [100], respectively. (Numbers given in the square-parentheses refer to % of the open circular form of DNA, Form II, in each case)

observed when the DNA samples containing  $[\text{Co}(\text{phen})_2(\text{dppz})]^{3+}$  (irradiated or not) were ethanol precipitated prior to loading onto the gel suggesting that DNA binding by this complex involves non-covalent interactions. Thus, the mobility change of DNA noticed for  $[\text{Co}(\text{phen})_2(\text{dppz})]^{3+}$  and  $[\text{Ni}(\text{phen})_2(\text{dppz})]^{2+}$  can be rationalized in terms of strong intercalative binding of these complexes with DNA.<sup>16</sup>

In attempts to unravel the probable DNA photocleavage mechanism of  $[\text{Co}(\text{phen})_2(\text{dppz})]^{3+}$ , a few more control experiments were conducted. The results of these control experiments are summarized below.

- (i) phen and dppz (free ligands dissolved in aqueous buffered solutions containing 5% DMF) are not detectably active under our irradiation conditions.
- (ii) No perceptible DNA cleavage was observed when samples of pBR 322 containing  $[\text{Co}(\text{phen})_3]^{3+}$  or  $[\text{Co}(\text{phen})_2(\text{phen-dione})]^{3+}$  were irradiated at 350 nm, as both these complexes do not appreciably absorb at this wavelength.
- (iii) Under experimental conditions similar to those employed for studies with  $[\text{Co}(\text{phen})_2(\text{dppz})]^{3+}$ , the  $d^8$   $[\text{Ni}(\text{phen})_2(\text{dppz})]^{2+}$  system did not show any light-induced nuclease activity, probably because of the paramagnetic nature of the complex that, in principle, would render the excited state of the molecule ineffective.
- (iv) Irradiation of pBR 322 samples containing the cobalt complex was also carried out in the presence of various 'inhibitors' (Fig. 5.6). Neither DABCO (lane 5) - a  $^1\text{O}_2$  'quencher', nor SOD - a  $\text{O}_2^{\cdot-}$  'scavenger' (lane 6) inhibit the photocleavage by the complex. Interestingly, purging the

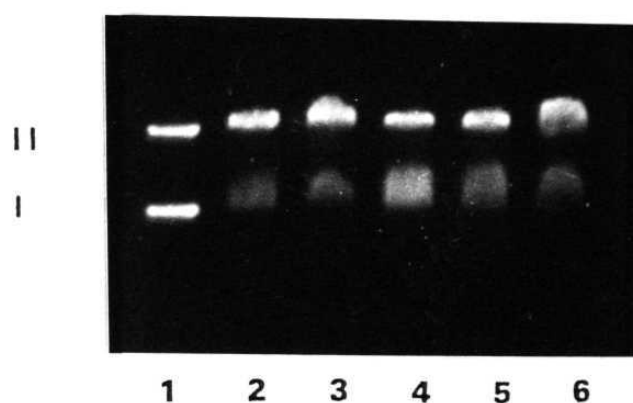


**Fig. 5.6.** Photograph showing effects of 'inhibitors' on the light-induced nuclease activity of  $[\text{Co}(\text{phen})_2(\text{dppz})]^{3+}$ : Lane 1: Untreated pBR 322 (100  $\mu\text{M}$  nucleotide phosphate) [41], Lane 2: pBR 322 +  $[\text{Co}(\text{phen})_2(\text{dppz})]^{3+}$  (100  $\mu\text{M}$ ) [65], Lanes 3 - 6: pBR 322 +  $[\text{Co}(\text{phen})_2(\text{dppz})]^{3+}$  in the presence of  $\text{N}_2$  [70], DMSO (0.2 M) [45], DABCO (10 mM) [62] and SOD (20  $\mu\text{g}/\text{ml}$ ) [72], respectively. Irradiation time = 45 min. in each case and  $\lambda_{\text{irr}} = 350 \text{ nm}$ . Numbers given in the square-parentheses refer to % of Form II DNA.

reaction mixture with N<sub>2</sub> (15 min, to remove O<sub>2</sub>) (lane 3) or with O<sub>2</sub> (data not shown) also does not inhibit the reaction. On the other hand, DMSO which scavenges OH• radical was found to inhibit the photocleavage (lane 4).

These results collectively suggest that the major pathway of DNA photodamage by [Co(phen)<sub>2</sub>(dppz)]<sup>3+</sup> involves a OH• -mediated mechanism.

Further support for the generation of OH• upon photolysis of the complex comes from the spin trapping experiments. In the presence of PBN as the spin trap, irradiated solutions of [Co(phen)<sub>2</sub>(dppz)]<sup>3+</sup> in acetonitrile solution containing ca. 1% water showed an ESR spectrum ( $g = 2.0036$ ,  $a^N = 13.6$ ) that is somewhat typical of the OH• spin adduct of PBN, Fig. 5.7.<sup>17</sup> Apart from a major three-line pattern due to the nitrogen hyperfine coupling, the spectrum also shows several splitting which are ascribable to the hyperfine interaction due to hydrogen of the PBN-OH• adduct and to the resonances of an unknown, as-yet unidentified paramagnetic species. It is possible that this unknown species could be a ligand - based radical similar to that obtained upon irradiation of 'aqueous' acetonitrile solutions containing a spin trap and a cobalt(III) complex of a bleomycin mimic or [Co(bpy)<sub>3</sub>]<sup>3+</sup>.<sup>18</sup> Thus, it is possible that irradiation facilitates, ultimately, a process of ligand reduction in [Co(phen)<sub>2</sub>(dppz)]<sup>3+</sup> - a process that leads to the production of OH• radical *via* the reaction of a C/N (ligand)-based radical intermediate with the aqueous buffer. A metal-centered photoreduction could precede the ligand reduction. Indeed, metal centered photoreduction reactions have been implicated in the DNA photocleavage by a few cobalt(III) complexes.<sup>19</sup> In this regard, it should be noted that irradiated aqueous solutions of [Co(phen)<sub>2</sub>(dppz)]<sup>3+</sup> did not

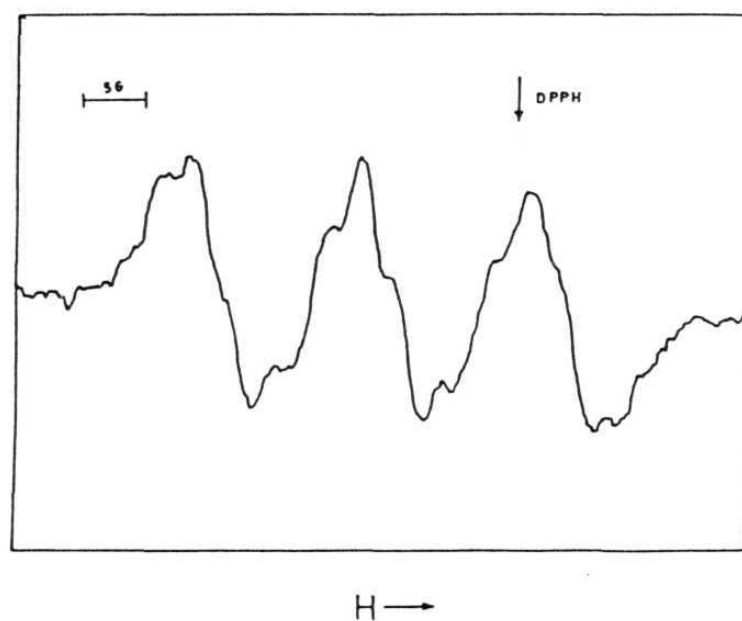


**Fig. 5.7.** ESR spectrum of the PBN spin adduct of  $[\text{Co}(\text{phen})_2(\text{dppz})]^{3+}$  under anaerobic and irradiated conditions ( $\lambda > 350 \text{ nm}$ ) in acetonitrile solution containing ca. 1% water (spin trap concentration, 20 mM;  $[\text{Co}(\text{phen})_2(\text{dppz})]^{3+}$  concentration, 1 mM). Spectrometer settings are microwave power = 5 mW, field modulation = 100 KHz, modulation width = 2 G.

release any  $\text{Co}^{2+}$  as evidenced by both UV-visible spectra and analytical method using  $\text{KSCN}$ .<sup>18a</sup>

## 5.6 Summary

Two new mixed-ligand complexes,  $[\text{Co}(\text{phen})_2(\text{dppz})]^{3+}$  and  $[\text{Ni}(\text{phen})_2(\text{dppz})]^{2+}$ , have been synthesized and fully characterized by elemental analysis, FABMS, IR, UV-visible,  $^1\text{H}$  NMR, magnetic susceptibility and electrochemical methods. Results of absorption titration, thermal denaturation and differential-pulse voltammetric experiments reveal that both these +3 and +2 complexes are avid binders of CT DNA and that the dipyridophenazine ligand on them is engaged in the intercalative interaction with DNA. On the other hand, while the cobalt(III) complex has been found to effect photocleavage of the supercoiled pBR 322 DNA *via*, most probably, a  $\text{OH}^\bullet$ -mediated mechanism, the nickel(II) complex is ineffective under similar experimental conditions. The results described in this study while underscoring the importance of dppz in the DNA-binding, also demonstrate that substitution by different metal ions can bring about subtle modulation in the properties and, consequently, in the DNA interaction of this new class of mixed-ligand complexes containing the versatile dipyridophenazine ligand.

## 5.7 References

1. Amouyal, E.; Homsí, A.; Chambron, J. -C; Sauvage, J.-P. *J. Chem. Soc. Dalton Trans.* **1990**, 1841. (b) Friedman, A. E.; Chambron, J. C.; Sauvage, J. P.; Turro, N. J.; Barton, J. K. *J. Am. Chem. Soc.* **1990**, 112, 4960. (c) Friedman, A. E.; Kumar, C. V.; Turro, N. J.; Barton, J. K.

- Nucl. Acid Res.* **1991**, 19, 2595. (d) Jenkins, Y.; Friedman, A. E.; Turro, N. J.; Barton, J. K. *Biochemistry* **1992**, 31, 10809. (e) Hiort, C. H.; Lincoln, P.; Norden, B. *J. Am. Chem. Soc.* **1993**, 115, 3448. (f) Dupureur, C. M.; Barton, J. K. *J. Am. Chem. Soc.* **1994**, 116, 10286. (g) Eriksson, M.; Leijon, M.; Hirot, C.; Norden, B.; Graslund, A. *Biochemistry* **1994**, 33, 5031. (h) Turro, C.; Bossman, S. H.; Jenkins, Y.; Barton, J. K.; Turro, N. J. *J. Am. Chem. Soc.* **1995**, 117, 9026. (i) Haq, I.; Linclon, P.; Suh, D.; Norden, B.; Chowdhry, B. Z.; Chaires, J. B. *J. Am. Chem. Soc.* **1995**, 117, 4788. (j) Stoeffler, H. D.; Thornton, N. B.; Temkin, S. L.; Schanze, K. S. *J. Am. Chem. Soc.* **1995**, 117, 7119. (k) Maggini, M.; Dono, A.; Scorrano, G.; Prato, M. *J. Chem. Soc., Chem. Commun.*, **1995**, 845. (l) Bogler, J.; Gourdon, A.; Ishow, E.; Launay, J. -P. *Inorg. Chem.*, **1996**, 35, 2937. (m) Linncoln, B.; Broo, A.; Norden, B. *J. Am. Chem. Soc.* **1996**, 118, 2644. (n) Lincoln, P.; Norden, B. *J. Chem. Soc. Chem. Commun.* **1996**, 2145.
2. Hartshorn, R. M.; Barton, J. K. *J. Am. Chem. Soc.* **1992**, 114, 5919.
  3. Holmlin, R. E.; Barton, J. K.; *Inorg. Chem.* **1995**, 34, 7. (b) Yam, V. W.-W.; Lo, K. K.-W.; Cheung, K.-K.; Kong, R. Y.-C. *J. Chem. Soc.; Chem. Commun.* **1995**, 1191.
  4. Sentagne, C.; Chambron, J.-C., Sauvage, J. P.; Paillous, N. *J. Photochem. Photobiol. B: Biol.* **1994**, 26, 165.
  5. Gupta, N.; Grover, N.; Neyhart, G. A.; Liang, W.; Singh, P.; Thorp, H. H. *Angew. Chem. Int. Ed. Engl.* **1992**, 31, 1048. (b) Neyhart, G. A.; Grover, N.; Smith, S. R.; Kalsbeck, W. A.; Fairley, T. A.; Cory, M.; Thorp, H. H. *J. Am. Chem. Soc.* **1993**, 115, 4423.

6. See for example (and also references therein): (a) Sigman, D. S. *Acc. Chem. Res.* **1986**, *19*, 180. (b) Barton, J. K. *Science* **1986**, *233*, 727. (c) *Metal-DNA Chemistry*; Tullis, T.D., Ed.; ACS Symposium Series 402; American Chemical Chemistry: Washington, DC, **1989**. (d) Pyle, A. M.; Barton, J. K. *Prog. Inorg. Chem.* **1990**, *38*, 413. (e) Turro, N. J.; Barton, J. K.; Tamalia, D. A. *Acc. Chem. Res.* **1991**, *24*, 332. (f) Sigman, D. S.; Mazumder, A.; Perrin, D. M. *Chem. Rev.* **1993**, *93*, 2295. (g) Murphy, C. J.; Barton, J. K. *Methods Enzymol.* **1993**, *226*, 576.
7. Barton, J. K.; Raphael, A. L. *J. Am. Chem. Soc.* **1984**, *106*, 2466. (b) Kelly, J. M.; Tossi, A. B.; McConnell, D. J.; OhUigin, C. *Nucl. Acid. Res.* **1985**, *13*, 6017. (c) Barton, J. K.; Raphael, A. L. *Proc. Natl. Acad. Sci. U. S. A.* **1985**, *82*, 6460. (d) Krischenbaum, M. R.; Tribolet, R.; Barton, J. K. *Nucleic Acid Res.* **1988**, *16*, 7943. (e) Mei, H. -Y.; Barton, J. K. *Proc. Natl. Acad. Sci. U. S. A.* **1988**, *85*, 1339. (f) Sammes, P. G. ; Yahiloglu, G. *Chem. Soc. Rev.* **1994**, 327.
8. Yamada, M.; Tanaka, Y.; Yoshimoto, Y.; Kuroda, S.; Shimao, I. *Bull. Chem. Soc. Jpn.* **1992**, *65*, 1006.
9. Dickenson, J. E.; Summers, L. A. *Aust. J. Chem.* **1970**, *23*, 1023. (b) Amouyal, E.; Homsy, A.; Chambron, J.-C.; Sauvage, J.-P. *J. Chem. Soc.; Dalton Trans.* **1990**, 1841.
10. Brustall, F. H.; Nyholm, R. S. *J. Chem. Soc.* **1952**, 3570. (b) Vlcek, A. *Inorg. Chem.* **1967**, *6*, 1425.
11. Harris, C. M.; Mckenzie, E. D. *J. Inorg. Nucl. Chem.* **1967**, *29*, 1047.

12. Ackermann, M. N.; Interrante, L. V.; *Inorg. Chem.* **1984**, 23, 3904. (b) Fees, J.; Kaim, W.; Moscherosch, M.; Matheis, W.; Klima, J.; Krejcik, M.; Zalis, S. *Inorg. Chem.* **1993**, 32, 166.
13. Nicholson, R. S. ; Shain, I. *Anal. Chem.* **1964**, 36, 706
14. Maki, N.; Tanaka, N. In Encyclopedia of Electrochemistry of The Elements; Bard, A. J.; Ed.; Marcel Dekker: New York. 1975; Vol. 3, pp 43-210 and references cited therein.
15. Carter, M. T.; Bard, A. J. *J. Am. Chem. Soc.* **1987**, 109, 7528. (b) Carter, M. T.; Rodriguez, M.; Bard, A. J. *J. Am. Chem. Soc.* **1989**, 111, 8901.
16. Waring, M. J. *J. Mol. Biol.* **1966**, 54, 247. (b) Espejo, R. T.; Lebowitz, J. *Anal. Biochem.* **1976**, 72, 95. (c) Keck, M. V.; Lippard, S. J. *J. Am. Chem. Soc.* **1992**, 114, 3386. (d) Goulle, V.; Lehn, J. M.; Schoentjes, B.; Schmitz, F. J. *Helv. Chim. Acta* **1991**, 74, 1471.
17. Harbour, J. R.; Chow, V.; Bolton, J. R. *Can. J. Chem.* **1974**, 52, 3549. (b) Kotake, Y.; Janzen, E. G. *J. Am. Chem. Soc.* **1991**, 113, 9503.
18. Tan, J. D.; Hudson, S. E.; Brown, S. J.; Olmstead, M. M.; Mascharak, P. K. *J. Am. Chem. Soc.* **1992**, 114, 3841. (b) Chang, C.-H.; Meares, C. F. *Biochemistry* **1982**, 21, 6332. (c) Farinas, E.; Tan, J. D.; Baidya, N.; Mascharak, P. K. *J. Am. Chem. Soc.* **1993**, 115, 2996
19. Barton, J. K.; Paranawithana, S. R. *Biochemistry* **1986**, 25, 2205. (b) Subramanian, R.; Meares, C. F. *J. Am. Chem. Soc.* **1986**, 108, 6427. (c) Basile, L. A.; Barton, J. K. *J. Am. Chem. Soc.* **1987**, 109, 7548. (d) Basile, L. A.; Raphael, A. L.; Barton, J. K. *J. Am. Chem. Soc.* **1987**, 109, 7550.

## CHAPTER 6

### *Photonuclease Activity of Porphyrin-Anthraquinone Diads and Diazoarene Chromophores*

As delineated in Chapter 1, DNA photocleavage by a class of porphyrin-based diads and a few diazoarene chromophores have also been investigated during the present study. Results of these investigations are described in this Chapter.

#### 6.1 Introduction

##### 6.1.1 Porphyrin-anthraquinone diads

A recently emerging application of porphyrin and related macrocyclic chromophores is concerned with their role as sensitizers in the photodynamic therapy (PDT) of malignant tumors.<sup>1</sup> The haematoporphyrin derivative (HpD), a first generation photosensitizer, and its commercial variant Photofrin<sup>®</sup> have been extensively employed both in experimental and clinical studies of PDT.<sup>2-4</sup> However, the uncertainty about the chemical structure and mechanism of action of HpD combined with the fact that HpD absorbs weakly in the red region of the visible spectrum (where the greatest penetration of light into tissue occurs) necessitated the development of other porphyrin and related macrocycles as PDT photosensitizers.<sup>5-7</sup> A plethora of new photosensitizers including modified phthalocyanines,<sup>8-11</sup> chlorins and bacteriochlorins,<sup>12-16</sup> purpurins,<sup>17</sup> benzoporphyrin derivatives,<sup>18,19</sup> expanded/contracted porphyrins,<sup>20,22</sup> and picket fence porphyrins<sup>23-25</sup> have been

reported recently. However, many of these new generation photosensitizing drugs suffer from their inability to accumulate selectively in tumors, leading to lower levels of tumor necrosis.

One possible way to circumvent the problem of low accumulation of a given porphyrin-based drug in the cells is to equip the drug with an intracellular recognition element *viz.* a DNA or membrane binding agent. This approach has the potential to deliver a better tumor-targeting device as the appended intracellular recognition element can, in principle, enhance the tumor accumulation ability of the drug. The modified drug is also expected to be more effective, even at low concentrations, in cleaving the DNA by either photochemical or other means. Thus, porphyrin conjugates endowed with oligonucleotide,<sup>26-29</sup> monoclonal antibody,<sup>30,31</sup> ellipticine,<sup>32-34</sup> or other intracellular recognition elements<sup>35-38</sup> have been reported recently. It is interesting to note that most of the hitherto reported such porphyrin conjugates effect the DNA cleavage only *via* chemical means and that very little effort seems to have been done to induce the photocleavage of DNA utilizing these modified photosensitizers. However, very recently, photonuclease activity of photoactive porphyrins which bind selectively to DNA owing to their linkage to either an intercalator<sup>39</sup> (e.g. acridone, phenothiazine), a minor groove binder<sup>40</sup> (e.g. ellipticine) or a cross-linking agent<sup>41</sup> (e.g. chlorambucil) have been reported.

During the course of this work, it was realized that utilization of a photoactive, intercalatable moiety in conjunction with the porphyrin chromophore might accentuate the photochemical activity of the so-derived 'hybrid' molecules leading to an efficient DNA cleavage. Among the various

non-porphyrinic chromophores that can be linked to the porphyrin in such new hybrids, anthraquinone seemed to be an ideal candidate because, this ubiquitous electron acceptor has been recently established to be an avid binder- and also an efficient photonic agent of DNA.<sup>42</sup> Thus, conjugates derived from a union of a porphyrin and an anthraquinone subunit are expected to not only absorb light all through in the visible region but also initiate photocleavage of DNA by  $^1\text{O}_2$  (porphyrin)<sup>1,43</sup> as well as electron transfer/H-abstraction (anthraquinone)<sup>42</sup> mechanisms. Moreover, the prospect of generation of the anthraquinone anion radical triggered by the visible light irradiation and the subsequent photoinduced electron transfer (PET) reaction from the photoexcited porphyrin donor to the appended anthraquinone acceptor in these hybrids, as previously reported for the covalently-linked, biomimetic porphyrin-anthraquinone donor-acceptor systems,<sup>44</sup> can be considered as an attractive attribute of this approach.

Accordingly, a series of porphyrin-anthraquinone (**4** - **10**) hybrids have been investigated in the present study inquiring, mainly, into their photonuclease activity. The molecular structures of these new systems are shown in Fig 6.1.

#### 6.1.2 Diazoarene compounds

A plethora of photochemically reactive molecules including quinones, naphthalimides, chlorobithiazoles, triazoles, thiopyridones, porphyrins and metal complexes, amongst others, are currently being scrutinized for their photonuclease activity.<sup>45</sup> Photogenerated ion, radical or oxygen-centered reactive species have been proposed to be responsible for cleaving DNA in a

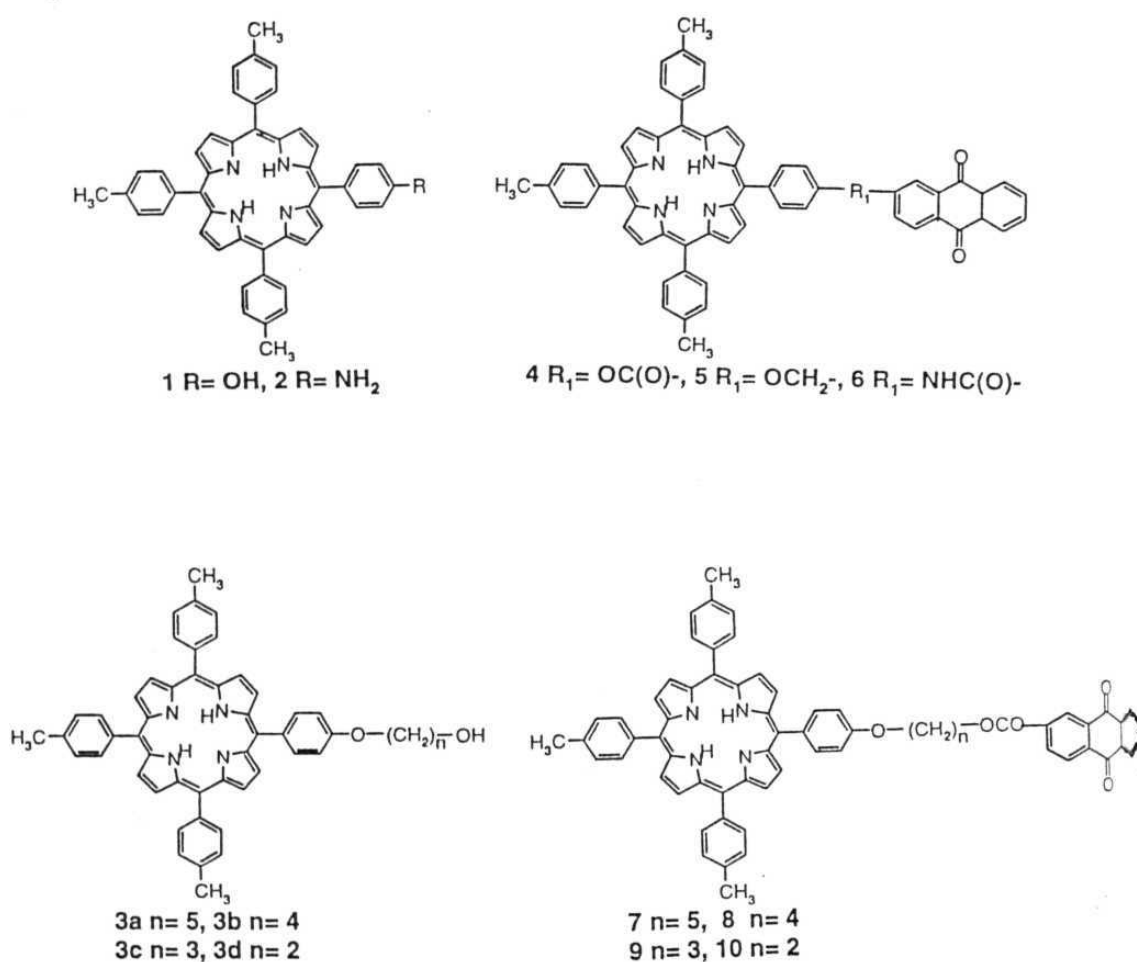


**Fig. 6.1** Structures of the porphyrins investigated in this study

majority of these cases. However, carbenes, which are known to be generated upon photoirradiation of diazo compounds and to be reactive towards a wide

variety of organic and bioorganic substrates including proteins, have never been tested for their ability to cleave DNA.<sup>46,47</sup> This is all the more surprising considering the fact that the naturally occurring anti-tumor agents kinamycin and prekinamycin, probably derive their DNA cleaving ability from the diazo group present in them. Nevertheless, arene diazonium salts<sup>48</sup> and also  $\alpha$ -diazo ketones<sup>49</sup> have been employed in studies aimed at DNA photocleavage but, participation of carbenes has not been invoked in both the cases. In this Chapter, it is demonstrated that carbenes which can be generated upon photoirradiation of simple, readily available arene diazo compounds (9-diazafluorene **11**, 9-diazoanthrone **12** and 9-diazoxanthene **13**, see Fig. 6.2) are capable of cleaving DNA.

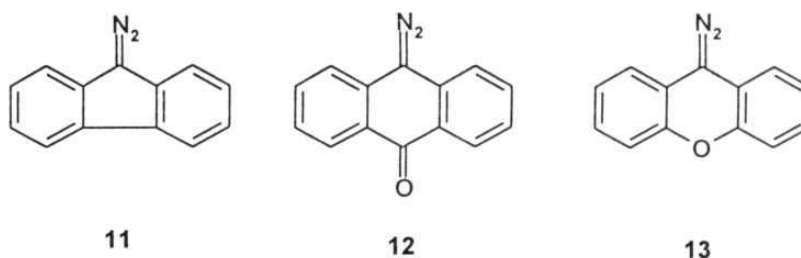


Fig. 6.2

## 6.2 Experimental details

All the porphyrin-anthraquinone hybrids and the three diazoarene compounds were obtained as kind gifts from Professor G. Mehta and Professor M. Nagarajan, respectively. Each porphyrin was purified on a short alumina column before the spectral and other measurements were made. All the spectroscopic and electrochemical experiments have been carried out as

described in Chapter 2. FAB-MS and  $^1\text{H}$  NMR spectral data of a few representative porphyrin-anthraquinone hybrids are given below.

**Compound 4**

FABMS (m/z): 907  $[\text{M}]^+$

$^1\text{H}$  NMR ( $\text{CDCl}_3$ , 200 MHz, TMS)  $\delta$ , ppm: -2.81(br s, 2H), 2.73(9H, s), 7.59(d, 6H), 7.70(d, 2H), 7.85(2H, m), 8.12(d, 6H), 8.34(4H, m), 8.52(1H, m), 8.90(8H, m).

**Compound 8**

FABMS (m/z): 993  $[\text{M}]^+$

$^1\text{H}$  NMR ( $\text{CDCl}_3$ , 200 MHz, TMS)  $\delta$ , ppm: -2.79(br s, 2H), 1.87(m, 2H), 2.06(m, 4H), 2.72(s, 9H), 4.32(t, 2H), 4.56(t, 4H), 7.30(d, 2H), 7.57(d, 6H), 7.74(m, 2H), 8.11(d, 8H), 8.26(m, 2H), 8.44(m, 2H), 8.86(s, 8H), 8.99(br s, 1H).

**Compound 10**

FABMS (m/z): 951  $[\text{M}]^+$

$^1\text{H}$  NMR ( $\text{CDCl}_3$ , 200 MHz, TMS)  $\delta$ , ppm: -2.81(br s, 4H), 2.72(s, 9H), 4.60(t, 2H), 4.92(t, 2H), 7.33(d, 2H), 7.57(d, 6H), 7.73(m, 2H), 8.12(d, 6H), 8.18(m, 4H), 8.38(m, 2H), 8.87(s, 8H), 8.96(s, 1H).

Singlet oxygen quantum yields ( $\Phi(^1\text{O}_2)$ ) of the porphyrin-anthraquinone hybrids were determined as detailed in Chapter 2. For the gel electrophoresis experiments with the porphyrin-anthraquinone diads and also

with the diazo compounds, supercoiled pBR 322 DNA (100  $\mu$ M in nucleotide phosphate; buffer B: 10 mM Tris, pH 8.0) was treated with an 100  $\mu$ M (buffer B + 2 - 3% DMF) of the drug (and the 'inhibitor' in cases where applicable) and the mixture was incubated for 1 h. in the dark. Irradiation experiments were carried out by keeping these pre-incubated samples inside the sample chamber of a JASCO Model FP-777 spectrofluorometer. The samples were analyzed by 0.8% agarose gel electrophoresis as described in Chapter 2.

### **6.3 Results and discussion**

#### **6.3.1 Porphyrin-anthraquinone diads**

##### **6.3.1.1 Ground and singlet excited state properties of porphyrin-anthraquinone diads**

The UV-visible spectral data of the hybrid porphyrin systems are summarized in Table 6.1 and representative UV-visible spectra are illustrated in Fig 6.3. As seen from this Figure and Table 6.1, the porphyrin moiety in each compound shows absorption bands between 400 - 700 nm and the appended intercalator moiety absorbs below 400 nm. The  $\lambda_{\text{max}}$  and log  $\epsilon$  values of these linked compounds are in the same range as those of the corresponding unlinked compounds viz: porphyrins **1** and **3** and anthraquinone (or anthraquinone 2-carboxylic acid, AnQ2-COOH / 2-bromomethyl anthraquinone, AnQ2-Br).

Table 6.2 summarizes the redox potential data of the hybrid porphyrins measured in  $\text{CH}_2\text{Cl}_2$ , 0.1 M TABPF<sub>6</sub> (vs. SCE) by the cyclic voltammetric method and representative cyclic voltammograms are shown in

**Table 6.1** UV-visible data of the porphyrin-anthraquinone diads in CH<sub>2</sub>Cl<sub>2</sub>

Compound	$\lambda_{\text{max}}$ , nm (log $\epsilon$ )	
	Porphyrin transition	Intercalator transition
4	647 (3.46), 591 (3.52), 551 (3.77), 516 (4.09), 419 (5.50)	259 (4.67)
5	647 (3.58), 592 (3.61), 551 (3.89), 516 (4.16), 419 (5.60)	257 (4.83)
6	678 (3.93), 591 (3.90), 551 (4.11), 517 (4.26), 420 (5.41)	260 (4.91)
7	649 (3.43), 592 (3.46), 552 (3.76), 516 (4.03), 420 (5.46)	258 (4.62)
8	648 (3.56), 592 (3.59), 553 (3.89), 516 (4.18), 420 (5.59)	258 (4.81)
9	650 (3.55), 591 (3.59), 552 (3.91), 517 (4.18), 420 (5.54)	258 (4.75)
10	647 (3.47), 592 (3.49), 552 (3.78), 517 (4.05), 420 (5.49)	259 (4.69)
1	650 (3.76), 592 (3.64), 551 (3.90), 516 (4.17), 418 (5.30)	-

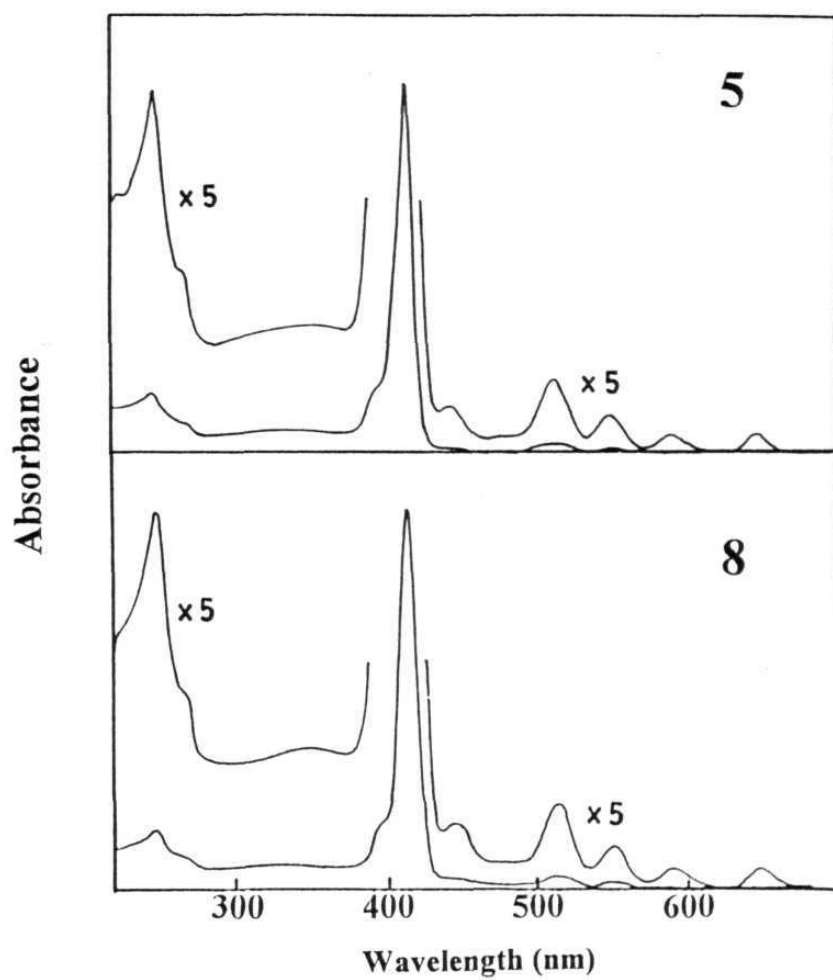


**Fig. 6.3.** UV-visible spectra of porphyrin-anthraquinone diads 5 and 8 in  $\text{CH}_2\text{Cl}_2$ .

**Table 6.2** Cyclic voltammetric data of the porphyrin-anthraquinone diads in  $\text{CH}_2\text{Cl}_2$ , 0.1 M TBAPF<sub>6</sub>

Compound	Potential, V vs SCE		
	Oxidation	Reduction	
		Intercalator	Porphyrin
4	+0.99	−0.76	−1.23
5	+0.93	−0.90	−1.23
7	+0.95	−0.77	−1.21
8	+0.93	−0.80	−1.23
9	+0.93	−0.79	−1.23
10	+0.92	−0.88	−1.28
1	+1.02	-	−1.20
Anthraquinone		−0.97	-

Fig 6.4. While porphyrin part of the hybrids investigated in this study is oxidized and reduced typically at 0.93 to 1.02 and -1.23 to -1.28 V, electron addition to the appended intercalator occurs at -0.76 to -0.90 V (reduction of the free anthraquinone occurs at -0.97 V). All these cyclic voltammetric responses were found to be reversible, diffusion-controlled one electron transfer reactions ( $i_p$  vs.  $\nu^{1/2}$  = constant where  $i_p$  is the peak current and  $\nu$  is the scan rate,  $i_{pa}/i_{pc}$  = 0.9 - 1.0 where  $i_{pa}$  and  $i_{pc}$  refer to anodic and cathodic peak currents, respectively and  $\Delta E_p$  = 60 - 80 mV where  $E_p$  is the peak potential).

Thus, the UV-visible and redox potential data of these new porphyrin-anthraquinone diads are in the same range as those of the corresponding reference compounds **1** and **3** as well as AnQ2-COOH or AnQ2-Br and indicate that there is minimal ground state interaction between the porphyrin and the intercalator. This is an expected result if one considers the fact that the connection between the porphyrin and the quinone is at the para position of one of the phenyl rings on the macrocycle in each case.

When excited with light of wavelength corresponding to the porphyrin absorption maximum (550 nm), all of the hybrid porphyrins exhibited a characteristic porphyrin fluorescence spectrum in CH<sub>2</sub>Cl<sub>2</sub> solutions with peak maxima appearing at (655 ± 2) and (717 ± 2) nm in each case, Fig 6.5. However, their fluorescence ( $\Phi_f$ ) and singlet oxygen ( $\Phi(^1O_2)$ ) quantum yields were seen to be drastically reduced in comparison with the corresponding values for the control porphyrins **1-3**, Table 6.3. Quenching of fluorescence in these hybrids can be attributed to the occurrence of a PET reaction from the porphyrin singlet state to the appended quinone, as is true with the

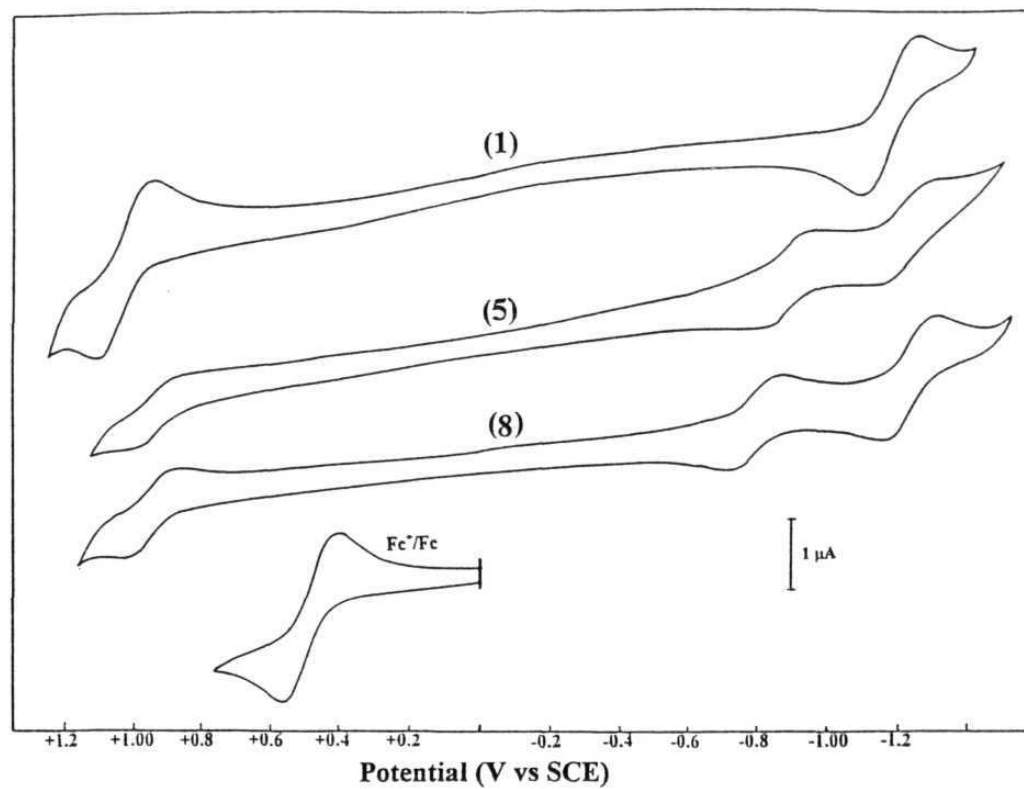


**Fig. 6.4.** Cyclic voltammograms (scan rate,  $100 \text{ mV s}^{-1}$ ) of **1**, **5** and **8** in  $\text{CH}_2\text{Cl}_2$ ,  $0.1 \text{ M TBAPF}_6$ . ( $\text{Fc}$  = Ferrocene)

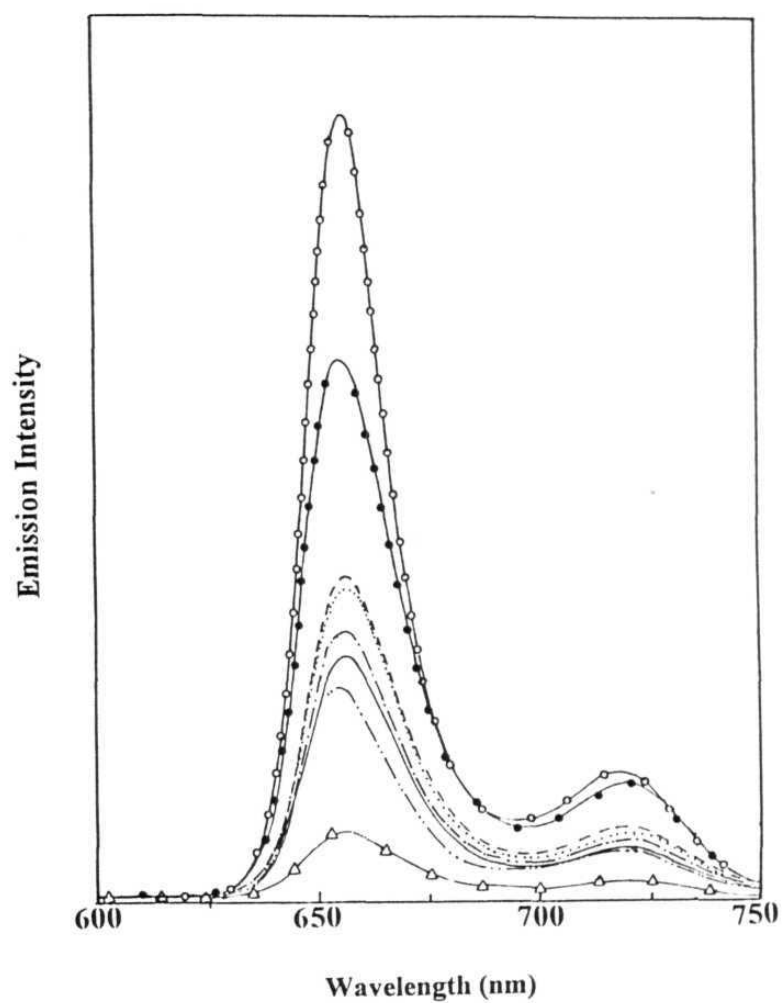


Fig. 6.5. Fluorescence spectra of equi-absorbing (O. D = 0.07) solutions of (top to bottom) 1 (—○—○—), 5 (—●—●—), 8 (— — — —), 7 (.....), 10 (— · — · —), 9 (———), 4 (— · · — · —) and 6 (—Δ—Δ—) in  $\text{CH}_2\text{Cl}_2$  ( $\lambda_{\text{exc}} = 550 \text{ nm}$ )

covalently-linked, porphyrin-anthraquinone systems reported earlier.<sup>44</sup> The low values of  $\Phi(^1\text{O}_2)$  are probably a consequence of an inefficient porphyrin triplet state generation in these compounds due, in part, to the PET mentioned above. Nonetheless, the photophysical data presented here collectively suggest that it is possible to photocleave DNA *via* both  $^1\text{O}_2$  and radical based mechanism by irradiation into the porphyrin absorption envelope ( $\lambda = 410\text{--}700\text{ nm}$ ) of these bichromophoric systems. On the other hand, excitation into the bands corresponding to the absorption due to their anthraquinone subunit ( $\lambda < 375\text{ nm}$ ) would generate the localized triplet quinone which is known to react with the DNA either directly or *via* the formation of the corresponding anion radical.<sup>42</sup>

**Table 6.3** Fluorescence ( $\Phi_f$ )<sup>a</sup> and singlet oxygen ( $\Phi(^1\text{O}_2)$ )<sup>b</sup> quantum yield data

Compound	1	4	5	6	7	8	9	10
$\Phi_f$	0.13	0.037	0.090	0.013	0.053	0.056	0.041	0.047
$\Phi(^1\text{O}_2)$	0.65	0.43	0.65	0.49	0.49	0.50	0.43	0.46

a: in  $\text{CH}_2\text{Cl}_2$

b: in DMF

### 6.3.1.2 Nuclease activity of porphyrin-anthraquinone diads

The nuclease activity of hybrids **4-10** was investigated using the supercoiled plasmid DNA pBR 322 in the presence and absence of light.

While no nicking was observed in the absence of light, irradiation at either 550 nm (porphyrin absorption) or 350 nm (anthraquinone absorption) caused nicking and generation of relaxed circular DNA, Fig 6.6 (note: there is <5% competitive absorption by the other chromophore at each of these wavelengths). On the other hand, the reference porphyrins **1** and **2** showed only marginal nicking when irradiated at 550 nm but, quinones AnQ2-COOH and AnQ2-Br (or anthraquinone itself) were seen to efficiently photocleave the DNA upon excitation by 350 nm light. Under the identical experimental conditions of concentration and light-dose, the nicking efficiency was found to be better for irradiation at 350 nm compared to that at 550 nm, thus revealing the superior DNA-photonicking ability of the *intercalated* quinone. On the other hand, although both the  $^1\text{O}_2$  and the radical based mechanisms can, in principle, participate in the photocleavage induced by excitation of the porphyrin chromophore, the lower efficiency observed during 550 nm irradiation can be rationalized if one considers that porphyrin is situated away from the duplex. The DNA photocleavage efficiency would then be necessarily dictated by (i) diffusion of  $^1\text{O}_2$ , within its lifetime, to the site of action on DNA and (ii) rate of production of the anthraquinone anion radical through an indirect (PET) mechanism. In any case, DNA nicking was found to be extremely efficient for each of these hybrids under the conditions of white-light ( $\lambda > 350$  nm) irradiation, as expected; complete conversion of Form I to Form II DNA could be achieved within half the time-duration used for 550/350 nm excitation.

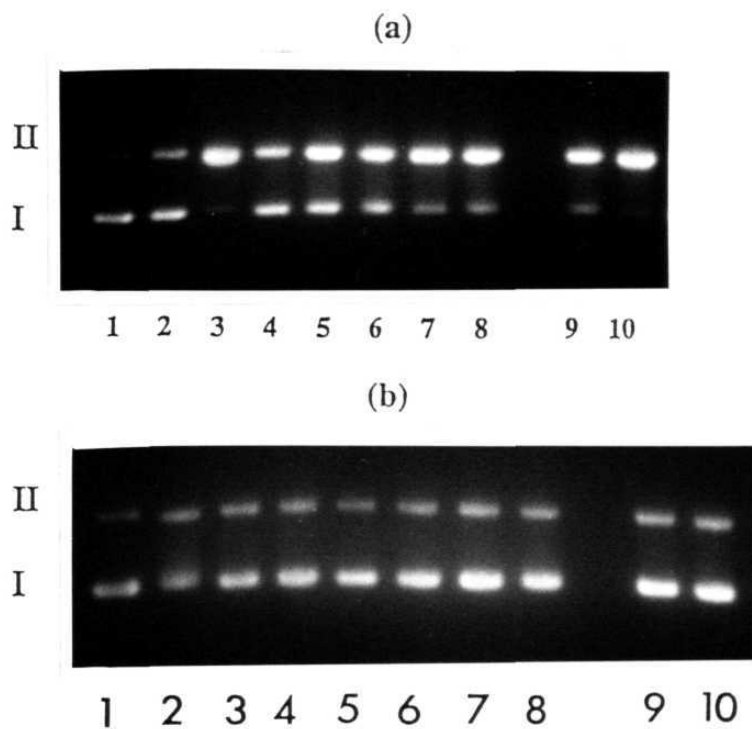


**Fig. 6.6.** Photograph showing the light-induced nuclease activity of porphyrin-anthraquinone diads. **(a)**  $\lambda_{\text{exc}} = 350 \text{ nm}$  ( $1 \text{ mW/cm}^2$ ; 30 min.); Lane 1: Untreated pBR 322, Lanes 2 - 10 : pBR 322 + 1, AnQ, 7, 8, 9, 10, 5, 4 or 6, respectively. **(b)**  $\lambda_{\text{exc}} = 550 \text{ nm}$  ( $1 \text{ mW/cm}^2$ ; 30 min.); Lane 1: untreated pBR 322, Lanes 2 - 10: pBR 322 + 1, AnQ, 7, 8, 9, 10, 5, 4 or 6, respectively. In each case, the proportion DNA/Drug = 1 and the samples were incubated for 1 h. before irradiated using a 150 W Xe-arc lamp/monochromator assembly.

### 6.3.2. Photonuclease activity of diazoarene compounds

9-Diazo fluorene (**11**), 9-diazoanthrone (**12**) and 9-diazoxanthene (**13**) were chosen for studies with DNA not only because of their ready availability and well-known photochemical reactivity<sup>50</sup> but also for their planar, aromatic structures<sup>51</sup> which are desirable (but not essential) features for binding with DNA. These diazo compounds were freshly prepared just prior to experiments with DNA either by the reaction of HgO/AgO and ethanolic KOH with the corresponding hydrazones in diethyl ether (**11** and **13**) or by the diazo transfer reaction using tosyl azide (**12**).<sup>52</sup> Each compound showed the expected UV-visible spectra in DMF with the peak maxima of the longest wavelength bands appearing at 348, 431 and 344 nm for **11**, **12** and **13**, respectively. Addition of increasing amounts of CT DNA (1 - 200  $\mu$ M base pairs in buffer A: 5 mM tris, 50 mM NaCl, pH 8.0) to solutions containing **11**, **12** or **13** ( $\approx$  20  $\mu$ M, buffer A + 2 - 3% DMF) resulted in hypochromism (20 - 45%) and bathochromic shifts (11 - 13 nm) of their peak maxima and also in the appearance of isosbestic points in the corresponding spectra suggesting DNA-binding. The intrinsic binding constants as obtained from the absorption titration method (eqn. 2.17, Chapter 2) are as high as  $1 - 3 \times 10^4 \text{ M}^{-1}$ . All these observations are reminiscent of those reported earlier for DNA-intercalation by various planar, aromatic molecules<sup>53</sup> and argue in favor of a similar intercalative mode of binding by **11**, **12** and **13** with DNA.

Photoirradiation ( $\lambda_{\text{ex}}$ :  $350 \pm 5$  nm for **11** and **13**,  $430 \pm 5$  nm for **12**) experiments probing the reactivity of these diazo compounds (10 - 100  $\mu$ M) with the duplex were carried out using supercoiled pBR 322 DNA (100  $\mu$ M nucleotide phosphate) and, the reaction was followed by the agarose gel

electrophoresis method as described earlier. Control runs showed that untreated DNA does not undergo any cleavage in the dark and even upon irradiation by a 350 (or 450) nm light for 2 h., Fig. 6.7 (a). Similarly, DNA nicking was not observed for pBR 322 treated with each of the diazo compounds in the dark (Lanes 1-3, Fig. 6.7 (a)) and only for compound **11** upon irradiation for 30 min (Lane 5). On the other hand, irradiation of DNA in the presence of compounds **12** and **13**, caused generation of the circular form (Form II) as shown in Lanes 4 and 6 of this Figure. Thus, under identical experimental conditions, the DNA nicking efficiencies follow an order: **13** > **12** > **11**. Accordingly, increasing the irradiation time to 60 min. resulted in further significant relaxation of the supercoiled DNA only for **12** and **13**, with **13** being able to completely convert the supercoiled form to the circular form.

Effects due to 2-propanol, triphenylphosphine (PPh<sub>3</sub>) and cumene on the observed photonuclease activity of **12** and **13** are illustrated in Fig. 6.7(b). Results obtained upon photoirradiation of these two reactive compounds in the presence of DNA and various 'inhibitors' including the above three are summarized in Fig. 6.8. While D<sub>2</sub>O, mannitol, DMSO and SOD do not affect the DNA-nicking efficiencies of these compounds, there is a moderate-to-strong inhibition by DABCO, 2-propanol, PPh<sub>3</sub> and cumene. The inability of D<sub>2</sub>O to enhance the DNA-nicking efficiency can be taken as an evidence to show that <sup>1</sup>O<sub>2</sub> is not involved in the reaction. That neither OH• nor O<sub>2</sub><sup>-</sup> play a role in the cleavage mechanism is established by the lack of inhibition of DNA cleavage in the presence of mannitol, DMSO and SOD. Thus, inhibition exhibited by the other added reagents can be collectively taken as evidence for the participation of carbenes in the observed DNA cleavage by

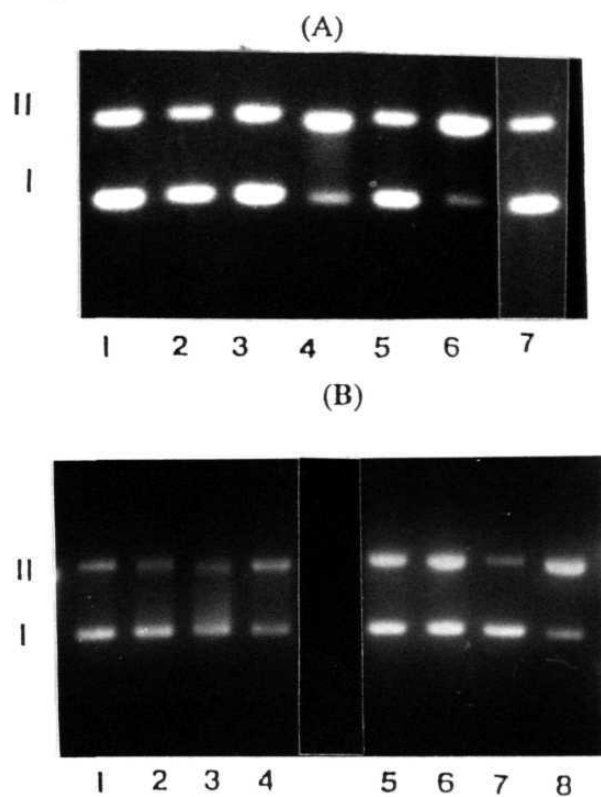


**Fig. 6.7.** Photograph showing the light-induced nuclease activity of diazo compounds **11**, **12** and **13** (100  $\mu$ M) with pBR 322 DNA (100  $\mu$ M in nucleotide phosphate): (A) 'Dark' and 'Light' (30 min,  $350 \pm 5$  nm for **11** and **13**,  $430 \pm 5$  nm for **12**) experiments: Lanes 1, 2 and 3: DNA + **12** (45), **11** (49) or **13** (47) in dark. Lanes 4, 5 and 6, DNA + **12** (70), **11** (45) or **13** (73) upon irradiation, lane 7: pBR 322 DNA dark control (45): (B) Results of 'inhibition' studies carried out with **12** and **13**, 'Light' Experiments: Lanes 1 - 3: (DNA + **12**) + 2-propanol (38),  $\text{PPh}_3$  (32) or cumene (31), respectively, Lane 4: DNA + **12** (60), Lanes 5 -7: (DNA + **13**) + 2-propanol (52),  $\text{PPh}_3$  (51) and cumene (51), respectively, Lane 8: DNA + **13** (70). Numbers in the parenthesis refer to % of Form II DNA.

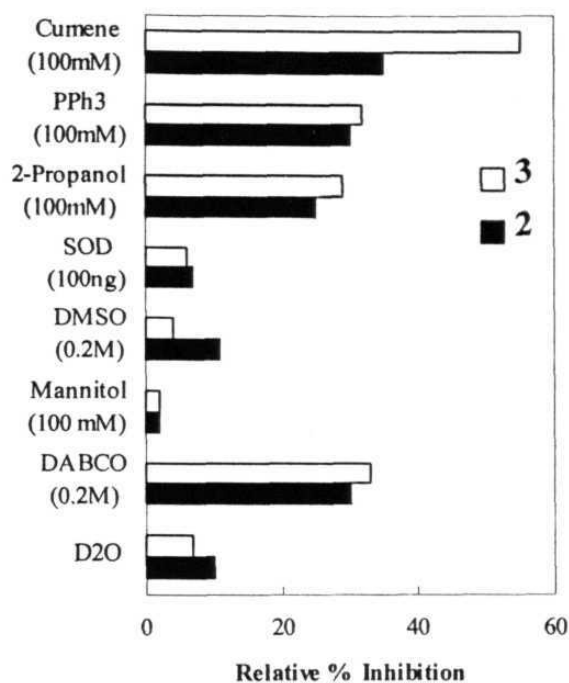


**Fig. 6.8.** Effect of various 'inhibitors' on the light-induced nuclease activity of **12** and **13** (Error limits  $\pm 5\%$ ).

the two reactive diazo compounds. Indeed, reaction of carbenes with  $\text{PPh}_3$  is known to be fast, yielding ylides.<sup>46</sup> Similarly, reaction of carbenes with 2-propanol and cumene is also known to be efficient.<sup>46, 50b</sup>

Generally, DABCO is employed for probing the participation of  $^1\text{O}_2$  in the DNA cleavage experiments. However, carbenes are also capable of reacting with amines, including tertiary amines, at their nitrogen centres.<sup>46</sup> This fact together with the observed inability of  $\text{D}_2\text{O}$  to enhance the DNA photocleavage of **12** and **13** suggests that the inhibitory effect exhibited by

DABCO here can be rationalized in terms of its reactivity with carbenes and not with  $^1\text{O}_2$ . By the same token, it is not unreasonable to expect that carbenes are capable of alkylating the nucleobases on the DNA and initiate the cleavage. An additional mechanism which involves hydrogen abstraction by the carbene as the key step cannot be ruled out.

#### 6.4 Summary

The ground- and excited state properties of porphyrin-anthraquinone diads have been investigated in some detail. The  $^1\text{H}$  NMR, UV-visible and electrochemical data of these hybrids suggests that there is no appreciable ground state interaction between the porphyrin and anthraquinone sub units. Fluorescence from the porphyrin part of these hybrids was seen to be quenched by the anthraquinone moiety and, this can be attributed to the occurrence of a PET reaction from the singlet porphyrin to the quinone. The nuclease activity of these hybrids as investigated using the supercoiled plasmid DNA pBR 322 suggests that these molecules are capable of displaying wavelength dependent DNA cleavage activity. The photonuclease activity of the three readily available diazoarenes compounds have also been reported. Inhibitor studies suggest that compounds **12** and **13** effectively photocleave the pBR 322 DNA *via* a carbene-mediated pathway.

#### 6.5 References.

1. (a) Gomer, C. J.; Doiron, D. R.; Dunn, S.; Rucker, N.; Razum, N.; Fountain, S. *Photochem. Photobiol.* **1983**, 37S, S91. (b) Girotti, A. W.

- Photochem. Photobiol.* **1983**, 38, 745. (c) Dougherty, T. J.; Weishaupt, K. R.; Boyle, D. G. *Principles and Practice of Oncology*; Devita Jr, V.; Hellman, S.; Rosenberg, S., Eds.; Lippincott, J. B. Philadelphia. **1985**, 2272. (d) Dougherty, T. J. *Sem. Surg. Oncol.* **1986**, 2, 24. (e) Kessel, D. *Int. J. Radiat. Biol.* **1986**, 49, 901. (f) Moan, J. *Photochem. Photobiol.* **1986**, 43, 681. (g) Dougherty, T. J. *Photochem. Photobiol.* **1987**, 45, 879. (h) *Photodynamic Therapy: Basic Principles and Clinical Application*; Henderson, B. W., Dougherty, T. J., Eds.; Marcel Dekker: New York, **1992**. (i) Dolphin, D. *Can. J. Chem.* **1994**, 72, 1005. (j) Bohm, F.; Marston, G.; Truscott, T. G.; Wayne, R. P. *J. Chem. Soc. Faraday Trans.* **1994**, 90, 2453. (k) Bonnet, R. *Chem. Soc. Rev.* **1995**, 19. (l) Morgan, A. R. *Curr. Med. Chem.*, **1995**, 2, 604.
2. (a) Diamond, I.; McDonagh, A. F.; Wilson, C. B.; Granelli, S. G.; Nielsen, S.; Jaenicke, R. *Lancet* **1972**, 2, 1175. (b) Henderson, B. W.; Fingar, V. H. *Cancer Res.* **1987**, 47, 3110.
  3. (a) Dougherty, T. J.; Kaufman, J. E.; Goldfarb, A. Weishaupt, K. R.; Boyle, D. G.; Mittleman, A. *Cancer Res.* **1978**, 38, 2628. (b) Henderson, B. W.; Fingar, V. H. *Photochem. Photobiol.* **1989**, 49, 299.
  4. (a) Kessel, D.; Cheng, M.-L. *Photochem. Photobiol.* **1985**, 41, 277. (b) Kessel, D.; Thompson, P.; Musselman, B.; Chang, C. K. *Cancer Res.* **1987**, 47, 4642. (c) Byrne, C. J.; Marshallsay, L. V.; Sek, S. Y.; Ward, A. D. In *Photodynamic therapy of neoplastic disease*; Kessel, D., Ed.; CRC: Boca Raton, **1990**; Vol. 2, p 131.
  5. (a) Kessel, D. *Photochem. Photobiol.* **1984**, 39, 851. (b) Ben-Hur, E.; Rosenthal, I. *Int. J. Radiat. Biol.* **1985**, 47, 145. (c) Ben-Hur, E.;

- Rosenthal I. *Photochem. Photobiol.* **1985**, 42, 129. (d) Brasseur, N.; Hasrat, A.; Langlois, R.; Wagner, J. R.; Rosseau, J.; van Lier, J. E. *Photochem. Photobiol.* **1987**, 45, 581.
6. (a) Moan, J.; Berg, K. *Photochem. Photobiol.* **1992**, 55, 931. (b) Kessel, D. *Cancer Res.* **1986**, 46, 2248. (c) Berenbaum, M. D.; Akande, S. L.; Bonnett, R.; Kaur, H.; Ivannow, S.; White, R. D.; Winfield, U. J. *Br. J. Cancer.* **1986**, 54, 717.
  7. Pandey, R. K.; Shiau, F. -Y.; Ramachandran, K.; Dougherty, T. J.; Smith, K. M. *J. Chem. Soc. Perkin Trans. I* **1992**, 1377 and references therein.
  8. Shopova, M.; Mantareva, V.; Krastev, K.; Hadjiolov, D.; Milev, A.; Spirov, K.; Jor, G.; Ricchelli, F. J. *Photochem. Photobiol., B. Biol.* **1992**, 16, 83.
  9. Bishop, S. M.; Khoo, B. J.; MacRobert, A. J.; Simpson, M. S. C.; Phillips, D.; Beeby, A. J. *Chromatogr.* **1993**, 646, 345.
  10. Boyle, B. W.; Lecznoff, C. C.; van Lier, J. E. *Br. J. Cancer* **1993**, 67, 1177.
  11. Segalla, A.; Milanesi, C.; Jori, G.; Capraro, H. -G.; Isele, U.; Schieweck, K. *Br. J. Cancer* **1994**, 69, 817.
  12. Kostenich, G. A.; Zhuravkin, I. N.; Zhavrid, E. A. *J. Photochem. Photobio. B. Biol.* **1994**, 22, 211.
  13. Bonnett, R.; Benzie, R.; Grahn, M. F.; Salgado, A.; Valles, M. A. *Proc. SPIE* **1994**, 2078, 171.
  14. Leach, M. W.; Higgins, R. J.; Autrey, S. A.; Boggan, J. E.; Lee, S. -J. H.; Smith, K. M. *Photochem. Photobiol.* **1993**, 58, 653.

15. Pandey, R. K.; Shiau, F. -Y.; Ramachandran, K.; Dougherty, T. J.; Smith, K. M. *J. Chem. Soc. Perkin Trans I* **1992**, 1377.
16. Richter, A. M.; Kelly, B.; Chow, J.; Liu, D. J.; Towers, G. M. N.; Dolphin, D.; Levy, J. G. *J. Natl. Cancer Inst.* **1987**, 79, 1327.
17. Morgan, A. R.; Garbo, G. M.; Keck, R. W.; Skalkos, D.; Selman, S. H. *Photochem. Photobiol.* **1990**, 6, 133.
18. Ritcher, A. M.; Watterfield, M. E.; Jain, A. K.; Allison, B.; Sternberg, E. D.; Dolphin, D.; Levy, J. G. *Br. J. Cancer* **1991**, 63, 87.
19. Hunt, D. W. C.; Jiang, J. -H.; Levy, G. J.; Kabn. A. H. *Photochem. Photobiol.* **1995**, 61, 417.
20. Vogel, E.; Kocher, M.; Schmickler, H.; Lex, J. *Angew. Chem., Int. Ed. Engl.* **1986**, 25, 197.
21. Leung, M.; Richert, C.; Gamarra, F.; Lumper, W.; Voge. E.; Jochanji, D.; Goetz, A. E. *Br. J. Cancer* **1993**, 68, 225.
22. Sessler, J. L.; Hemmi, G.; Mody, T. D.; Murai, T.; Burrell, A.; Young, S. W. *Acc. Chem. Res.* **1994**, 27, 43 and references therein.
23. Hegan, W. J.; Barber, D. C.; Whitten, D. G.; Kelly, M.; Albrecht, F.; Gibson, S. L.; Hilf, R. *Cancer Res.* **1988**, 48, 1148.
24. Barber, D. C.; Van Der Meid, K. R.; Gibson, S. L.; Hilf, R.; Whitten, D. G. *Cancer Res.* **1991**, 51, 1836.
25. Lawrence, D. S.; Gibson, S. L.; Nguyen, M. L.; Whittemore, K. R.; Whitten, D. G.; Ressel, H. *Photochem. Photobiol.* **1995**, 61, 90.
26. Bigey, P.; Pratviel, G.; Meunier, B. *J. Chem. Soc., Chem. Commun.* **1995**, 181.

27. Mastruzzo, L.; Woisard, A.; Ma, D. D. F.; Rizzarelli, E.; Favre, A.; Doan, T. L. *Photochem. Photobiol.* **1994**, 60, 316.
28. Le Doan, T. Praseuth, D.; Perrouault, L.; Chassignol, M.; Thuong, N. T.; Helene, C. *Bioconjugate Chem.* **1990**, 2, 108.
29. Fedorova, O. S.; Savitskii, A. P.; Shoikhet, K. G.; Ponomarev, G. V. *FEBS Lett.* **1990**, 259, 335.
30. Milgrom, L. R.; O'Neill, F. *Tetrahedron* **1995**, 51, 2137.
31. Harada, A.; Shiotsuki, K.; Fukushima, H.; Yamaguchi, H.; Kamachi, M. *Inorg. Chem.* **1995**, 34, 1070.
32. Ding, L.; Etemad-Moghadam, G.; Cros, S.; Auclair, C.; Meunier, B. *J. Chem. Soc., Chem. Commun.* **1989**, 1711.
33. Etemad-Moghadam, G.; Ding, L.; Tadj, F.; Meunier, B. *Tetrahedron* **1989**, 45, 2641.
34. Ding, L.; Etemad-Moghadam, G.; Meunier, B. *Biochemistry* **1990**, 29, 7868.
35. Perrecc-Fauvet, M.; Gresh, N. *Tetrahedron Lett.* **1995**, 36, 4227.
36. Mathews, S. E.; Pouton, C. W.; Threadgill, M. D. *J. Chem. Soc., Chem. Commun.* **1995**, 1809.
37. Herbelin, G. A.; Perrecc-Fauvet, M.; Gaudemer, A.; Helissey, P.; Renault, S. G.; Gresh, N. *Tetrahedron Lett.* **1993**, 45, 7263.
38. Hashimoto, Y.; Lee, C. -S.; Shudo, K.; Okamoto, T. *Tetrahedron Lett.* **1983**, 24, 1523.
39. (a) Mehta, G.; Sambaiah, T.; Maiya, B. G.; Sirish, M.; Chatterjee, D. *J. Chem. Soc. Perkin Trans. 1.* **1993**, 2667. (b) Mehta, G.; Sambaiah, T.; Maiya, B. G.; Sirish, M.; Dattagupta, A. *J. Chem. Soc. Perkin Trans. 1.*

- 1995, 295. (c) Mehta, G.; Muthusamy, S.; Maiya, B. G.; Sirish, M. *J. Chem. Soc. Perkin Trans. 1*. **1996**, 2421.
40. (a) Milder, S. J.; Ding, L.; Etemad-Moghadam, G.; Meunier, B.; Paillous, N. *J. Chem. Soc. Chem. Commun.* **1990**, 1131. (b) Sentagne, C.; Meunier, B.; Paillous, N. *J. Photochem. Photobiol B: Biol.* **1992**, 16, 47.
41. Mehta, G.; Sambaiah, T.; Maiya, B. G.; Sirish, M.; Dattagupta, A. *Tetrahedron Lett.* **1994**, 35, 4201.
42. (a) Bhattacharya, S.; Mandal, S. S. *J. Chem. Soc. Chem. Commun.* **1996**, 1515 (b) Breslin, D. T.; Coury, J. E.; Anderson, J. R.; Mcfail-Isom, L.; Kan, Y.; Williams, L. D.; Bottomley, L. A.; Schuster, G. B. *J. Am. Chem. Soc.* **1997**, 119, 5043 (and references therein).
43. (a) Bonnett, R.; Lambert, C. R.; Land, E. J.; Scourides, P. A.; Sinclair, R. S.; Truscott, T. G. *Photochem. Photobiol.* **1983**, 38, 1. (b) Foote, C. S.; Shook, F. C.; Abakerli, R. B. *Methods Enzymol.* **1984**, 105, 36. (c) Foote, C. S. *Porphyrin Localization and Treatment of Tumors*; Doiron, D. R.; Gomer, C. J., Eds.; Alan R. Liss: New York. **1984**, 3. (d) Foote, C. S. *Photochem. Photobiol.* **1991**, 54, 659. (e) Girotte, A. W. *Photochem. Photobiol.* **1990**, 51, 497.
44. Wasielewski, M. R. *Chem. Rev.* **1992**, 92, 435.
45. (a) Saito, I.; Takayama, I.; Sugiyama, H.; Nakatani, K. *J. Am. Chem. Soc.*, **1995**, 117, 6406; (b) Ly, D.; Kan, D.; Armitage D.; Schuster, G. B. *J. Am. Chem. Soc.*, **1996**, 118, 8747; (c) Quada, Jr. J. C.; Levy, M. J.; Hecht, S. M. *J. Am. Chem. Soc.*, **1993**, 115, 12171; (d) Wender, P. A.; Touami, S. M.; Alayrac, C.; Philipp, U. C. *J. Am. Chem. Soc.*, **1996**,

- 118, 6522; (e) Theodorakis, E. A.; Wilcoxon, K. M. *Chem. Commun.*, **1996**, 1927; (f) Magada, D.; Wright, M.; Miller, R. A.; Sessler, J. L.; Sansom, P. I. *J. Am. Chem. Soc.*, **1995**, 117, 3629.
46. (a) Kirmse, W. *Carbene Chemistry*, (vol 1) 2nd edn., Academic Press, **1971**; (b) Jones, Jr., M.; Moss, R. A. *Carbenes*, (vol 1, A volume in Reactive Intermediates in Organic Chemistry), Wiley-Interscience, **1973**.
47. Bayley, H.; Knowles, J. R. *Methods Enzymol.*, **1977**, 46, 69 (and references therein).
48. (a) Behr, J. P. *J. Chem. Soc., Chem. Commun.*, **1989**, 101. (b) Arya, D. P.; Warner, P. M.; Jebaratnam, D. J. *Tetrahedron Lett.*, **1993**, 34, 7823. (c) Griffiths, J.; Murphy, J. A. *J. Chem. Soc., Chem. Commun.*, **1992**, 24; (d) Arya, D. P.; Jebaratnam, D. J. *J. Org. Chem.*, **1995**, 60, 3268.
49. (a) Naakatani, K.; Maekawa, S.; Tanabe, K.; Saito, I. *J. Am. Chem. Soc.*, **1995**, 117, 10635; (b) Naakatani, K.; Isoe, S.; Maekawa, S.; Saito, I. *Tetrahedron Lett.*, **1994**, 35, 605; (c) Nakatani, K. *J. Syn. Org. Chem. JPN.*, **1995**, 53, 1068. (d) Saito, I.; Nakatani, K. *Bull. Chem. Soc. Jpn.*, **1996**, 69, 3007. (e) Nielsen, P. E.; Jeppesen, C.; Egholm, M.; Buchardt, O. *Nucleic Acids Res.*, **1988**, 16, 3877.
50. (a) Grasse, P. B., Brauer, B.E., Zupancic, J. J., Kaufmann, K. J., Schuster, G. B. *J. Am. Chem. Soc.*, **1983**, 105, 6833; (b) Fleming, J. C., Shechter, H. *J. Org. Chem.*, **1969**, 34, 3962; (c) Lapin, S. C., Schuster, G. B. *J. Am. Chem. Soc.*, **1985**, 107, 4243.
51. (a) Tulip, T. H.; Corfield, P. W. R.; Ibers, J. A. *Acta Crystallogr., Sect. B*, **1978**, 34, 1549; (b) Sander, W.; Bucher, G.; Komnick, P.;

- Morawictz, J.; Bubenitschek, P.; Jones, P. G.; Chrapkowski, A. *Chem. Ber.*, **1993**, 126, 2101; (c) Goodman, J. M.; James, J. J.; Whiting, A. *J. Chem. Soc. Perkin trans. 2*, **1994**, 109.
52. (a) Schönberg, A.; Awad, W. I.; Latif, N. *J. Chem. Soc.*, **1951**, 1368; (b) Raasch, M. S. *J. Org. Chem.*, **1979**, 44, 632; (c) Reverdy, G. *Bull. Soc. Chim. Fr.* **1976**, 1131.
53. (a) Kumar, C.V.; Asuncion, E. H. *J. Am. Chem. Soc.*, **1993**, 115, 8547; (b) Lerman, L.S. *J. Mol. Biol.*, **1961**, 3, 18.



## **CHAPTER 7**

### ***Conclusions***

The present study deals with the DNA-binding and cleavage aspects of new, rationally-designed photonucleases based on metallopolypyridyl, porphyrin and diazoarene chromophores.

Chapter 1 of this thesis summarizes research related to DNA interactions of previously reported metallopolypyridyl, porphyrin and diazoarene chromophores. The literature survey presented in this Chapter is not intended to be exhaustive but, is only representative with emphasis being laid on those examples that bear relevance to the main theme of this thesis. Chapters 3, 4 and 5 deal with the design, synthesis, DNA-binding and photocleavage of ruthenium(II), cobalt(III) and nickel(II) complexes containing modified phenanthroline ligands. The ligands were designed in such a way that their architecture promotes DNA intercalation and the electronic structures of the ensuing complexes promote efficient photocleavage of DNA. Molecular light switching and redox switching of luminescence effects observed in a few of these new complexes are also discussed in these Chapters. In Chapter 6 are presented DNA photocleavage characteristics of porphyrin and diazoarene chromophores. Results described in this Chapter are not necessarily an extension of what was described in the earlier Chapters; they need to be viewed more like an “off-shoot” of the investigations carried out with metallopolypyridyl systems.

While CT DNA was used for binding studies, supercoiled pBR 322 DNA was used for the photocleavage experiments throughout this work. Various techniques including absorption and emission titration, thermal denaturation, viscometry, differential-pulse voltammetry, agarose gel electrophoresis, topoisomerase assay etc. have been employed to monitor DNA binding by the new and old drugs. DNA photocleavage studies have been accomplished by the agarose gel electrophoresis method. Studies with various inhibitors and on-line irradiation/ESR experiments were also carried out in a few cases wherein attempts have been made to identify the reactive species responsible for cleaving DNA.

### **7.1 DNA-binding and photocleavage by Ru(II), Co(III) and Ni(II) complexes containing modified phenanthroline ligands**

DNA-binding and photocleavage characteristics of Ru(II), Co(III) and Ni(II) complexes containing modified phenanthroline ligands have been discussed in Chapters 3, 4 and 5. While Chapter 3 deals with the design, synthesis, characterization and DNA interactions of new mixed-ligand ruthenium(II) complexes incorporating either a quinone-fused dipyridophenazine ligand qdppz (qdppz = naphtho[2,3-*a*]dipyrido[3,2-*h*:2',3'-*f*]phenazine-5,18-dione) or its hydroquinone form, Chapter 4 presents similar results obtained with a series of ruthenium(II) complexes containing a new ligand - 6,7-dicyanodipyridoquinoxaline (dicnq). In Chapter 5 are discussed DNA binding and photocleavage characteristics of cobalt(III) and nickel(II) complexes containing dipyrdo[3,2-*a*:2',3'-*c*]-phenazine (dppz).

As mentioned earlier, the new ligands employed in this study were so designed that their architecture promotes strong DNA intercalation and the electronic structures of the complexes derived out of these ligands assist efficient photocleavage of DNA. Dipyridophenazine, a near-planar, hetero-aromatic entity whose metal-complexes have found various applications<sup>1-6</sup>, was chosen as the “platform” for building more elaborate ligand systems. Thus, besides dppz, newly synthesized ligands, viz: qdppz, hqdppz and dicnq were employed for complexation during this work, Fig. 7.1.

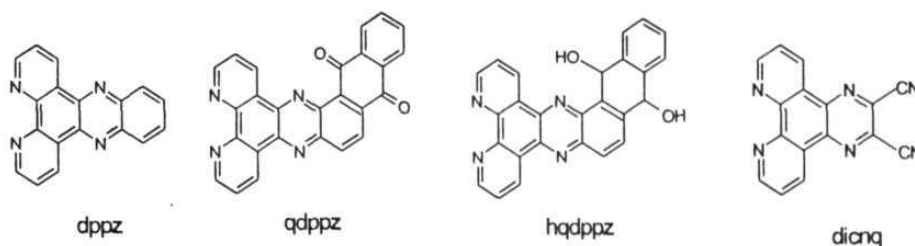


Fig. 7.1

While this study was in progress, synthesis and characterization of qdppz and a rhenium complex containing it ( $\text{Re}(\text{qdppz})(\text{CO})_3\text{Cl}$ ) have been reported by Lopez et al<sup>7</sup> but, neither the DNA interaction nor the influence of redox chemistry on the luminescence properties of this rhenium complex was investigated in that study. These have been accomplished in the present study with the new complex derived from qdppz viz:  $[\text{Ru}(\text{phen})_2(\text{qdppz})]^{2+}$ . It is demonstrated in Chapter 3 that  $[\text{Ru}(\text{phen})_2(\text{qdppz})]^{2+}$  is not only an avid binder of DNA but also an efficient photocleaving agent of the plasmid. On the other hand, the corresponding reduced species,  $[\text{Ru}(\text{phen})_2(\text{hqdppz})]^{2+}$ ,

binds and photocleaves DNA with less efficiency. Specifically, results of absorption titration, thermal denaturation, viscometry, differential-pulse voltammetric experiments have revealed that the DNA binding constant,  $K_b$ , for  $[\text{Ru}(\text{phen})_2(\text{qdppz})]^{2+}$  is as high as  $> 10^6 \text{ M}^{-1}$  and the corresponding value for  $[\text{Ru}(\text{phen})_2(\text{hqdpz})]^{2+}$  is only  $\sim 10^5 \text{ M}^{-1}$ . DNA photocleavage efficacies of these complexes also follow the same trend with the oxidized form being a better photonuclease. Experiments carried out in the presence of various 'inhibitors' have suggested that none of the reactive oxygen species ( $^1\text{O}_2$ ,  $\text{OH}^\bullet$  or  $\text{O}_2^{\cdot-}$ ) play a significant role in the DNA photocleavage by  $[\text{Ru}(\text{phen})_2(\text{qdppz})]^{2+}$  (see Fig. 3.9). This situation is unlike the case with  $\text{OH}^\bullet$ -mediated DNA cleavage by  $[(\eta^5\text{-C}_5\text{Me}_5)\text{Ru}(\text{NO})(\text{dppz})]^{2+8a}$  but, is quite similar to that reported recently for  $[\text{Re}(\text{dppz})(\text{CO})_3(\text{py})]^+$  (py = pyridine)<sup>8b</sup>, indicating the possibility of photoinduced DNA cleavage by  $[\text{Ru}(\text{phen})_2(\text{qdppz})]^{2+}$  *via* a direct oxidation of the biopolymer. In this regard, it is interesting to note that while irradiation into the MLCT band of  $[\text{Ru}(\text{phen})_2(\text{qdppz})]^{2+}$  can generate a species containing oxidized ruthenium and reduced qdppz (1  $e^-$  transfer), direct excitation of the bound-qdppz is expected to provide the triplet quinone. Both these quinone-based, transient species are known to be potent DNA cleaving agents capable of reacting with the duplex *via* various mechanisms including hydrogen abstraction, electron transfer etc.<sup>9</sup>

DNA binding and photocleavage properties of a series of new ruthenium(II) complexes containing dicnq are described in Chapter 4. Results of absorption and emission titration, thermal denaturation and agarose gel

electrophoresis experiments suggest that while binding of DNA by  $[\text{Ru}(\text{phen})_2(\text{dicnq})]^{2+}$  and  $[\text{Ru}(\text{phen})(\text{dicnq})_2]^{2+}$  is *via* an intercalative mode, that by the tris- complex,  $[\text{Ru}(\text{dicnq})_3]^{2+}$ , on the other hand, may not involve intercalation. The  $K_b$  values for all the three dicnq containing complexes are in the range of  $1 - 4 \times 10^4 \text{ M}^{-1}$ . These values are close to the  $K_b$  for DNA binding by  $[\text{Ru}(\text{phen})_3]^{2+}$  but, are too low in comparison with the strong ( $K_b > 10^6 \text{ M}^{-1}$ ) DNA binding exhibited by  $[\text{Ru}(\text{phen})_2(\text{dppz})]^{2+}$  and  $[\text{Ru}(\text{phen})_2(\text{qdppz})]^{2+}$  described in Chapter 3. Obviously, dicnq is not as an extended  $\pi$ -system as dppz is and, nor does its architecture is endowed with a fused quinone moiety as in the case of qdppz. Interestingly, DNA photocleavage efficiencies of the three complexes follow the order:  $[\text{Ru}(\text{phen})_2(\text{dicnq})]^{2+} > [\text{Ru}(\text{phen})(\text{dicnq})_2]^{2+} \gg [\text{Ru}(\text{dicnq})_3]^{2+}$ . As discussed in Chapter 4, while the precise mechanism of the DNA cleavage by these complexes has not been explored, it is tempting to suggest, based on the absorption and luminescence results, that the DNA nicking ability of these complexes depends on their mode of binding with DNA.

It was noticed, during the course of this work, that notwithstanding the well-documented importance of dppz in DNA interactions of the complexes containing it, binding studies using such complexes having a metal ion other than ruthenium have attracted much less attention.<sup>1a, 10</sup> Moreover, only a few studies seem to have addressed DNA cleavage aspects of dppz-based complexes.<sup>3, 11</sup> Thus, in the present study, two new mixed-ligand complexes,  $[\text{Co}(\text{phen})_2(\text{dppz})]^{3+}$  and  $[\text{Ni}(\text{phen})_2(\text{dppz})]^{2+}$ , have been synthesized and fully characterized by various physico-chemical methods.

Results of absorption titration, thermal denaturation and differential-pulse voltammetric experiments reveal that both these +3 and +2 complexes are avid binders ( $K_b = (9 \pm 2) \times 10^5 \text{ M}^{-1}$ ) of CT DNA and that the dipyridophenazine ligand on them is engaged in the intercalative interaction with DNA. Thus, although the two complexes investigated in the present study provide a good opportunity to compare directly the binding of isosteric intercalating species of +2 and +3 charge to DNA, such a comparison could not be made. On the other hand, while the cobalt(III) complex has been found to effect the photocleavage of the supercoiled pBR 322 DNA *via*, most probably, a  $\text{OH}^\bullet$ -mediated mechanism, the nickel(II) complex, being paramagnetic, is ineffective under similar experimental conditions. The participation of hydroxyl radical in the DNA photocleavage by  $[\text{Co}(\text{phen})_2(\text{dppz})]^{3+}$  is not only substantiated by a series of control experiments involving various inhibitors but also, by ESR spin-trapping studies. Finally, it is interesting to note that while the Co-dppz complex reported here cleaves DNA *via*  $\text{OH}^\bullet$ -mediated mechanism. The DNA nicking by the corresponding Ru-dppz complex has been reported to involve a Type II process.<sup>5a</sup>

The results described in these three Chapters while underscoring the importance of dppz in the DNA-binding, also demonstrate that substitution of dppz-based complexes by different metal ions and/or modifying this versatile ligand with appropriate substituents can bring about modulation in the structural and electronic properties of the ensuing complexes and, consequently, in their DNA binding and photocleaving efficacies.

## 7.2 Luminescence properties of Ru(II) complexes

Luminescence studies carried out with the new ruthenium(II) complexes synthesized during this work have yielded interesting results. Specifically, it has been demonstrated in this thesis that (i) the redox couple  $[\text{Ru}(\text{phen})_2(\text{qdppz})]^{2+}/[\text{Ru}(\text{phen})_2(\text{hqdpz})]^{2+}$  represents an 'electro-photoswitch' (Chapter 3) and (ii) both  $[\text{Ru}(\text{phen})_2(\text{dinq})]^{2+}$  and  $[\text{Ru}(\text{phen})(\text{dicnq})_2]^{2+}$  are moderately efficient molecular light switches for DNA (Chapter 4).

$[\text{Ru}(\text{phen})_2(\text{qdppz})]^{2+}$  was found to be weakly luminescent ( $\phi \leq 10^{-4}$ ) in rigorously dried  $\text{CHCl}_3$ ,  $\text{CH}_2\text{Cl}_2$ , dichloroethane and  $\text{CH}_3\text{CN}$  and to be essentially non-luminescent in aqueous buffer, aqueous  $\text{CH}_3\text{CN}$  (10%  $\text{H}_2\text{O}$ ) and micellar solutions. On the other hand, the reduced complex  $[\text{Ru}(\text{phen})_2(\text{hqdpz})]^{2+}$  was found to be non-luminescent in aqueous solutions with or without buffer as was the case with its oxidized form but, it showed the MLCT luminescence in aqueous  $\text{CH}_3\text{CN}$  and micellar media (Fig. 3.10). The weak luminescence observed for the oxidized complex in non-aqueous solvents has been rationalized in terms of an intramolecular photoinduced electron transfer (PET) quenching of its MLCT state by the appended quinone fragment. An additional process involving the sensitivity of the excited state to quenching by water, and the subsequent increase in the non-radiative decay rate has also been invoked in explaining the total lack of emission observed for this complex in the aqueous environments.<sup>1, 4</sup> We believe that the PET reaction does not operate in the hydroquinone-containing complex. A 'partial recovery' of luminescence has been suggested to occur in SDS medium and

CH<sub>3</sub>CN solutions where the complex can reside in a hydrophobic environment with the dipyrrophenazine ligand protected from water.<sup>1, 4</sup>

Based on the emission characteristics described above, it was possible to demonstrate the redox switching of luminescence with the redox couple  $[\text{Ru}(\text{phen})_2(\text{qdppz})]^{2+}/[\text{Ru}(\text{phen})_2(\text{hqdpz})]^{2+}$ . Exhaustive Coulometric reduction and re-oxidation of  $[\text{Ru}(\text{phen})_2(\text{qdppz})]^{2+}$  were conducted in CH<sub>3</sub>CN, 0.1 M TBAPF<sub>6</sub>. It was observed that while the quinone form is almost non-luminescent, the electrochemically generated hydroquinone form shows moderate luminescence at 601 nm. Thus, the couple  $[\text{Ru}(\text{phen})_2(\text{qdppz})]^{2+}/[\text{Ru}(\text{phen})_2(\text{hqdpz})]^{2+}$ , which combines an electroactive component with a light-emitting center, represents a redox-activated luminescence on/off switching device,<sup>12</sup> Fig. 7.2.

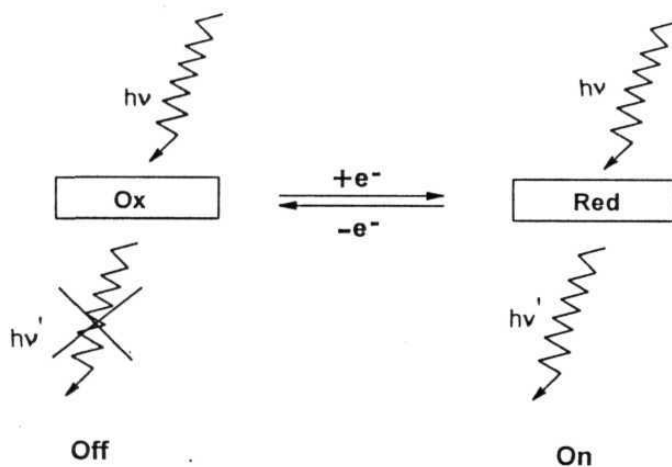


Fig. 7.2

Both  $[\text{Ru}(\text{phen})_2(\text{dicnq})]^{2+}$  and  $[\text{Ru}(\text{phen})(\text{dicnq})_2]^{2+}$  were seen to act as molecular light switches for DNA, albeit with less efficiency compared to the behavior previously reported for the light switches  $[\text{Ru}(\text{phen})_2(\text{dppz})]^{2+}$

and its osmium(II) analogue.<sup>1, 4</sup> As seen in Fig. 4.10, both  $[\text{Ru}(\text{phen})_2(\text{dicnq})]^{2+}$  and  $[\text{Ru}(\text{phen})(\text{dicnq})_2]^{2+}$  are weakly luminescent in buffered aqueous solutions but, show enhancement of luminescence upon successive additions of CT DNA. The luminescence enhancement factor for  $[\text{Ru}(\text{phen})(\text{dicnq})_2]^{2+}$  (16) is approximately twice that for  $[\text{Ru}(\text{phen})_2(\text{dicnq})]^{2+}$  (8) but, both these enhancement factors are too low in comparison with that for  $[\text{Ru}(\text{phen})_2(\text{dppz})]^{2+}$  ( $>10^4$ ).<sup>1</sup> In the latter case, emission enhancement has been ascribed to the protection of the imine nitrogen/s from attack by water and a consequent decrease in the non-radiative processes upon intercalation. dicnq being a quinoxaline ligand bearing imine nitrogens, the increase in emission intensity observed for  $[\text{Ru}(\text{phen})_2(\text{dicnq})]^{2+}$  and  $[\text{Ru}(\text{phen})(\text{dicnq})_2]^{2+}$  in the presence of DNA is also a consequence of a decrease in the non-radiative deactivation process of each excited complex due to the protection of the *complexed* dicnq by DNA. The low enhancement factors observed for these two complexes can be due to (i) an intramolecular PET process involving their  $^3\text{MLCT}$  states and the electron deficient dicnq ligand and/or (ii) their weak DNA binding in comparison with the corresponding dppz complex. Both these suppositions are consistent with the non-emissive nature of the corresponding tris-analogue ( $[\text{Ru}(\text{dicnq})_3]^{2+}$ ) in the absence and presence of DNA.

### 7.3 Photonuclease activity of porphyrin-anthraquinone diads and diazoarene chromophores

During the course of studies on metallointercalators described in Chapters 3, 4 and 5, we came across two interesting series of photonucleases

viz: porphyrin-anthraquinone (P-Q) diads and diazoarene systems.

The P-Q systems have been developed in Professor G. Mehta's group as part of their continuing research on new generation sensitizers for photodynamic therapy (PDT) of cancer and allied diseases.<sup>13</sup> During the design of these P-Q conjugates, it was conceived that these bichromophoric systems, which absorb light all through in the UV-visible region, are capable of initiating the photocleavage of DNA by  $^1\text{O}_2$  (porphyrin,  $> 400$  nm excitation)<sup>14</sup> as well as electron transfer/H-abstraction (anthraquinone,  $< 400$  nm excitation)<sup>9</sup> mechanisms. Moreover, the prospect of generation of the anthraquinone anion radical triggered by the visible light irradiation and the subsequent PET reaction from the photoexcited porphyrin donor to the appended anthraquinone acceptor in these hybrids, as previously reported for the covalently-linked, biomimetic porphyrin-anthraquinone donor-acceptor systems,<sup>15</sup> can be considered as an attractive attribute of this approach. These concepts are illustrated in Fig. 7.3.

$^1\text{H}$  NMR, UV-visible and electrochemical data of these hybrids has suggested that there is no appreciable ground state interaction between the porphyrin and anthraquinone subunits. The fluorescence from the porphyrin part of these hybrids was seen to be quenched by the anthraquinone moiety and, this can be attributed to the occurrence of a PET reaction from the singlet porphyrin to the quinone. Nonetheless, each new P-Q diad investigated in this study, was seen to be able to generate  $^1\text{O}_2$  in moderate yields when irradiated into the porphyrin absorption band (550 nm). The nuclease activity of these hybrids measured using the supercoiled plasmid DNA pBR 322 suggested that they are capable of displaying wavelength

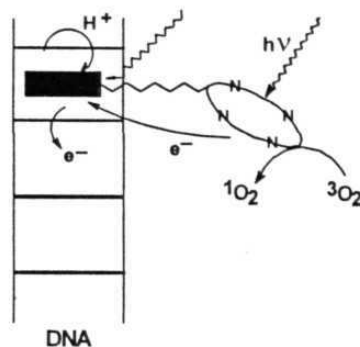


Fig. 7.3

dependent DNA cleavage activity (Fig. 6.6). In addition, efficient DNA photocleavage was observed by each new P-Q diad under white-light irradiation. Under these conditions, it is possible that the cleavage mechanism might involve  $^1\text{O}_2$ , PET and H-abstraction mechanisms as pictured in Fig. 7.3.

Finally, photonuclease activity of the three readily available diazoarenes compounds have also been reported in this thesis. To the best of our knowledge, carbenes, that are generated upon photoirradiation of diazoarenes, seem to have never been tested for their ability to cleave DNA. Both 9-diazoanthrone and 9-diazoxanthene are carbene-precursors and are capable of absorbing the visible light. Irradiation of supercoiled pBR 322 DNA by light in the presence of these diazoarenes resulted in a facile generation of the relaxed circular form. Careful experiments with various 'inhibitors' established the participation of carbene species in this photoconversion.

#### 7.4 Overall conclusions

Overall, it has been demonstrated in this thesis that it is possible to accomplish potent photonucleases by suitably modifying the structures of visible-light-absorbing chromophores. A highlight of this approach is that the chromophores either themselves can intercalate between the base-pairs of DNA (e.g. metallointercalators and diazo arenes) or can employ other structural components crafted on them to strongly bind to the duplex by intercalative interactions (eg, P-Q diads). The principal themes common to these new photonucleases is that (i) they all bind DNA with high affinity with  $K_b$  ranging from ca.  $10^4$  -  $10^6$   $M^{-1}$  and (ii) they all absorb light in the 400-650 nm region and (iii) they generate cytotoxic species such as reactive oxygen intermediates ( $^1O_2$  or  $OH^\bullet$ ), radical or carbene species and lead to DNA cleavage.

The photonucleases described here also have several practical applications. The ‘dual wavelength-dual mechanism’ theme as exemplified here in studies with the P-Q conjugates can be perceived to have immense application not only in photodynamic therapy but also in the design of photo-footprinting agents. The ‘light-switching’ abilities of  $[Ru(phen)_2(dicnq)]^{2+}$  and  $[Ru(phen)(dicnq)_2]^{2+}$  in the presence of DNA permit the use of these complexes as ‘luminescence reporters’ of DNA. Finally, DNA-binding and photocleavage by  $[Ru(phen)_2(qdppz)]^{2+}$  and  $[Ru(phen)_2(hqdppz)]^{2+}$  together with the finding that this redox couple represents an ‘electro-photoswitch’ testify to the suitability of these complexes in the design of both photonucleases and molecule-based, opto-electronic devices.

### 7.5 Future scope

Notwithstanding the fact that the present study has been helpful, to some extent, in providing new directions to the construction of novel photonucleases, an in-depth analysis of the results described in various chapters of this thesis suggests that a lot remains to be done.

One of the main problems associated with the DNA-binding studies presented in this thesis is concerned with an evaluation of the exact binding constants ( $K_b$ ) of a few new complexes. For example,  $[\text{Ru}(\text{phen})_2(\text{qdppz})]^{2+}$ ,  $[\text{Co}(\text{phen})_2(\text{dppz})]^{2+}$  and  $[\text{Ni}(\text{phen})_2(\text{dppz})]^{2+}$  all bind to DNA too strongly even at micromolar concentrations. The binding data in these cases could not be analyzed using eqn. 2.17, because the treatment involved in formulating this eqn. is valid only for weak-to-moderate binding situations. The data could not be satisfactorily fit even to the McGhee and von Hippel equation with and without incorporating the cooperativity parameters as is true for a recently reported strongly binding ruthenium(II) complex.<sup>16</sup> However, curve-fitting to eqn. 2.18 was found to be somewhat better and, the apparent binding constants thus obtained were in the range of ca.  $10^6 \text{ M}^{-1}$ . As mentioned earlier, these  $K_b$  values can be taken only as the lower limits of the effective binding constants for these complexes as was the case with the previously studied dppz complexes.<sup>1-6</sup> Thus, we note that while it is desirable to have the exact binding constants for these new complexes, and attempts will have to be made in this direction, the lack of such data has no significant impact on the main conclusions drawn from the present work. In a similar vein, while details of DNA photocleavage mechanisms have been unraveled in cases where possible, absence of discussion in a few other cases is only a

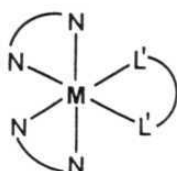
---

minor aberration. Nevertheless mechanistic studies inquiring into the details of DNA photocleavage by each photonuclease reported in this study, will have to be carried out.

A critical analysis of the wealth of information amassed during the present work suggests that there exists ample future scope in this field of research. The most trivial, but an important, future task is concerned with identifying the site specificity of DNA photocleavage by the various photonucleases investigated in this study. It should be possible to take this study to the next higher level and to find out the site specificity involved in the DNA photocleavage by the metallointercalators, P-Q systems and diazoarenes. The results obtainable in such studies are expected to be useful in the design of more effective artificial photonucleases and photo footprinting agents. The results described in Chapters 3-5 also provide some hints with regard to the design of new, architecturally more-appealing systems such as those shown in Fig. 7.4.

As far as the photochemical and photophysical properties of these photonucleases are concerned, it would be of interest to inquire into the detailed dynamics of these systems by using time-resolved fluorescence and absorbance methods. In this regard, the question of proton transfer quenching of the luminescence of Ru(II)-dicnq and qdppz complexes in aqueous solution is the most interesting one to be investigated. The dicnq complexes can also be tested for their shape selective binding affinity towards A or Z forms of DNA.

Finally, new generation photodynamic therapeutic agents based on water-soluble P-Q complexes can be developed. Water-soluble, red-light



$M = Ru(II), Co(III), Ni(II)$

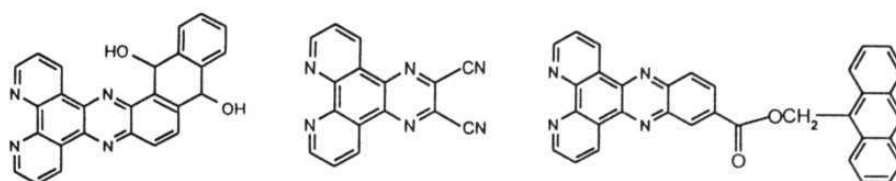
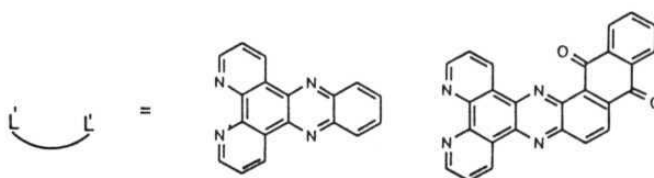
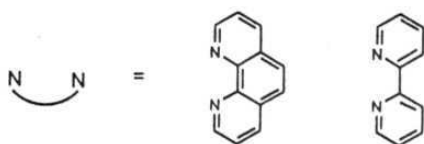


Fig. 7.4

absorbing diazoarene chromophores can also be designed to investigate the carbene-mediated DNA photocleavage by such novel photonucleases.

## 7.5 References

1. (a) Holmlin, R. E.; Barton, J. K. *Inorg. Chem.* **1995**, 34, 7. (b) Turro, C.; Bossman, S. H.; Jenkins, Y.; Barton, J. K.; Turro, N. J. *J. Am. Chem. Soc.* **1995**, 117, 9026. (c) Dupureur, C. M.; Barton, J. K. *J. Am. Chem. Soc.* **1994**, 116, 10286. (d) Hartshorn, R. M.; Barton, J. K. *J. Am. Chem. Soc.* **1992**, 114, 5919. (e) Jenkins, Y.; Friedman, A. E.; Turro, N. J.; Barton, J. K. *Biochemistry* **1992**, 31, 10809. (f) Friedman, A. E.; Kumar, C. V.; Turro, N. J.; Barton, J. K. *Nucl. Acid Res.* **1991**, 19, 2595. (g) Friedman, A. E.; Chambron, J. C.; Sauvage, J. P.; Turro, N. J.; Barton, J. K. *J. Am. Chem. Soc.* **1990**, 112, 4960.
2. (a) Bogler, J.; Gourdon, A.; Ishow, E.; Launay, J. -P. *Inorg. Chem.*, **1996**, 35, 2937. (b) Lincoln, B.; Broo, A.; Norden, B. *J. Am. Chem. Soc.* **1996**, 118, 2644. (c) Lincoln, P.; Norden, B. *J. Chem. Soc. Chem. Commun.* **1996**, 2145. (d) Stoeffler, H. D.; Thornton, N. B.; Temkin, S. L.; Schanze, K. S. *J. Am. Chem. Soc.* **1995**, 117, 7119. (e) Haq, I.; Lincoln, P.; Suh, D.; Norden, B.; Chowdhry, B. Z.; Chaires, J. B. *J. Am. Chem. Soc.* **1995**, 117, 4788. (f) Maggini, M.; Dono, A.; Scorrano, G.; Prato, M. *J. Chem. Soc., Chem. Commun.*, **1995**, 845. (g) Hiort, C. H.; Lincoln, P.; Norden, B. *J. Am. Chem. Soc.* **1993**, 115, 3448. (h) Eriksson, M.; Leijon, M.; Hiort, C.; Norden, B.; Graslund, A. *Biochemistry* **1994**, 33, 5031.

3. (a) Gupta, N.; Grover, N.; Neyhart, G. A.; Liang, W.; Singh, P.; Thorp, H. H. *Angew. Chem. Int. Ed. Engl.* **1992**, 31, 1048. (b) Neyhart, G. A.; Grover, N.; Smith, S. R.; Kalsbeck, W. A.; Fairley, T. A.; Cory, M.; Thorp, H. H. *J. Am. Chem. Soc.* **1993**, 115, 4423
4. Olson, E. J. C.; Hu, D.; Hormann, A.; Jonkman, A. M.; Arkin, M. R.; Stemp, E. D. A.; Barton, J. K.; Barbara, P. F. *J. Am. Chem. Soc.* **1997**, 119, 11458.
5. (a) Sentagne, C.; Chambron, J.-C.; Sauvage, J. P.; Paillous, N. *J. Photochem. Photobiol. B: Biol.* **1994**, 26, 165. (b) Schoch, K.; Hubbard, J. L.; Zoch, C. R.; Yi, G. -B.; Sorlie, M. *Inorg. Chem.* **1996**, 35, 4383. (c) Yam, V. W.-W.; Lo, K. K.-W.; Cheung, K.-K.; Kong, R. Y.-C. *J. Chem. Soc. Dalton Trans.*, **1997**, 2067.
6. (a) Arkin, R.; Stemp, E. D. A.; Turro, C.; Turro, N. J.; Barton, J. K. *J. Am. Chem. Soc.*, **1996**, 118, 2267. (b) Stemp, E. D. A.; Arkin, M. R.; Barton, J. K. *J. Am. Chem. Soc.* **1995**, 117, 2375. (c) Murphy, C. J.; Arkin, M. R.; Ghatlia, N. D.; Bossman, S. H.; Turro, N. J.; Barton, J. K. *Proc. Natl. Acad. Sci. USA*. **1994**, 91, 5315. (d) Murphy, C. J.; Arkin, M. R.; Jenkins, Y.; Ghatlia, N. D.; Bossman, S. H.; Turro, N. J.; Barton, J. K. *Science* **1993**, 262, 1025.
7. Lopez, R. B.; Loeb, B. L.; Boussie, T.; Meyer, T. J. *Tetrahedron Lett.*, **1996**, 37, 5437.
8. (a) Schoch, K.; Hubbard, J. L.; Zoch, C. R.; Yi, G. -B.; Sorlie, M. *Inorg. Chem.* **1996**, 35, 4383. (b) Yam, V. W.-W.; Lo, K. K.-W.; Cheung, K.-K.; Kong, R. Y.-C. *J. Chem. Soc. Dalton Trans.*, **1997**, 2067.

9. (a) Breslin, D. T.; Coury, J. E.; Anderson, J. R.; Mcfail-Isom, L.; Kan, Y.; Williams, L. D.; Bottomley, L. A.; Schuster, G. B. *J. Am. Chem. Soc.* **1997**, 119, 5043. (b) Koch, T.; Ropp, J. D.; Sligar, S. D.; Schuster, G. B. *Photochem. Photobiol.* **1993**, 58, 554. (c) Bhattacharya, S.; Mandal, S. S. *J. Chem. Soc. Chem. Commun.* **1996**, 1515.
10. Yam, V. W.-W.; Lo, K. K.-W.; Cheung, K.-K.; Kong, R. Y.-C. *J. Chem. Soc.; Chem. Commun.* **1995**, 1191.
11. Sentagne, C.; Chambron, J.-C.; Sauvage, J. P.; Paillous, N. *J. Photochem. Photobiol. B: Biol.* **1994**, 26, 165.
12. Goulle, V.; Harriman, A.; Lehn, J. -M. *J. Chem. Soc., Chem. Commun.*, **1993**, 1034.
13. (a) Mehta, G.; Sambaiah, T.; Maiya, B. G.; Sirish, M.; Chatterjee, D. *J. Chem. Soc. Perkin Trans. 1.* **1993**, 2667. (b) Mehta, G.; Sambaiah, T.; Maiya, B. G.; Sirish, M.; Dattagupta, A. *Tetrahedron Lett.* **1994**, 35, 4201. (c) Mehta, G.; Sambaiah, T.; Maiya, B. G.; Sirish, M.; Dattagupta, A. *J. Chem. Soc. Perkin Trans. 1.* **1995**, 295. (d) Mehta, G.; Muthusamy, S.; Maiya, B. G.; Sirish, M. *J. Chem. Soc. Perkin Trans. 1.* **1996**, 2421.
14. (a) Morgan, A. R. *Curr. Med. Chem.*, **1995**, 2, 604. (b) Bonnett, R., *Chem. Soc. Rev.* **1995**, 19. (c) *Photodynamic Therapy: Basic Principles and Clinical Applications*, Henderson, R. W.; Dougherty, T. J., Eds.; Marcel Dekker: New York, **1992**.
15. Wasielewski, M. R. *Chem. Rev.* **1992**, 92, 435.
16. Carlson, D. L.; Hutchital, D. H.; Mantilla, E. J.; Sheardy, R. D.; Murphy Jr., W. R. *J. Am. Chem. Soc.*, **1993**, 115, 6424.

## APPENDIX I

### List of Publications

1. Arounaguiri, S.; Maiya, B. G. 'Dipyridophenazine Complexes of Cobalt(III) and Nickel(II): DNA-Binding and Photocleavage Studies' *Inorg. Chem.* **1996**, 35, 4267.
2. Arounaguiri, S.; Dattagupta, A.; Maiya, B. G. 'Redox-Activated Luminescence and Light-Induced Nuclease Activity of a New Mixed-Ligand Ruthenium(II) Complex' *Proc. Indian Acad. Sci. (Chem. Sci)* **1997**, 109, 155.
3. Maiya, B. G.; Ramana, C. V.; Arounaguiri, S.; Nagarajan, M. 'DNA Cleavage by Photoexcited Diazoarenes' *Bioorg. & Med. Chem. Lett.* **1997**, 7, 2141.
4. Mehta, G.; Muthusamy, S.; Maiya, B. G.; Arounaguiri, S. 'Porphyrin-Anthraquinone Hybrids: Wavelength Dependent DNA Photonucleases' *Tetrahedron Lett.* **1997**, 38, 7125.
5. Arounaguiri, S.; Maiya, B. G. 'A New Metallointercalator Containing an Electroactive Dipyridophenazine Ligand: DNA Binding, Photonuclease Activity and Luminescence Properties' (Submitted for Publication).